NEW AGE

HIGH VOLTAGE ENGINEERING

C.L. Wadhwa

NEW AGE INTERNATIONAL PUBLISHERS

HIGH VOLTAGE ENGINEERING

THIS PAGE IS BLANK

HIGH VOLTAGE ENGINEERING

(Second Edition)

C.L. WADHWA

Formerly Professor
Department of Electrical Engineering,
Delhi College of Engineering, Delhi
Formerly Dean, Faculty of Technology
University of Delhi

PUBLISHING FOR ONE WORLD

NEW AGE INTERNATIONAL (P) LIMITED, PUBLISHERS

New Delhi • Bangalore • Chennai • Cochin • Guwahati • Hyderabad
Jalandhar • Kolkata • Lucknow • Mumbai • Ranchi

Visit us at **www.newagepublishers.com**

Published by New Age International (P) Ltd., Publishers

ISBN (10) : 81-224-2323-X

ISBN (13) : 978-81-224-2323-5

PUBLISHING FOR ONE WORLD

NEW AGE INTERNATIONAL (P) LIMITED, PUBLISHERS
4835/24, Ansari Road, Daryaganj, New Delhi - 110002
Visit us at **www.newagepublishers.com**

To

My mother, who taught me how to hold pen in my little fingers.
My father, who taught me modesty and tolerance.
My wife, a symbol of mutual trust and mutual respect.
My daughter and son, who exhibited a high degree of patience.
My students, who made me learn the subject.
The Almighty, who has created such a beautiful world.

THIS PAGE IS BLANK

Preface to the Second Edition

"High Voltage Engineering" has been written for the undergraduate students in Electrical Engineering of Indian and foreign Universities as well as the practising electrical engineers.

The author developed interest in the field of High Voltage Engineering when he was a student at the Govt. Engineering College, Jabalpur. It used to be thrilling to observe large metal spheres flashing over, corona phenomenon on a wire placed along the axis of a cylinder and then recording the corona loss, controlling the wave shapes of impulse voltages etc.

The author has taught the subject at the Delhi College of Engineering for quite a number of years and while preparing lecture notes he referred to some of the books and journals and some literature from the internationally famed manufacturers of High Voltage equipments e.g. Haefely, Tettex etc. The lecture notes so prepared, thus, have a touch of both the class room requirements and a practising engineer's requirements.

In this edition, zeroth chapter on Electric Stress estimation and c ontrol has been added where in different methods viz. finite difference, finite element, charge simmulation method and surface charge simulation methods have been discussed per estimation of metric stresses in complex dielectric media and electrode configuration. a brief view of optimisation of electrode configuration is also given in this chapter.

Chapter 1 deals with the breakdown of gases, liquids, and solid materials. Even though it has not been possible to explain the physical phenomenon associated with breakdown of the materials, with accuracy and precisiveness, an attempt has been made to bring out some of the theories advocated by researchers in this field in a simple lucid and organised way.

Chapters 2 and 3 discuss the generation of high d.c. and a.c. voltages and high impulse voltages and currents. Some of the latest circuits have been discussed and rigorous mathematical treatment of the circuit has been given to make the subject more interesting and to make the student understand the subject better.

Measurement of transient voltage and currents and high voltage and current require different skills and equipment as compared with common a.c. or d.c. voltages we normally come across. Chapter 4 discusses various techniques and circuits for measurement of such quantities.

Chapter 5 deals into high voltage testing of electrical equipments like insulators, cables, transformers, circuit breakers etc.

The measurements using high voltage Schering bridge, transformer ratio arm bridge and partial discharges yield information regarding the life expectancy and the long term stability or otherwise of the insulating materials. These techniques have been discussed elaborately in Chapter 6. These tests are very important both during design and operation of the equipments.

Electrical transients last for a very short duration but these play a very important role in the insulation design of power system. Chapter 7 takes a view of various types of transients in power system and suggests classical and more modern statistical methods of coordinating the insulation requirements of various equipments of the system and the devices required for protection of these equipments.

In this edition of the book following articles have been added in chapter 1 of the book :

(*i*) Breakdown in SF_6 gas and Vacuum.

(*ii*) Insulating materials used in power apparatus.

(*iii*) Application of gases, liquid and solid insulating materials in different power apparatus.

A suitable number of problems have been solved to help understand the relevant theory. At the end, a large number of multiple choice questions have been added to help the reader to test himself. An extensive bibliography will help the reader to locate detailed information on various topics of his interest.

There are very few High Voltage Laboratories all over the world and the reader may not have an opportunity to visit such a laboratory. Therefore, a few photoplates have been added at suitable locations in the book to give a physical feel of various equipments in a well equipped high voltage laboratory. The author feels that with the inclusion of photoplates of high voltage equipments the student as well the practising engineers would be greatly benefited.

I wish to express my sincere thanks to M/s Emile Haefely & Co. Ltd., Switzerland for permitting inclusion of photoplates in the book which has enhanced the utility of the book.

I also wish my express my gratitude to my wife Usha, daughter Meenu and son Sandeep for their patience and encouragement during the preparation of the book.

Any constructive suggestion for the improvement of the book will be gratefully acknowledged.

New Delhi **C.L. WADHWA**

Contents

THIS PAGE IS BLANK

0 Electric Stress Estimation and Control

0.1 INTRODUCTION

The potential at a point plays an important role in obtaining any information regarding the electrostatic field at that point. The electric field intensity can be obtained from the potential by gradient operation on the potential

i.e. $$E = -\nabla V \quad ...(1)$$

which is nothing but differentiation and the electric field intensity can be used to find electric flux density using the relation

$$D = \varepsilon E \quad ...(2)$$

The divergence of this flux density which is again a differentiation results in volume charge density.

$$\nabla . D = \rho_v \quad ...(3)$$

Therefore, our objective should be to evaluate potential which of course can be found in terms of, charge configuration. However it is not a simple job as the exact distribution of charges for a particular potential at a point is not readily available. Writing $\varepsilon E = D$ in equation (3) we have

$$\nabla . \varepsilon E = \rho_v$$

or $$-\nabla . \varepsilon . \nabla V = \rho_v$$

or $$\varepsilon \nabla^2 V = -\rho_v$$

or $$\nabla^2 V = -\frac{\rho_v}{\varepsilon} \quad ...(4)$$

This is known as Poisson's equation. However, in most of the high voltage equipments, space charges are not present and hence $\rho_v = 0$ and hence equation (4) is written as

$$\nabla^2 V = 0 \quad ...(5)$$

Equation (5) is known as Laplace's equation

If $\rho_v = 0$, it indicates zero volume charge density but it allows point charges, line charge, ring charge and surface charge density to exist at singular location as sources of the field.

Here ∇ is a vector operator and is termed as del operator and expressed mathematically in cartesian coordinates as

$$\nabla = \frac{\partial}{\partial x}\bar{a}_x + \frac{\partial}{\partial y}\bar{a}_y + \frac{\partial}{\partial z}\bar{a}_z \quad ...(6)$$

where $\bar{a}_x, \bar{a}_y$ and $\bar{a}_z$ are unit vectors in the respective increasing directions.

Hence Laplace's equation in cartesian coordinates is given as

$$\nabla^2 V = \frac{\partial^2 V}{\partial x^2} + \frac{\partial^2 V}{\partial y^2} + \frac{\partial^2 V}{\partial z^2} = 0 \qquad ...(7)$$

Since $\nabla \cdot \nabla$ is a dot produce of two vectors, it is a scalar quantity. Following methods are normally used for determination of the potential distribution

(*i*) Numerical methods

(*ii*) Electrolytic tank method.

Some of the numerical methods used are

(*a*) Finite difference method (FDM)

(*b*) Finite element method (FEM)

(*c*) Charge simulation method (CSM)

(*d*) Surface charge simulation method (SCSM).

0.2 FINITE DIFFERENCE METHOD

Let us assume that voltage variations is a two dimensional problem *i.e.* it varies in *x-y* plane and it does not vary along *z*-co-ordinate and let us divide the interior of a cross section of the region where the potential distribution is required into squares of length *h* on a side as shown in Fig. 0.1.

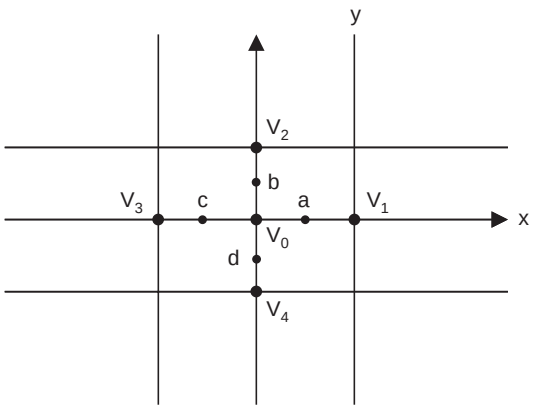

Fig. 0.1 A portion of a region containing a two-dimensional potential field divided into square of side *h* .

Assuming the region to be charge free

$$\nabla \cdot D = 0 \quad \text{or} \quad \nabla \cdot E = 0$$

and for a two-dimensional situation

$$\frac{\partial E_x}{\partial x} + \frac{\partial E_y}{\partial y} = 0$$

and from equation (7) the Laplace equation is

$$\frac{\partial^2 V}{\partial x^2} + \frac{\partial^2 V}{\partial y^2} = 0 \qquad ...(8)$$

Approximate values for these partial derivatives may be obtained in terms of the assumed values (Here V_0 is to be obtained when V_1, V_2, V_3 and V_4 are known Fig. 1.

$$\left.\frac{\partial V}{\partial x}\right|_a = \frac{V_1 - V_0}{h} \quad \text{and} \quad \left.\frac{\partial V}{\partial x}\right|_c = \frac{V_0 - V_3}{h} \qquad ...(9)$$

From the gradients

$$\left.\frac{\partial^2 V}{\partial x^2}\right|_0 = \frac{\left.\frac{\partial V}{\partial x}\right|_a - \left.\frac{\partial V}{\partial x}\right|_c}{h} = \frac{V_1 - V_0 - V_0 + V_3}{h^2} \qquad ...(10)$$

Similarly $$\left.\frac{\partial^2 V}{\partial y^2}\right|_0 = \frac{V_2 - V_0 - V_0 + V_4}{h^2}$$

Substituting in equation (8) we have

$$\frac{\partial^2 V}{\partial x^2} + \frac{\partial^2 V}{\partial y^2} = \frac{V_1 + V_2 + V_3 + V_4 - 4V_0}{h^2} = 0$$

or $$V_0 = \frac{1}{4}(V_1 + V_2 + V_3 + V_4) \qquad ...(11)$$

As mentioned earlier the potentials at four corners of the square are either known through computations or at start, these correspond to boundary potentials which are known a priori. From equation (11) it is clear that the potential at point *O* is the average of the potential at the four neighbouring points. The iterative method uses equation (11) to determine the potential at the corner of every square subdivision in turn and then the process is repeated over the entire region until the difference in values is less than a prespecified value.

The method is found suitable only for two dimensional symmetrical field where a direct solution is possible. In order to work for irregular three dimensional field so that these nodes are fixed upon boundaries, becomes extremely difficult. Also to solve for such fields as very large number of $V(x, y)$ values of potential are required which needs very large computer memory and computation time and hence this method is normally not recommended for a solution of such electrostatic problems.

0.3 FINITE ELEMENT METHOD

This method is not based on seeking the direct solution of Laplace equation as in case of FDM, instead in Finite element method use is made of the fact that in an electrostatic field the total energy enclosed in the whole field region acquires a minimum value. This means that this voltage distribution under given conditions of electrode surface should make the enclosed energy function to be a minimum for a given dielectric volume *v*.

We know that electrostatic energy stored per unit volume is given as

$$W = \frac{1}{2} \in E^2 \qquad ...(12)$$

For a situation where electric field is not uniform, and if it can be assumed uniform for a differential volume δv, the electric energy over the complete volume is given as

$$W = \frac{1}{2}\int_V \frac{1}{2} \in (-\nabla V)\, dv \qquad ...(13)$$

To obtain voltage distribution, our performance index is to minimise W as given in equation (13).

Let us assume an isotropic dielectric medium and an electrostatic field without any space charge. The potential V would be determined by the boundaries formed by the metal electrode surfaces.

Equation (13) can be rewritten in cartesian co-ordinates as

$$W = \frac{1}{2} \in \iiint \left[\left(\frac{\partial V}{\partial x} \right)^2 + \left(\frac{\partial V}{\partial y} \right)^2 + \left(\frac{\partial V}{\partial z} \right)^2 \right] dxdydz \qquad ...(14)$$

Assuming that potential distribution is only two-dimensional and there is no change in potential along z-direction, then $\frac{\partial V}{\partial z} = 0$ and hence equation (14) reduces to

$$W_A = z \iint \left[\frac{1}{2} \in \left\{ \left(\frac{\partial V}{\partial x} \right)^2 + \left(\frac{\partial V}{\partial y} \right)^2 \right\} \right] dxdy \qquad ...(15)$$

Here z is constant and W_A represents the energy density per unit area and the quantity within integral sign represents differential energy per elementary area $dA = dxdy$.

In this method also the field between electrodes is divided into discrete elements as in FDM. The shape of these elements is chosen to be triangular for two dimensional representation and tetrahedron for three dimensional field representation Fig. 0.2 (*a*) and (*b*).

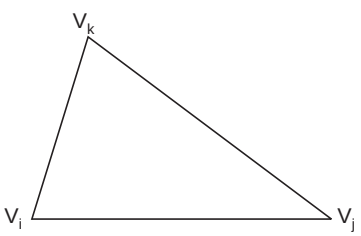

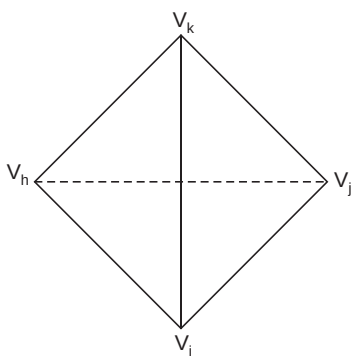

Fig. 0.2 (a) Triangular finite element (b) Tetrahedron finite element.

The shape and size of these finite elements is suitably chosen and these are irregularly distributed within the field. It is to be noted that wherever within the medium higher electric stresses are expected *e.g.* corners and edges of electrodes, triangles of smaller size should be chosen.

Let us consider an element e_1 as shown in Fig. 0.2(*a*) as part of the total field having nodes i, j and k in anti-clockwise direction. There will be a large no. of such elements e_1, e_2 .....e_N . Having obtained the potential of the nodes of these elements, the potential distribution within each elements is required to be obtained. For this normally a linear relations of V on x and y is assumed and hence the first order approximation gives

$$V(x, y) = a_1 + a_2 x + a_3 y \qquad ...(16)$$

It is to be noted that for better accuracy of results higher order approximation *e.g.* square or cubic would be required. Equation (16) implies that electric field intensity within the element is constant and potentials at any point within the element are linearly distributed. The potentials at nodes *i*, *j* and *k* are given as

$$V_i = a_1 + a_2 x_i + a_3 y_i$$
$$V_j = a_1 + a_2 x_j + a_3 y_j$$
$$V_k = a_1 + a_2 x_k + a_3 y_k \quad \text{...(17)}$$

Equation (17) can be rewritten in matrix form as

$$\begin{bmatrix} V_i \\ V_j \\ V_k \end{bmatrix} = \begin{bmatrix} 1 & x_i & y_i \\ 1 & x_j & y_j \\ 1 & x_k & y_k \end{bmatrix} \begin{bmatrix} a_1 \\ a_2 \\ a_3 \end{bmatrix} \quad \text{...(18)}$$

By using Cramer's rules, the coefficient a_1, a_2, a_3 can be obtained as follows

$$a_1 = \frac{1}{2\Delta_e}(\alpha_i V_i + \alpha_j V_j + \alpha_k V_k) \quad \text{...(19)}$$

$$a_2 = \frac{1}{2\Delta_e}(\beta_i V_i + \beta_j V_j + \beta_k V_k)$$

and

$$a_3 = \frac{1}{2\Delta_e}(\gamma_i V_i + \gamma_j V_j + \gamma_k V_k)$$

where

$$\alpha_i = x_j y_k - x_k y_j, \quad \alpha_j = x_k y_i - x_i y_k, \quad \alpha_k = x_i y_j - x_j y_i$$
$$\beta_i = y_i - y_k, \quad \beta_j = y_k - y_i, \quad \beta_k = y_i - y_j$$
$$\gamma_i = x_k - x_j, \quad \gamma_j = x_i - x_k, \quad \gamma_k = x_j - x_i$$

and

$$2\Delta_e = \alpha_i + \alpha_j + \alpha_k = \beta_i \gamma_j - \beta_j \gamma_i$$

where Δ_e represents the area of the triangular element under consideration. As mentioned earlier the nodes must be numbered anticlockwise, else Δ_e may turn out to be negative.

From equation (16), the partial derivatives of V are

$$\frac{\partial V}{\partial x} = a_2 = f(V_i, V_j, V_k) \quad \text{and} \quad \frac{\partial V}{\partial y} = a_3 = f(V_i, V_j, V_k) \quad \text{...(20)}$$

We know that for obtaining the voltage at various nodes we have to minimise the energy within the whole system for which derivatives of energies with respect to potential distribution in each element is required. For the element *e* under consideration, let W_e be the energy enclosed in the element, then energy per unit length in the *z*-direction W_e/z denoted by $W_{\Delta e}$ can be obtained by using equation (15) as follows

$$W_{\Delta e} = \frac{W_e}{z} = \frac{1}{2} \in \Delta e \left\{ \left(\frac{\partial V}{\partial x} \right)^2 + \left(\frac{\partial V}{\partial y} \right)^2 \right\}_e \quad \text{...(21)}$$

Here

$$\Delta e = \iint_e dx dy$$

To obtain condition for energy minimisation we differentiate partially equation (21) with respect to V_i, V_j and V_k separately. Thus partially differentiating equation (21) with respect to V_i and making use of equations (19) and (20).

We have $$\frac{\partial W_{\Delta e}}{\partial V_i} = \frac{1}{2} \in \Delta_e \left(2a_2 \frac{\partial a_2}{\partial V_i} + \frac{\partial a_3}{\partial V_i} \right) = \frac{1}{2} \in (a_2 \beta_i + a_3 \gamma_i)$$

$$= \frac{\varepsilon}{4\Delta_e} [(\beta_i^2 + \gamma_i^2) V_i + (\beta_i \beta_j + \gamma_i \gamma_j) V_j + (\beta_i \beta_k + \gamma_i \gamma_k) V_k] \quad ...(22)$$

Similarly, finding partial derivatives of equation (21) with respect to V_j and V_k and following the procedure outlined above for partial derivative with respect to V_i and arranging all the three equation in matrix from we have

$$\frac{\partial W_{\Delta e}}{\partial V_e} = \frac{\varepsilon}{4\Delta_e} \begin{bmatrix} (\beta_i^2 + \gamma_i^2) & (\beta_i \beta_j + \gamma_i \gamma_j) & (\beta_i \beta_k + \gamma_i \gamma_k) \\ (\beta_j \beta_i + \gamma_j \gamma_i) & (\beta_j^2 + \gamma_j^2) & (\beta_j \beta_k + \gamma_j \gamma_k) \\ (\beta_k \beta_i + \gamma_k \gamma_i) & (\beta_k \beta_j + \gamma_k \gamma_j) & (\beta_k^2 + \gamma_k^2) \end{bmatrix} \begin{bmatrix} V_i \\ V_j \\ V_k \end{bmatrix} \quad ...(22a)$$

$$= \frac{\varepsilon}{4\Delta_e} \begin{bmatrix} (C_{ii}) & (C_{ij}) & C_{ik} \\ (C_{ji}) & C_{jj} & C_{jk} \\ C_{ki} & C_{kj} & C_{kk} \end{bmatrix}_e \begin{bmatrix} V_i \\ V_j \\ V_k \end{bmatrix}_e = [C]_e [V]_e \quad ...(23)$$

After considering a typical element *e*, the next step is to take into account all such elements in the region under consideration and the energy associated with all the elements will then be

$$W = \sum_{e=1}^{N} W_e = \frac{1}{2} \in [V^T] [C] [V] \quad ...(24)$$

where $$[V] = \begin{bmatrix} V_1 \\ V_2 \\ \vdots \\ V_n \end{bmatrix}$$

and n is the total number of nodes in the system and N is the no. of elements and $[C]$ is called the global stiffness matrix which is the sum of the individual matrices.

In general $\frac{\partial W}{\partial V_h}$ leads to

$$\sum_{i=1}^{n} V_i C_{ik} = 0 \quad ...(25)$$

The solution of the above equations gives voltage distribution in the region. Of course while seeking the final solution the boundary conditions must be satisfied and hence this would require some iterative method for the exact solution.

The second approach could be to formulate energy function in terms of the unknown nodal voltage. This energy function is subjected to certain constraints in terms of boundary conditions. The objective then is to min. $[W]$ subject to certain constraints. For this various mathematical programming techniques like, Fletcher Powell technique, Fletcher technique, direct search techniques, self scaling variable metric techniques can be used. A computer program can be developed and accuracy of the result can be obtained depending upon the convergence critsion fed into the computer. A suitable initial guess for the solution can always be made depending upon the system configuration and during every iteration the voltage can be updated till all the boundary conditions are satisfied and the energy

function is minimised that is when the change in the energy function between two consecutive iterations is less than a prespecified value.

The finite element method is useful for estimating electric fields at highly curved and thin electrode surfaces with composite dielectric materials especially when the electric fields are uniform or weakly non-uniform and can be expressed in two dimensioned geometrics. The method is normally not recommended for three dimensional non-uniform fields.

0.4 CHARGE SIMULATION METHOD

As suggested by the name itself, in this method, the distributed charges on the surface of a conductor/electrode or dielectric interfaces is simulated by replacing these charges by n discrete fictitious individual charges arranged suitably inside the conductor or outside the space in which the field is to be computed. These charges could be in the form of point, line or ring, depending upon the shape of the electrode under consideration. It could be a suitable combination of these fictitious charges. The position and type of simulation charges are to be determined first and then the field on the electrode surface is determined by the potential function of these individual charges. In order to determine the magnitude of these charges n no. of points are chosen on the surface of the conductor. These points are known as "contour points''. The sum of the potentials due to fictitious charge distribution at any contour points should correspond to the conductor potential V_c which is known a priori.

Suppose q_i, is one of the fictitious charges and V_i is the potential of any point P_i in space which is independent of the coordinate system chosen, the total potential V_i due to all the charges is given as

$$V_i = \sum_{j=1}^{n} p_{ij} q_j \qquad ...(26)$$

where p_{ij} are known as ''potential Co-efficient'' which are to be determined for different types of charges by using Laplace's equation. We know that potential at a point P at a distance 'a' from a point charge q is given as

$$V = \frac{q}{4\pi \in a} \qquad ...(27)$$

So here the potential co-efficient p is $\dfrac{1}{4\pi \in a}$

Similarly, these co-efficients for linear and ring or circular charges can also be obtained. It is found these are also dependent upon various distance of these charges from the point under consideration where potential is to be obtained and the permittivity of the medium as in case of a point charge and hence potential co-efficients are constant number and hence the potential due to various types of charges are a linear function of charges and this is how we get the potential at a point due to various charges as an algebraic sum of potential due to individual charges.

A few contour points must also be taken at the electrode boundaries also and the potential due to the simulated charge system should be obtained at these points and this should correspond to the equipotentials or else, the type and location of charges should be changed to acquire the desired shape and the given potential. Suppose we take 'n' number of contour points and n no. of charges, the following set of equations can be written

$$\begin{bmatrix} p_{11} & p_{12} & \cdots & p_{1n} \\ p_{21} & p_{22} & \cdots & p_{2n} \\ \vdots & & & \\ p_{n1} & p_{n2} & \cdots & p_{nn} \end{bmatrix} \begin{bmatrix} q_1 \\ q_2 \\ \vdots \\ q_n \end{bmatrix} = \begin{bmatrix} V_1 \\ V_2 \\ \vdots \\ V_n \end{bmatrix} \quad ...(28)$$

The solution of these equations gives the magnitude of the individual charges and which corresponds to electrode potential (V_1 ..... V_n) at the given discrete points. Next, it is necessary to check whether the type and location of charges as obtained from the solution of equation (28) satisfies the actual boundary conditions every where on the electrode surfaces. It is just possible that at certain check points the charges may not satisfy the potential at those points. This check for individual point is carried out using equation (26). If simulation does not meet the accuracy criterion, the procedure is repeated by changing either the number or type or location or all, of the simulation charges till adequate charge system (simulation) is obtained. Once, this is achieved, potential or electric field intensity at any point can be obtained.

The field intensity at a point due to various charges is obtained by vector addition of intensity due to individual charges at that point. However, it is desirable to obtain the individual directional components of field intensity separately. In cartesion coordinate system, the component of electric field intensity along *x*-direction for *n* number of charges is given as

$$\overline{E}_x = \sum_{j=1}^{n} \frac{\partial p_{ij}}{\partial x} q_j = \sum_{j=1}^{n} (f_{ij})_x \, q_j \quad ...(29)$$

where $(f_{ij})_x$ are known as field intensity co-efficients in *x*-direction.

In this method it is very important to select a suitable type of simulation charges and their location for faster convergence of the solution *e.g.* for cylindrical electrodes finite line charges are suitable, spherical electrodes have point charges or ring charges as suitable charges. However, for fields with axial symmetry having projected circular structures, ring charges are found better. Experience of working on such problems certainly will play an important role for better and faster selection. The procedure for CSM is summarised as follows :

1. Choose a suitable type and location of simulation charges within the electride system.
2. Select some contour point on the surface of the electrodes. A relatively larger no. of contour points should be selected on the curved or corner points of the electrode.
3. Calculate the p_{ij} for different charges and locations (contour points) and assemble in the form of a matrix.
4. Obtain inverse of this matrix and calculate the magnitude of charges (simulation).
5. Test whether the solution so obtained is feasible or not by selecting some check points on the conductor surface. If the solution is feasible stop and calculate the electric field intensity at requisite point. If not, repeat the procedure by either changing the type or location of the simulation charges.

CSM has proved quite useful for estimation of electric field intensity for two and three dimensional fields both with or without axial symmetry. It is a simple method and is found computationally efficient and provides accurate results.

The simplicity with which CSM takes care of curved and rounded surfaces of electrodes or interfaces of composite dielectric medium makes it a suitable method for field estimation. The computation time is much less as compared to FDM and FEM.

However, it is difficult to apply this methods for thin electrodes *e.g.* foils, plates or coatings as some minimum gap distance between the location of a charge and electrode contours is required. Also, it is found difficult to apply this method for electrodes with highly irregular and complicated boundaries with sharp edges etc.

However, as mentioned earlier a good experience of selecting type and location of simulation charge may solve some of these problem.

An improved version of CSM known as surface charge simulation method (SCSM) described below is used to overcome the problem faced in CSM.

0.5 SURFACE CHARGE SIMULATION METHOD

Here a suitably distributed surface charge is used to simulate the complete equipotential surface *i.e.* the electrode contour since the surface charge is located on the contour surface itself. In actual practice the existing surface charge on the electrode configuration is simulated by integration of ring charges placed on the electrode contour and dielectric boundaries. This results into a physically correct reproduction of the whole electrode configuration.

The electrode contours are segmented as shown in Fig. 0.3 and to each segment '*S*' a surface charge density is assigned by a given function $S_k(x)$ which could be a first degree approximation or a polynomial as follows

$$\sigma(x) = \sum_{k=0}^{n} S_k(x).\sigma_k \qquad ...(29)$$

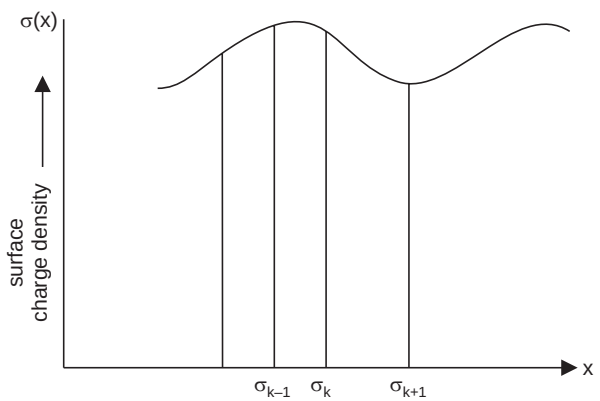

Fig. 0.3. Segmented Contour path with assigned σ

The individual segments along the contour path can be represented as shown in Fig. 0.4.

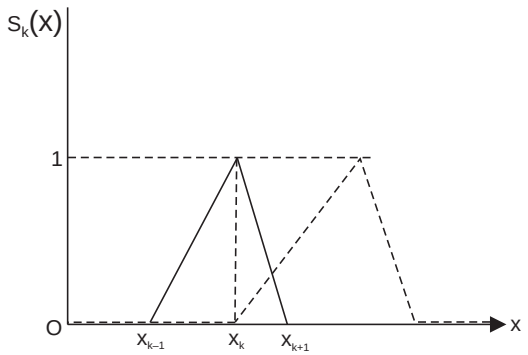

Fig. 0.4. Representation of a segment $S_k(x)$

The value of $S_k(x)$ is zero for $x < x_{k-1}$ and is unity at $x = x_k$ and in between x_{k-1} and x_k is given as $\frac{x - x_{k-1}}{x_k - x_{k-1}}$.

With the representation the contour sarface is reproduced accurately and exactly and thus the continuity of charge between the segments is assumed. Surface charges can be simulated either by line or ring charges. Ring charge simulation is found to be more useful for fields with symmetry of rotation. Each contour segment is assigned m no. of charges and the potential due to a charge q_j, is given by equation (26) and is rewritten here

$$V_i = \sum_{j=1}^{m} p_i q_j$$

The potential co-efficient p_{ik} for a contour point i due to kth contour segment is obtained as shown in Fig. 05.

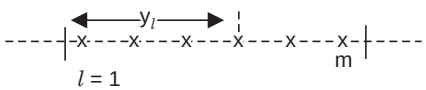

Fig. 0.5. Concentrated charges to simulate surface charges

and is give as

$$p_{ik}\,\sigma_k = \int_x \sigma(x)\,.\,p_{ix}\,dx \qquad ...(30)$$

Now substituting equation (29) in equation (30) we have

$$p_{ik}\sigma_k = \int_x \sum_{k=0}^{n} S_k(x)\,.\,\sigma_k\,p_{ix}\,dx \qquad ...(31)$$

Since each segment is divided into m intervals as shown in Fig. 0.5, equation (31) can be rewritten as

$$p_{ik}\sigma_k = \int_{x_{k-1}}^{xk} s_k(x)\,p_{ix}\,dx = \sum_{l=1}^{m} s_k(y_l)\,p_{il}\sigma_k \qquad ...(32)$$

The potential coefficient p_{il} are similar to the coefficients derived from a single concentrated charge in CSM. This coefficient, therefore, can be obtained for a line charge or by solving elliptical integral for a ring charge. The electric field intensity at any contour point i due to kth contour segment is given as

$$E_i = \sum_{x=1}^{m} \sigma_k \; f_{ik} \qquad ...(33)$$

where f_{ik} are the field intensity co-efficients.

As discussed this method requires a large number of elements, normally more than 2500, independent of the surface shape and thus require large computational efforts. Also, due to certain practical difficulties this method is not used as frequently as other numerical methods for estimation of electric fields.

0.6 COMPARISON OF VARIOUS TECHNIQUES

Out of the various techniques FDM is the simplest to compute and understand but the computation effort and computer memory requirements are the highest. Also, since all difference equations are approximation to the actual field conditions, the final solution may have considerable error.

Finite element method is a general method and has been used for almost all fields of engineering. The method is suitable for estimating fields at highly curved and thin electrode surfaces with different dielectric materials. However, this method is more useful for uniform or weakly non-uniform fields and which can be represented by two dimensional geometries. This method is recommended for three dimensional complicated field configurations.

Charge Simulation Method (CSM) is considered to be one of the most superior and acceptable method for two and three dimensional configuration with more than one dielectric and with electrode systems of any desired shape since this method is based on minimization of the energy function which could be subjected to any operating constraints *e.g.* environmental condition, it has proved to be highly accurate method. Because of inherent features of the technique, this method also helps in optimising electrode configuration. In this electrode configuration optimisation problems the objective is to have field intensity as low as possible subject to the condition that a constant field intensity exists on the complete electrode surface. With this optimisation, a higher life expectancy of high voltage equipments can be achieved.

However, as mentioned earlier this method can not be used for thin electrodes *e.g.* foils, plates or coatings due to the requirement of a minimum gap distance between the location of a charge and electrode contour. Also, this method is not suitable for highly irregular electrode boundaries.

The surface charge simulation method even though takes into account the actual surface charge distribution on the electrode surface, this method is not normally recommended for solution of field problem due to some practical difficulties.

An important difference between the various method is that the FDM and FEM can be used only for bounded field whereas CSM and SCMS can also be used for unbounded fields.

0.7 ELECTROLYTIC TANK

For assessing electric field distribution in complex three dimensional situations, analytical methods are unsuitable. Two other approaches in use are, experimental analog and numbrical techniques. The numerical techniques have already been discussed in the previous section. We now study analog techniques especially the use of electrolytic tank.

The potential distribution in conductive media in current equilibrium condition satisfies Laplace's equation the same as the electric fields in space-charge-free regions *i.e.* $\rho_v = 0$. This fact makes it possible to obtain solutions to many difficult electrostatic field problems by constructing an analyogous potential distribution in a conductive medium where the potential and field distributions can be measured directly. The conductors and insulation arrangements can be represented using an electrolytic tank. Due to its simplicity and accuracy this method has been used for decades.

A scale model of the electrode configuration is set up in a tank with insulating walls, filled with suitable electrolyte *e.g.* tap water. An alternating voltage is the appropriate choice of working voltage to avoid polarisation voltage arising in the case of direct voltages. The equipotential lines or equipotential areas in the case of the electric field are measured by means of a probe which can be fed with different voltages from a potential divider *via* a null indicator.

Guiding the probe along the lines corresponding to the potential selected on the divider as well as their graphical representation, can be undertaken manually or automatically in large systems. For the two-dimensional field model, various dielectric constants can be simulated by different heights of electrolyte as shown in Fig. 0.5 for a cylinder-plane configuration.

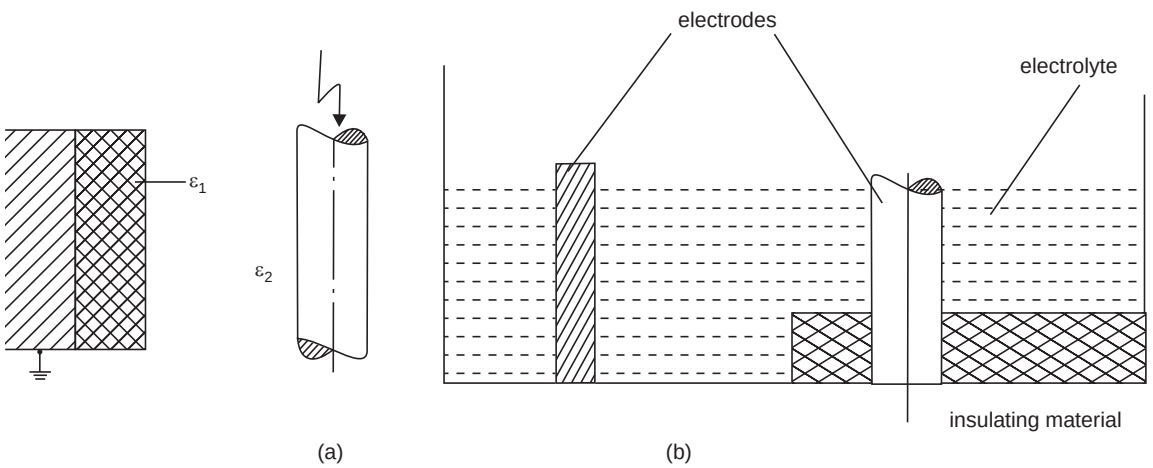

Fig. 0.5. Simulation of a cylinder-plane configuration in the electrolytic tank
(a) Original (b) Simulation for the case $\varepsilon_1 = 2\varepsilon_2$

Three dimensional fields with rotational symmetry can be readily simulated in a wedge shaped tank where as for fields with no rotational symmetry one has to resort to much more complex forms of three dimensional simulation.

Equipotential boundaries are represented in the tank by specially formed sheets of metal. For example a single dielectric problem such as a three core cable may be represented using a flat tank as shown in Fig. 0.6. Different permittivities are represented by electrolytes of different conductivities separated by special partitions. Otherwise, the tank base can be specially shaped.

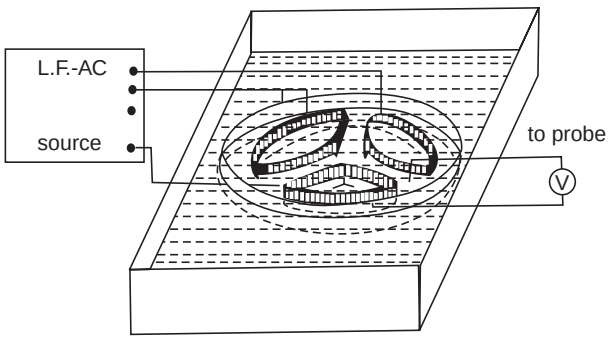

Fig. 0.6. Electrolytic tank model of a three-core cable represented at the instant when one core is at zero voltage, the same as the sheath.

0.8 CONTROL OF ELECTRIC FIELD INTENSITY

It is a common knowledge that if the field in a dielectric material is uniform, the material is properly utilised. If it is non-uniform the material is under-utilised. Under normal situation an electric field is not uniform due to imperfection in the dielectric material during manufacture or it could be due to undesirable shapes and sizes of electrodes.

Sudden change in shape of electrodes in the form of corners or edges in high voltage equipments leads to concentration of electric fields at such locations resulting in higher electric stresses on the dielectric. The area around such location becomes highly vulnerable to breakdown of insulation. In order to avoid this breakdown, the electrodes should be suitably designed and shaped so that concentration of the field is not allowed. The electrodes are extended and so shaped that a higher field intensity than the main field does not appear anywhere in the dielectric material. To achieve this objective Rogowaski suggested a shape by which electrodes should be extended known as Rogowaski profile as shown in Fig. 0.7(*b*).

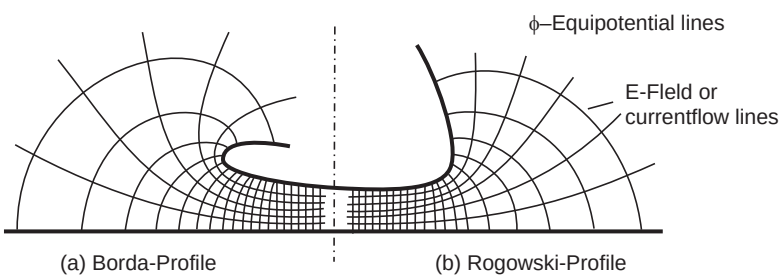

Fig. 0.7 equipotential and the field (current flow) lines between plane and brim field.

It is clear from the Fig. 0.7 that the electric field intensity continuously reduces beyond the edges of the electrodes. Another profile of electrodes suggested by Borda for reducing electric field stresses is shown in Fig. 0.7(*a*) . Comparing the two profiles, it is found that the Borda profile achieves a lower field intensity beyond the edges as compared to Rogowski profile.

Also, it is found that the space requirements for high voltage equipments is smaller with Borda profile electrodes as compared to Rogowski profile. In many situations for high voltage equipment

space requirements become a serious problem and hence electric field optimisation techniques have received a great importance.

A visit to a high voltage laboratory shows that electrodes at high potential are given large, smooth shaped dome like shapes to bring down the electric field stress surrounding the area *i.e.* the atmospheric air. The modern trend is to design segmented electrodes in which a number of small, identical, smooth discs are given a desired continuous shapes as per requirement.

Electric stress control shields of various shapes and sizes are used for high voltage equipments Fig. 0.8. Sometimes sharp electrode ends are enclosed by a large dimeter hemispherical electrode having a smooth aperture.

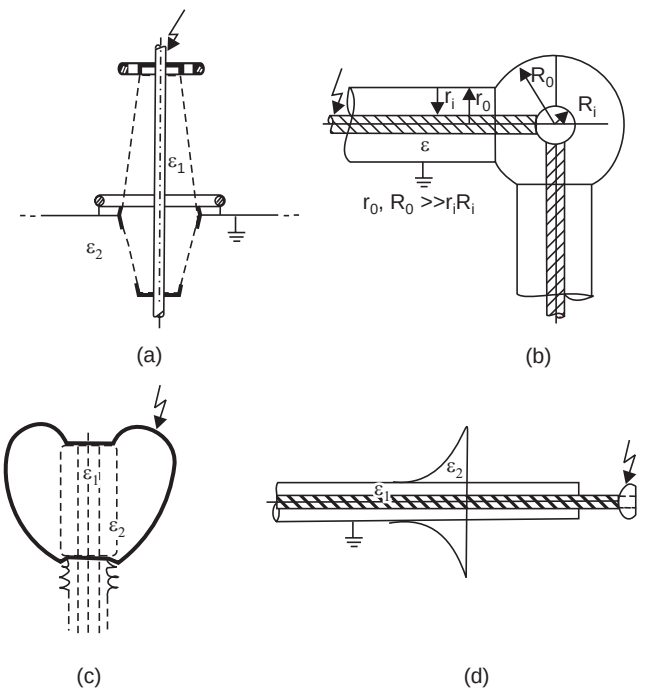

Fig. 0.8. Extended shapes of electrodes for stress control (a) A bushing with toroids (b) Right angle turn of a bus bar in gas insulated switchgear (*GIS*), (c) HV electrode on a condenser, (d) Stress cone on a screened cable end.

Circular and tubular electrodes are provided with spherical shields at bends. In high voltage laboratories tubular electrodes of large diameter are used for connection rather than insulated wire thereby electric field intensity is reduced considerably.

For transmission voltage 400 kV and above we make use of more than one conductor which is known as bundling of conductors or these conductors are known as bundled conductor. This is done to reduce electric field intensity in the atmospheric air thereby the corona loss on the line and radio interference with communication lines is reduced.

The design of high voltage bushing used for large capacity power transformers, potential transformers or cable termination is based on capacitance grading thereby a uniform voltage distribution is achieved which results in a uniform electric field intensity within the dielectric. This is done by

interposing concentric sheets of metals of suitable lengths and position. This is known as "inter-sheath grading" to control electric field intensity. The inter-sheaths are held at suitable potential which enables economic utilisation of the insulating material by evenly distributing the equipotential surfaces.

A simple rule to control electric field intensity in high voltage equipments is to avoid sharp points and edges in the electrodes. These electrodes should be large symmetrical and should have smooth surface. The surface should not be rough as this would lead to higher stresses at high voltages. Micro protrusion on the surface of the electrode may penetrate deeper into the dielectric material which may result in high electric field intensity at those points and may lead to breakdown of the dielectric material.

0.9 OPTIMISATION OF ELECTRODE CONFIGURATION

Various numerical techniques have been used to optimise the electrode configuration so that the dielectric material is optimally utilised as a result a considerable improvement in dielectric behaviour is achieved and a higher life expectancy of high voltage equipments can be anticipated. When we talk of electrode configuration optimisation, we really mean the electric field intensity optimisation. Even though some work has been dedicated for electrode configurations optimisation by FDM and FEM methods, yet the inherent suitability of CSM for optimisation, lot of work has been reported in literature using this technique.

The objective of optimisation is to determine the configuration of electrodes which may result into a minimum and constant field intensity on the complete electrode surface. The optimisation technique is based on the partial discharge inception electric field intensity E_{pd} which depends upon the dielectric material, its pressure (if gas is the medium) and the electrode configuration. It is to be noted that if the electric field is uniform or weakly non-uniform, the partial discharge or normal breakdown takes place at the same electric field intensity. Therefore, it is only the electrode configuration which can be optimised. If E_{pd} is more than the electric field intensity E applied, partial discharge can not take place which means the electrode can be said to be optimised, if at a given voltage the maximum value of $\frac{E}{E_{pd}}$ on its surface is as small as possible. Since the maximum value of E/E_{pd} depends upon three parametres the shape, size and position of electrodes, three different types of optimisation possibilities exist. The optimum shape of an electrode in characterised by

$$\text{Min. } (E/E_{pd})_{\max} = \text{constant} \qquad \text{...(34)}$$

The optimisation methods are based on iterative process and when equation (0.34) is satisfied, the optimum electrode configuration is obtained. While using CSM, following strategies are used for optomisation of electrode configuration.

(*i*) Displacement of contour points perpendicular to the surface

(*ii*) Changing the position of the ''optimisation charges'' and contour points

(*iii*) Modification of contour elements

A brief view of these methods is given below.

0.9.1. Displacement of Contour Points

In this method a constant magnitude of electric field intensity is achieved using an iterative process by differential displacement of contour points perpendicular to the surface during every iteration. We start with a suitable contour of the electrode and on this we fix some contour points, and, electric field intensity is evaluated for this contour. If this field intensity is within the permissible value of desired field intensity we stop as the optimal configuration is obtained right at the first step. However, it is very unlikely to hit at the optimal configuration in the first step itself and hence the curvature of this contour is changed step by step depending upon the difference between the calculated electric field intensity and the desired field intensity. A good experience in field theory will be quite helpful in deciding the new contour points during different iterations. Fig. 0.9 shows the flows chart for the optimisation process.

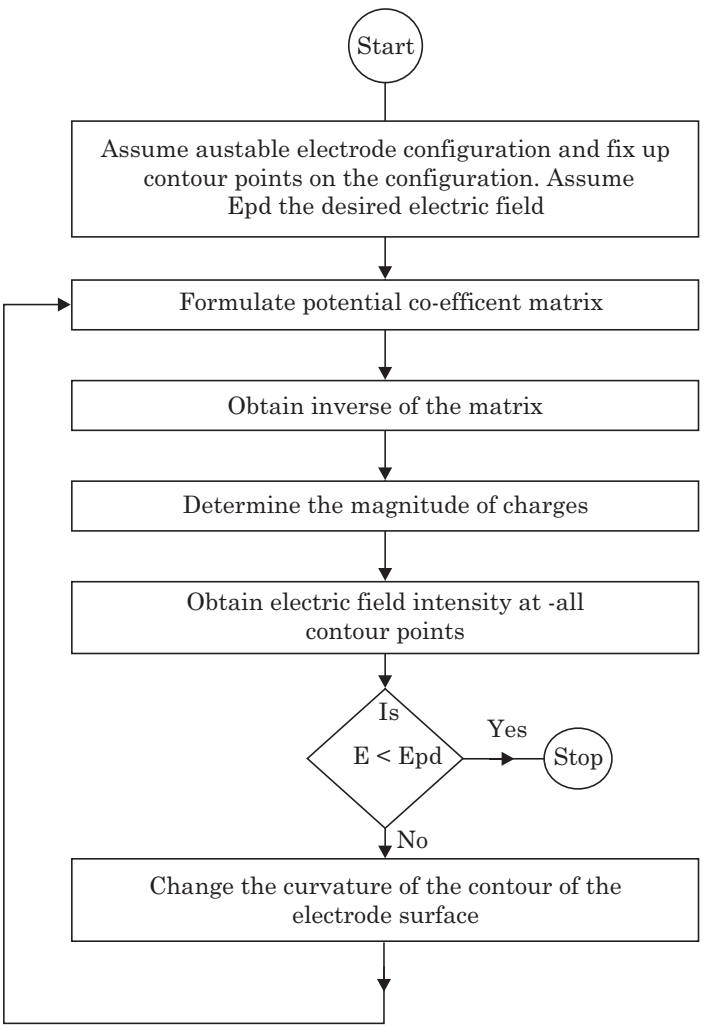

Fig. 0.9. Flow chart for optimisation by displacement of contour points method

It is to be noted that for electric field calculation on the electrode surface (assumed or updated) is caried out using CSM technique. Since during every iteration the complete CSM technique is to be used for calculation of electric field intensity, computer time requirement is high and this is its major disadvantage.

0.9.2. Changing the Position of the Optimisation Charges and Contour Points

In CSM we start with certain configuration of the electrode and we calculate electrode field intensity at various contour points of the electrode and from this we should be able to identity which part of the electrode surface needs optimisation (the contour points where $E > E_{pd}$). Normally in CSM, the identified region of electrode configuration is reproduced by a set of contour points and a set of simulation charges at fixed locations but of unknown magnitudes. However, in optimisation method, the optimisation region is reproduced like in CSM by a suitable '*n*' number of contour optimisation points as shown in Fig. 0.10.

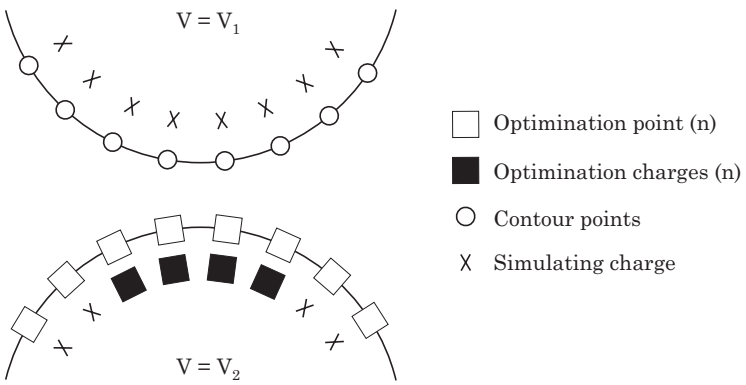

Fig. 0.10. Optimisation region in an electrode configuration

This optimisation region is then provided with '*n*' optimisation charges which have fixed position and known magnitudes. The optimisation charges are obtained corresponding to a partial solution of mathematical problem.

The optimisation procedure proceeds with iterative steps as follows :

(*i*) The optimisation charges which affect the field intensity in optimisation region more than the simulation charges are shifted in position such that the field intensity in the optimisation region is less than a prespecificd value.

(*ii*) When we shift the optimisation charges the potential at the contour points in the region is changed. In order to bring the known potential (new) at the contour points, the magnitude of the simulation charges should be changed to fulfil the new potential requirement at the contour points.

(*iii*) The new equipotential line having the known potential is calculated with the help of a complete new set of optimisation charges. This will be our new optimised contour of the electrode.

(*iv*) The field intensity in the optimisation region is calculated and compared it with a prespecified value of *E* and this may not satisfy equation (34) or even after changing the shape of the electrode and the charge magnitudes in the other region.

(*v*) The optimisation points are now located at the newly obtained contour of the electrode. The location of the respective optimisation charges should, therefore, be suitably corrected to start the next iteration.

The iteration procedure is continued with lower magnitude of electric field intensity till it converges to a prespecified value or instruct to stop the computation process if it goes to a very low value which is physically not feasible.

0.9.3. Modification of Contour Elements

This method is based on the qualitative correlation between the curvature of an electrode surface and its electric field intensity. The larger yer the curvature the larger is the value E/E_{pd}. Therefore, the radii of the contour element will have to be increased for the region where E/E_{pd} is large and decreased where E/E_{pd} is small. The optimisation method is explained here for a cylindrical rod and plane electrode configuration. It is required to optimise the contour of the rod end. Suppose r is the radius of the rod end and 'd' is its distance from the plane as shown as Fig. 0.11(*a*). As an initial approximation, the rod end is assumed to be hemispherical. Since the rod end is symmetrical about the vertical axis, the corresponding semicircle is divided into segments Fig. 0.11(*b*). Depending upon the accuracy requirements of the final result a suitable number of segments are selected. The circular arcs on the periphery are called the 'contour segment'. The procedure is explained as follows :

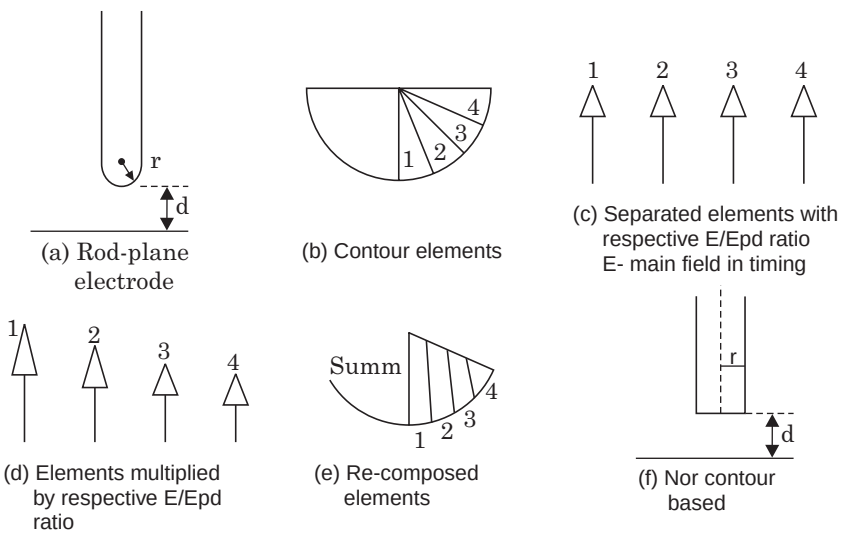

Fig. 0.11. Optimisation by contour elements

(*i*) At the outset, mean electric field intensity E on each contour element is calculated using any of the numerical techniques mentioned in article 0.8. Contour elements are shown separately with their corresponding magnitudes of E/E_{pd} ratio in Fig. 0.11(*c*).

(*ii*) The radius of each element which is same in this case as all elements lie along the arc of a circle is multiplied by their respective $(E/E_{pd})^n$ whereas the angles of the elements and therefore, the shapes remain unchanged. The exponent which represents no. of iterations required to converge, is recommended to be four. As a result of multiplication a new set of elements of different sizes is obtained Fig. 0.11(*d*). The new set of elements are recomposed as shown in Fig 0.11(*e*) thereby a new contour is obtained. The radius of the new contour is made equal to r by multiplying the radius of the new contour by a suitable scale factor.

(*iii*) The new contour is placed at the distance '*d*' from the plane as shown in Fig. 0.11(*f*). The steps (*i*) and (*ii*) are repeated until the remaining differences in E/E_{pd} ratio are sufficiently small. As seen in Fig. 0.11(*e*) during each iteration the surface region is flattened where E/E_{pd} exceeds its mean value whereas the remaining region becomes more curved which results into a more uniform distribution of E/E_{pd} . It is to be noted that in step (*ii*) if the E_{pd} depends upon the curvature of the electrode surface, then instead of the element radii, the reciprocal of the curvature is multiplied by $(E/E_{pd})^n$. It is to be noted with caution that the boundary conditions in terms of operating constraints if any must be included during the process of optimisation of electrode configuration otherwise it may turn out to an infeasible solution.

For further details a few references are given at the end of the chapter.

QUESTIONS

0.1. ''The potential at a point plays an important role in obtaining any information regarding the electrostatic field'' Justify the statement.

0.2. Starting with Laplace's equation in two dimension explain the Finite Differentce method for Evaluation of field distribution. Discuss its advantages and disadvantages.

0.3. What is Finite Element Method for evaluation of field distribution. Discuss the procedure associated with this method and discuss its advantages and limitations.

0.4. What is a global stiffness matrix when referred to Finite Element Method used for evaluation of electric field ?

0.5. Discuss the basic philosophy associated with charge simulation method for evaluation of electric field distribution.

0.6. Obtain expressions for potential coefficients *p* for a (*i*) point charge (*ii*) line charge (*iii*) ring charge distribution.

0.7. What are field intensity co-efficients when referred to charge simulation method.

0.8. Explain briefly in a few steps the procedure associated with charge simulation method. Discuss its advantages and limitations.

0.9. Explain briefly an improved version of charge simulation method and discuss its advantages and limitations.

0.10. Compare in brief various numerical techniques to study or evaluate the electric field distribution in dielectric medium.

0.11. Explain with neat diagrams the application of an Electrolytic tank for evaluating electric field distribution in dielectric medium or electrical equipments.

0.12. Explain with neat diagrams the procedure to control electric field intensity in high voltage equipments.

0.13. Explain clearly what you mean by optimisation of Electrode configuration. Mention various techniques used for the purpose.

0.14. Discuss briefly the optimisation techniques listed here :

(*i*) Displacement of contour points with flow chart.

(*ii*) Changing the location of optimisation charges and contour points.

(*iii*) Modification of contour elements.

REFERENCES

1. Alston High Voltage Technology Oxford University Press 1968.
2. E. Kuffel and W.S. Zaengl, High Voltage Engineering-Fundamentals, Pergamon Press, 1984.
3. Arora R. & Wolfgang Mosch, High Voltage Insulation Engg., New Age International.
4. Reister M. Weib P. "Computation of Electric fields by use of surface charge simulation method" Int. Symp on HV Engg. Athens (1983) Report 11.06.
5. Welly J. D. "Optimisation of electrode contours in high voltage equipment using circular contour elements" Int. Symp on HV Engg. Braunschweig (1987).
6. Singer H., computation of optimised electrode geometries Int. Symp. on HV Engg. Milano (1979) Report 11.06.

1 Breakdown Mechanism of Gaseous, Liquid and Solid Materials

1.0 INTRODUCTION

With ever increasing demand of electrical energy, the power system is growing both in size and complexities. The generating capacities of power plants and transmission voltage are on the increase because of their inherent advantages. If the transmission voltage is doubled, the power transfer capability of the system becomes four times and the line losses are also relatively reduced. As a result, it becomes a stronger and economical system. In India, we already have 400 kV lines in operation and 800 kV lines are being planned. In big cities, the conventional transmission voltages (110 kV–220 kV etc.) are being used as distribution voltages because of increased demand. A system (transmission, switchgear, etc.) designed for 400 kV and above using conventional insulating materials is both bulky and expensive and, therefore, newer and newer insulating materials are being investigated to bring down both the cost and space requirements. The electrically live conductors are supported on insulating materials and sufficient air clearances are provided to avoid flashover or short circuits between the live parts of the system and the grounded structures. Sometimes, a live conductor is to be immersed in an insulating liquid to bring down the size of the container and at the same time provide sufficient insulation between the live conductor and the grounded container. In electrical engineering all the three media, viz. the gas, the liquid and the solid are being used and, therefore, we study here the mechanism of breakdown of these media.

1.1 MECHANISM OF BREAKDOWN OF GASES

At normal temperature and pressure, the gases are excellent insulators. The current conduction is of the order of 10^{-10} A/cm^2. This current conduction results from the ionisation of air by the cosmic radiation and the radioactive substances present in the atmosphere and the earth. At higher fields, charged particles may gain sufficient energy between collision to cause ionisation on impact with neutral molecules. It is known that during an elastic collision, an electron loses little energy and rapidly builds up its kinetic energy which is supplied by an external electric field. On the other hand, during elastic collision, a large part of the kinetic energy is transformed into potential energy by ionising the molecule struck by the electron. Ionisation by electron impact under strong electric field is the most important process leading to breakdown of gases.

This ionisation by radiation or photons involves the interaction of radiation with matter. Photoionisation occurs when the amount of radiation energy absorbed by an atom or molecule exceeds its ionisation energy and is represented as $A + h\nu \rightarrow A^+ + e$ where A represents a neutral atom or

molecule in the gas and $h\nu$ the photon energy. Photoionization is a secondary ionization process and is essential in the streamer breakdown mechanism and in some corona discharges. If the photon energy is less than the ionization energy, it may still be absorbed thus raising the atom to a higher energy level. This is known as *photoexcitation.*

The life time of certain elements in some of the excited electronic states extends to seconds. These are known as metastable states and these atoms are known as *metastables*. Metastables have a relatively high potential energy and are, therefore, able to ionize neutral particles. Let A be the atom to be ionized and B^m the metastable, when B^m collides with A, ionization may take place according to the reaction.

$$A + B^m \longrightarrow A^+ + B + e$$

Ionization by metastable interactions comes into operation long after excitation and it has been shown that these reactions are responsible for long-time lags observed in some gases.

Thermal Ionisation: The term thermal ionisation in general applies to the ionizing actions of molecular collisions, radiation and electron collisions occurring in gases at high temperatures. When a gas is heated to high temperature, some of the gas molecules acquire high kinetic energy and these particles after collision with neutral particles ionize them and release electrons. These electrons and other high-velocity molecules in turn collide with other particles and release more electrons. Thus, the gas gets ionized. In this process, some of the electrons may recombine with positive ions resulting into neutral molecule. Therefore, a situation is reached when under thermodynamic equilibrium condition the rate of new ion formation must be equal to the rate of recombination. Using this assumption, Saha derived an expression for the degree of ionization β in terms of the gas pressure and absolute temperature as follows:

$$\frac{\beta^2}{1-\beta^2} = \frac{1}{p}\frac{(2\pi m_e)^{3/2}}{h}(KT)^{5/2}\, e^{-W/KT}$$

or

$$\frac{\beta^2}{1-\beta^2} = \frac{2.4\times 10^{-4}}{p} T^{5/2}\, e^{-W_i/KT}$$

where p is the pressure in Torr, W_i the ionization energy of the gas, K the Boltzmann's constant, β the ratio n_i/n and n_i the number of ionized particles of total n particles. Since β depends upon the temperature it is clear that the degree of ionization is negligible at room temperature. Also, if we substitute the values of p, W_i, K and T, it can be shown that thermal ionization of gas becomes significant only if temperature exceeds 1000° K.

1.2 TOWNSEND'S FIRST IONIZATION COEFFICIENT

Consider a parallel plate capacitor having gas as an insulating medium and separated by a distance d as shown in Fig. 1.1. When no electric field is set up between the plates, a state of equilibrium exists between the state of electron and positive ion generation due to the decay processes. This state of equilibrium will be disturbed moment a high electric field is applied. The variation of current as a function of voltage

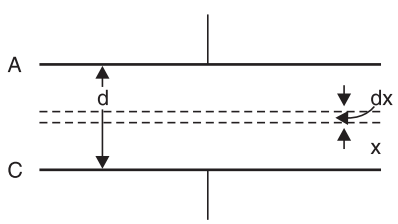

Fig. 1.1 Parallel plate capacitor

was studied by Townsend. He found that the current at first increased proportionally as the voltage is increased and then remains constant, at I_0 which corresponds to the saturation current. At still higher voltages, the current increases exponentially. The variation of current as a function of voltage is shown in Fig. 1.2. The exponential increase in current is due to ionization of gas by electron collision. As the voltage increases *V/d* increases and hence the electrons are accelerated more and more and between collisions these acquire higher kinetic energy and, therefore, knock out more and more electrons.

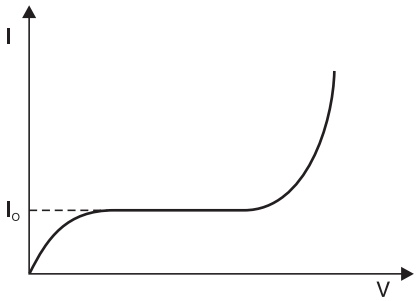

Fig. 1.2 Variation of current as a function of voltage

To explain the exponential rise in current, Townsend introduced a coefficient α known as *Townsend's first ionization coefficient* and is defined as the number of electrons produced by an electron per unit length of path in the direction of field. Let n_0 be the number of electons leaving the cathode and when these have moved through a distance *x* from the cathode, these become *n*. Now when these *n* electrons move through a distance *dx* produce additional *dn* electrons due to collision. Therefore,

$$dn = \alpha\, n\, dx$$

or
$$\frac{dn}{n} = \alpha\, dx$$

or
$$\ln n = \alpha x + A$$

Now at $x = 0$, $n = n_0$. Therefore,

$$\ln n_0 = A$$

or
$$\ln n = \alpha x + \ln n_0$$

or
$$\ln \frac{n}{n_0} = \alpha x$$

At $x = d$, $n = n_0\, e^{\alpha d}$. Therefore, in terms of current

$$I = I_0\, e^{\alpha d}$$

The term $e^{\alpha d}$ is called the *electron avalanche* and it represents the number of electrons produced by one electron in travelling from cathode to anode.

1.3 CATHODE PROCESSES—SECONDARY EFFECTS

Cathode plays an important role in gas discharges by supplying electrons for the initiation, sustainance and completion of a discharge. In a metal, under normal condition, electrons are not allowed to leave the surface as they are tied together due to the electrostatic force between the electrons and the ions in the lattice. The energy required to knock out an electron from a Fermi level is konwn as the *work function* and is a characteristic of a given material. There are various ways in which this energy can be supplied to release the electron.

Thermionic Emission: At room temperature, the conduction electrons of the metal do not have sufficient thermal energy to leave the surface. However, if the metals are heated to temperature 1500°K and above, the electrons will receive energy from the violent thermal lattice in vibration sufficient to cross the surface barrier and leave the metal. After extensive investigation of electron emission from metals at high temperature, Richardson developed an expression for the saturation current density J_s as

$$J_s = \frac{4\pi m_e K^2}{h^3} T^2 e^{-W\alpha/KT} \ A/m^2$$

where the various terms have their usual significance.

Let $$A = \frac{4\pi m_e K^2}{h^3}$$

the above expression becomes

$$J_s = AT^2 e^{-W/KT}$$

which shows that the saturation current density increases with decrease in work function and increase in temperature. Substituting the values of m_e, K and h, A is found to be $120 \times 10^4 \ A/m^2 K^2$. However, the experimentally obtained value of A is lower than what is predicted by the equation above. The discrepancy is due to the surface imperfections and surface impurities of the metal. The gas present between the electrode affects the thermionic emission as the gas may be absorbed by the metal and can also damage the electrode surface due to continuous impinging of ions. Also, the work function is observed to be lowered due to thermal expansion of crystal structure. Normally metals with low work function are used as cathode for thermionic emission.

Field Emission: If a strong electric field is applied between the electrodes, the effective work function of the cathode decreases and is given by

$$W' = W - \varepsilon^{3/2} E^{1/2}$$

and the saturation current density is then given by

$$J_s = AT^2 e^{-W'/KT}$$

This is known as *Schottky effect* and holds good over a wide range of temperature and electric fields. Calculations have shown that at room temperature the total emission is still low even when fields of the order of 10^5 V/cm are applied. However, if the field is of the order of 10^7 V/cm, the emission current has been observed to be much larger than the calculated thermionic value. This can be explained only through quantum mechanics at these high surface gradients, the cathode surface barrier becomes very thin and quantum tunnelling of electrons occurs which leads to field emission even at room temperature.

Electron Emission by Positive Ion and Excited Atom Bombardment

Electrons may be emitted by the bombardment of positive ion on the cathode surface. This is known as *secondary emission*. In order to effect secondary emission, the positive ion must have energy more than twice the work function of the metal since one electron will neutralize the bombarding positive ion and the other electron will be released. If W_k and W_p are the kinetic and potential energies, respectively of the positive ion then for secondary emission to take place $W_k + W_p \geq 2W$. The electron emission by positive ion is the principal secondary process in the Townsend spark discharge mechanism. Neutral

excited atoms or molecules (metastables) incident upon the cathode surface are also capable of releasing electron from the surface.

1.4 TOWNSEND SECOND IONISATION COEFFICIENT

From the equation

$$I = I_0 e^{\alpha x}$$

We have, taking log on both the sides.

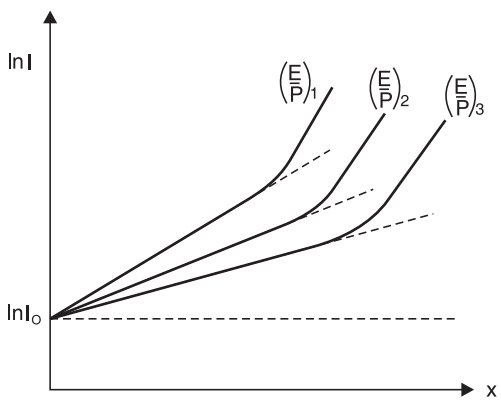

Fig. 1.3 Variation of gap current with electrode spacing in uniform E

$$\ln I = \ln I_0 + \alpha x$$

This is a straight line equation with slope α and intercept $\ln I_0$ as shown in Fig. 1.3 if for a given pressure p, E is kept constant.

Townsend in his earlier investigations had observed that the current in parallel plate gap increased more rapidly with increase in voltage as compared to the one given by the above equation. To explain this departure from linearity, Townsend suggested that a second mechanism must be affecting the current. He postulated that the additional current must be due to the presence of positive ions and the photons. The positive ions will liberate electrons by collision with gas molecules and by bombardment against the cathode. Similarly, the photons will also release electrons after collision with gas molecules and from the cathode after photon impact.

Let us consider the phenomenon of self-sustained discharge where the electrons are released from the cathode by positive ion bombardment.

Let n_0 be the number of electrons released from the cathode by ultraviolet radiation, n_+ the number of electrons released from the cathode due to positive ion bombardment and n the number of electrons reaching the anode. Let ν, known as *Townsend second ionization co-efficient* be defined as the number of electrons released from cathode per incident positive ion, Then

$$n = (n_0 + n_+)e^{\alpha d}$$

Now total number of electrons released from the cathode is $(n_0 + n_+)$ and those reaching the anode are n, therefore, the number of electrons released from the gas = $n - (n_0 + n_+)$, and corresponding to each electron released from the gas there will be one positive ion and assuming each positive ion releases ν effective electrons from the cathode then

$$n_+ = \nu\,[n - (n_0 + n_+)]$$

or $$n_+ = \nu n - \nu n_0 - \nu n_+$$

or $$(1 + \nu)\, n_+ = \nu(n - n_0)$$

or $$n_+ = \frac{\nu(n - n_0)}{1 + \nu}$$

Substituting n_+ in the previous expression for n, we have

$$n = \left[n_0 + \frac{\nu(n - n_0)}{1 + \nu} \right] e^{\alpha d} = \frac{(1 + \nu)\, n_0 + \nu n - \nu n_0}{1 + \nu}\, e^{\alpha d}$$

$$= \frac{n_0 + \nu n}{1 + \nu}\, e^{\alpha d}$$

or $$(n + \nu n) = n_0\, e^{\alpha d} + \nu n e^{\alpha d}$$

or $$n + \nu n - \nu n e^{\alpha d} = n_0 e^{\alpha d}$$

or $$n[1 + \nu - \nu e^{\alpha d}] = n_0 e^{\alpha d}$$

or $$n = \frac{n_0 e^{\alpha d}}{1 + \nu n(1 - e^{\alpha d})} = \frac{n_0 e^{\alpha d}}{1 - \nu\,(e^{\alpha d} - 1)}$$

In terms of current

$$I = \frac{I_0\, e^{\alpha d}}{1 - \nu(e^{\alpha d} - 1)}$$

Earlier Townsend derived an expression for current as

$$I = I_0 \frac{(\alpha - \beta)\, e^{(\alpha - \beta)d}}{\alpha - \beta\, e^{(\alpha - \beta)d}}$$

where β represents the number of ion pairs produced by positive ion travelling 1 cm path in the direction of field. Townsend's original suggestion that the positive ion after collision with gas molecule releases electron does not hold good as ions rapidly lose energy in elastic collision and ordinarily are unable to gain sufficient energy from the electric field to cause ionization on collision with gas molecules or atoms.

In practice positive ions, photons and metastable, all the three may participate in the process of ionization. It depends upon the experimental conditions. There may be more than one mechanism producing secondary ionization in the discharge gap and, therefore, it is customary to express the net secondary ionization effect by a single coefficient ν and represent the current by the above equation keeping in mind that ν may represent one or more of the several possible mechanism.

$$\nu = \nu_1 + \nu_2 + \nu_3 + ...$$

It is to be noted that the value of ν depends upon the work function of the material. If the work function of the cathode surface is low, under the same experimental conditions will produce more emission. Also, the value of ν is relatively small at low value of E/p and will increase with increase in E/p. This is because at higher values of E/p, there will be more number of positive ions and photons of sufficiently large energy to cause ionization upon impact on the cathode surface. It is to be noted that the influence of ν on breakdown mechanism is restricted to Townsend breakdown mechanism *i.e.*, to low-pressure breakdown only.

1.5 TOWNSEND BREAKDOWN MECHANISM

When voltage between the anode and cathode is increased, the current at the anode is given by

$$I = \frac{I_0 e^{\alpha d}}{1 - \nu (e^{\alpha d} - 1)}$$

The current becomes infinite if

$$1 - \nu(e^{\alpha d} - 1) = 0$$

or $$\nu(e^{\alpha d} - 1) = 1$$

or $$\nu e^{\alpha d} \approx 1$$

Since normally $$e^{\alpha d} >> 1$$

the current in the anode equals the current in the external cirrcuit. Theoretically the current becomes infinitely large under the above mentioned condition but practically it is limited by the resistance of the external circuit and partially by the voltage drop in the arc. The condition $\nu e^{\alpha d} = 1$ defines the condition for beginning of spark and is known as the *Townsend criterion* for spark formation or Townsend breakdown criterion. Using the above equations, the following three conditions are possible.

(1) $\nu e^{\alpha d} = 1$

The number of ion pairs produced in the gap by the passage of arc electron avalanche is sufficiently large and the resulting positive ions on bombarding the cathode are able to relase one secondary electron and so cause a repetition of the avalanche process. The discharge is then said to be self-sustained as the discharge will sustain itself even if the source producing I_0 is removed. Therefore, the condition $\nu e^{\alpha d} = 1$ defines the threshold sparking condition.

(2) $\nu e^{\alpha d} > 1$

Here ionization produced by successive avalanche is cumulative. The spark discharge grows more rapidly the more $\nu e^{\alpha d}$ exceeds unity.

(3) $\nu e^{\alpha d} < 1$

Here the current I is not self-sustained *i.e.*, on removal of the source the current I_0 ceases to flow.

1.6 STREAMER OR KANAL MECHANISM OF SPARK

We know that the charges in between the electrodes separated by a distance d increase by a factor $e^{\alpha d}$ when field between electrodes is uniform. This is valid only if we assume that the field $E_0 = V/d$ is not affected by the space charges of electrons and positive ions. Raether has observed that if the charge concentration is higher than 10^6 but lower than 10^8 the growth of an avalanche is weakened *i.e.*, $dn/dx < e^{\alpha d}$. Whenever the concentration exceeds 10^8, the avalanche current is followed by steep rise in current and breakdown of the gap takes place. The weakening of the avalanche at lower concentration and rapid growth of avalanche at higher concentration have been attributed to the modification of the

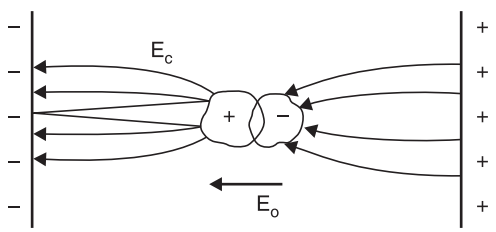

Fig. 1.4 Field redistribution due to space charge

electric field E_0 due to the space charge field. Fig. 1.4 shows the electric field around an avalanche as it progresses along the gap and the resultant field *i.e.*, the superposition of the space charge field and the original field E_0. Since the electrons have higher mobility, the space charge at the head of the avalanche is considered to be negative and is assumed to be concentrated within a spherical volume. It can be seen from Fig. 1.4 that the filed at the head of the avalanche is strengthened. The field between the two assumed charge centres *i.e.*, the electrons and positive ions is decreased as the field due to the charge centres opposes the main field E_0 and again the field between the positive space charge centre and the cathode is strengthened as the space charge field aids the main field E_0 in this region. It has been observed that if the charge carrier number exceeds 10^6, the field distortion becomes noticeable. If the distortion of field is of 1%, it would lead to a doubling of the avalanche but as the field distortion is only near the head of the avalanche, it does not have a significance on the discharge phenomenon. However, if the charge carrier exceeds 10^8, the space charge field becomes almost of the same magnitude as the main field E_0 and hence it may lead to initiation of a streamer. The space charge field, therefore, plays a very important role in the mechanism of electric discharge in a non-uniform gap.

Townsend suggested that the electric spark discharge is due to the ionization of gas molecule by the electron impact and release of electrons from cathode due to positive ion bombardment at the cathode. According to this theory, the formative time lag of the spark should be at best equal to the electron transit time t_r. At pressures around atmospheric and above *p.d.* > 10^3 Torr-cm, the experimentally determined time lags have been found to be much shorter than t_r. Study of the photographs of the avalanche development has also shown that under certain conditions, the space charge developed in an avalanche is capable of transforming the avalanche into channels of ionization known as *streamers* that lead to rapid development of breakdown. It has also been observed through measurement that the transformation from avalanche to streamer generally takes place when the charge within the avalanche head reaches a critical value of

$$n_0 e^{\alpha x} \approx 10^8 \quad \text{or} \quad \alpha x_c \approx 18 \text{ to } 20$$

where X_c is the length of the avalanche parth in field direction when it reaches the critical size. If the gap length $d < X_c$, the initiation of streamer is unlikely.

The short-time lags associated with the discharge development led Raether and independently Meek and Meek and Loeb to the advancement of the theory of streamer of Kanal mechanism for spark formation, in which the secondary mechanism results from photoionization of gas molecules and is independent of the electrodes.

Raether and Meek have proposed that when the avalanche in the gap reaches a certain critical size the combined space charge field and externally applied field E_0 lead to intense ionization and excitation of the gas particles in front of the avalanche head. There is recombination of electrons and positive ion resulting in generation of photons and these photons in turn generate secondary electrons by the photoionization process. These electrons under the influence of the electric field develop into secondary avalanches as shown in Fig. 1.5. Since photons travel with velocity of light, the process leads to a rapid development of conduction channel across the gap.

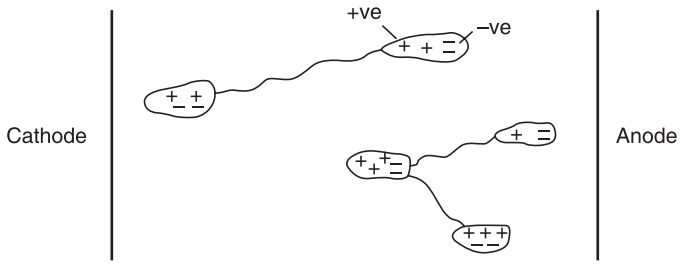

Fig. 1.5 Secondary avalanche formation by photoelectrons

Raether after thorough experimental investigation developed an empirical relation for the streamer spark criterion of the form

$$\alpha x_c = 17.7 + \ln x_c + \ln \frac{E_r}{E_0}$$

where E_r is the radial field due to space charge and E_0 is the externally applied field.

Now for transformation of avalanche into a streamer $E_r \approx E$

Therefore, $\alpha x_c = 17.7 + \ln x_c$

For a uniform field gap, breakdown voltage through streamer mechanism is obtained on the assumption that the transition from avalanche to streamer occurs when the avalanche has just crossed the gap. The equation above, therefore, becomes

$$\alpha d = 17.7 + \ln d$$

When the critical length $x_c \geq d$ minimum breakdown by streamer mechanism is brought about. The condition $X_c = d$ gives the smallest value of α to produce streamer breakdown.

Meek suggested that the transition from avalanche to streamer takes place when the radial field about the positive space charge in an electron avalanche attains a value of the order of the externally applied field. He showed that the value of the radial field can be otained by using the expression.

$$E_r = 5.3 \times 10^{-7} \frac{\alpha e^{\alpha x}}{(x/P)^{1/2}} \text{ volts/cm.}$$

where x is the distance in cm which the avalanche has progressed, p the gas pressure in Torr and α the Townsend coefficient of ionization by electrons corresponding to the applied field E. The minimum breakdown voltage is assumed to correspond to the condition when the avalanche has crossed the gap of length d and the space charge field E_r approaches the externally applied field *i.e.*, at $x = d$, $E_r = E$. Substituting these values in the above equation, we have

$$E = 5.3 \times 10^{-7} \frac{\alpha e^{\alpha d}}{(d/p)^{1/2}}$$

Taking ln on both the sides, we have

$$\ln E = -14.5 + \ln \alpha - \frac{1}{2} \ln \frac{d}{p} + \alpha d$$

$$\ln E - \ln p = -14.5 + \ln \alpha - \ln p - \frac{1}{2} \ln \frac{d}{p} + \alpha d$$

$$1n\ \frac{E}{p} = -14.5 + \ln\frac{\alpha}{p} - \frac{1}{2}\ln\frac{d}{p} + \alpha d$$

The experimentally determined values of α/p and the corresponding E/p are used to solve the above equation using trial and error method. Values of α/p corresponding to E/p at a given pressure are chosen until the equation is satisfied.

1.7. THE SPARKING POTENTIAL—PASCHEN'S LAW

The Townsend's Criterion

$$\nu(e^{\alpha d} - 1) = 1$$

enables the evaluation of breakdown voltage of the gap by the use of appropriate values of α/p and ν corresponding to the values E/p when the current is too low to damage the cathode and also the space charge distortions are minimum. A close agreement between the calculated and experimentally determined values is obtained when the gaps are short or long and the pressure is relatively low.

An expression for the breakdown voltage for uniform field gaps as a function of gap length and gas pressure can be derived from the threshold equation by expressing the ionization coefficient α/p as a function of field strength E and gas pressure p *i.e.*,

$$\frac{\alpha}{p} = f\left(\frac{E}{p}\right)$$

Substituting this, we have

$$e^{f(E/p)\ pd} = \frac{1}{\nu} + 1$$

Taking ln both the sides, we have

$$f\left(\frac{E}{p}\right)pd = \ln\left[\frac{1}{\nu} + 1\right] = K \text{ say}$$

For uniform field $E = \dfrac{V_b}{d}$.

Therefore, $f\left(\dfrac{V_b}{pd}\right).\ pd = K$

or $$f\left(\frac{V_b}{pd}\right) = \frac{K}{pd}$$

or $$V_b = F\ (p.d)$$

This shows that the breakdown voltage of a uniform field gap is a unique function of the product of gas pressure and the gap length for a particular gas and electrode material. This relation is known as *Paschen's law*. This relation does not mean that the breakdown voltage is directly proportional to product *pd* even though it is found that for some region of the product *pd* the relation is linear *i.e.*, the breakdown voltage varies linearly with the product *pd*. The variation over a large range is shown in Fig. 1.6.

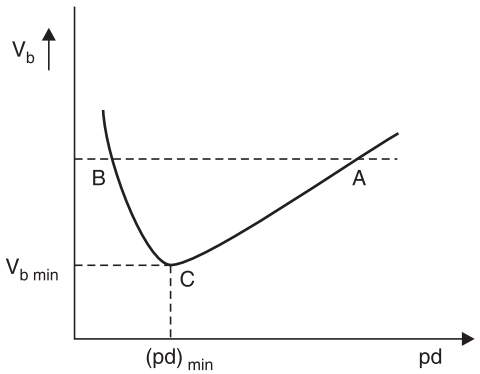

Fig. 1.6 Paschen's law curve

Let us now compare Paschen's law and the Townsend's criterion for spark potential. We draw the experimentally obtained relation between the ionization coefficient α/p and the field strength $f(E/p)$ for a given gas. Fig. 1.7. Here point $\left(\frac{E_b}{p}\right)_c$ represents the onset of ionization.

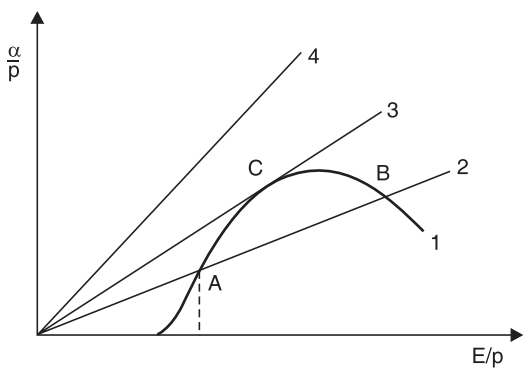

Fig. 1.7 The relation between Townsend's criterion for spark = k and Paschen's criterion

Now the Townsend's criterion $\alpha d = K$ can be re-written as

$$\frac{\alpha}{p} \cdot \frac{V}{E} = \frac{K}{p} \quad \text{or} \quad \frac{\alpha}{p} = \frac{K}{V} \cdot \frac{E}{P}$$

This is equation to a straight line with slope equal to K/V depending upon the value of K. The higher the voltage the smaller the slope and therefore, this line will intersect the ionization curve at two points *e.g.*, A and B in Fig. 1.7. Therefore, there must exist two breakdown voltages at a constant pressure (p = constant), one corresponding to the small value of gap length *i.e.*, higher E ($E = V/d$) *i.e.*, point B and the other to the longer gap length *i.e.*, smaller E or smaller E/p *i.e.*, the point A. At low values of voltage V the slope of the straight line is large and, therefore, there is no intersection between the line and the curve 1. This means no breakdown occurs with small voltages below Paschen's minimum irrespective of the value of pd. The point C on the curve indicates the lowest breakdown voltage or the minimum sparking potential. The spark over voltages corresponding to points A, B, C are shown in the Paschen's curve in Fig. 1.6.

The fact that there exists a minimum sparking potential in the relation between the sparking potential and the gap length assuming p to be constant can be explained quantitatively by considering the efficiency of ionization of electrons traversing the gap with different electron energies. Assuming that the Townsend's second ionization coefficient ν is small for values $pd > (pd)$min., electrons crossing the gap make more frequent collision with the gas molecules than at (pd)min. but the energy gained between the successive collision is smaller than at (pd). Hence, the probability of ionization is lower unless the voltage is increased. In case of $(pd) < (pd)$ min., the electrons cross the gap without making any collision and thus the sparking potential is higher. The point (pd)min., therefore, corresponds to the highest ionization efficiency and hence minimum sparking potential.

An analytical expression for the minimum sparking potential can be obtained using the general expression for α/p.

$$\frac{\alpha}{p} = Ae^{Bp/E} \quad \text{or} \quad \alpha = pAe^{-Bpd/V_b}$$

or $$e^{-Bpd/V_b} = \frac{pA}{\alpha} \quad \text{or} \quad \frac{1}{\alpha} = \frac{e^{Bpd/V_b}}{pA}$$

or $$d \cdot \frac{1}{\alpha d} = \frac{e^{B^{pd}/V_b}}{pA}$$

We know that $$\alpha d = 1\text{n}\left(1 + \frac{1}{\nu}\right)$$

Therefore, $$d = \frac{e^{Bpd/V_b}}{pA} 1\text{n}\left(1 + \frac{1}{\nu}\right)$$

Assuming ν to be constant, let $$1\text{n}\left(1 + \frac{1}{\nu}\right) = k$$

Then $$d = \frac{e^{Bpd/V_b}}{pA} K$$

In order to obtain minimum sparking potential, we rearrange the above expression as

$$V_b = f(pd)$$

Taking 1n on both sides, we have

$$\frac{Bpd}{V_b} = \ln \frac{Apd}{K}$$

or $$V_b = \frac{Bpd}{\ln Apd/k}$$

Differentiating V_b w.r. to pd and equating the derivative to zero

$$\frac{dV_b}{d(pd)} = \frac{\ln \frac{Apd}{K} \cdot B - Bpd \cdot \frac{K}{Apd} \cdot \frac{A}{K}}{\left(1\text{n} \frac{Apd}{K}\right)^2} = \frac{B \ln \frac{Apd}{K}}{\left(1\text{n} \frac{Apd}{K}\right)^2} - \frac{B}{\left(1\text{n} \frac{Apd}{K}\right)^2} = 0$$

or $$\frac{1}{\ln \frac{Apd}{K}} = \frac{1}{\left(\ln \frac{Apd}{K}\right)^2}$$

or $$1\text{n}\frac{Apd}{K} = 1$$

or $$1\text{n}\frac{Apd}{K} = e$$

or $$(pd)_{\min} = \frac{e}{A}K$$

or $$V_{b\,\min} = \frac{B\,e^{K/A}}{1} = \frac{B}{A}.eK$$

$$V_{b\min} = 2.718\ \frac{B}{A}1\text{n}\left(1+\frac{1}{\nu}\right)$$

If values of A, B and ν are known both the (pd) min and $V_{b\min}$ can be obtained. However, in practice these values are obtained through measurements and values of some of the gases are given in the following Table 1.1.

Table 1.1. Minimum Sparking Constant for various gases

Gas	*(pd)min*	V_b *min volts*
Air	0.55	352
Nitrogen	0.65	240
Hydrogen	1.05	230
SF_6	0.26	507
CO_2	0.57	420
O_2	0.70	450
Neon	4.0	245
Helium	4.0	155

Typical values for A, B and ν for air are $A = 12$, $B = 365$ and $\nu = 0.02$.

Schuman has suggested a quadratic formulation between α/p and E/p under uniform field over a wide but restricted range as

$$\text{s}\frac{\alpha}{p} = C\left[\frac{E}{p} - \left(\frac{E}{p}\right)\right]^2$$

where $(E/p)_c$ is the minimum value of E at which the effective ionization begins and p is the pressure, C a constant.

We know that Townsend's spark criterion for uniform fields is $\alpha d = k$ where $k = (1 + 1/\nu)$.

Therefore, the equation above can be re-written as

$$\frac{K}{dp} = C\left[\frac{E}{p} - \left(\frac{E}{p}\right)_c\right]^2$$

or $$\left(\frac{K}{C}.\frac{1}{pd}\right)^{1/2} = \frac{E}{p} - \left(\frac{E}{p}\right)_c$$

or $$\frac{E}{p} = \left(\frac{E}{p}\right)_c + \left(\frac{K/C}{pd}\right)^{1/2}$$

$$\frac{V}{dp} = \left(\frac{E}{p}\right)_c + \left(\frac{K/C}{pd}\right)^{1/2}$$

or

$$V_b = \left(\frac{E}{p}\right)_c pd + \left(\frac{K}{c}\right)^{1/2} \cdot \sqrt{pd}$$

Sohst and Schröder have suggested values for E_c = 24.36 kV/cm K/C = 45.16 (kV)^2 /cm for air at p = 1 bar and temperature 20°C.

Substituting these values in the above equation, we have

$$V_b = 6.72\sqrt{pd} + 24.36\ (pd)\ kV$$

The breakdown voltages suggested in tables or obtained through the use of empirical relation normally correspond to ambient temperature and pressure conditions, whereas the atmospheric air provides basic insulation between various electrical equipments. Since the atmospheric conditions (Temperature, pressure) vary widely from time to time and from location to location, to obtain the actual breakdown voltage, the voltage obtained from the STP condition should be multiplied by the air density correction factor. The air density correction factor is given as

$$\delta = \frac{3.92\ b}{273 + t}$$

where b is the atmospheric pressure in cm of Hg and t the temperature in °C.

1.8 PENNING EFFECT

Paschen's law does not hold good for many gaseous mixtures. A typical example is that of mixture of Argon in Neon. A small percentage of Argon in Neon reduces substantially the dielectric strength of pure Neon. In fact, the dielectric strength is smaller than the dielectric strengths of either pure Neon or Argon. The lowering of dielectric strength is due to the fact that the lowest excited stage of neon is metastable and its excitation potential (16 ev) is about 0.9 ev greater than the ionization potential of Argon. The metastable atoms have a long life in neon gas, and on hitting Argon atoms there is a very high probability of ionizing them. This phenomenon is known as Penning Effect.

1.9 CORONA DISCHARGES

If the electric field is uniform and if the field is increased gradually, just when measurable ionization begins, the ionization leads to complete breakdown of the gap. However, in non-uniform fields, before the spark or breakdown of the medium takes place, there are many manifestations in the form of visual and audible discharges. These discharges are known as *Corona discharges*. In fact Corona is defined as a self-sustained electric discharge in which the field intensified ionization is localised only over a portion of the distance (non-uniform fields) between the electrodes. The phenomenon is of particular importance in high voltage engineering where most of the fields encountered are non-uniform fields unless of course some design features are involved to make the filed almost uniform. Corona is responsible for power loss and interference of power lines with the communication lines as corona frequency lies between 20 Hz and 20 kHz. This also leads to deterioration of insulation by the combined action of the discharge ion bombarding the surface and the action of chemical compounds that are formed by the corona discharge.

When a voltage higher than the critical voltage is applied between two parallel polished wires, the glow is quite even. After operation for a short time, reddish beads or tufts form along the wire, while around the surface of the wire there is a bluish white glow. If the conductors are examined through a stroboscope, so that one wire is always seen when at a given half of the wave, it is noticed that the reddish tufts or beads are formed when the conductor is negative and a smoother bluish white glow when the conductor is positive. The a.c. corona viewed through a stroboscope has the same apperance as direct current corona. As corona phenomenon is initiated a hissing noise is heard and ozone gas is formed which can be detected by its chracteristic colour.

When the voltage applied corresponds to the critical disruptive voltage, corona phenomenon starts but it is not visible because the charged ions in the air must receive some finite energy to cause further ionization by collisions. For a radial field, it must reach a gradient (visual corona gradient) g_u at the surface of the conductor to cause a gradient g_0, finite distance away from the surface of the conductor. The distance between g_0 and g_v is called the energy distance. According to Peek, this distance is equal to $(r + 0.301 \sqrt{r})$ for two parallel conductors and $(r + 0.308 \sqrt{r})$ for coaxial conductors. From this it is clear that g_v is not constant as g_0 is, and is a function of the size of the conductor. The electric field intensity for two parallel wires is given as

$$E = 30 \left(1 + \frac{0.301}{\sqrt{r}\,\delta}\right) \delta \text{ kV/cm}$$

and for a coaxial wire

$$E = 30 \left(1 + \frac{0.308}{\sqrt{r}\delta}\right) \delta$$

Investigation with point-plane gaps in air have shown that when point is positive, the corona current increases steadily with voltage. At sufficiently high voltage, current amplification increases rapidly with voltage upto a current of about 10^{-7} *A*, after which the current becomes pulsed with repetition frequency of about 1 kHz composed of small bursts. This form of corona is known as *burst corona*. The average current then increases steadily with applied voltage, leading to breakdown.

With point-plane gap in air when negative polarity voltage is applied to the point and the voltage exceeds the onset value, the current flows in vary regular pulses known as *Trichel pulses*. The onset voltage is independent of the gap length and is numerically equal to the onset of streamers under positive voltage for the same arrangement. The pulse frequency increases with voltage and is a function of the radius of the cathode, the gap length and the pressure. A decrease in pressure decreases the frequency of the pulses. It should be noted that the breakdown voltage with negative polarity is higher than with positive polarity except at low pressure. Therefore, under alternating power frequency voltage the breakdown of non-uniform field gap invariably takes place during the positive half cycle of the voltage wave.

Fig. 1.8 gives comparision between the positive and negative point-plane gap breakdown characteristics measured in air as a function of gas pressure.

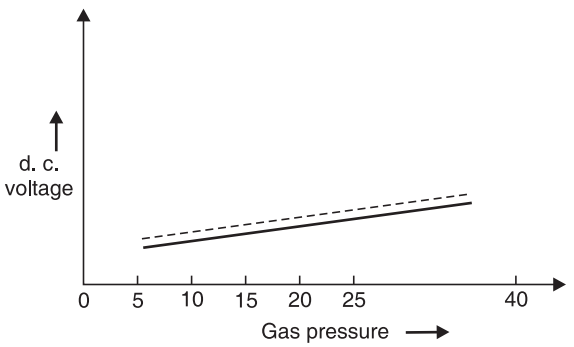

Fig. 1.8. Point-plane breakdown for +ve and –ve polarities

When the spacing is small the breakdown characteristics for the two polarities nearly coincide and no corona stabilised region is observed. As the spacing is increased, the positive characteristics display the distinct high corona beakdown upto a pressure of about 7 bars, followed by a sudden drop in breakdown strengths. Under the negative polarity, the corona stabilised region extends to much higher pressures.

Fig. 1.9 shows the corona inception and breakdown voltages of the sphere-plane arrangement. From the figure, it is clear that—

(*i*) For small spacings (Zone–I), the field is uniform and the breakdown voltage depends mainly on the gap spacing.

(*ii*) In zone–II, where the spacing is relatively larger, the electric field is non-uniform and the breakdown voltage depends on both the sphere diameter and the spacing.

(*iii*) For still larger spacings (Zone-III) the field is non-uniform and the breakdown is preceded by corona and is controlled only by the spacing. The corona inception voltage mainly depends on the sphere diameter.

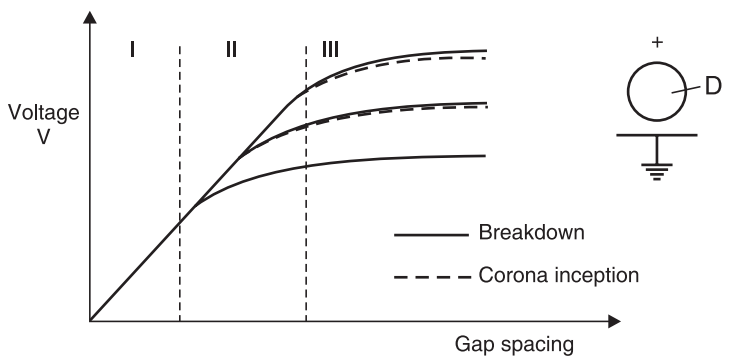

Fig. 1.9 Breakdown and corona inception characteristics for spheres of different diameters in sphere-plane gap geometry

1.10 TIME-LAG

In order to breakdown a gap, certain amount of energy is required. Also it depends upon the availability of an electron between the gap for initiation of the avalanche. Normally the peak value of a.c. and d.c. are smaller as compared to impulse wave as the duration of the former are pretty large as compared to the letter and the energy content is large. Also with d.c. and a.c. as the duration is large there are usually sufficient initiatory electrons created by cosmic ray and naturally occuring radioactive sources.

Suppose V_d is the maximum value of d.c. voltage applied for a long time to cause breakdown of a given gap. Fig. 1.10.

Let the same gap be subjected to a step voltage of peak value $V_{d1} > V_d$ and of a duration such that the gap breaks down in time *t*. If the breakdown

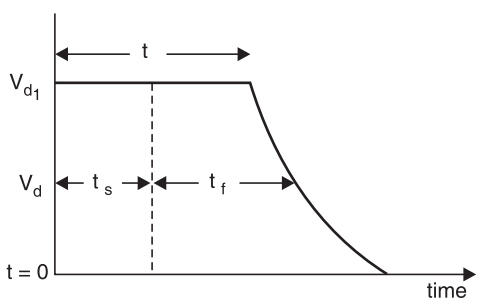

Fig. 1.10 Time lag components under a step voltage

were purely a function of voltage magnitude, the breakdown should have taken place the moment the step voltage had just crossed the voltage V_d.

The time that elapses between the application of the voltage to a gap sufficient to cause breakdown, and the breakdown, is called the *time lag*. In the given case shown in Fig. 1.10, t is the time lag. It consists of two components. One is the that elapses during the voltage applications until a primary electron appears to initiate the discharge and is known as the *statistical time lag* t_s and the other is the time required for the breakdown to develop once initiated and is known as the *formative time lag* t_f.

The statistical time lag depends upon (*i*) The amount of pre-ionization present in between the gap (*ii*) Size of the gap (*iii*) The amount of over voltage ($V_{d1} - V_d$) applied to the gap. The larger the gap the higher is going to be the statistical time lag. Similarly, a smaller over voltage results in higher statistical time lag. However, the formative time lag depends mainly on the mechanism of breakdown. In cases when the secondary electrons arise entirely from electron emission at the cathode by positive ions, the transit time from anode to cathode will be the dominant factor determining the formative time. The formative time lag increases with increase in gap length and field non-uniformity, decreases with increase in over voltage applied.

1.10.1 Breakdown in Electronegative Gases

SF_6, has excellent insulating strength because of its affinity for electrons (electronegativity) *i.e.,* whenever a free electron collides with the neutral gas molecule to form negative ion, the electron is absorbed by the neutral gas molecule. The attachment of the electron with the neutral gas molecule may occur in two ways:

$$SF_6 + e \longrightarrow SF_6^-$$

$$SF_6 + e \longrightarrow SF_5^- + F$$

The negative ions formed are relatively heavier as compared to free electrons and, therefore, under a given electric field the ions do not attain sufficient energy to lead cumulative ionization in the gas. Thus, these processes represent an effective way of removing electrons from the space which otherwise would have contributed to form electron avalanche. This property, therefore, gives rise to very high dielectric strength for SF_6. The gas not only possesses a good dielectric strength but it has the unique property of fast recombination after the source energizing the spark is removed.

The dielectric strength of SF_6 at normal pressure and temperature is 2–3 times that of air and at 2 atm its strength is comparable with the transformer oil. Although SF_6 is a vapour, it can be liquified at moderate pressure and stored in steel cylinders. Even though SF_6 has better insulating and arc-quencling properties than air at an equal pressure, it has the important disadvantage that it can not be used much above 14 kg/cm^2 unless the gas is heated to avoid liquifaction.

1.10.2 Application of Gases in Power System

The gases find wide application in power system to provide insulation to various equipments and substations. The gases are also used in circuit breakers for arc interruption besides providing insulation between breaker contacts and from contact to the enclosure used for contacts. The various gases used are (*i*) air (*ii*) oxygen (*iii*) hydrogen (*iv*) nitrogen (*v*) CO_2 and (*vi*) electronegative gases like sulphur hexafluoride, arcton etc.

The various properties required for providing insulation and arc interruption are:

(*i*) High dielectric strength.

(*ii*) Thermal and chemical stability.

(*iii*) Non-inflammability.

(*iv*) High thermal conductivity. This assists cooling of current carrying conductors immersed in the gas and also assists the arc-extinction process.

(*v*) Arc extinguishing ability. It should have a low dissociation temperature, a short thermal time constant (ratio of energy contained in an arc column at any instant to the rate of energy dissipation at the same instant) and should not produce conducting products such as carbon during arcing.

(*vi*) Commercial availability at moderate cost. Of the simple gases air is the cheapest and most widely used for circuit breaking. Hydrogen has better arc extinguishing property but it has lower dielectric strength as compared with air. Also if hydrogen is contaminated with air, it forms an explosive mixture. Nitrogen has similar properties as air, CO_2 has almost the same dielectric strength as air but is a better arc extinguishing medium at moderate currents. Oxygen is a good extinguishing medium but is chemically active. SF_6 has outstanding arc-quenching properties and good dielectric strength. Of all these gases, SF_6 and air are used in commercial gas blast circuit breakers.

Air at atmospheric pressure is 'free' but dry air costs a lot when stored at say 75 atmosphere. The compressed air supply system is a vital part of an air blast C.B. Moisture from the air is removed by refrigeration, by drying agents or by storing at several times the working pressure and then expanding it to the working pressure for use in the C.B. The relative cost of storing the air reduces with increase in pressure. If the air to be used by the breaker is at 35 kg/cm^2 it is common to store it at 210 kg/cm^2.

Air has an advantage over the electronegative gases in that air can be compressed to extremely high pressures at room temperature and then its dielectric strength even exceeds that of these gases.

The SF_6 gas is toxic and its release in the form of leakage causes environmental problems. Therefore, the electrical industry has been looking for an alternative gas or a mixture of SF_6 with some other gas as an insulating and arc interrupting medium. It has been observed that a suitable mixture of SF_6 with N_2 is a good replacement for SF_6. This mixture is not only finding acceptability for providing insulation *e.g.*, gas insulated substation and other equipments, it is able to quench high current magnitude arcs. The mixture is not only cost effective, it is less sensitive to find non-uniformities present within the equipment. Electric power industry is trying to find optimum SF_6 to N_2 mixture ratio for various components of the system *viz.*, GIS, C.B., capacitors, CT, PT and cables. A ratio 70% of SF_6 and 30% of N_2 is found to be optimum for circuit breaking. With this ratio, the C.B. has higher recovery rate than pure SF_6 at the same partial pressure. The future of using SF_6 with N_2 or He for providing insulation and arc interruption is quite bright.

1.11 BREAKDOWN IN LIQUID DIELECTRICS

Liquid dielectrics are used for filling transformers, circuit breakers and as impregnants in high voltage cables and capacitors. For transformer, the liquid dielectric is used both for providing insulation between the live parts of the transformer and the grounded parts besides carrying out the heat from the transformer to the atmosphere thus providing cooling effect. For circuit breaker, again besides providing insulation between the live parts and the grounded parts, the liquid dielectric is used to quench the arc developed between the breaker contacts. The liquid dielectrics mostly used are petroleum oils. Other oils used are synthetic hydrocarbons and halogenated hydrocarbons and for very high temperature applications sillicone oils and fluorinated hyrocarbons are also used.

The three most important properties of liquid dielectric are (*i*) The dielectric strength (*ii*) The dielectric constant and (*iii*) The electrical conductivity. Other important properties are viscosity, thermal stability, specific gravity, flash point etc. The most important factors which affect the dielectric

strength of oil are the, presence of fine water droplets and the fibrous impurities. The presence of even 0.01% water in oil brings down the dielectric strength to 20% of the dry oil value and the presence of fibrous impurities brings down the dielectric strength much sharply. Therefore, whenever these oils are used for providing electrical insulation, these should be free from moisture, products of oxidation and other contaminants.

The main consideration in the selection of a liquid dielectric is its chemical stability. The other considerations are the cost, the saving in space, susceptibility to environmental influences etc. The use of liquid dielectric has brought down the size of equipment tremendously. In fact, it is practically impossible to construct a 765 kV transformer with air as the insulating medium. Table 1.2. shows the properties of some dielectrics commonly used in electrical equipments.

Table 1.2. Dielectric properties of some liquids

S.No.	*Property*	*Transformer Oil*	*Capacitor Oil*	*Cable Oil*	*Silicone Oil*
1.	Relative permittivity 50 Hz	2.2 – 2.3	2.1	2.3 – 2.6	2.7 – 3.0
2.	Breakdown strength at 20°C 2.5 mm 1 min	12 kV/mm	18 kV/mm	25 kV/mm	35 kV/mm
3.	(*a*) Tan δ 50 Hz	10^{-3}	2.5×10^{-4}	2×10^{-3}	10^{-3}
	(*b*) 1 kHz	5×10^{-4}	10^{-4}	10^{-4}	10^{-4}
4.	Resistivity ohm-cm	$10^{12} – 10^{13}$	$10^{13} – 10^{14}$	$10^{12} – 10^{13}$	2.5×10^{14}
5.	Maximum permissible water content (ppm)	50	50	50	< 40
6.	Acid value mg/gm of KOH	NIL	NIL	NIL	NIL
7.	Sponification mg of KOH/gm of oil	0.01	0.01	0.01	< 0.01
8.	Specific gravity at 20°C	0.89	0.89	0.93	1.0–1.1

Liquids which are chemically pure, structurally simple and do not contain any impurity even in traces of 1 in 10^9, are known as *pure liquids*. In contrast, commercial liquids used as insulating liquids are chemically impure and contain mixtures of complex organic molecules. In fact their behaviour is quite erratic. No two samples of oil taken out from the same container will behave identically.

The theory of liquid insulation breakdown is less understood as of today as compared to the gas or even solids. Many aspects of liquid breakdown have been investigated over the last decades but no general theory has been evolved so far to explain the breakdown in liquids. Investigations carried out so far, however, can be classified into two schools of thought. The first one tries to explain the breakdown in liquids on a model which is an extension of gaseous breakdown, based on the avalanche ionization of the atoms caused by electon collisiron in the applied field. The electrons are assumed to be ejected from the cathode into the liquid by either a field emission or by the field enhanced thermionic effect (Shottky's effect). This breakdown mechanism explains breakdown only of highly pure liquid and does not apply to explain the breakdown mechanism in commercially available liquids. It has been observed that conduction in pure liquids at low electric field (1 kV/cm) is largely ionic due to dissociation of impurities and increases linearly with the field strength. At moderately high fields the conduction saturates but at high field (electric), 100 kV/cm the conduction increases more rapidly and thus breakdown takes place. Fig. 1.11 (*a*) shows the variation of current as a function of electric field for

hexane. This is the condition nearer to breakdown. However, if the figure is redrawn starting with low fields, a current-electric field characteristic as shown in Fig. 1.11 (*b*) will be obtained. This curve has three distinct regions as discussed above.

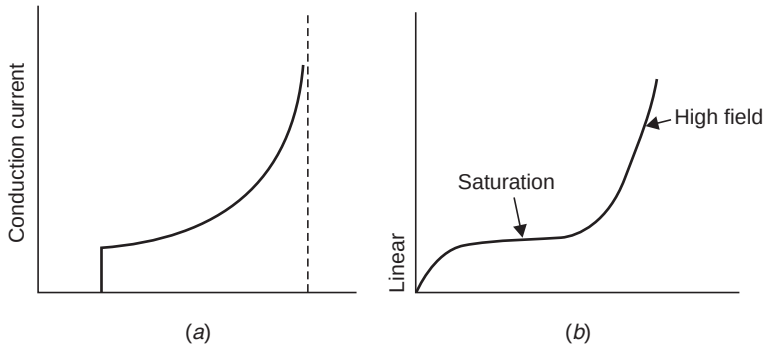

Fig. 1.11 Variation of current as a function of electric field
(*a*) High fields (*b*) Low fields

The second school of thought recognises that the presence of foreign particles in liquid insulations has a marked effect on the dielectric strength of liquid dielectrics. It has been suggested that the suspended particles are polarizable and are of higher permittivity than the liquid. These particles experience an electrical force directed towards the place of maximum stress. With uniform field electrodes the movement of particles is presumed to be initiated by surface irregularities on the electrodes, which give rise to local field gradients. The particles thus get accumulated and tend to form a bridge across the gap which leads finally to initiation of breakdown. The impurities could also be in the form of gaseous bubbles which obviously have lower dielectric strength than the liquid itself and hence on breakdown of bubble the total breakdown of liquid may be triggered.

Electronic Breakdown

Once an electron is injected into the liquid, it gains energy from the electric field applied between the electrodes. It is presumed that some electrons will gain more energy due to field than they would lose during collision. These electrons are accelerated under the electric field and would gain sufficient energy to knock out an electron and thus initiate the process of avalanche. The threshold condition for the beginning of avalanche is achieved when the energy gained by the electron equals the energy lost during ionization (electron emission) and is given by

$$e \lambda E = Chv$$

where λ is the mean free path, hv is the energy of ionization and C is a constant. Table 1.3 gives typical values of dielectric strengths of some of the highly purified liquids.

Table 1.3. Dielectric strengths of pure liquids

Liquid	*Strength (MV/cm)*
Benzene	1.1
Goodoil	1.0–4.0
Hexane	1.1–1.3
Nitrogen	1.6–1.88
Oxygen	2.4
Silicon	1.0–1.2

The electronic theory whereas predicts the relative values of dielectric strength satisfactorily, the formative time lags observed are much longer as compared to the ones predicted by the electronic theory.

1.11.1 Suspended Solid Particle Mechanism

Commercial liquids will always contain solid impurities either as fibers or as dispersed solid particles. The permittivity of these solids (E_1) will always be different from that of the liquid (E_2). Let us assume these particles to be sphere of radisus r. These particles get polarized in an electric field E and experience a force which is given as

$$F = r^3 \frac{\varepsilon_1 - \varepsilon_2}{\varepsilon_1 + 2\varepsilon_2} E \cdot \frac{dE}{dx}$$

and this force is directed towards a place of higher stress if $\varepsilon_1 > \varepsilon_2$ and towards a place of lower stress if $\varepsilon_1 < \varepsilon_2$ when ε_1 is the permittivity of gas bubbles. The force given above increases as the permittivity of the suspended particles (ε_1) increases. If $\varepsilon_1 \to \infty$

$$F = r^3 \frac{1 - \varepsilon_2/\varepsilon_1}{1 + 2\varepsilon_2/\varepsilon_1} E \frac{dE}{dx}$$

Let $\varepsilon_1 \to \infty$

$$F = r^3 E \cdot \frac{dE}{dx}$$

Thus, the force will tend the particle to move towards the strongest region of the field. In a uniform electric field which usually can be developed by a small sphere gap, the field is the strongest in the uniform field region. Here $dE/dx \to 0$ so that the force on the particle is zero and the particle remains in equilibrium. Therefore, the particles will be dragged into the uniform field region. Since the permittivity of the particles is higher than that of the liquid, the presence of particle in the uniform field region will cause flux concentration at its surface. Other particles if present will be attracted towards the higher flux concentration. If the particles present are large, they become aligned due to these forces and form a bridge across the gap. The field in the liquid between the gap will increase and if it reaches critical value, brakdown will take place. If the number of particles is not sufficient to bridge the gap, the particles will give rise to local field enhancement and if the field exceeds the dielectric strength of liquid, local breakdown will occur near the particles and thus will result in the formation of gas bubbles which have much less dielectric strength and hence finally lead to the breakdown of the liquid.

The movement of the particle under the influence of electric field is oposed by the viscous force posed by the liquid and since the particles are moving into the region of high stress, diffusion must also be taken into account. We know that the viscous force is given by (Stoke's relation) $F_V = 6\pi n r \nu$ where η is the viscosity of liquid, r the raidus of the particle and v the velocity of the particle.

Equating the electrical force with the viscous force we have

$$6\pi\eta r\nu = r^3 E \frac{dE}{dx} \quad \text{or} \quad \nu = \frac{r^2 E}{6\pi\eta} \frac{dE}{dx}$$

However, if the diffusion process is included, the drift velocity due to diffusion will be given by

$$\nu_d = -\frac{D}{N}\frac{dN}{dx} = -\frac{KT}{6\pi\eta r}\frac{dN}{Ndx}$$

where $D = KT/6\pi\eta r$ a relation known as Stokes-Einstein relation. Here K is Boltzmann's constant and T the absolute temperature. At any instant of time, the particle should have one velocity and, therefore, equation $v = v_d$

We have

$$-\frac{KT}{6\pi\eta r}\cdot\frac{dN}{Ndx}=\frac{r^2E}{6\pi\eta}\cdot\frac{dE}{dx}$$

or
$$\frac{KT}{r}\frac{dN}{N}=-r^2E\,dE$$

or
$$\frac{KT}{r}\ln N=-\frac{r^2E^2}{2}$$

It is clear that the breakdown strength E depends upon the concentration of particles N, radius r of particle, viscosity η of liquid and temperature T of the liquid.

It has been found that liquid with solid impurities has lower dielectric strength as compared to its pure form. Also, it has been observed that larger the size of the particles impurity the lower the overall dielectric strength of the liquid containing the impurity.

1.11.2 Cavity Breakdown

It has been observed experimentally that the dielectric strength of liquid depnds upon the hydrostatic pressure above the gap length. The higher the hydrostatic pressure, the higher the electric strength, which suggests that a change in phase of the liquid is involved in the breakdown process. In fact, smaller the head of liquid, the more are the chances of partially ionized gases coming out of the gap and higher the chances of breakdown. This means a kind of vapour bubble formed is responsible for the breakdown. The following processes might lead to formation of bubbles in the liquids:

(*i*) Gas pockets on the surface of electrodes.

(*ii*) Due to irregular surface of electrodes, point charge concentration may lead to corona discharge, thus vapourizing the liquid.

(*iii*) Changes in temperature and pressure.

(*iv*) Dissociation of products by electron collisions giving rise to gaseous products.

It has been suggested that the electric field in a gas bubble which is immersed in a liquid of permittivity ε_2 is given by

$$E_b=\frac{3E_0}{\varepsilon_2+2}$$

Where E_0 is the field in the liquid in absence of the bubble. The bubble under the influence of the electric field E_0 elongates keeping its volume constant. When the field E_b equals the gaseous ionization field, discharge takes place which will lead to decomposition of liquid and breakdown may follow.

A more accurate expression for the bubble breakdown strength is given as

$$E_b=\frac{1}{\varepsilon_2-\varepsilon_1}\left\{\frac{2\pi\sigma(2\varepsilon_2+\varepsilon_1)}{r}\left[\frac{\pi}{4}\sqrt{\frac{V_b}{2rE_0}-1}\right]\right\}^{1/2}$$

where σ is the surface tension of the liquid, ε_2 and ε_1 are the permittivities of the liquid and bubble, respectively, r the initial radius of the bubble and V_b the voltage drop in the bubble. From the expression it can be seen that the breakdown strength depends on the initial size of the bubble which of course depends upon the hydrostatic pressure above the bubble and temperature of the liquid. Since the above formation does not take into account the production of the initial bubble, the experimental values of breakdown were found to be much less than the calculated values. Later on it was suggested that only incompressible bubbles like water bubbles can elongate at constant volume according to the simple gas law $pV = RT$. Such a bubble under the influence of electric field changes its shape to that of a prolate spheroid and reaches a condition of instability when β, the ratio of the longer to the shorter diameter of the spheroid is about 1.85 and the critical field producing the instability will be given by

$$E_c = 600 \frac{\sqrt{\pi \sigma}}{\varepsilon_2 r} \left[\frac{\varepsilon_2}{\varepsilon_2 - \varepsilon_1} - G \right] H$$

where

$$G = \frac{1}{\beta^2 - 1} \left[\frac{\beta \cosh^{-1} \beta}{(\beta^2 - 1)^{1/2}} - 1 \right]$$

and

$$H^2 = 2\beta^{1/3} \left(2\beta - 1 - \frac{1}{\beta^2} \right)$$

For transformer oil $\varepsilon_2 = 2.0$ and water globule with $r = 1$ μm, $\sigma = 43$ dynes/cm, the above equation gives $E_c = 226$ KV/cm.

Electroconvection Breakdown

It has been recognized that the electroconvection plays an important role in breakdown of insulating fluids subjected to high voltages. When a highly pure insulating liquid is subjected to high voltage, electrical conduction results from charge carriers injected into the liquid from the electrode surface. The resulting space charge gives rise to coulombic forces which under certain conditions causes hydrodynamic instability, yielding convecting current. It has been shown that the onset of instability is associated with a critical voltage. As the applied voltage approaches the critical voltage, the motion at first exhibits a structure of hexagonal cells and as the voltage is increased further the motion becomes turbulent. Thus, interaction between the space charge and the electric field gives rise to forces creating an eddy motion of liquid. It has been shown that when the voltage applied is near to breakdown value, the speed of the eddy motion is given by $\nu_e = \sqrt{\varepsilon_2 / \rho}$ where ρ is the density of liquid. In liquids, the ionic drift velocity is given by

$$\nu_d = KE$$

where K is the mobility of ions.

Let

$$M \frac{\nu_e}{\nu_d} = \sqrt{\frac{\varepsilon_2}{\rho}} / KE$$

The ratio M is usually greater than unity and sometimes much greater than unity (Table 1.4).

Table 1.4

Medium	*Ion*	ε	*M*
Air NTP	O^-_2	1.0	2.3×10^{-2}
Ethanol	Cl^-	2.5	26.5
Methanol	H^+	33.5	4.1
Nitrobenzene	Cl^-	35.5	22
Propylene Carbonate	Cl^-	69	51
Transformer Oil	H^+	2.3	200

Thus, in the theory of electroconvection, *M* plays a dominant role. The charge transport will be largely by liquid motion rather than by ionic drift. The criterion for instability is that the local flow velocity should be greater than drift velocity.

1.12 TREATMENT OF TRANSFORMER OIL

Even though new synthetic materials with better mechanical and thermal properties are being developed, the use of oil/paper complex for high voltages is still finding applications. Oil, besides being a good insulating medium, it allows better dispersion of heat. It allows transfer and absorption of water, air and residues created by the ageing of the solid insulation. In order to achieve operational requirements, it must be treated to attain high degree of purity.

Whatever be the nature of impurities whether solid, liquid or gaseous, these bring down the dielectric strength of oil materially. Oil at 20°C with water contents of 44 ppm will have 25% of its normal dielectric strength. The presence of water in paper not only increases the loss angle tan δ, it accelerates the process of ageing. Similarly, air dissolved in oil produces a risk of forming bubble and reduces the dielectric strength of oil.

Air Absorption: The process of air absorption can be compared to a diffusing phenomenon in which a gaseous substance in this case air is in contact with liquid (oil here).

If the viscosity of the liquid is low, the convection movements bring about a continuous intermixing whereby a uniform concentration is achieved. This phenomenon can, for example, be checked in a tank where the air content or the water content measured both at the top and the bottom are approximately equal.

Let $G(t)$ = Air content of the oil after time t

G_m = Air content under saturation condition

p = Probability of absorption per unit time

S = Surface of oil

V = Volume of oil

The absorption of air by oil can be given by the equation

$$\frac{dG}{dt} = p \cdot \frac{S}{V}[G_m - G(t)]$$

with boundary condition at $t = 0$ $G = G_0$

Solving the above equation

$$\frac{dG}{G_m - G(t)} = p\,\frac{S}{V}\,dt$$

or $$1\text{n}\,\{G_m - G\,(t)\} = -\,p\,\frac{S}{V}\,t + A$$

At $t = 0$ $G = G_{0.}$ Therefore, $A = +\ 1\text{n} \leftarrow \{G_m - G_0\}$

or $$1\text{n}\,\frac{G_m - G(t)}{G_m - G_0} = -\,p\,\frac{S}{V}\,t$$

or $$G_m - G\,(t) = (G_m - G_0)\,e^{\,-pSt/V}$$

Fig. 1.12 (*a*) shows the schematic for the measurement of air absorption by insulating oil which has previously been degassed as a function of the absorption time. The oil is degassed and dried with the help of the vacuum pump (1) and then introduced into the installation until the desired pressure is reached. A part of this air is absorbed by the oil, the pressure being maintained at a constant (2) Value by reducing the volume in absorption meter (3) Thus, air content of oil by volume can be measured. Precision manometer (4) is used to calibrate the absorption meter. Phosphorus pentaoxide trap (5) takes in the remainder of the water vapour.

In case of a completely degassed oil *i.e.*, at $t = 0$ $G = 0$, we obtain

$$G(t) = G_m\,(1 - e^{-pSt/V})$$

To have an estimate of air absorbed by oil, let us consider a hermetically sealed bushing impregnated under vacuum contains 20 litres of degassed oil ($G_0 = 0$). Suppose the bushing is opened at 25°C and remains under atmospheric pressure for 10 hours, the oil surface $S = 10^3$ cm^2. Assume a typical value of $p = 0.4$ cm/hr, the percentage of air absorbed in given as

$$G\,(10\ hr) = 10(1 - e^{-10^3/10^4 \times 0.4 \times 10})$$

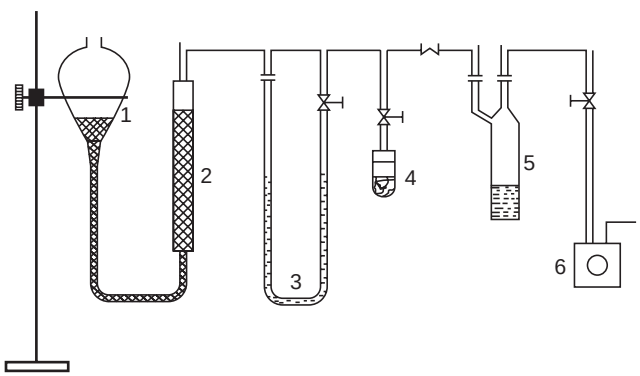

(*a*)

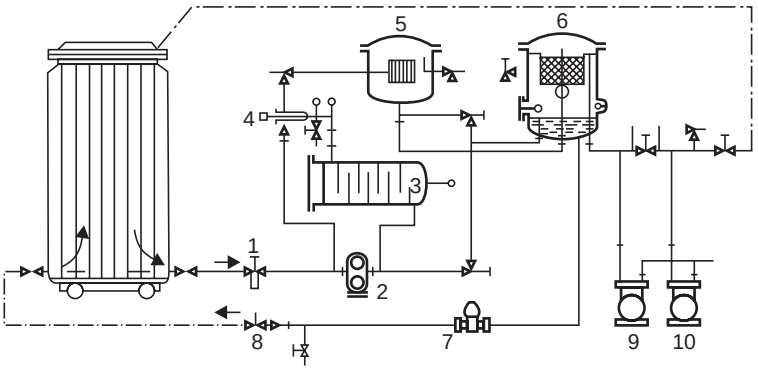

(*b*)

Fig. 1.12 (*a*), (*b*)

The molecules of oil are held together by their internal binding energy. In order that water molecule takes the place of oil molecule and is dissolved in the mixture, it is necessary to provide this molecule with a quantity of energy E in the form of heat.

Let N be the number of oil molecule n, the number of water molecules.

P_n the number of possibilities of combination for n water molecules among $(N + n)$ molecules.

i.e.,
$$P_n = \frac{N+n!}{N!\,n!}$$

S = Entropy of the oil

T = Absolute temperature of mixture

K = Boltzamann's constant

$E(T)$ = Energy required for a water molecule to take the palce of an oil molecule

W = Water content of the oil (p.p.m.)

W_m = Maximum water content of the oil, at saturation point

Thermal equilibrium will be reached when free energy F is minimum *i.e.*,

$$\frac{\partial F}{\partial n} = 0$$

where $F = E\,(T) - TS$

and $S = k\ 1\text{n}\ P_n$

Now
$$\frac{\partial F}{\partial n} = \frac{\partial E\,(T)}{\partial n} - T\,\frac{\partial S}{\partial n} = 0$$

Since
$$P_n = \frac{(N+n)!}{N!\,n!}$$

Taking 1n both sides, we have

$$1\text{n}\ P_n = 1\text{n}\ (N+n)! - 1\text{n}\ N\ ! - 1\text{n}\ n\ !$$
$$= 1\text{n}\ (N+n) + 1\text{n}\ (N+n-1) + 1\text{n}\ (N+n-2)$$
$$\ldots - 1\text{n}\ N\ ! - 1\text{n}\ n - \ln\ (n-1) - 1\text{n}\ (n-2) - 1\text{n}\ (n-3)\ \ldots$$

Differentiating both sides,

$$\frac{1}{P_n}\frac{\partial P_n}{\partial n} = \frac{1}{N+n} + \frac{1}{N+n-1} + \ldots - \frac{1}{n} - \frac{1}{n-1} \ldots$$

$$\approx \frac{1}{N+n} - \frac{1}{n} = -\frac{N}{n(N+n)}$$

Since $$\frac{\partial S}{\partial n} = \frac{K}{P_n}\frac{\partial P_n}{\partial n} \approx -\frac{KN}{n(N+n)}$$

Substituting for $\partial S/\partial n$ in the equation

We have, $$\frac{\partial E(T)}{\partial n} - T\frac{\partial S}{\partial n} = 0$$

$$\frac{\partial E(T)}{\partial n} + T\frac{TKN}{n(N+n)} = 0$$

or $$\frac{\partial E}{\partial n} = -\frac{TKN}{n(N+n)}$$

$$\partial E = -TK\frac{N\,dn}{n(N+n)}$$

Since $$N >> N + n \approx N$$

Therefore, $$\partial E = -TK\frac{dn}{n}$$

or $$E = -TK \ln n + A$$

when $E = 0$, $n = N$. Therefore, $0 = -TK \ln N + A$ or $A = TK \ln N$

or $$E = TK \ln \frac{N}{n}$$

or $$\ln \frac{n}{N} = -\frac{E}{TK} \quad \text{or} \quad \frac{n}{N} \approx e^{-E/TK}$$

or $$n = N e^{-E/TK} \approx W_m$$

Following impurities should be considered for purification of oil (*i*) solid impurities (*ii*) free and dissolved water particles (*iii*) dissolved air. Some of the methods used to remove these impurities have been described below.

Filtration and Treatment Under Vacuum: Different types of filters have been used. Filter press with soft and hard filter papers is found to be more suitable for insulating oil. Due to hygroscopic properties of the paper, oil is predried before filtering. Therefore, this oil can not be used for high voltage insulation. The subsequent process of drying is carried out in a specially, designed tank under vacuum. The oil is distributed over a large surface by a so-called ''Rasching-ring'' degassing column. Through this process, both the complete drying and degassing are achieved simultaneously. By suitable selection of the various components of the plant *e.g.*, rate of flow of oil, degassing surface, vacuum pump etc., a desired degree of purity can be obtained.

Fig. 1.12 (*b*) shows a typical plant for oil treatment. The oil from a transformer or a storage tank is prefiltered (1) so as to protect the feeder pump (2). In (3), the oil is heated up and is allowed to flow

through filter press (4) into degassing tank (5). The degassing tank is evacuated by means of vacuum pump (6) whereas the second vacuum pump (7) is either connected with the degassing tank in parallel with pump (6) or can be used for evacuating the transformer tank which is to be treated.

The operating temperature depends upon the quality and the vapour pressure of oil. In order to prevent an excessive evaporation of the aromatics, the pressure should be greater than 0.1 Torr. The filteration should be carried out at a suitable temperature as a higher temperature will cause certain products of the ageing process to be dissolved again in the oil.

Centrifugal Method: This method is helpful in partially extracting solid impurities and free water. It is totally ineffective as far as removal of water and dissolved gases is concerned and oil treated in this manner is even over-saturated with air as air, is thoroughly mixed into it during the process. However, if the centrifugal device is kept in a tank kept under vacuum, partial improvement can be obtained. But the slight increase in efficiency of oil achieved is out of proportion to the additional costs involved.

Adsorption Columns: Here the oil is made to flow through one or several columns filled with an adsorbing agent either in the form of grains or powder. Following adsorbing agents have been used:

(*i*) Fuller earth

(*ii*) Silica gel

(*iii*) Molecular sieves

Activated Fuller earths absorb carbonyl and hydroxyl groups which from the principal ageing products of oil and small amount of humidity. Best results of oil treatment are obtained by a combination of Fuller earth and subsequent drying under vacuum.

Silica gel and in particular molecular sieves whose pore diameter measures 4 Å show a strong affinity for water. Molecular sieves are capable of adsorbing water 20% of its original weight at 25°C and water vapour pressure of 1 Torr whereas sillica gel and Fuller earth take up 6 and 4 per cent respectively.

Molecular sieves are synthetically produced Zeolites which are activated by removal of the crystallisation water. Their adsorption capacity remains constant upto saturation point. The construction of an oil drying plant using molecular sieves is, therefore, simple. The plant consists of an adsorption column containing the sieves and of an oil circulating pump.

The adsorption cycle is followed by a desorption cycle once the water content of the sieves has exceeded 20 per cent. It has been found that the two processes adsorption and desorption are readily reversible. In order to attain disorption of the sieves, it is sufficient to dry them in air stream of 200°C.

Electrostatic Filters: The oil to be treated is passed between the two electrodes placed in a container. The electrostatic field charges the impurities and traces of water which are then attracted and retained by the foam coated electrodes. This method of drying oil is found to be economical if the water content of the oil is less than 2 ppm. It is, therefore, essential that the oil is dried before hand if the water content is large. Also, it is desirable that the oil flow should be slow if efficient filtering is required. Therefore, for industrial application where large quantity of oil is to be filtered, large number of filters will have to be connected in parallel which may prove uneconomical.

1.13 TESTING OF TRANSFORMER OIL

The oil is poured in a container known as *test-cell* which has internal dimensions of 55 mm × 90 mm × 100 mm high. The electrodes are polished spheres of 12.7 to 13 mm diameter, preferably of brass, arranged horizontally with their axis not less than 40 mm above the bottom of the cell. For the test, the

distance between the spheres shall be 4 + 0.02 mm. A suitable gauge is used to adjust the gap. While preparing the oil sample, the test-cell should be thoroughly cleaned and the moisture and suspended particles should be avoided. Fig. 1.13 shows an experimental set-up for finding out the dielectric strength of the given sample of oil. The voltmeter is connected on to the primary side of the high voltage transformer but calibrated on the high voltage side.

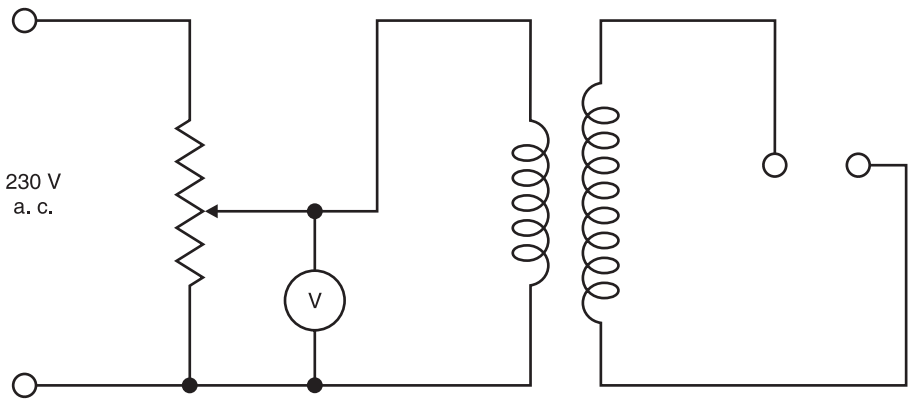

Fig. 1.13

The gap between the spheres is adjusted to 4 mm with the help of a gauge and the spheres are immersed in oil to a depth as mentioned earlier. The voltage is increased gradually and continuously till a flash over of the gap is seen or the MCB operates. Note down this voltage. This voltage is known as *rapidly-applied voltage*. The breakdown of the gap has taken place mainly due to field effect. The thermal effect is minimal as the time of application is short.

Next bring the voltage back to zero and start with 40% of the rapidly applied voltage and wait for one minute. See if the gap has broken. If not, increase the voltage everytime by 2.1/2% of the rapidly applied voltage and wait for one minute till the flash over is seen or the MCB trips. Note down this voltage.

Start again with zero voltage and increase the voltage to a value just obtained in the previous step and wait for a minute. It is expected that the breakdown will take place. A few trials around this point will give us the breakdown value of the dielectric strength. The acceptable value is 30 kV for 4 mm applied for one minute. In fact these days transformer oils with 65 kV for 4 mm 1 minute value are available. If it is less than 30 kV, the oil should be sent for reconditioning. It is to be noted that if the electrodes are immersed vertically in the oil, the dielectric strength measured may turn out to be lower than what we obtained by placing the electrodes in horizontal position which is the normal configuration. It is due to the fact that when oil decomposes carbon particles being lighter rise up and if the electrodes are in vertical configuration, these will bridge the gap and the breakdown will take place at a relatively lower value.

1.13.1 Application of Oil in Power Apparatus

Oil is normally used for providing insulation between the live parts of different phases and between phases and the grounded enclosure containing the oil and the main parts of the apparatus. Also it provides cooling effect to the apparatus placed within the enclosure. Besides providing insulation, the oil helps the C.B. to quench the arc produced between the breaker contacts when they begin to separate to eliminate the faulted section from the healthy section of the system.

In an oil circuit breaker, the heat of the oil decomposes the oil which boils at 658 K. The gases liberated are approx. (*i*) Hydrogen, 70%, (*ii*) Acetylene, 20%, (*iii*) Methane, 5% and (*iv*) Ethane, 5%. (the abbreviation for these gases could be used as HAME).

The temperature about the arc is too high for the three last-named gases to exist and the arc itself runs into a mixture of hydrogen, carbon and copper vapour at temperature above 6000 K. The hydrogen being a diatomic gas gets dissociated into the atomic state which changes the characteristics of the arc on account of its associated change in its thermal conductivity. The outcome of this is that the discharge suddenly contracts and acquires an appreciably higher core temperature. In certain cases, the thermal ionization may be so great that the discharge runs with a lower voltage which may stop the ionization due to the electric field strength. The transition from the field ionization to thermal ionization is most marked in hydrogen and, therefore, in oil circuit breakers.

The separation of the C.B. contacts which are carrying current gives rise to an arc without changing much the current wave form. Initially when the contacts just begin to separate the magnitude of current is very large but the contact resistance being very small, a small voltage appears across them. But the distance of separation being very very small, a large voltage gradient is set up which is good enough to cause ionization of the particles between the contacts. Also it is known that with the copper contacts which are generally used for the circuit breakers very little thermal ionization can occur at temperature below the melting point. For effective field emission, the voltage gradient required is 10^6 V/cm. From this it is clear that the arc is initiated by the field emission rather than the thermal ionization. This high voltage gradient exists only for a fraction of a micro-second. But in this short period, a large number of electrons would have been liberated from the cathode and these electrons while reaching anode, on their way would have collided with the atoms and molecules of the gases. Thus, each emitted electron tends to create others and these in turn derive energy from the field and multiply. In short, the work done by the initially-emitted electrons enables the discharge to be maintained. Finally, if the current is high, the discharge attains the form of an arc having a temperature high enough for thermal ionization, which results in lower voltage gradient. Thus, an arc is initiated due to field effect and then maintained due to thermal ionization.

1.14 BREAKDOWN IN SOLID DIELECTRICS

Solid insulating materials are used almost in all electrical equipments, be it an electric heater or a 500 MW generator or a circuit breaker, solid insulation forms an integral part of all electrical equipments especially when the operating voltages are high. The solid insulation not only provides insulation to the live parts of the equipment from the grounded structures, it sometimes provides mechanical support to the equipment. In general, of course, a suitable combination of solid, liquid and gaseous insulations are used.

The processes responsible for the breakdown of gaseous dielectrics are governed by the rapid growth of current due to emission of electrons from the cathode, ionization of the gas particles and fast development of avalanche process. When breakdown occurs the gases regain their dielectric strength very fast, the liquids regain partially and solid dielectrics lose their strength completely.

The breakdown of solid dielectrics not only depends upon the magnitude of voltage applied but also it is a function of time for which the voltage is applied. Roughly speaking, the product of the breakdown voltage and the log of the time required for breakdown is almost a constant *i.e.*,

$$V_b = 1\text{n}\ t_b = \text{constant}$$

The characteristics is shown in Fig. 1.14.

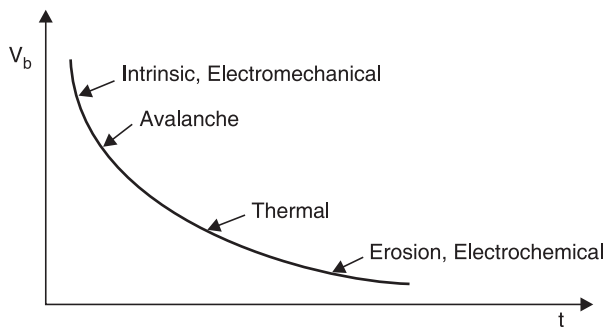

Fig. 1.14. Variation of V_b with time of application

The dielectric strength of solid materials is affected by many factors viz. ambient temperature, humidity, duration of test, impurities or structural defects whether a.c., d.c. or impulse voltages are being used, pressure applied to these electrodes etc. The mechanism of breakdown in solids is again less understood. However, as is said earlier the time of application plays an important role in breakdown process, for discussion purposes, it is convenient to divide the time scale of voltage application into regions in which different mechanisms operate. The various mechanisms are:

(*i*) Intrinisic Breakdown

(*ii*) Electromechanical Breakdown

(*iii*) Breakdown Due to Treeing and Tracking

(*iv*) Thermal Breakdown

(*v*) Electrochemical Breakdown

1.14.1 Intrinsic Breakdown

If the dielectric material is pure and homogeneous, the temperature and environmental conditions suitably controlled and if the voltage is applied for a very short time of the order of 10^{-8} second, the dielectric strength of the specimen increases rapidly to an upper limit known as *intrinsic dielectric strength*. The intrinsic strength, therefore, depends mainly upon the structural design of the material *i.e.*, the material itself and is affected by the ambient temperature as the structure itself might change slightly by temperature condition. In order to obtain the intrinsic dielectric strength of a material, the samples are so prepared that there is high stress in the centre of the specimen and much low stress at the corners as shown in Fig. 1.15.

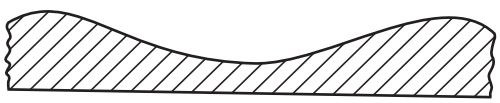

Fig. 1.15 Specimen designed for intrinsic breakdown

The intrinsic breakdown is obtained in times of the order of 10^{-8} sec. and, therefore, has been considered to be electronic in nature. The stresses required are of the order of one million volt/cm. The intrinsic strength is generally assumed to have been reached when electrons in the valance band gain sufficient energy from the electric field to cross the forbidden energy band to the conduction band. In pure and homogenous materials, the valence and the conduction bands are separated by a large energy gap at room temperature, no electron can jump from valance band to the conduction band. The

conductivity of pure dielectrics at room temperature is, therfore, zero. However, in practice, no insulating material is pure and, therefore, has some impurities and/or imperfections in their structural designs. The impurity atoms may act as traps for free electrons in energy levels that lie just below the conduction band is small. An amorphous crystal will, therefore, always have some free electrons in the conduction band. At room temperature some of the trapped electrons will be excited thermally into the conduction band as the energy gap between the trapping band and the conduction band is small. An amorphous crystal will, therefore, always have some free electrons in the conduction band. As an electric field is applied, the electrons gain energy and due to collisions between them the energy is shared by all electrons. In an amorphous dielectric the energy gained by electrons from the electric field is much more than they can transfer it to the lattice. Therefore, the temperature of electrons will exceed the lattice temperature and this will result into increase in the number of trapped electrons reaching the conduction band and finally leading to complete breakdown.

When an electrode embeded in a solid specimen is subjected to a uniform electric field, breakdown may occur. An electron entering the conduction band of the dielectric at the cathode will move towards the anode under the effect of the electric field. During its movement, it gains energy and on collision it loses a part of the energy. If the mean free path is long, the energy gained due to motion is more than lost during collision. The process continues and finally may lead to formation of an electron avalanche similar to gases and will lead finally to breakdown if the avalanche exceeds a certain critical size.

1.14.2 Electromechanical Breakdown

When a dielectric material is subjected to an electric field, charges of opposite nature are induced on the two opposite surfaces of the material and hence a force of attraction is developed and the speciment is subjected to electrostatic compressive forces and when these forces exceed the mechanical withstand strength of the material, the material collapses. If the initial thickness of the material is d_0 and is compressed to a thickness d under the applied voltage V then the compressive stress developed due to electric field is

$$F = \frac{1}{2}\varepsilon_0\varepsilon_r \frac{V^2}{d^2}$$

where ε_r is the relative permittivity of the specimen. If γ is the Young's modulus, the mechanical compressive strength is

$$\gamma \ln \frac{d_0}{d}$$

Equating the two under equilibrium condition, we have

$$\frac{1}{2}\varepsilon_0\varepsilon_r \frac{V^2}{d^2} = \gamma \ln \frac{d_0}{d}$$

or

$$V^2 = d^2 \cdot \frac{2\gamma}{\varepsilon_0\varepsilon_r} \ln \frac{d_0}{d} = Kd^2 \ln \frac{d_0}{d}$$

Differentiating with respect to d, we have

$$2V \frac{dV}{dd} = K\left[2d \ln \frac{d_0}{d} - d^2 \cdot \frac{d}{d_0} \cdot \frac{d_0}{d^2}\right] = 0$$

or $$2d \ln \frac{d_0}{d} = d$$

or $$\ln \frac{d_0}{d} = \frac{1}{2}$$

or $$\frac{d}{d_0} = 0.6$$

For any real value of voltage *V,* the reduction in thickness of the specimen can not be more than 40%. If the ratio *V/d* at this value of *V* is less than the intrinsic strength of the specimen, a further increase in *V* shall make the thickness unstable and the specimen collapses. The highest apparent strength is then obtained by substituting $d = 0.6\ d_0$ in the above expressions.

$$\frac{V}{d} = \sqrt{\frac{2\gamma}{\varepsilon_0 \varepsilon_r} \ln 1.67} \quad \text{or} \quad \frac{V}{d_0} = E_a = 0.6 \left[\frac{\gamma}{\varepsilon_0 \varepsilon_r}\right]^{1/2}$$

The above equation is approximate only as γ depends upon the mechanical stress. The possibility of instability occuring for lower average field is ignored *i.e.,* the effect of stress concentration at irregularities is not taken into account.

1.14.3 Breakdown due to Treeing and Tracking

We know that the strength of a chain is given by the strength of the weakest link in the chain. Similarly whenever a solid material has some impurities in terms of some gas pockets or liquid pockets in it the dielectric strength of the solid will be more or less equal to the strength of the weakest impurities. Suppose some gas pockets are trapped in a solid material during manufacture, the gas has a relative permittivity of unity and the solid material ε_r, the electric field in the gas will be ε_r times the field in the solid material. As a result, the gas breaks down at a relatively lower voltage. The charge concentration here in the void will make the field more non-uniform. The charge concentration in such voids is found to be quite large to give fields of the order of 10 MV/cm which is higher than even the intrinsic breakdown. These charge concentrations at the voids within the dielectric lead to breakdown step by step and finally lead to complete rupture of the dielectric. Since the breakdown is not caused by a single discharge channel and assumes a tree like structure as shown in Fig. 1.6, it is known as breakdown due to treeing. The treeing phenomenon can be readily demonstrated in a laboratory by applying an impulse voltage between point plane electrodes with the point embedded in a transparent solid dielectric such as perspex.

The treeing phenomenon can be observed in all dielectric wherever non-uniform fields prevail.

Suppose we have two electrodes separated by an insulating material and the assembly is placed in an outdoor environment. Some contaminants in the form of moisture or dust particles will get deposited on the surface of the insulation and leakage current starts between the electrode through the contaminants say moisture. The current heats the moisture and causes breaks in the moisture films. These small films then act as electrodes and sparks are drawn between the films. The sparks cause carbonization and volatilization of the insulation and lead to formation of permanent carbontracks on the surface of insulations. Therefore, tracking is the formation of a permanent conducting path usually carbon across the surface of insulation. For tracking to occur, the insulating material must contain organic substances. For this reason, for outdoor equipment, tracking severely limits the use of insulation having organic substances. The rate of tracking can be slowed down by adding filters to the polymers which inhibit carbonization.

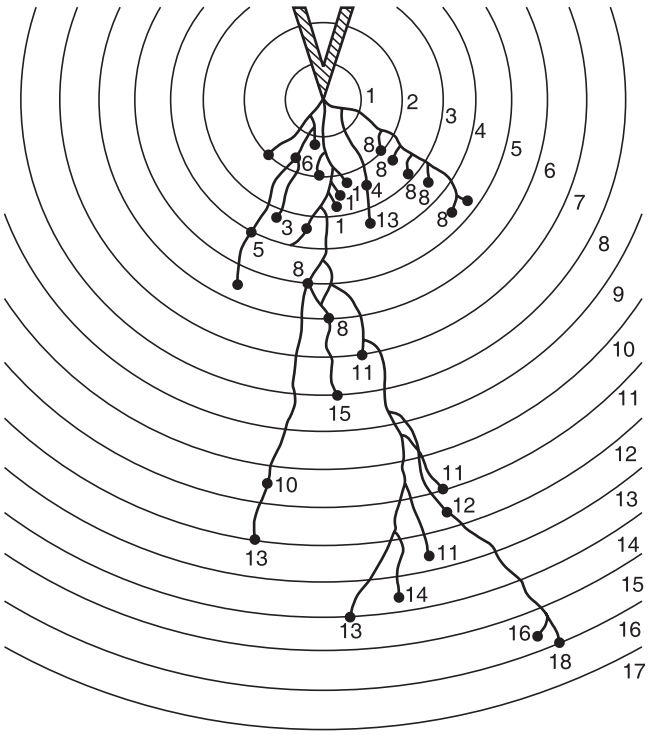

Fig. 1.16

1.14.4 Thermal Breakdown

When an insulating material is subjected to an electric field, the material gets heated up due to conduction current and dielectric losses due to polarization. The conductivity of the material increases with increase in termperature and a condition of instability is reached when the heat generated exceeds the heat dissipated by the material and the material breaks down. Fig. 1.17 shows various heating curves corresponding to different electric stresses as a function of specimen temperature. Assuming that the temperature difference between the ambient and the specimen temperature is small, Newton's law of cooling is represented by a straight line.

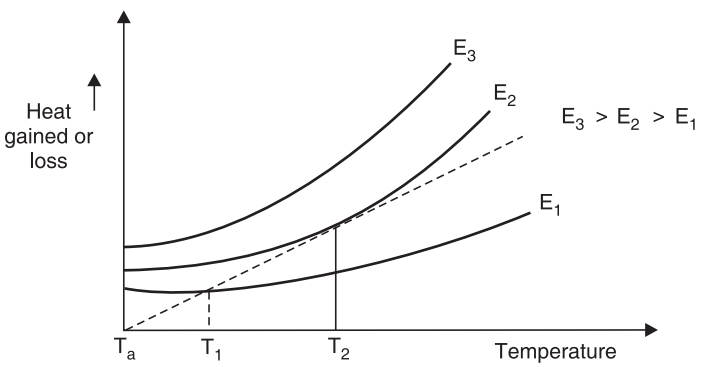

Fig. 1.17 Thermal stability or instability of different fields

The test specimen is at thermal equilibrium corresponding to field E_1 at temperature T_1 as beyond that heat generated is less than heat lost. Unstable equilibrium exists for field E_2 at T_2, and for field E_3 the state of equilibrium is never reached and hence the specimen breaks down thermally.

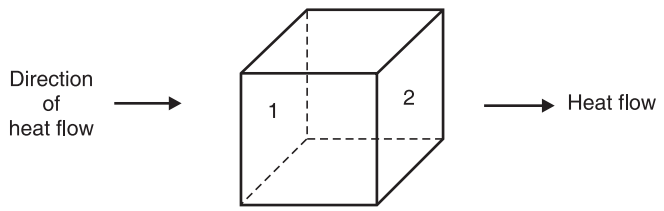

Fig. 1.18. Cubical speciman—Heat flow

In order to obtain basic equation for studying thermal breakdown, let us consider a small cube (Fig. 1.18) within the dielectric specimen with side Δx and temperature difference across its faces in the direction of heat flow (assume here flow is along x-direction) is ΔT. Therefore, the temperature gradient is

$$\frac{\Delta T}{\Delta x} \approx \frac{dT}{dx}$$

Let $\Delta x^2 = A$. The heat flow across face 1

$$KA \frac{dT}{dx} \text{ Joules}$$

Heat flow across face 2

$$KA \frac{dT}{dx} - KA \frac{d}{dx}\left(\frac{dT}{dx}\right)\Delta x$$

Here the second term indicates the heat input to the differential specimen. Therefore, the heat absorbed by the differential cube volume

$$= \frac{KA \frac{d}{dx}\left(\frac{dT}{dx}\right)\Delta x}{\Delta V} = K \frac{d}{dx}\left(\frac{dT}{dx}\right)$$

The heat input to the block will be partly dissipated into the surrounding and partly it will raise the temperature of the block. Let C_V be the thermal capacity of the dielectric, σ the electrical conductivity, E the electric field intensity. The heat generated by the electric field = σE^2 watts, and suppose the rise in temperature of the block is ΔT, in time dt, the power required to raise the temperature of the block by ΔT is

$$C_V \frac{dT}{dt} \text{ watts}$$

Therefore,
$$C_V \frac{dT}{dt} + K \frac{d}{dx}\left(\frac{dT}{dx}\right) = \sigma E^2$$

The solution of the above equation will give us the time required to reach the critical temperature T_c for which thermal instability will reach and the dielectric will lose its insulating properties. However, unfortunately the equation can be solved in its present from C_V, K and σ are all functions of temperature and in fact σ may also depend on the intensity of electrical field.

Therefore, to obtain solution of the equation, we make certain practical assumptions and we consider two extreme situations for its solution.

Case I: Assume that the heat absorbed by the block is very fast and heat generated due to the electric field is utilized in raising the temperature of the block and no heat is dissipated into the surroundings. We obtain, therefore, an expression for what is known as impulse thermal breakdown. The main equation reduces to

$$C_V \frac{dT}{dt} = \sigma E^2$$

The objective now is to obtain critical field strength E_c which will generate sufficient heat very fast so that above requirement is met. Let

$$E = \left(\frac{E_c}{t_c}\right) t$$

i.e., the field is a ramp function

$$\sigma E^2 = C_V \frac{dT}{dt} = C_V \frac{dT}{dE} \cdot \frac{dE}{dt}$$

and Let $$\sigma = \sigma_0 \, e^{-u/KT}$$

where K is Boltzamann's constant and σ_0 is the conductivity at ambinent temperature T_0.

Substituting these values in the simplified equation, we have

$$\sigma_0 e^{-u/KT} \, E^2 = C_V \frac{dE}{dt} \cdot \frac{dT}{dE}$$

Now $$\frac{dE}{dt} = \frac{E_c}{t_c}$$

Therefore, $$\sigma_0 e^{-u/KT} E^2 = C_V \frac{E_c}{t_c} \frac{dT}{dE}$$

or $$\sigma_0 \, E^2 \frac{t_c}{E_c} dE = C_V e^{u/KT} dT$$

or $$\frac{\sigma_0}{C_V} \frac{t_c}{E_c} \int_0^{E_c} E^2 dE = \int_{T_0}^{T_c} e^{\frac{u}{KT}} \, dT$$

The integral on the left hand side

$$\frac{\sigma_0}{C_V} \frac{t_c}{E_c} \int_0^{E_c} E^2 \, dE = \frac{\sigma_0}{C_V} \frac{t_c}{E_c} \cdot \frac{1}{3} E_c^3 = \frac{1}{3} t_c \frac{\sigma_0}{C_V} {E_c}^2$$

The integral on the right hand side

$$\int_{T_0}^{T_c} e^{\frac{u}{KT}} \, dt \to {T_0}^2 \frac{K}{u} e^{u/KT_0}$$

when $T_c >> T_0$

Therefore, $$E_c = \frac{3C_V}{\sigma_0 t_c} \cdot \frac{K {T_0}^2}{u} e^{u/KT_0}$$

From the above expression, it is clear that the critical condition requires a combination of critical time and critical field. However, the critical field is independent of the critical temperature due to the fast rise in temperature.

Case II: Here we assume that the voltage applied is the minimum voltage for indefinite time so that the thermal breakdown takes place. For this, we assume that we have a thick dielectric slab that is subjected to constant ambient temperature at its surface by using sufficiently large electrodes as shown in Fig. 1.19

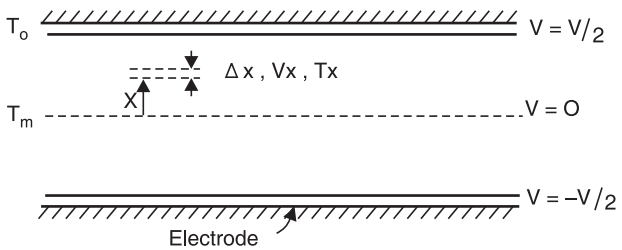

Fig. 1.19 Arrangement of electrode and specimen for minimum thermal B.D. voltage

Suppose that minimum voltage is applied which brings thermal breakdown. As a result after some time, a temperature distribution will be set up within the specimen with maximum temperature T_m at its centre and it decreases as we approach the surface.

In order to calculate maximum thermal voltage, let us consider a point inside the dielectric at a distance x from the central axis and let the voltage and temperature at the point are V_x and T_x, respectively. We further assume that all the heat generated in the dielectric will be carried away to its surroundings through the electrodes. Therefore, neglecting the term

$$C_V \frac{dT}{dt}$$

the main equation reduces to

$$\frac{d}{dx}\left(K \frac{dT}{dx}\right) = \sigma E^2$$

Now using the relations $\sigma E = J$ and $E = -\frac{\partial V}{\partial x}$

We have $$K \frac{d}{dx}\left(\frac{dT}{dx}\right) = -J \frac{\partial V}{\partial x}$$

Integrating both the sides w.r. to x

We have $$\int_0^x \frac{d}{dx}\left(K \frac{dT}{dx}\right) dx = -J \int_0^{V_x} \frac{\partial V}{\partial x} dx$$

or $$K \frac{dT}{dx} = -JV_x = -\sigma E V_x = -\sigma V_x \frac{dv}{dx}$$

Let $\sigma = \sigma_0 e^{-u/KT}$.

We have

$$K \frac{dT}{dx} = \sigma_0 e^{-u/KT} V_x \frac{\partial V}{\partial x}$$

or $$\frac{K}{\sigma_0} E^{u/KT} dT = V_x \frac{\partial V}{\partial x} dx$$

or $$\frac{K}{\sigma_0}\int_{T_0}^{T_c} e^{u/KT}\, dT = \int_0^{V_{m/2}} V_x\, dV$$

This shows that the maximum thermal voltage depends upon the critical temperature T_c at the centre of dielectric at which the specimen loses is insulating properties. However, V_m is independent of the thickness of the insulating material but for thin specimens the thermal breakdown becomes touching asymptotically to a constant value for thick specimen. Under alternating currents the total heat generated will be

$$\sigma E^2 + V^2\, \omega c \tan \delta$$

and, therefore, this being higher than what we have in d.c. circuits, the maximum thermal breakdown voltage will be lower in a.c. supplies. In fact, higher the frequency the lower the thermal breakdown voltage.

Table 1.5 gives for thick specimen, thermal breakdown values for some dielectric under a.c. and d.c. voltages at 20°C.

Table 1.5. Thermal breakdown voltage

Material		*Maximum thermal voltage in MV/cm*	
		d.c.	*a.c.*
Ceramics	HV Steatite	—	9.8
	LF Steatite	—	1.5
	High grade porcelain		2.8
Organic materials	Ebonite	—	1.45–2.75
	Polythene		3.5
	Polystyrene		5.0
	Polystyrene at 1 MHz		0.05
	Acrylic resins		0.3–1.0
Crystals	Mica muscovite	24	7–18
	Rock salt	38	1.4
Quartz	Perpendiculars to axis	12000	—
	Paralle to axis	66	—
	Impure	—	2.2

1.14.5 Electrochemical Breakdown

Whenever cavities are formed in solid dielectrics, the dielectric strength in these solid specimen decreases. When the gas in the cavity breaks down, the surfaces of the specimen provide instantaneous anode and cathode. Some of the electrons dashing against the anode with sufficient energy shall break the chemical bonds of the insulation surface. Similarly, positive ions bombarding against the cathode may increase the surface temperature and produce local thermal instability. Similarly, chemical degradation may also occur from the active discharge products *e.g.*, O_3, NO_2 etc. formed in air. The net effect of all these processes is a slow erosion of the material and a consequent reduction in the thickness of the specimen. Normally, it is desired that with ageing, the dielectric strength of the specimen should not decrease. However, because of defects in manufacturing processes and/or design, the dielectric strength

decreases with time of voltage application or even without voltage application and in many cases; the decrease in dielectric strength (E_b) with time follows the following empirical relation.

$$t \ E_b^{\,n} = \text{constant}$$

where the exponent n depends upon the dielectric material, the ambient temperature humidity and the quality of manufacture. This is the main reason why high a.c. voltage testing is not recommended. In fact, these days very low frequency testing is being suggested (0.1 HZ) which simulates the effects of both a.c. 50 HZ and d.c. voltages and yet the dielectric strength of the specimen is not affected much with VLF voltage application.

The breakdown of solid dielectric due to internal discharges or partial discharges has been elaborately explained in section 6.9 of the book.

1.14.6 Solid Dielectrics Used in Power Apparatus

The main requirements of the insulating materials used for power apparatus are:

1. High insulation resistance
2. High dielectric strength
3. Good mechanical properties *i.e.*, tenacity and elasticity
4. It should not be affected by chemicals around it
5. It should be non-hygroscopic because the dielectric strength of any material goes very much down with moisture content

Vulcanized rubber : Rubber in its natural form is highly insulating but it absorbs moisture readily and gets oxidized into a resinous material; thereby it loses insulating properties. When it is mixed with sulphur alongwith other carefully chosen ingredients and is subjected to a particular temperature it changes into vulcanized rubber which does not absorb moisture and has better insulating properties than even the pure rubber. It is elastic and resilient.

The electrical properties expected of rubber insulation are high breakdown strength and high insulation resistance. In fact the insulation strength of the vulcanized rubber is so good that for lower voltages the radial thickness is limited due to mechanical consideration.

The physical properties expected of rubber insulation are that the cable should withstand normal hazards of installation and it should give trouble-free service.

Vulcanized rubber insulated cables are used for wiring of houses, buildings and factories for low-power work.

There are two main groups of synthetic rubber material : (*i*) general purpose synthetics which have rubber-like properties and (*ii*) special purpose synthetics which have better properties than the rubber *e.g.*, fire resisting and oil resisting properties. The four main types are: (*i*) butyl rubber, (*ii*) silicon rubber, (*iii*) neoprene, and (*iv*) styrene rubber.

Butyl rubber: The processing of butyl rubber is similar to that of natural rubber but it is more difficult and its properties are comparable to those of natural rubber. The continuous temperature to which butyl rubber can be subjected is 85°C whereas for natural rubber it is 60°C. The current rating of

butyl insulated cables is approximately same as those of paper or PVC insulated cables. Butyl rubber compound can be so manufactured that it has low water absorption and offers interesting possibilities for a non-metallic sheathed cable suitable for direct burial in the ground.

Silicone rubber: It is a mechanically weak material and needs external protection but it has high heat resistant properties. It can be operated at temperatures of the order of 150°C. The raw materials used for the silicon rubber are sand, marsh gas, salt, coke and magnesium.

Neoprene: Neoprene is a polymerized chlorobutadiene. Chlorobutadiene is a colourless liquid which is polymerized into a solid varying from a pale yellow to a darkish brown colour. Neoprene does not have good insulating properties and is used upto 660 V a.c. but it has very good fire resisting properties and therefore it is more useful as a sheathing material.

Styrene rubber: Styrene is used both for insulating and sheathing of cables. It has properties almost equal to the natural rubber.

Polyvinyl Chloride (PVC)

It is a polymer derived generally from acetylene and it can be produced in different grades depending upon the polymerization process. For use in cable industry the polymer must be compounded with a plasticizer which makes it plastic over a wide range of temperature. The grade of PVC depends upon the plasticizer. PVC is inferior to vulcanized in respect of elasticity and insulation resistance. PVC material has many grades.

General purpose type: It is used both for sheathing and as an insulating material. In this compound monomeric plasticizers are used. It is to be noted that a V.R. insulated PVC sheathed cable is not good for use.

Hard grade PVC: These are manufactured with less amount of plasticizer as compared with general purpose type. Hard grade PVC are used for higher temperatures for short duration of time like in soldering and are better than the general purpose type. Hard grade can not be used for low continuous temperatures.

Heat resisting PVC: Because of the use of monomeric plasticizer which volatilizes at temperature 80°C–100°C, general purpose type compounds become stiff. By using polymeric plasticizers it is possible to operate the material continuously around 100°C.

PVC compounds are normally costlier than the rubber compounds and the polymeric plasticized compounds are more expensive than the monomeric plasticized ones. PVC is inert to oxygen, oils, alkalis and acids and, therefore, if the environmental conditions are such that these things are present in the atmosphere, PVC is more useful than rubber.

Polythene

This material can be used for high frequency cables. This has been used to a limited extent for power cables also. The thermal dissipation properties are better than those of impregnated paper and the impulse strength compares favourably with an impregnated paper-insulated device. The maximum operating temperature of this material under short circuits is 100°C.

Cross-linked polythene: The use of polythene for cables has been limited by its low melting point. By cross-linking the molecules, in roughly the same way as vulcanising rubber, a new material is produced which does not melt but carbonizes at 250 to 300°C. By using chemical process it has been

made technically possible to cross-link polythene in conventional equipment for the manufacture of rubber. This is why the product is said to be "vulcanised" or "cross-linked" polythene.

The polythene is inert to chemical reactions as it does not have double bonds and polar groups. Therefore, it was thought that polythene could be cross-linked only through special condition, *e.g.*, by irradiating polythene with electrons, thereby it could be given properties of cross-linking such as change of tensile strength and better temperature stability. Many irradiation processes have been developed in the cable making industry even though large amounts of high energy radiations are required and the procedure is expensive.

Polythene can also be irradiated with ultraviolet light, after adding to it a smal quantity of ultra-violet sensitive material such as benzophenone. Under the influence of ultraviolet light on benzophenone, a radical is formed of the same type as in the decomposition of peroxide by the radical mechanism. Organic peroxides have also been used successfully to crosslink the polythene.

Impregnated paper

A suitable layer of the paper is lapped on the conductor depending upon the operating voltage. It is then dried by the combined application of heat and vacuum. This is carried out in a hermetically sealed steam heated chamber. The temperature is 120°–130°C before vacuum is created. After the device is dried, an insulating compound having the same temperature as that of the chamber is forced into the chamber. All the pores of the paper are completely filled with this compound. After impregnation the device is allowed to cool under the compound so that the void formation due to compound shrinkage is minimized.

In case of pre-impregnated type the papers are dried and impregnated before they are applied on the conductor.

The compound used in case of impregnated paper is a semifluid and when the cables are laid on gradients the fluid tends to move from higher to lower gradient. This reduces the compound content at higher gradients and may result in void formation at higher gradients. This is very serious for cables operating at voltages higher than 3.3 kV. In many cases, the failures of the cables have been due to the void formation at the higher levels or due to the bursting of the sheath at the lower levels because of the excessive internal pressure of the head of compound.

Insulating press boards. If the thickness of paper is 0.8 mm or more, it is called paper board. When many layers of paper are laminated with an adhesive to get desired thickness, these are known as press boards and are used in bushings, transformers as insulating barriers or supporting materials. The electrical properties of press boards varies depending upon the resin content. The application of these press boards depends upon the thickness and density of paper used. For high frequency capacitors and cables usually low density paper (0.8 gm/cm^3) is used where medium density paper is used for power capacitors and high density papers are used in d.c. machines and energy storage capacitors. The electric strength of press board is higher than that of resins or porcelain. However, it is adversely affected by temperature above 20°C. The loss angle tan δ also decreases with increase in temperature. The main advantage of this material is that it provides good mechanical support even at higher temperatures upto 120°C.

Mica. Mica consists of crystalline mineral silicates of alumina and potash. It has high dielectric strength, low dielectric losses and good mechanical strength. All these properties make it useful for

many electrical devices *e.g.*, commutator segment separator, aremature windings, electrical heating and cooling equipments and switchgear. Thin layers of mica are laminated with a suitable resin or varnish to make thick sheets of mica. Mica can be mixed with the required type of resin to obtain its application at different operating temperatures. Mica is used as a filler in insulating materials to improve their dielectric strength, reduce dielectric loss and improve heat resistance property.

Ceramics. Ceramics materials are produced from clay containing aluminium oxide and other inorganic materials. The thick parts of these substances is given the desired shape and form at room temperature and then baked at high temperature about (1450°C) to provide a solid inelastic final structure. Ceramics also known as porcelain in one of its forms have high mechanical strength and low permittivity ($\varepsilon_r < 12$) are widely used for insulators and bushings. These have 40% to 50% of clay, 30-20% of aluminium oxide and 30% of fieldspar. The ceramics with higher permittivity ($\varepsilon_r > 12$) are used in capacitors and transducers.

The specific insulation resistance of ceramics is comparatively low. The tan δ of these materials is high and increases with increase in temperature resulting in higher dielectric loss. The breakdown strength of porecelain compared to other insulating material is low but it remains unaffected over a wide range of temperature variation. Porcelain is chemically insert to alkalies and acids and, therefore, corrosion resistant and does not get contaminated. Alumina (Al_2O_3) has replaced quartz because of its better thermal conductivity, insulating property and mechanical strength. It is used for the fabrication of high current vacuum circuit breakers.

Glass. Glass is a thermoplastic inorganic material consisting of silicondioxide (SiO_2), which is available in nature in the form of quartz. Different types of metal oxides could be used for producing different types of glasses but for use in electrical engineering only non-alkaline glasses are suitable having alkaline content less than 0.8%.

The dielectric constant of glass varies between 3.6 and 10.0 and the density varies between 2000 kg/m^3 and 6000 kg/m^3. The loss angle tan δ is less than 10^{-3} and losses are higher for lower frequencies. Its dielectric strength varies between 300 and 500 kV/mm and it decreases with increase in temperature. Glass is used for X-ray equipments, electronic valves, electric bulbs etc.

Epoxy Resins. Epoxy resins are low molecular but soluble thermosetting plastics which exhibit sufficient hardening quality in their molecules. The chemical cross-linking of epoxy resins is normally carried out at room temperatures either by a catalytic mechanism or by bridging across epoxy molecule through the epoxy or hydroxyl group.

Epoxy resins have high dielectric and mechanical strength. They can be cast into desired shapes even at room temperature. They are highly elastic and it is found that when it is subjected to a pressure of 175000 psi, it returned to its original shape after the load is removed. The dielectric constant varies between 2.5 and 4.0. Epoxy resins basically being non-polar substances have high dc specific insulation resistance and low loss tan δ compared to polar materials like PVC. However, when the temperature exceeds 100°C the specific insulation resistance begins to decrease considerably and tan δ increases. Compared to porcelain the breakdown strength of epoxy resin is almost double at temperatures upto 100°C but decreases rapidly at higher temperatures.

As filler materials, the inorganic substances like quartz powder (SiO_2) are used for casting applications. In SF_6 gas insulated systems having epoxy resin spacers, aluminium oxide and also dolo-

mite are used as filler materials. These are found to be more compatible to the decomposed products of SF_6 by partial discharge and arcing discharges.

It is to be noted that the cast or encapsulation should not contain voids or humidity especially in high voltage applications and the material is desired to be homogeneous. It is, therefore, desirable to dry and degas the individual components of the mixture and casting is preferably carried out in vacuum.

The epoxy resins casts are inert to ether, alcohol and benzol. However, most of them are soluble in mineral oils at about 70°C. It is for this reason that they are not found suitable for applications in filled transformers.

There are certain application which require insulating materials to operate between a high range of temperature *e.g.*, –270°C to 400°C. Some of the applications are space shuttle solar arrays, capacitors, transformers high speed locomotive, microprocessor chip carriers, cryogenic cables and other applications at cryogenic temperatures. For this some thermoplastic polymer films are used which have unique combination of electrical, mechanical and physical quantities and these materials are able to retain these properties over a wide range of temperatures where other insulating materials may fail. Perfluoro carbon films have high dielectric strength very low dielectric constant of 2 and low dielectric loss of 2×10^{-4} at 100 Hz and 7.5×10^{-4} at 100 MHz. These films are used under extreme conditions of temperature and environment. These films are used for insulation on high temperature wires, cables, motor coils phase and ground insulation and for capacitors. This is also used as a substrate for flexible printed circuits and flexible cables.

Another insulating film in which has the best thermal properties in this category of insulating materials is polyimide film under the trade name of Kapton manufactured by DuPont of America. These films can be used between a very wide range of temperature variation varying between –270°C and 350°C. Its continuous temperature rating is 240°C. It has high dielectric and tensile strength. The disadvantages of the film are

(*i*) high moisture absorption rate and (*ii*) it is affected by alkalies and strong inorganic acids.

Kepton films can be used capacitors, transformers formed coil insulation, motor state insulation and flexible printed circuits. The film is selectively costlier and is mainly used where its unique characteristics makes it the only suitable insulation. The use of this insulation for motors reduces the overall dimensions of the motors for the same ratings. It is, therefore, used in almost all situations whose space is a serious problem and the other nature insulation result in bigger dimension.

Another recently developed resins is poly carbonate (PC) which is good heat resistant; it is flexible and has good dielectric characteristic. It is not affected by oils, fats and dilute acids but is adversely affected by alkalies, esters and aromatic hydrocarbons. The film being cost effective and fast resistant, it is used for coil insulation, slot insulation for motors and for capacitor insulation. This is known as the lexon polymer.

General Electric Co. of USA has developed a film under the trade name Ultem which is a poly etherimine (PEI) film which has dielectric strength comparable to that of polyimide film and has higher thermal conductivity and lower moisture absorption and is relatively less costlier. It is used as insulation for transformers and motors.

1.14.7 Application of Insulating Materials

Insulating fluids (gases and liquids) provide insulation between phases and between phase and grounded parts of electrical equipments. These also carry out heat from the windings of the electrical equipments. However, solid insulating materials are used only to provide insulation only.

International Electrotechincal Commission has categories various insulating materials depending upon the temperature of operations of the equipments under the following categories.

Class Y	90°C Natural rubber, PVC, paper cotton, silk without impregnation.
Class A	105°C Same as class Y but impregnated
Class E	120°C Polyethylene, terephthalate, cellulose tricetrate, polyvinyl acetate enamel
Class B	130°C Bakelite, bituminised asbestos, fibre glass, mica, polyester enamel
Class F	155°C As class B but with epoxy based resin
Class H	180°C As class B with silicon resin binder silicone rubber, aromatic polyamide (nomex paper and fibre), polyimide film (enamel, varnish and film) and estermide enamel
Class C	Above 180°C, as class B but with suitable non-organic binders, teflon and other high temperature polymers.

While describing the dielectric and other properties of various insulating materials, their application for various electrical apparatus has also been mentioned in the previous paragraphs. However, a reverse process *i.e.,* what insulating materials are used for a particular apparatus depending upon its ratings and environmental condition where the apparatus is required to operate, is also desirable and a brief review is given here.

Power Transformers. For small rating, the coils are made of super-enamelled copper wire. For layer to layer, coil to coil and coil to ground (iron core) craft paper is used.

However, for large size transformers paper or glass tape is rapped on the rectangular conductors whereas for coil to coil or coil to ground, insulation is provided using thick radial spacers made of press board or glas fibre.

In oil-filled transformers, the transformer oil is the main insulation. However between various layers of low voltage and high voltage winding oil-impregnated press boards are placed.

SF_6 gas insulated power transformers make use of sheet aluminium conductors for windings and turn to turn insulation is provided by a polymer film. The transformer has annular cooling ducts through which SF_6 gas circulates for cooling the winding. SF_6 gas provides insulations to all major gaps in the transformer. This transformer is used where oil filled transform is not suitable *e.g.,* in cinema halls, high rise buildings and some especial circumstances: The end turns of a large power transformer are provided with extra insulation to avoid damage to coil when lighting or switching surges of high frequency are incident on the transformer winding.

The terminal bushings of large size power transformer are made of condenser type bushing. The terminal itself consists of a brass rod or tube which is wound with alternate layers of treated paper and tin foil, so proportioned, as to length, that the series of condensers formed by the tin foil cylinders and the intervening insulation have equal capacitances, thereby the dielectric stress is distributed uniformly.

Circuit Breakers. The basic construction of any circuit breaker requires the separation of contacts in an insulating fluid which serves two functions here:

(*i*) It extinguishes the arc drawn between the contacts when the CB, opens.

(*ii*) It provides adequate insulation between the contacts and from each contact to earth.

Many insulating fluids are used for arc extinction and the fluid chosen depends upon the rating and type of C.B. The insulating fluids commonly used for circuit breakers are

(*i*) Air at atmospheric pressure: Air break circuit breaker upto 11 kV.

(*ii*) Compressed air (Air blast circuit breaker between 220 kV and 400 kV)

(*iii*) Mineral oil which produces hydrogen for arc extrictrion (transformer oil)

(*a*) Plain break oil, C.B. 11 kV–66 kV

(*b*) Controlled break oil C.B. or bulk oil C.B. between 66 kV–220 kV

(*c*) Minimum oil C.B. between 66 kV and 132 kV.

(*iv*) Ultra high vacuum C.B. upto 33 kV.

(*v*) SF_6 circuit breakers above 220 kV.

The controlled break and minimum oil circuit breakers enclose the breaker contacts in an arcing chamber made of insulating materials such as glassfibre reinforced synthetic resins etc.

Rotating Machines. For low voltage a.c. and d.c. machines, the winding wire are super enamelled wire and the other insulation used are vulcanised rubber and varnished cambric and paper. For high voltage and large power capacity machines, the space limitations demand the use of insulating materials having substantially greater dielectric strength. Mica is considered to be a good choice not only due to space requirements but because of its ability to withstand higher temperatures. However, the brittleness of mica makes it necessary to build up the required thickness by using thin flakes cemented together by varnish or bakelite generally with a backing of thin paper or cloth and then baking it under pressure. Epoxy resin bounded mica paper is widely used for both low and high voltage machines. Multilayer slot insulation is made of press board and polyester film. However, for machines with high operating temperatures kapton polymide is used for slot insulation. Mica has always been used for stator insulations. In addition to mica, conducting non-woven polyesters are used for corona protection both inside and at the edges of the slots. Glass fibre reinforced epoxy wedge profiles are used to provide support between the winding bars, slots and the core laminations.

Power Cables. The various insulating materials used are vulcanised rubber, PVC, Polyethylene and impregnated papers.

Vulcanised rubber, insulated cables are used for wiring of houses, buildings and factories for low power work.

PVC is inert to oxygen, oils, alkalies and acids and therefore, if the environmental conditions are such that these things are present in the atmosphere, PVC is more useful than rubber.

Polyethylene is used for high frequency cables. This has been used to a limited extent for power cables also. The thermal dissipation properties are better than those of impregnated poper. The maximum oprating temperature of this cable under short circuits is 100°C.

In case of impregnated paper, a suitable layer of the paper is lapped on the conductor depending upon the operating voltage. It is then dried by the combined application of heat and vacuum. The compound used in case of impregnated paper is semifluid and when the cables are laid on gradients the fluid tends to move from higher to lower gradients which reduces the compound content at higher gradients and may result in void formation at higher gradients. For this reason, impregnated paper cables are used upto 3.3 kV.

Following methods are used for elimination of void formation in the cables:

(*i*) The use of low viscosity mineral oil for the impregnation of the dielectric and the inclusion of oil channels so that any tendency of void formation (due to cyclic heating and cooling of impregnate) is eliminated.

(*ii*) The use of inert gas at high pressure within the metal sheath and indirect contact with the dielectric.

Because of the good thermal characteristics and high dielectric strength of the gas SF_6, it is used for insulating the cables also. SF_6 gas insulated cables can be matched to overhead lines and can be operated corresponding to their surge impedance loading. These cables can be used for transporting thousands of MVA even at UHV, whereas the conventional cables are limited to 1000 MVA and 500 kV.

Power Capacitors. Capacitor design economics suggests the use of individual unit assembled in appropriate series and parallel connected groups to obtain the desired bank voltage and reactive power ratings both in shunt and series capacitor equipments. Series capacitor duty usually requires that a unit designated for a series application be more conservatively rated than a shunt unit. However, there is no basic difference in the construction of the two capacitors.

The most commonly used capacitor for the purpose is the impregnated paper capacitor. This consists of a pair of aluminium foil electrodes separated by a number of Kraft paper tissues which are impregnated with chlorinated diphenyl and has a higher permittivity and results in reduction in the quantity of materials required for a given capacitance and the cost.

The working stress of an impregnated paper is 15 to 25 V/μ and papers of thickness 6–12μ are available and hence depending upon the operating voltage of the capacitor, a suitable thickness of the paper can be selected. Because of imperfection involved in the manufacturing process of the dielectric paper it is desirable to use at least two layers of tissues between metal foils so that the possibility of coincidence of weak spots is avoided.

The effective relative permittivity depends upon the paper and the impregnant. For chlorinated diphenyl impregnant the relative permittivity lies between 5 and 6. Normally through past experience, the area of the plate for a particular material of paper and impregnant per microfarad of capacitance is known and hence it is possible to obtain the number of turns of paper to be wound on a given diameter of mandrel for a specified foil width and for the particular lay-up of foil and paper.

The method of laying up the paper and metallic foil and the connection of lugs is shown in Fig. 1.20. Two layers of dielectric are used as without it rolling would short circuit the plates. As a result of this, two capacitors in parallel are formed by the roll. The foil and the paper interleaved in this fashion are wound on to a mandrel which is split to allow easy removal of the finished roll. If the section of the container is same as that of the roll, minimum overall value for the capacitor is obtained. As a result of this, quantity of free impregnant is a minimum thereby the risk of leakage of impregnant with variation in temperature is reduced. Sometimes a high resistance (for discharge) is connected across the terminals of the capacitor for safety reasons.

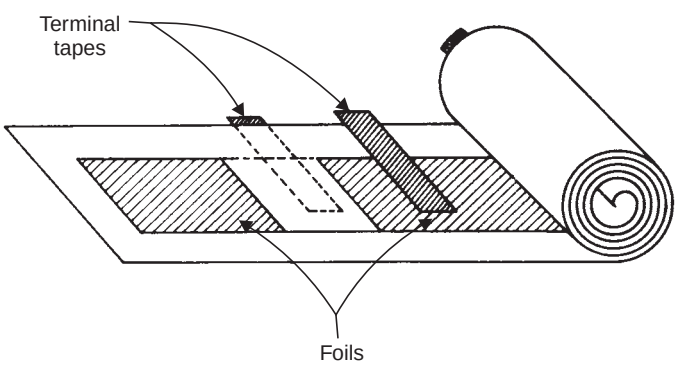

Fig. 1.20. Impregnated paper capacitor-terminal tape type

The replacement of linen by the Kraft paper and oil by askarel made it possible to have individual unit ratings upto 15 kVAr by 1930. After making some costly refinements in basic paper/askarel dielectric 100 kVAr rating capacitor were manufactured by 1960.

General Electric Company designed a 150 kVAr unit using a paper/poly propylene film/askarel dielectric.

Further advances in the manufacture of dielectric materials led to single unit of 600 kVAr even though the rating of a single unit based on economy ranges between 200 and 300 kVAr. Replacement of askarel with non-PCB fluids did not have much effect on unit sizes or ratings. The newer all polypropylene film dielectric units offer distinct advantages in reduced losses and probability of case rapture as well as improvement in unit ratings. The large size units have made it possible to reduce the physical equipment size and the site area requirements.

With further development, it has now been possible to have series and shout capacitor rating upto 550 kV and bank rating of upto 800 MVAr. The average price of smaller units in terms of 100 kVAr is Rs. 100 per kVAr or $2 per kVAr. It is to be noted that aluminium foil are used in these capacitors as it has high thermal and electrical conductivity, has high tensile strength, high melting point, is light in weight, low cost and is easily available.

Capacitor Bushings. Capacitor bushing is used for the terminals of high voltage transformers and switch gears. The power conductor is insulated from the flange by a capacitor bushing consisting of some dielectric material with metal foils cylinderical sheaths of different lengths and radii embedded in it as shown in Fig. 1.21 thus splitting up what essentially a capacitor having high voltage conductor and flange as it's plates, into a number of capacitors in series.

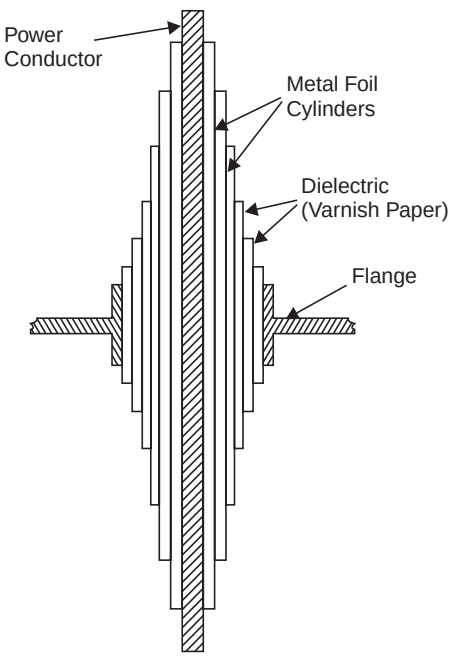

Fig. 1.21. Capacitor bushing

The capacitance of the capacitors formed by the metal foil cylinders is given by

$$C = \frac{\varepsilon l}{2 \ln \frac{R_2}{R_1}}$$

where l is the axial length of the capacitor R_1 and R_2 are the radii of its cylinderical plates. If these capacitor have the same capacitance, the potential difference between their plates will be equal. The equal capacitance between different layers is made possible by choosing suitable axial length together with ratio $\frac{R_2}{R_1}$. With this strategy the potential gradient in the dielectric is uniform but the edges of the foil sheets lie on a curve, thus giving unequal surfaces of dielectric between the edges of successive sheets. This is undesirable as this would result into flashovers by "Creeping" along the surface. However, if the differences between the lengths of successive sheets are made equal, the radial stress is not uniform and hence a compromise between the two conditions is usually adopted.

There are three types of papers used as insulating materials for capacitor bushings; oil impregnated paper, resin bonded paper and resin impregnated paper. The oil impregnated paper bushing is made by wrapping untreated paper after inserting foil sheets at the appropriate position and then impregnating with transformer oil after vacuum drying. Before impregnation, it is ensured that moisture and air voids are avoided. This bushing can work at a radial stress of 40 kV/cm.

In case of resin impregnated bushing creped paper tape is wrapped round the conductor and then dried in an autoclave under controlled heat and vacuum. Epoxyresin is then sprayed to fill the winding. The permissible radial stress in this case is 30 kV/cm.

In case of resin bonded paper bushing, the paper is first coated with epoxyresin and wrapped round a cylinderical form under heat and pressure after inserting foil sheets at appropriate position. The permissible radial stress in this case in 20 kV/cm.

1.15 BREAKDOWN IN VACUUM

A vacuum system is one in which the pressure maintained is at a value below the atmospheric pressure and is measured in terms of mm of mercury. One standard atmospheric pressure at 0°C is equal to 760 mm of mercury. One mm of Hg pressure is also known as *one torr* after the name of Torricelli who was the first to obtain pressures below atmosphere, with the help of mercury barometer. Sometimes 10^{-3} torr is known as one micron. It is now possible to obtain pressures as low as 10^{-8} torr.

In a Townsend type of discharge, in a gas, the mean free path of the particles is small and electrons get multiplied due to various ionization processes and an electron avalanche is formed. In a vacuum of the order of 10^{-5} torr, the mean free path is of the order of few metres and thus when the electrodes are separated by a few mm an electron crosses the gap without any collision. Therefore, in a vacuum, the current growth prior to breakdown can not take place due to formation of electron avalanches. However, if it could be possible to liberate gas in the vacuum by some means, the discharge could take place according to Townsend process. Thus, a vacuum arc is different from the general class of low and high pressure arcs. In the vacuum arc, the neutral atoms, ions and electrons do not come from the medium in which the arc is drawn but they are obtained from the electrodes themselves by

evaporating its surface material. Because of the large mean free path for the electrons, the dielectric strength of the vacuum is a thousand times more than when the gas is used as the interrupting medium. In this range of vacuum, the breakdown strength is independent of the gas density and depends only on the gap length and upon the condition of electrode surface. Highly polished and thoroughly degassed electrodes show higher breakdown strength. Electrodes get roughened after use and thus the dielectric strength or breakdown strength decreases which can be improved by applying successive high voltage impulses which of course does not change the roughened surface but removes the loosely adhering metal particles from the electrodes which were deposited during arcing. It has been observed that for a vacuum of 10^{-6} torr, some of the metals like silver, bismuth-copper etc. attain their maximum breakdown strength when the gap is slightly less than 3 mm. This property of vacuum switches permits the use of short gaps for fast operation.

Electric Discharge in Vacuum

The electric discharge in vacuum results from the neutral atoms, ions and electrons emitted from the electrodes themselves. Cathode spots are formed depending upon the current flowing. For low currents a highly mobile cathode spot is formed and for large currents a multiple number of cathode spots are formed. These spots constitute the main source of vapour in the arc. The processes involved in drawing the discharge will be due to high electric field between the contacts or resistive heating produced at the point of operation or a combination of the two. The cathode surfaces, normally, are not perfectly smooth but have many micro projections. Due to their small area of cross-section, the projections will suffer explosive evaporation by resistive heating and supply sufficient quantity of vapour for the arc formation. Since in case of vacuum, the emission occurs only at the cathode spots and not from the entire surface of the cathode, the vacuum discharge is also known as *cold cathode discharge*. In cold cathode the emission of electrons could be due to any of the combinations of the following mechanisms: (*i*) Field emission; (*ii*) Thermionic emission; (*iii*) Field and Thermionic emission; (*iv*) Secondary emission by positive ion bombardment; (*v*) Secondary emission by photons; and (*vi*) Pinch effect.

The stability of discharge in vacuum depends upon: (*i*) the contact material and its vapour pressure, and (*ii*) circuit parameters such as voltage, current, inductance and capacitance. It has been observed that higher the vapour pressure at low temperature the better is the stability of the discharge. There are certain metals like Zn, Bi which show these characteristics and are better electrode materials for vacuum breakers. Besides the vapour pressure, the thermal conductivity of the metal also affects the current chopping level. A good heat conducting metal will cool its surface faster and hence its electrode surface temperature will fall which will result into reduction in evaporation rate and arc will be chopped because of insufficient vapour. On the other hand, a bad heat conductor will maintain its temperature and vaporization for a longer time and the arc will be more stable.

The process of multiplication of charged particles by the process of collision is very small in the space between the electrode in vacuum, electron avalanche is not possible. If somehow a gas cloud could be formed in vacuum, the usual kind of breakdown process can take place. This is the line of action adopted by the researchers to study mechanism of breakdown in vacuum. By finding the way, gas cloud could be created in a vacuum.

1.15.1 Non-metallic Electron Emission Mechanism

The pre-breakdown conduction current in vacuum normally originates from a nonmetallic electrode surface. These are present in the form of insulating/semiconducting oxide layer on the surfaces or as impurities in the electrode material. These microinclusions present in the electrode surface can produce strong electron emission and significantly reduce the break down strength of the gap.

Even when a vacuum system is completely sealed off, the electrode surfaces may still get contaminated. It has been observed that when glass is heated to 'its' working temperature for sealing the electrodes into a closed container, fluxes are vaporised from the glass which get deposited in the cool inner surfaces in the form of spherical particles upto a μm diameter . Therefore, the surface of a sealed electrode may have on its surface contaminates *e.g.*, sodium, potassium, boron aluminium and silicon. When an electric field is applied across such electrodes the oxides adsorbates and dust particles, then undergo chemical changes *e.g.*, oxides and adsorbates undergo chemical reactions which are initiated by photons, electrons and ions and thus these contaminants limit the maximum field intensity for the following reasons:

(*i*) The adsorbates and dust enhance the field emission of electrons.

(*ii*) The oxides adsorbates and dust particles enhance the secondary electron emission.

(*iii*) The oxides adsorbates and dust particles exhibit stimulated desorption of molecules and ions under the impact of electrons, protons or ions.

Due to these mechanism, there is increase in electron emission process and therefore, more electric field energy is converted into kinetic energy of electron and ions which leads to an increase in surface energy of the metal. Thus, the electric strength of the gap may reduce to a level as low as 10 kV/cm as compared to 10^4 kV/cm which is required for the field emission process.

1.15.2 Clump Mechanism

The vacuum breakdown mechanism based on this theory makes following assumption:

(*i*) A loosely bound particle known as *clump* exists on one of the electrode surfaces.

(*ii*) When a high voltage is applied between the two electrodes, this clump gets charged and subsequently gets detached from the mother electrode and is attracted by the other electrode.

(*iii*) The breakdown occurs due to a discharge in the vapour or gas released by the impact to the particle at the opposite electrode.

It has been observed that for a certain vacuum gap if frequent recurrent electric breakdowns are carried out, the withstand voltage of the gap increases and after certain number of breakdown, it reaches an optimum maximum value. This is known as *conditioning* of electrodes and is of paramount importance from practical reasons. In this electrode conditioning, the microemission sites are supposed to have been destroyed.

Various methods for conditioning the electrodes have been suggested. Some of these are

(*i*) To treat the electrodes by means of hydrogen glow discharge. This method gives more consistent results.

(*ii*) Allowing the pre-breakdown currents in the gap to flow for some time or to heat the electrodes in vacuum to high temperature.

(*iii*) Treating the electrodes with repeated spark breakdown. This method is however quite time consuming.

The area of electrodes for breakdown of gases, liquids, solids or vacuum plays an important role. It has been observed that if the area of electrodes is increased for the same gap distance in uniform field, the breakdown voltages are reduced.

1.15.3 Effect of Pressure on Breakdown Voltage

It has been observed that in case of very small gaps of less than a mm and the gas pressure between the gap lies in the range 10^{-9} to 10^{-2} Torr, there is no change in the breakdown voltage *i.e.*, if the gap length is small a variation of gas pressure in the range given above doesn't affect the breakdown voltage. However, if the gap length is large say about 20 cm, the variation of gas pressure between the gap adversely affects the withstand voltage and the withstand voltage lowers drastically.

EXAMPLES

Example 1.1 *A steady current of 600 μA flows through the plane electrode separated by a distance of 0.5 cm when a voltage of 10 kV is applied. Determine the Townsend's first ionization coefficient if a current of 60 μA flows when the distance of separation is reduced to 0.1 cm and the field is kept constant at the previous value.*

Solution: Since the field is kept constant (*i.e.*, if distance of separation is reduced, the voltage is also reduced by the same ratio so that *V/d* is kept constant).

$$I = I_0 e^{\alpha x}$$

Substituting two different sets of values,

we have $600 = I_0 e^{0.5\alpha}$ and $60 = I_0 e^{0.1\alpha}$

or $10 = e^{0.4\alpha}$ or $0.4\ \alpha = 1n\ 10$

$$0.4\ \alpha = 2.3026$$

$$\alpha = 5.75 \text{ ionizing collisions/cm.}$$

Example 1.2. *The following table gives two sets of experimental results for studying Townsend's mechanism. The field is kept constant in each set:*

I set 30 kV/cm *Gap distance (mm)*	*II set kV/cm* *Observed current A*	
	I set	*II set*
0.5	1.5×10^{-13}	6.5×10^{-14}
1.0	5×10^{-13}	2.0×10^{-13}
1.5	8.5×10^{-13}	4×10^{-13}
2.0	1.5×10^{-12}	8×10^{-13}
2.5	5.6×10^{-12}	1.2×10^{-12}
3.0	1.4×10^{-10}	6.5×10^{-12}
3.5	1.4×10^{-10}	6.5×10^{-11}
4.0	1.5×10^{-9}	4.0×10^{-10}
5.0	7.0×10^{-7}	1.2×10^{-8}

The manimum current observed is 6×10^{-14} A. Determine the values of Townsend's first and second ionization coefficients.

Solution: 1st Set. Since there is gradual increase in current upto gap distance of 3 mm, slope between any two points

$$\left(\frac{1\text{n } I/I_0}{x}\right)$$

will give us the value of α.

Let us take gap distances of 2 and 2.5 mm.

The respective $1\text{n } I/I_0$ are

$$1\text{n}\left(\frac{1.5\times10^{-12}}{6\times10^{-14}}\right) = 3.2188$$

and

$$1\text{n}\left(\frac{1.5\times10^{-12}}{6\times10^{-14}}\right) = 4.5362$$

$\therefore$ The slope $= \dfrac{4.5362 - 3.2188}{0.05} = 26.34$

Since there is sudden rise in current at the last observation, this is used to evaluate γ.

We know that

or $$I = \frac{I_0 e^{\alpha x}}{1-\gamma\,(e^{\alpha x}-1)}$$

or $$\frac{I}{I_0} = \frac{7}{6}\times10^7 = \frac{e^{26.34\times0.5}}{1-\gamma(e^{13.17}-1)}$$

$$= \frac{5.24\times10^5}{1-5.24\times10^5\,\gamma}$$

or $$\frac{7}{6}\times10^7\,\frac{1}{5.24\times10^5} = \frac{1}{1-5.24\times10^5\,\gamma}$$

or $$0.0449 = 1 - 5.24\times10^5\,\gamma$$

or $$0.9551 = 5.24\times10^5\,\gamma$$

or $$\gamma = 0.182\times10^{-5}\text{ /cm.}$$

Set-II. For the same gap distance the slope will be α = 1n (12/8)/0.05 = 8.1 collisions/cm and therefore

$$\frac{I}{I_0} = 2\times10^5 = \frac{e^{8.1\times0.5}}{1-\gamma(e^{4.05}-1)}$$

$$2\times10^5 = \frac{57.39}{1-\gamma\,(56.39)}$$

or $$\frac{200\times10^3}{57.39} = 3.4849\times10^3 = \frac{1}{1-56.39\gamma}$$

$$2.87\times10^{-4} = 1 - 56.39\,\gamma$$

$$56.39\gamma = 1.0$$

or $$\gamma = 1.7 \times 10^{-2} \text{ collisions/cm}$$

Example 1.3. *The following observations were made in an experiment for determination of dielectric strength of transformer oil. Determine the power law equation.*

Gap spacing	*4*	*6*	*8*	*10*
Breakdown Voltage (kV)	*88*	*135*	*165*	*212*

Solution: Let us assume that the relation between gap spacing and breakdown voltage be given as

$$V_b = Kd^n$$

Our objective is to find out values of K and n. Substituting values of two observations , we have

$$88 = K.4^n$$

$$165 = K.8^n$$

$\therefore$ $$\frac{165}{88} = \frac{8^n}{4^n} = 2^n$$

$$1.875 = 2^n$$

$$0.6286 = n \times 0.693$$

or $$n = 0.9068$$

and $$K = \frac{88}{4^{0.9068}} = 25.03$$

Similarly taking 2nd and 4th observation, we have

$$135 = K6^n$$

$$212 = K10^n$$

or $$\frac{212}{135} = 1.67^n$$

$$1.57 = 1.67^n$$

Taking 1n on both sides

$$0.4513 = 0.5128\ n$$

or $$n = 0.88$$

and $$K = \frac{135}{6^{0.88}} = 27.9$$

Therefore, average value of $n \approx 0.89$ and that of $K \approx 26.46$ Ans.

Example 1.4. *State and explain Paschen's law. Derive expression for $(pd)_{min}$ and V_{bmin}. Assume $A = 12$, $B = 365$ and $\gamma = 0.02$ for air. Determine $(pd)_{min}$ and V_{bmin}.*

Solution: We know that

$$(pd)_{\min} = \frac{ek}{A}$$

where $$K = \ln (1 + 1/\gamma)$$

Therefore, $(pd)_{\min} = \frac{e}{A} \ln (1 + 1/\gamma)$

Substituting the values, we have

$$(pd)_{\min} = \frac{2.718}{12} 1\text{n}\,(1 + 1/0.02) = 0.89 \quad \text{Ans.}$$

Now $$V_{bmin} = \frac{B}{A} e K = \frac{365}{12} \times 2.718\, 1\text{n}\, 51 = 325 \text{ Volts} \quad \text{Ans.}$$

PROBLEMS

1.1. Discuss various factors which affect breakdown of gases.

1.2. Define Townsend's first and second ionisation coefficients. Explain the Townsends criterion for a spark.

1.3. State and explain Paschen's law. How do you account for the minimum voltage for breakdown under a given *pd* condition?

1.4. Explain the mechanism of development of anode and cathode streamers and explain how these lead to breakdown.

1.5. What is time-lag? Discuss its components and the factors which affect these components.

1.6. Explain briefly various theories of breakdown in liquid dielectrics.

1.7. Explain clearly suspended particle mechanism of liquid breakdown.

1.8. State various process which lead to formation of bubbles in liquid dielectrics and explain clearly cavity breakdown mechanism in liquid dielectrics.

1.9. What is electroconvection? Explain liquid breakdown based on electroconvection.

1.10. Discuss various criteria suggested by researchers for transition from avalanche to streamer.

1.11. Explain Penning Effect when referred to gaseous discharges.

1.12. What is corona discharge? Explain clearly Anode and Cathode coronas.

1.13. Describe briefly various mechanism of breakdown in solids.

1.14. What are 'Treeing' and 'Tracking'? Explain clearly the two processes in solid dielectrics.

1.15. Derive an expression for maximum thermal voltage and show that the voltage is independent of thickness of specimen. State clearly the assumptions made.

1.16. Derive an expression for critical electric field and show that the field is independent of the critical temperature of the dielectric. State the assumptions made.

1.17. What do you mean by 'Intrinsic strength' of a solid dielectric? Explain electric breakdown of solid dielectrics.

1.18. Explain Thermal breakdown in solid dielectrics. How this mechanism is more significant than the other mechanisms?

1.19. Explain the process of breakdown in electronegative gases.

1.20. Explain the application of oil in power apparatus and discuss clearly its function with reference to a circuit breaker.

1.21. Describe the main requirements of solid insulating materials used for power apparatus and describe the dielectric characteristics of the following material:

(*i*) vulcanized rubber (*ii*) PVC (*iii*) cross-link polyethylene (*iv*) insulating press board (*v*) mica (*vi*) ceramics (*vii*) glass (*viii*) epoxy resins.

1.22. Describe the application of various insulating materials used in the following power apparatus:

(*i*) Power transformers (*ii*) Circuit breakers

(*iii*) Rotating machines (*iv*) Power cables

(*v*) Power capacitors (*vi*) Capacitor bushings

1.23. Explain clearly various processes which explain electric breakdown in vacuum.

1.24. What is ''conditioning of elecrodes''? How does it affect breakdown in vacuum?

1.25. Discuss the effect of ''Area of electrode'' and ''Effect of pressure'' on the breakdown of vacuum.

1.26. Discuss the application of gases in electric power apparatus.

REFERENCES

Alston, *High Voltage Technology*, Oxford University Press, 1968.

E.W. Mc Daniel, *Collision Phenomenon in Ionised Gases*, John Wiley, New York, 1964.

L.D. Loeb, *The kinetic Theory of Gases*, Johm Wiley, New York, 1963.

E. Kuffel and W.S. Zaengl, *High Voltage Engineering-Fundamentals*, Pergamon Press, 1984.

M.S. Naidu and V. Kamaraju, *High Voltage Engineering*, Tata McGraw-Hill 1982.

Ravindra Arora & W. Mosch, *High Voltage Insulation Engineering*, New Age International, 2005.

2 Generation of High D.C. and A.C. Voltages

There are various applications of high d.c. voltages in industries, research medical sciences etc. HVDC transmission over both overhead lines and underground cables is becoming more and more popular. HVDC is used for testing HVAC cables of long lengths as these have very large capacitance and would require very large values of currents if tested on HVAC voltages. Even though D.C. tests on A.C. cables is convenient and economical, these suffer from the fact that the stress distribution within the insulating material is different from the normal operating condition. In industry it is being used for electrostatic precipitation of ashing in thermal power plants, electrostatic painting, cement industry, communication systems etc. HVDC is also being used extensively in physics for particle acceleration and in medical equipments (X-Rays).

The most efficient method of generating high D.C. voltages is through the process of rectification employing voltage multiplier circuits. Electrostatic generators have also been used for generating high D.C. voltages.

According to IEEE standards 4-1978, the value of a direct test voltage is defined by its arithematic mean value V_d and is expressed mathematically as

$$V_d = \frac{1}{T}\int_0^T \upsilon(t)dt \tag{2.1}$$

where T is the *time period* of the voltage wave having a frequency $f = 1/T$. Test voltages generated using rectifiers are never constant in magnitude. These deviate from the mean value periodically and this deviation is known as *ripple*. The magnitude of the ripple voltage denoted by δV is defined as half the difference between the maximum and minimum values of voltage *i.e.*,

$$\delta V = \frac{1}{2}[V_{max} - V_{min}] \tag{2.2}$$

and ripple factor is defined as the ratio of ripple magnitude to the mean value V_d *i.e.*, $\delta V/V_d$. The test voltages should not have ripple factor more than 5% or as specified in a specific standard for a particular equipment as the requirement on voltage shape may differ for different applications.

2.1 HALF-WAVE RECTIFIER CIRCUIT

The simplest circuit for generation of high direct voltage is the half wave rectifier shown in Fig. 2.1 Here R_L is the load resistance and C the capacitance to smoothen the d.c. output voltage.

If the capacitor is not connected, pulsating d.c. voltage is obtained at the output terminals whereas with the capacitance *C*, the pulsation at the output terminal are reduced. Assuming the ideal transformer and small internal resistance of the diode during conduction the capacitor *C* is charged to the maximum voltage V_{max} during conduction of the diode *D*. Assuming that there is no load connected, the d.c. voltage across capacitance remains constant at V_{max} whereas the supply voltage oscillates between $\pm V_{max}$ and during negative half cycle the potential of point *A* becomes $-V_{max}$ and hence the diode must be rated for $2V_{max.}$ This would also be the case if the transformer is grounded at *A* instead of *B* as shown in Fig. 2.1 (*a*). Such a circuit is known as *voltage doubler* due to Villard for which the output voltage would be taken across *D*. This d.c. voltage, however, oscillates between zero and $2V_{max}$ and is needed for the Cascade circuit.

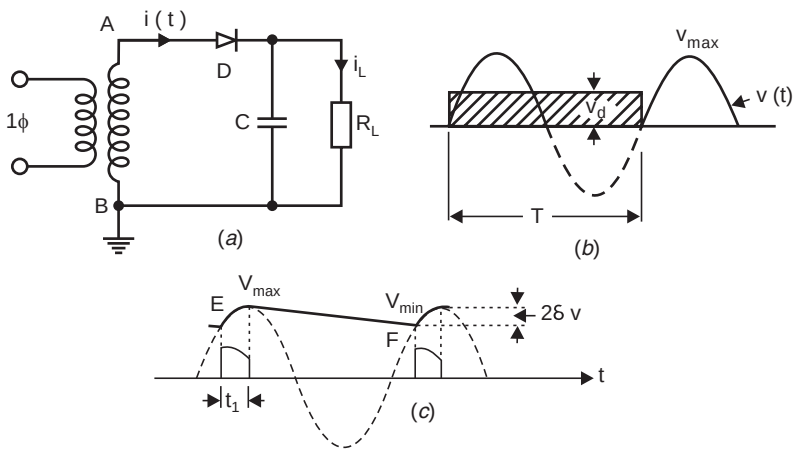

Fig. 2.1 (*a*) Single Phase rectifier (*b*) Output voltage without *C* (*c*) Output voltage with *C*

If the circuit is loaded, the output voltage does not remain constant at V_{max}. After point *E* (Fig. 2.1 (*c*)), the supply voltage becomes less than the capacitor voltage, diode stops conducting. The capacitor can not discharge back into the a.c. system because of one way action of the diode. Instead, the current now flows out of *C* to furnish the current i_L through the load. While giving up this energy, the capacitor voltage also decreases at a rate depending on the time constant *CR* of the circuit and it reaches the point *F* corresponding to V_{min}. Beyond *F*, the supply voltage is greater than the capacitor voltage and hence the diode *D* starts conducting charging the capacitor *C* again to V_{max} and also during this period it supplies current to the load also. This second pulse of $i_p(i_c + i_l)$ is of shorter duration than the initial charging pulse as it serve mainly to restore into *C* the energy that *C* meanwhile had supplied to load. Thus, while each pulse of diode current lasts much less than a half cycle, the load receives current more continuously from *C*.

Assuming the charge supplied by the transformer to the load during the conduction period *t*, which is very small to be negligible, the charge supplied by the transformer to the capacitor during conduction equals the charge supplied by the capacitor to the load. Note that $i_c >> i_L$. During one period $T = 1/f$ of the a.c voltage, a charge *Q* is transferred to the load R_L and is given as

$$Q = \int_T i_L(t)\, dt = \int_T \frac{V_{RL}(t)}{R_L} dt = IT = \frac{I}{f}$$

where I is the mean value of the d.c output $i_L(t)$ and $V_{RL}(t)$ the d.c. voltage which includes a ripple as shown in Fig. 2.1 (*c*).

This charge is supplied by the capacitor over the period T when the voltage changes from V_{max} to V_{min} over approximately period T neglecting the conduction period of the diode.

Suppose at any time the voltage of the capacitor is V and it decreases by an amount of dV over the time dt then charge delivered by the capacitor during this time is

$$dQ = CdV$$

Therefore, if voltage changes from V_{max} to V_{min}, the charge delivered by the capacitor

$$\int dQ = \int_{V_{max}}^{V_{\min}} CdV = -C\left(V_{max} - V_{min}\right)$$

Or the magnitude of charge delivered by the capacitor

$$Q = C\,(V_{max} - V_{min}) \tag{2.3}$$

Using equation (2.2)

$$Q = 2\delta VC \tag{2.4}$$

Therefore, $2\delta VC = IT$

or
$$\delta V = \frac{IT}{2C} = \frac{I}{2fC} \tag{2.5}$$

Equation (2.5) shows that the ripple in a rectifier output depends upon the load current and the circuit parameter like f and C. The product fC is, therefore, an important design factor for the rectifiers. The higher the frequency of supply and larger the value of filtering capacitor the smaller will be the ripple in the d.c. output.

The single phase half-wave rectifier circuits have the following disadvantages:

(*i*) The size of the circuits is very large if high and pure d.c. output voltages are desired.

(*ii*) The h.t. transformer may get saturated if the amplitude of direct current is comparable with the nominal alternating current of the transformer.

It is to be noted that all the circuits considered here are able to supply relatively low currents and therefore are not suitable for high current applications such as HVDC transmission.

When high d.c. voltages are to be generated, voltage doubler or cascaded voltage multiplier circuits are used. One of the most popular doubler circuit due to Greinacher is shown in Fig. 2.2.

Suppose B is more positive with respect to A and the diode D_1 conducts thus charging the capacitor C_1 to V_{max} with polarity as shown in Fig. 2.2. During the next half cycle terminal A of the capacitor C_1 rises to V_{max} and hence terminal M attains a potential of 2 V_{max}. Thus, the capacitor C_2 is charged to 2 V_{max} through D_2. Normally the voltage across the load will be less than 2 V_{max} depending upon the time constant of the circuit C_2R_L.

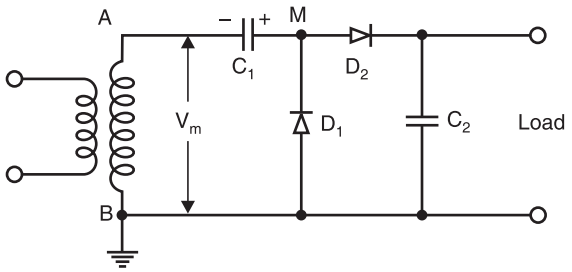

Fig. 2.2 Greinacher voltage doubler circuit

2.2 COCKROFT-WALTON VOLTAGE MULTIPLIER CIRCUIT

In 1932, Cockroft and Walton suggested an improvement over the circuit developed by Greinacher for producing high D.C. voltages. Fig. 2.3. shows a multistage single phase cascade circuit of the Cockroft-Walton type.

No Load Operation: The portion ABM′MA is exactly indentical to Greinarcher voltage doubler circuit and the voltage across C becomes $2V_{max}$ when M attains a voltage $2V_{max}$.

During the next half cycle when B becomes positive with respect to A, potential of M falls and, therefore, potential of N also falls becoming less than potential at M' hence C_2 is charged through D_2. Next half cycle A becomes more positive and potential of M and N rise thus charging C'_2 through D'_2. Finally all the capacitors C'_1, C'_2, C'_3, C_1, C_2, and C_3 are charged. The voltage across the column of capacitors consisting of C_1, C_2, C_3, keeps on oscillating as the supply voltage alternates. This column, therefore, is known as *oscillating column*. However, the voltage across the capacitances C'_1, C'_2, C'_3, remains constant and is known as *smoothening column*. The voltages at M', N', and O' are 2 V_{max} 4 V_{max} and 6 V_{max}. Therefore, voltage across all the capacitors is 2 V_{max} except for C_1 where it is V_{max} only. The total output voltage is $2n$ V_{max} where n is the number of stages. Thus, the use of multistages arranged in the manner shown enables very high voltage to be obtained. The equal stress of the elements (both capacitors and diodes) used is very helpful and promotes a modular design of such generators.

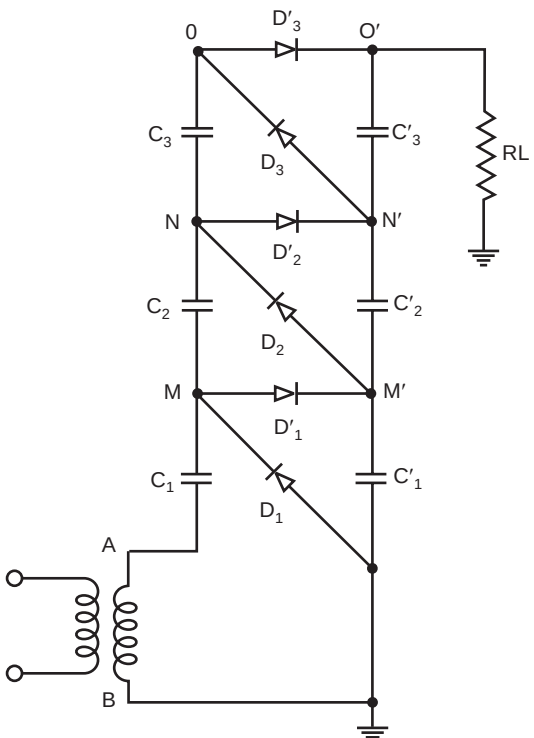

Fig. 2.3

Generator Loaded: When the generator is loaded, the output voltage will never reach the value $2n$ V_{max}. Also, the output wave will consist of ripples on the voltage. Thus, we have to deal with two quantities, the voltage drop ΔV and the ripple δV.

Suppose a charge q is transferred to the load per cycle. This charge is $q = I/f = IT$. The charge comes from the smoothening column, the series connection of C'_1, C'_2, C'_3,. If no charge were transferred during T from this stack via D_1, D_2, D_3, to the oscillating column, the peak to peak ripple would merely be

$$2\delta V = IT \sum_{n=0}^{n} \frac{1}{C'_i} \tag{2.6}$$

But in practice charges are transferred. The process is explained with the help of circuits in Fig. 2.4 (*a*) and (*b*).

Fig. 2.4 (*a*) shows arrangement when point A is more positive with reference to B and charging of smoothing column takes place and Fig. 2.4 (*b*) shows the arrangement when in the next half cycle B becomes positive with reference to A and charging of oscillating column takes place. Refer to Fig. 2.4 (*a*). Say the potential of point O' is now 6 V_{max}. This discharges through the load resistance and say the charge lost is $q = IT$ over the cycle. This must be regained during the charging cycle (Fig. 2.4 (*a*)) for stable operation of the generator. C_3 is, therefore supplied a charge q from C_3. For this C_2 must acquire a charge of $2q$ so that it can supply q charge to the load and q to C_3, in the next half cycle termed by cockroft and Walton as the transfer cycle (Fig. 2.4 (*b*)). Similarly C'_1 must acquire for stability reasons a charge $3q$ so that it can supply a charge q to the load and $2q$ to the capacitor C_2 in the next half cycle (transfer half cycle).

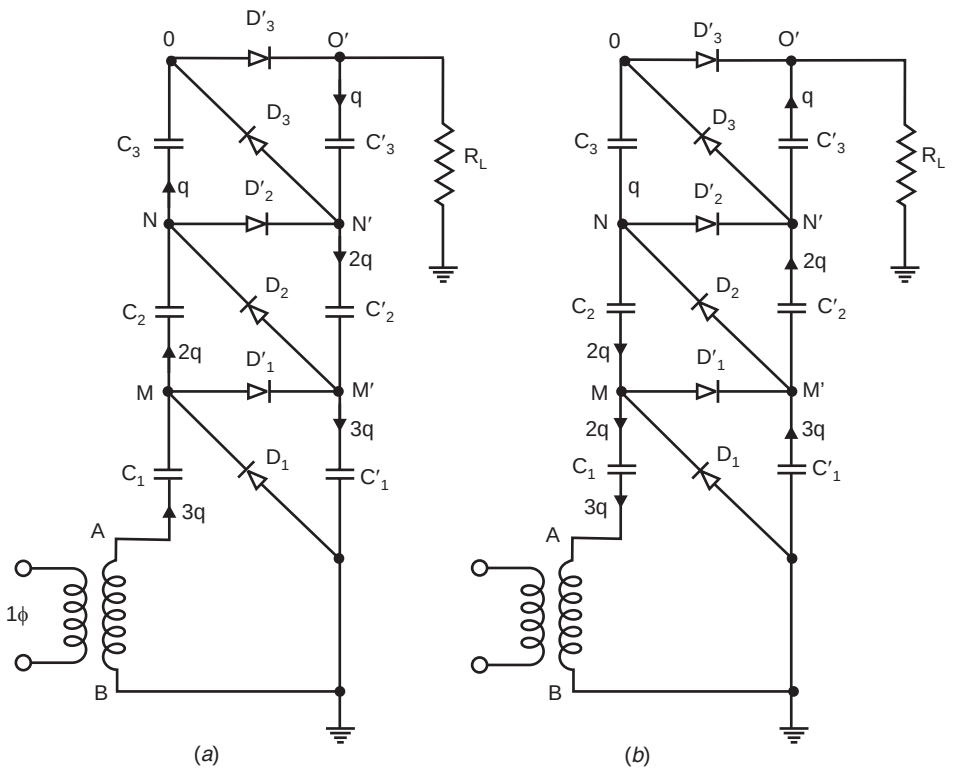

Fig. 2.4 (*a*) Charging of smoothening Column (*b*) Charging of oscillating column

During the transfer cycle shown in Fig. 2.4 (*b*), the diodes D_1, D_2, D_3, conduct when B is positive with reference to A. Here C'_2 transfers q charge to C_3, C_1 transfers charge $2q$ to C_2 and the transformer provides change $3q$.

For n-stage circuit, the total ripple will be

$$2\delta V = \frac{I}{f}\left(\frac{1}{C'_n} + \frac{2}{C'_{n-1}} + \frac{3}{C'_{n-2}} + \ldots + \frac{n}{C'_1}\right)$$

or

$$\delta V = \frac{I}{2f}\left(\frac{1}{C'_n} + \frac{2}{C'_{n-1}} + \frac{3}{C'_{n-2}} + \ldots + \frac{n}{C'_1}\right) \tag{2.7}$$

From equation (2.7), it is clear that in a multistage circuit the lowest capacitors are responsible for most ripple and it is, therefore, desirable to increase the capacitance in the lower stages. However, this is objectionable from the view point of High Voltage Circuit where if the load is large and the load voltage goes down, the smaller capacitors (within the column) would be overstressed. Therefore, capacitors of equal value are used in practical circuits *i.e.*, $C'_n = C'_{n-1} = \ldots C'_1 = C$ and the ripple is given as

$$\delta V = \frac{I}{2fC}\frac{n(n+1)}{2} = \frac{In(n+1)}{4fC} \tag{2.8}$$

The second quantity to be evaluated is the voltage drop ΔV which is the difference between the theoretical no load voltage $2nV_{max}$ and the onload voltage. In order to obtain the voltage drop ΔV refer to Fig. 2.4 (*a*).

Here C'_1 is not charged upto full voltage $2V_{max}$ but only to $2V_{max} - 3q/C$ because of the charge given up through C_1 in one cycle which gives a voltage drop of $3q/C = 3I/fC$

The voltage drop in the transformer is assumed to be negligible. Thus, C_2 is charged to the voltage

$$\left(2V_{max} - \frac{3I}{fC}\right) - \frac{3I}{fC}$$

since the reduction in voltage across C'_3 again is $3I/fC$. Therefore, C'_2 attains the voltage

$$2V_{max} - \left(\frac{3I + 3I + 2I}{fC}\right)$$

In a three stage generator

$$\Delta V_1 = \frac{3I}{fC}$$

$$\Delta V_2 = \{2 \times 3 + (3-1)\}\frac{I}{fC}$$

$$\Delta V_3 = (2 \times 3 + 2 \times 2 + 1)\frac{I}{fC}$$

In general for a *n*-stage generator

$$\Delta V_n = \frac{nI}{fC}$$

$$\Delta V_{n-1} = \frac{I}{fC}\{2n + (n-1)\}$$

$$\Delta V_{n-2} = \frac{I}{fC}\{2n + 2(n-1) + (n-2)\}$$

.
.
.

$$\Delta V_1 = \frac{I}{fC}\{2n + 2(n-1) + 2(n-2) + \ldots 2 \times 3 + 2 \times 2 + 1\}$$

$$\Delta V = \Delta V_n + \Delta V_{n-1} + \ldots + \Delta V_1$$

After omitting I/fC, the series can be rewritten as:

$$T_n = n$$
$$T_{n-1} = 2n + (n-1)$$
$$T_{n-2} = 2n + 2(n-1) + (n-2)$$
$$T_{n-3} = 2n + 2(n-1) + 2(n-2) + (n-3)$$

.
.
.

$$T_1 = 2n + 2(n-1) + 2(n-2) + \ldots + 2 \times 3 + 2 \times 2 + 1$$
$$T = T_n + T_{n-1} + T_{n-2} + \ldots + T_1$$

To sum up we add the last term of all the terms (T_n through T_1) and again add the last term of the remaining term and so on, *i.e.*,

$$[n + (n-1) + (n-2) + \ldots + 2 + 1]$$
$$+ [2n + 2(n-1) + 2(n-2) + \ldots + 2 \times 2]$$
$$+ [2n + 2(n-1) + \ldots + 2 \times 4 + 2 \times 3]$$
$$+ [2n + 2(n-1) + \ldots + 2 \times 4]$$
$$+ [2n + 2(n-1) + 2(n-2) + \ldots + 2 \times 5] + \ldots [2n]$$

Rearranging the above terms we have

$$n + (n-1) + (n-2) + \ldots + 2 + 1$$
$$+ [2n + 2(n-1) + 2(n-2) + \ldots + 2 \times 2 + 2 \times 1] - 2 \times 1$$
$$+ [2n + 2(n-1) + 2(n-2) + \ldots + 2 \times 3 + 2 \times 2 + 2 \times 1] - 2 \times 2 - 2 \times 1$$
$$+ [2n + 2(n-1) + 2(n-2) + \ldots + 2 \times 4 + 2 \times 3 + 2 \times 2 + 2 \times 1]$$
$$- 2 \times 3 - 2 \times 2 - 2 \times 1$$

.
.
.

$$[2 \times n + 2(n-1) + \ldots + 2 \times 2 + 2 \times 1] - [2(n-1)]$$
$$+ 2(n-2) + \ldots + 2 \times 2 + 2 \times 1]$$

or $n + (n-1) + (n-2) + ... + 2 + 1$

Plus $(n-1)$ number of terms of 2 $[n + (n-1) + ... + 2 + 1]$

minus 2 $[1 + (1+2) + (1+2+3) + ... + ... \{1 + 2 + 3 + ... (n-1)\}]$

The last term (minus term) is rewritten as

$$2 [1 + (1+2) + ... + \{1 + 2 + 3 + ... (n-1)\} + \{1 + 2 + ... + n\}]$$
$$- 2 [1 + 2 + 3 + ... + n]$$

The nth term of the first part of the above series is given as

$$t_n = \frac{2n(n+1)}{2} = (n^2 + n)$$

Therefore, the above terms are equal to

$$= \sum (n^2 + n) - 2 \sum n$$
$$= \sum (n^2 - n)$$

Taking once again all the term we have

$$T = \sum n + 2(n-1) \sum n - \sum (n^2 - n)$$
$$= 2n \sum n - \sum n^2$$
$$= 2n \cdot \frac{n(n+1)}{2} - \frac{n(n+1)(2n+1)}{6}$$
$$= \frac{6(n^3 + n^2) - n(2n^2 + 3n + 1)}{6}$$
$$= \frac{6n^3 + 6n^2 - 2n^3 - 3n^2 - n}{6}$$
$$= \frac{4n^3 + 3n^2 - n}{6} = \frac{2}{3}n^3 + \frac{n^2}{2} - \frac{n}{6} \qquad (2.9)$$

Here again the lowest capacitors contribute most to the voltage drop ΔV and so it is advantageous to increase their capacitance in suitable steps. However, only a doubling of C_1 is convenient as this capacitors has to withstand only half of the voltage of other capacitors. Therefore, ΔV_1 decreases by an amount nI/fC which rreduces ΔV of every stage by the same amount *i.e.*, by

$$n \cdot \frac{nI}{2fC}$$

Hence $$\Delta V = \frac{I}{fC}\left(\frac{2}{3}n^3 - \frac{n}{6}\right) \qquad (2.10)$$

If $n \geq 4$ we find that the linear term can be neglected and, therefore, the voltage drop can be approximated to

$$\Delta V \approx \frac{I}{fC} \cdot \frac{2}{3}n^3 \qquad (2.11)$$

The maximum output voltage is given by

$$V_{0\,max} = 2nV_{max} - \frac{I}{fC}\cdot\frac{2}{3}n^3 \tag{2.12}$$

From (2.12) it is clear that for a given number of stages, a given frequency and capacitance of each stage, the output voltage decrease linearly with load current I. For a given load, however, $V_0 = (V_{0max} - V)$ may rise initially with the number of stages n, and reaches a maximum value but decays beyond on optimum number of stage. The optimum number of stages assuming a constant V_{max}, I, f and C can be obtained for maximum value of $V_{0\,max}$ by differentiating equation (2.12) with respect to n and equating it to zero.

$$\frac{dV_{max}}{dn} = 2V_{max} - \frac{2}{3}\frac{I}{fC}3n^2 = 0$$

$$= V_{max} - \frac{I}{fC}n^2 = 0$$

or
$$n_{opt} = \sqrt{\frac{V_{max}\,fC}{I}} \tag{2.13}$$

Substituting n_{opt} in equation (2.12) we have

$$(V_{0\,max})_{max} = \sqrt{\frac{V_{max}\,fC}{I}}\left(2V_{max} - \frac{2I}{3fC}\frac{V_{max}\,fC}{I}\right)$$

$$= \sqrt{\frac{V_{max}\,fC}{I}}\left(2V_{max} - \frac{2}{3}V_{max}\right)$$

$$= \sqrt{\frac{V_{max}\,fC}{I}}\cdot\frac{4}{3}V_{max} \tag{2.14}$$

It is to be noted that in general it is more economical to use high frequency and smaller value of capacitance to reduce the ripples or the voltage drop rather than low frequency and high capacitance.

Cascaded generators of Cockroft-Walton type are used and manufactured world wide these days. A typical circuit is shown in Fig. 2.5. In general a direct current upto 20 mA is required for high voltages between 1 MV and 2 MV. In case where a higher value of current is required, symmetrical cascaded rectifiers have been developed. These consist of mainly two rectifiers in cascade with a common smoothing column. The symmetrical cascaded rectifier has a smaller voltage drop and also a smaller voltage ripple than the simple cascade. The alternating current input to the individual circuits must be provided at the appropriate high potential; this can be done by means of isolating transformer. Fig. 2.6 shows a typical cascaded rectifier circuit. Each stage consists of one transformer which feeds two half wave rectifiers.

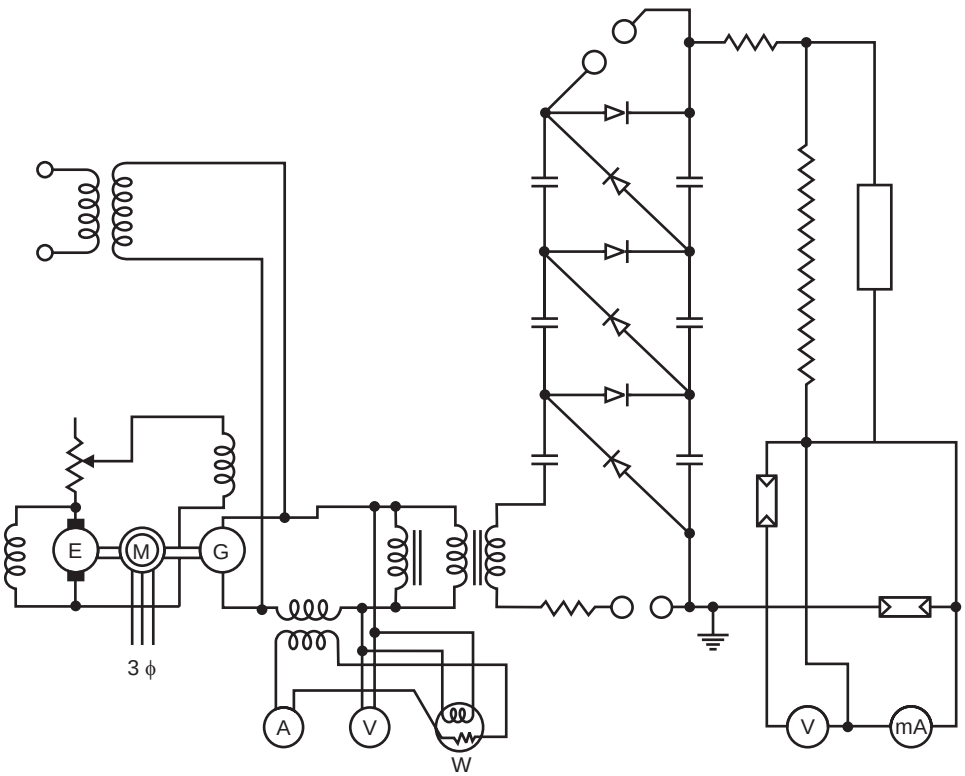

Fig. 2.5 A typical Cockroft circuit

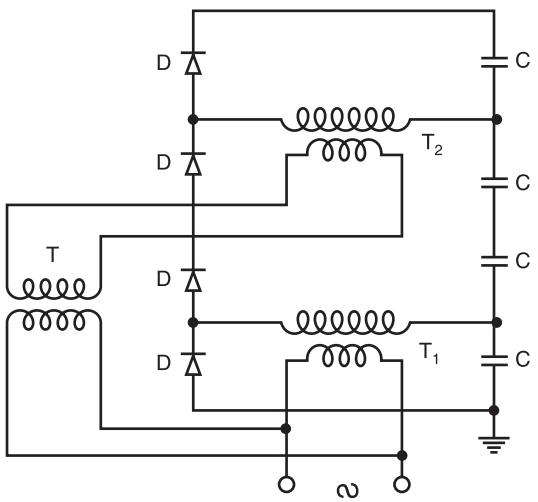

Fig. 2.6 Cascaded rectifier circuit

As the storage capacitors of these half wave rectifiers are series connected even the h.v. winding of T_1 can not be grounded. This means that the main insulation between the primary and the secondary winding of T_1 has to be insulated for a d.c. voltage of magnitude V_{max}, the peak voltage of T_1. The same is required for T_2 also but this time the high voltage winding is at a voltage of $3V_{max}$. It would be

difficult to provide the whole main insulation within this transformer, an isolating transformer T supplies T_2. The cascading of every stage would thus require an additional isolating transformer which makes this circuit less economical for more than two stages.

2.3 ELECTROSTATIC GENERATOR

In electromagnetic generators, current carrying conductors are moved against the electromagnetic forces acting upon them. In contrast to the generator, electrostatic generators convert mechanical energy into electric energy directly. The electric charges are moved against the force of electric fields, thereby higher potential energy is gained at the cost of mechanical energy.

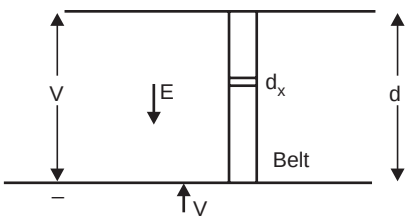

Fig. 2.7

The basic principle of operation is explained with the help of Fig. 2.7.

An insulated belt is moving with uniform velocity ν in an electric field of strength $E(x)$. Suppose the width of the belt is b and the charge density σ consider a length dx of the belt, the charge $dq = \sigma\, b dx$.

The force experienced by this charge (or the force experienced by the belt).

$$dF = Edq = E\,\sigma\, bdx$$

or
$$F = \sigma b \int Edx$$

Normally the electric field is uniform

$\therefore$
$$F = \sigma bV$$

The power required to move the belt

= Force × Velocity

$$= Fv = \sigma bV\nu \tag{2.15}$$

Now current
$$I = \frac{dq}{dt}\,\sigma b\,\frac{dx}{dt} = \sigma bv \tag{2.16}$$

$\therefore$ The power required to move the belt

$$P = F\nu = \sigma bV\nu = VI \tag{2.17}$$

Assuming no losses, the power output is also equal to VI.

Fig. 2.8 shows belt driven electrostatic generator developed by Van deGraaf in 1931. An insulating belt is run over pulleys. The belt, the width of which may vary from a few cms to metres is driven at a speed of about 15 to 30 m/sec, by means of a motor connected to the lower pulley. The belt near the lower pully is charged electrostatically by an excitation arrangement. The lower charge spray unit consists of a number of needles connected to the controllable d.c. source (10 kV–100 kV) so that the discharge between the points and the belt is maintained. The charge is conveyed to the upper end where it is collected from the belt by discharging points connected to the inside of an insulated metal electrode through which the belt passes. The entire equipment is enclosed in an earthed metal tank filled with insulating gases of good dielectric strength viz. SF_6 etc. So that the potential of the electrode could be

raised to relatively higher voltage without corona discharges or for a certain voltage a smaller size of the equipment will result. Also, the shape of the h.t., electrode should be such that the surface gradient of electric field is made uniform to reduce again corona discharges, even though it is desirable to avoid corona entirely. An isolated sphere is the most favourable electrode shape and will maintain a uniform field E with a voltage of Er where r is the radius of the sphere.

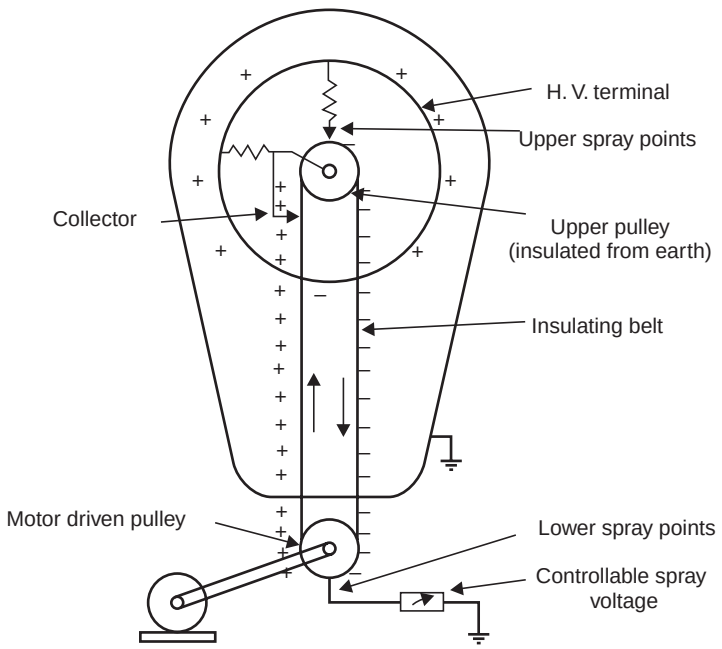

Fig. 2.8 Van de Graaf generator

As the h.t. electrode collects charges its potential rises. The potential at any instant is given as $V = q/C$ where q is the charge collected at that instant. It appears as though if the charge were collected for a long time any amount of voltage could be generated. However, as the potential of electrode rises, the field set up by the electrode increases and that may ionise the surrounding medium and, therefore, this would be the limiting value of the voltage. In practice, equilibrium is established at a terminal voltage which is such that the charging current

$$\left(I = C \frac{dV}{dt} \right)$$

equals the discharge current which will include the load current and the leakage and corona loss currents. The moving belt system also distorts the electric field and, therefore, it is placed within properly shaped field grading rings. The grading is provided by resistors and additional corona discharge elements.

The collector needle system is placed near the point where the belt enters the h.t. terminal. A second point system excited by a self-inducing arrangement enables the down going belt to be charged to the polarity opposite to that of the terminal and thus the rate of charging of the latter, for a given speed, is doubled. The self inducing arrangement requires insulating the upper pulley and maintaining it at a potential higher than that of the h.t. terminal by connecting the pulley to the collector needle

system. The arrangement also consists of a row of points (shown as upper spray points in Fig. 2.8) connected to the inside of the h.t. terminal and directed towards the pulley above its points of entry into the terminal. As the pulley is at a higher potential (positive), the negative charges due to corona discharge at the upper spray points are collected by the belt. This neutralises any remaining positive charge on the belt and leaves an excess of negative charges on the down going belt to be neutralised by the lower spray points. Since these negative charges leave the h.t. terminal, the potential of the h.t. terminal is raised by the corresponding amount.

In order to have a rough estimate of the current supplied by the generator, let us assume that the electric field E is normal to the belt and is homogeneous.

We know that $D = \varepsilon_0 E$ where D is the flux density and since the medium surrounding the h.t. terminal is say air $\varepsilon_r = 1$ and $\varepsilon_0 = 8.854 \times 10^{-12}$ F/metre.

According to Gauss law, $D = \sigma$ the surface charge density.

Therefore, $$D = \sigma = \varepsilon_0 E \qquad (2.18)$$

Assuming $E = 30$ kV/cm or 30,000 kV/m

$$\sigma = 8.854 \times 10^{-12} \times 3000 \times 10^3$$
$$= 26.562 \times 10^{-6} \text{ C/m}^2$$

Assuming for a typical system $b = 1$ metre and velocity of the belt $v = 10$ m/sec, and using equation (2.16), the current supplied by the generator is given as

$$I = \sigma b v$$
$$= 26.562 \times 10^{-6} \times 1 \times 10$$
$$= 26.562 \times 10^{-5} \text{ Amp}$$
$$= 265 \ \mu\text{A}$$

From equation (2.16) it is clear that current I depends upon σ, b and v. The belt width (b) and velocity v being limited by mechanical reasons, the current can be increased by having higher value of σ. σ can be increased by using gases of higher dielectric strength so that electric field intensity E could be increased without the inception of ionisation of the medium surrounding the h.t. terminal. However, with all these arrangements, the actual short circuit currents are limited only to a few mA even for large generators.

The advantages of the generator are:

(*i*) Very high voltages can be easily generated

(*ii*) Ripple free output

(*iii*) Precision and flexibility of control

The disadvantages are:

(*i*) Low current output

(*ii*) Limitations on belt velocity due to its tendency for vibration. The vibrations may make it difficult to have an accurate grading of electric fields

These generators are used in nuclear physics laboratories for particle acceleration and other processes in research work.

2.4 GENERATION OF HIGH A.C. VOLTAGES

Most of the present day transmission and distribution networks are operating on a.c. voltages and hence most of the testing equipments relate to high a.c. voltages. Even though most of the equipments on the system are 3-phase systems, a single phase transformer operating at power frequency is the most common from of HVAC testing equipment.

Test transformers normally used for the purpose have low power rating but high voltage ratings. These transformers are mainly used for short time tests on high voltage equipments. The currents required for these tests on various equipments are given below:

Insulators, C.B., bushings, Instrument transformers	= 0.1– 0.5 A
Power transformers, h.v. capacitors.	= 0.5–1 A
Cables	= 1 A and above

The design of a test transformer is similar to a potential transformer used for the measurement of voltage and power in transmission lines. The flux density chosen is low so that it does not draw large magnetising current which would otherwise saturate the core and produce higher harmonics.

2.4.1 Cascaded Transformers

For voltages higher than 400 KV, it is desired to cascade two or more transformers depending upon the voltage requirements. With this, the weight of the whole unit is subdivided into single units and, therefore, transport and erection becomes easier. Also, with this, the transformer cost for a given voltage may be reduced, since cascaded units need not individually possess the expensive and heavy insulation required in single stage transformers for high voltages exceeding 345 kV. It is found that the cost of insulation for such voltages for a single unit becomes proportional to square of operating voltage.

Fig. 2.9 shows a basic scheme for cascading three transformers. The primary of the first stage transformer is connected to a low voltage supply. A voltage is available across the secondary of this transformer. The tertiary winding (excitation winding) of first stage has the same number of turns as the primary winding, and feeds the primary of the second stage transformer. The potential of the tertiary is fixed to the potential V of the secondary winding as shown in Fig. 2.9. The secondary winding of the second stage transformer is connected in series with the secondary winding of the first stage transformer, so that a voltage of $2V$ is available between the ground and the terminal of secondary of the second stage transformer. Similarly, the stage-III transformer is connected in series with the second stage transformer. With this the output voltage between ground and the third stage transformer, secondary is $3V$. it is to be noted that the individual stages except the upper most must have three-winding transformers. The upper most, however, will be a two winding transformer.

Fig. 2.9 shows metal tank construction of transformers and the secondary winding is not divided. Here the low voltage terminal of the secondary winding is connected to the tank. The tank of stage-I transformer is earthed. The tanks of stage-II and stage-III transformers have potentials of V and $2V$, respectively above earth and, therefore, these must be insulated from the earth with suitable solid insulation. Through h.t. bushings, the leads from the tertiary winding and the h.v. winding are brought out to be connected to the next stage transformer.

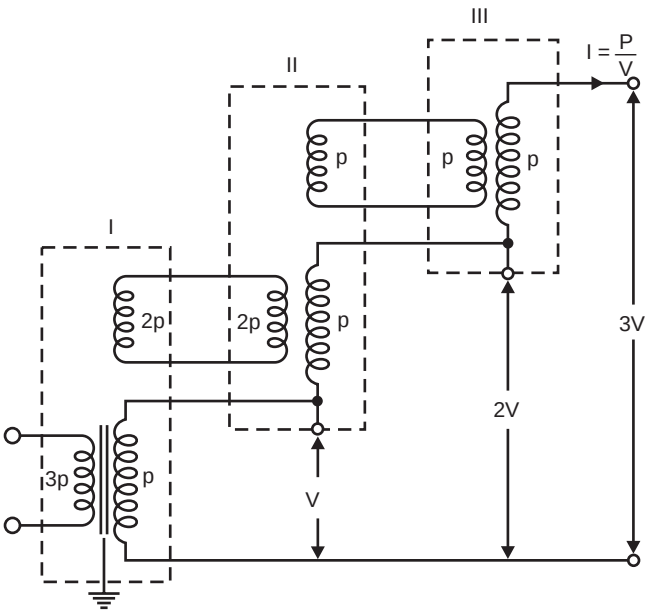

Fig. 2.9 Basic 3 stage cascaded transformer

However, if the high voltage windings are of mid-point potential type, the tanks are held at 0.5 V, 1.5 V and 2.5 V, respectively. This connection results in a cheaper construction and the high voltage insulation now needs to be designed for *V*/2 from its tank potential.

The main disadvantage of cascading the transformers is that the lower stages of the primaries of the transformers are loaded more as compared with the upper stages.

The loading of various windings is indicated by *P* in Fig. 2.9. For the three-stage transformer, the total output *VA* will be 3*VI* = 3*P* and, therefore, each of the secondary winding of the transformer would carry a current of *I* = *P*/*V*. The primary winding of stage-III transformer is loaded with *P* and so also the tertiary winding of second stage transformer. Therefore, the primary of the second stage transformer would be loaded with 2*P*. Extending the same logic, it is found that the first stage primary would be loaded with *P*. Therefore, while designing the primaries and tertiaries of these transformers, this factor must be taken into consideration.

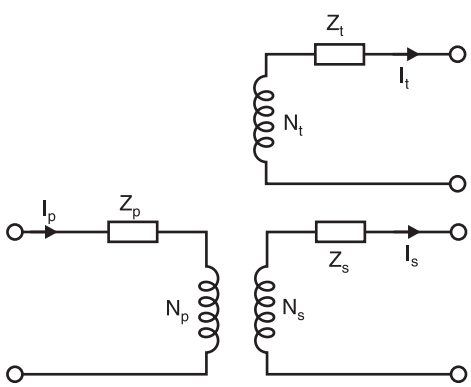

Fig. 2.10 Equivalent circuit of one stage

The total short circuit impedance of a cascaded transformer from data for individual stages can be obtained. The equivalent circuit of an individual stage is shown in Fig. 2.10.

Here Z_p, Z_s, and Z_t, are the impedances associated with each winding. The impedances are shown in series with an ideal 3-winding transformer with corresponding number of turns N_p, N_s and N_t. The impedances are obtained either from calculated or experimentally-derived results of the three short-circuit tests between any two windings taken at a time.

Let Z_{ps} = leakage impedance measured on primary side with secondary short circuited and tertiary open.

Z_{pt} = leakage impedance measured on primary side with tertiary short circuited and secondary open.

Z_{st} = leakage impedance on secondary side with tertiary short circuited and primary open.

If these measured impedances are referred to primary side then

$$Z_{ps} = Z_p + Z_s,\ Z_{pt} = Z_p + Z_t \quad \text{and} \quad Z_{st} = Z_s + Z_t$$

Solving these equations, we have

$$Z_p = \frac{1}{2}(Z_{ps} + Z_{pt} - Z_{st}),\ Z_s = \frac{1}{2}(Z_{ps} + Z_{st} - Z_{pt})$$

and

$$Z_t = \frac{1}{2}(Z_{pt} + Z_{st} - Z_{ps}) \tag{2.19}$$

Assuming negligible magnetising current, the sum of the ampere turns of all the windings must be zero.

$$N_p I_p - N_s I_s - N_t I_t = 0$$

Assuming lossless transformer, we have,

$$Z_p = jX_p, \quad Z_s = jX_s \quad \text{and} \quad Z_t = jX_t$$

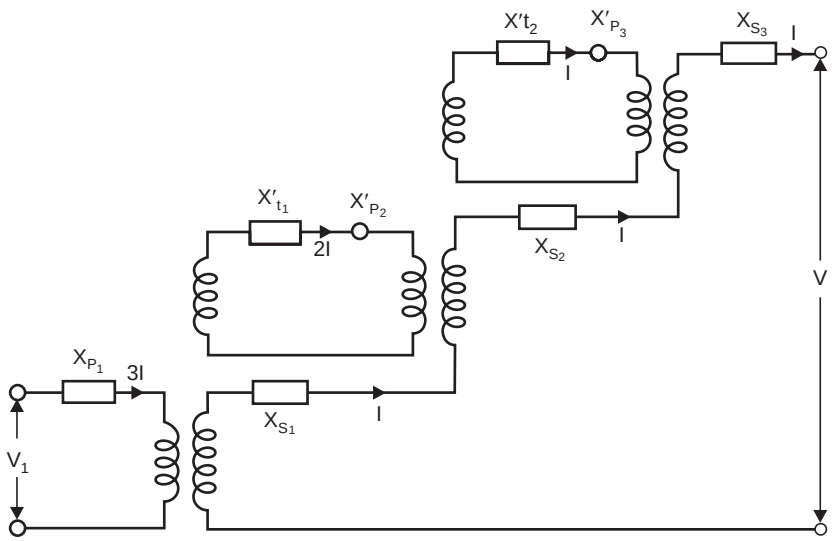

Fig. 2.11 Equivalent circuit of 3-stage transformer

Also let $N_p = N_t$ for all stages, the equivalent circuit for a 3-stage transformer would be given as in Fig. 2.11

Fig. 2.11 can be further reduced to a very simplified circuit as shown in Fig. 2.12. The resulting short circuit reactance X_{res} is obtained from the condition that

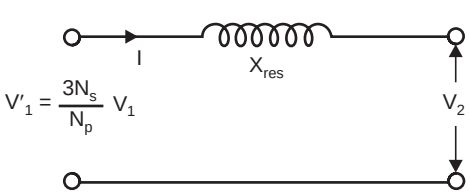

Fig. 2.12 A simplified equivalent circuit

the power rating of the two circuits be the same. Here currents have been shown corresponding to high voltage side.

$$I^2X_{res} = (3I)^2\, X_p + (2I)^2\, X_p + I^2\, X_p + I^2\, X_s + I^2\, X_s + I^2\, X_s + (2I)^2\, X_t + I^2\, X_t$$

$$X_{res} = 14X_p + 3X_s + 5x_t \qquad (2.20)$$

instead of $3(X_p + X_s + X_t)$ as might be expected. Equation (2.20) can be generalised for an n-stage transformer as follows:

$$X_{res} = \sum_{i=1}^{n} [(n - i + 1)^2\, X_{pi} + X_{si} + (i - 1)^2\, X_{ti}]$$

Where X_{pi}, X_{si} and X_{ti} are the short-circuit reactance of the primary, secondary and tertiary windings of ith transformer.

It has been observed that the impedance of a two-stage transformer is about 3–4 times the impedance of one unit and a three-stage impedance is 8–9 times the impedance of one unit transformer. Hence, in order to have a low impedance of a cascaded transformer, it is desirable that the impedance of individual units should be as small as possible.

2.4.2 Reactive Power Compensation

As is mentioned earlier, the test transformers are used for testing the insulation of various electrical equipments. This means the load connected to these transformers is highly capacitive. Therefore, if rated voltage is available at the output terminals of the test transformer and a test piece (capacitive load) is connected across its terminals, the voltage across the load becomes higher than the rated voltage as the load draws leading current. Thus, it is necessary to regulate the input voltage to the test transformer so that the voltage across the load, which is variable, depending on the test specimen, remains the rated voltage. Another possibility is that a variable inductor should be connected across the supply as shown in Fig. 2.13 so that the reactive power supplied by the load is absorbed by the inductor and thus the voltage across the test transformer is maintained within limits.

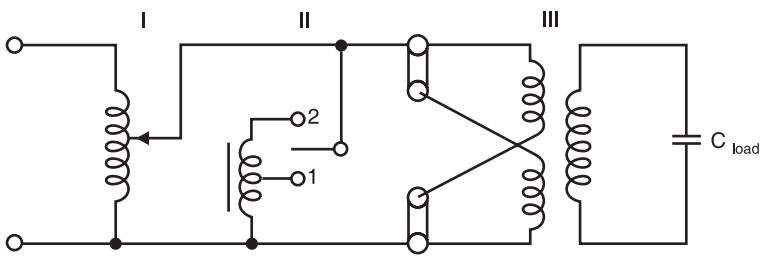

I. Regulating transformer II. Compensating reactor III. Test transformer with commutable primary

Fig. 2.13 Basic principle of reactive power compensation

It should be noted that the test transformer should be able to supply the maximum value of load current for which it has been designed at all intermediate voltages including the rated voltage. The power voltage characteristic is, therefore, a straight line as shown by line *A* in Fig. 2.14. The compensating reactive power absorbed by the air-cored inductor is shown on parabolas *B, C* and *D*. These will

be parabolas as the reactive power = V^2/X. Curve *B* corresponds to the condition when the transformer primary is connected in parallel and the reactor is connected at position 1 in Fig. 2.13.

Similarly Curve *C*—Transformer primary connected in parallel and reactor at position 1 connected.

Curve *D*—Transformer primary connected in series and reactor at position 2.

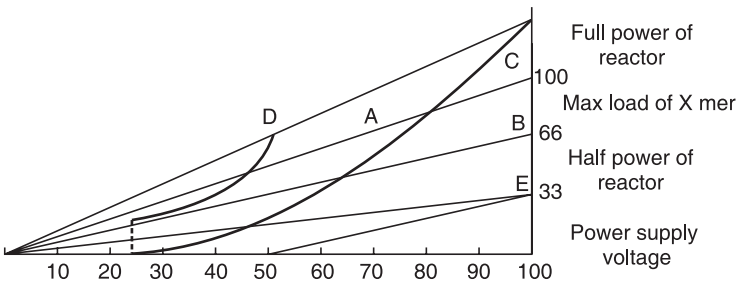

Fig. 2.14 Reactive power compensation

When the primary series is connected, for the same supply voltage, voltage per turn of primary becomes half its value when it is parallel connected and, therefore, the secondary voltage becomes 1/2 of the rated voltage and hence the curve starts at 50% of the rated voltage. The power of the voltage regulator is proportional to the supply voltage and, therefore, is represented by line *E* in Fig. 2.14 and the maximum power at rated voltage is 33.3% of the maximum power requirement of the transformer. All possible operating conditions of the test transformer lie within the triangular area enclosed by the line *A,* the abscissa and the 100% rated voltage line. This area has been sub-divided into different parts, so that the permissible supply power (Here 33% of maximum transformer load) is never exceeded. The value of the highest voltage is always taken for the evaluation of the compensation arrangement. Since the impedance of the test transformer is usually large (about 20–25%), the range under 25% of the rated voltage is not considered.

It is clear from the above considerations that the design of the compensating reactor depends upon

(*i*) The capacitance and operating voltage of test specimen.

(*ii*) The power rating of the available regulator.

(*iii*) The possibility of different connections of the winding of test transformer.

(*iv*) The power rating of the test transformer.

In order that the test laboratory meets all the different requirements, every particular case must be investigated and a suitable reactor must be designed for reactive power compensation.

In multistage transformers with large power output, it is desirable to provide reactive power compensation at every stage, so that the voltage stability of the test transformer is greatly improved.

2.5 SERIES RESONANT CIRCUIT

The equivalent circuit of a single-stage-test transformer alongwith its capacitive load is shown in Fig. 2.15. Here L_1 represents the inductance of the voltage regulator and the transformer primary, *L* the

exciting inductance of the transformer, L_2 the inductance of the transformer secondary and C the capacitance of the load. Normally inductance L is very large as compared to L_1 and L_2 and hence its shunting effect can be neglected. Usually the load capacitance is variable and it is possible that for certain loading, resonance may occur in the circuit suddenly and the current will then only be limited by the resistance of the circuit and the voltage across the test specimen may go up as high as 20 to 40 times the desired value.

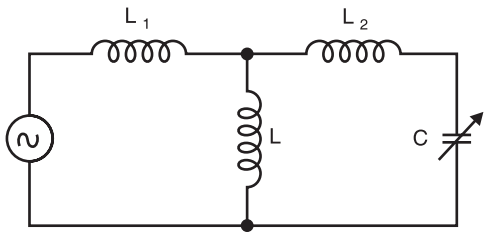

Fig. 2.15 Equivalent circuit of a single stage loaded transformer

Similarly, presence of harmonics due to saturation of iron core of transformer may also result in resonance. Third harmonic frequencies have been found to be quite disastrous.

With series resonance, the resonance is controlled at fundamental frequency and hence no unwanted resonance occurs.

The development of series resonance circuit for testing purpose has been very widely welcome by the cable industry as they faced resonance problem with test transformer while testing short lengths of cables.

In the initial stages, it was difficult to manufacture continuously variable high voltage and high value reactors to be used in the series circuit and therefore, indirect methods to achieve this objective were employed. Fig. 2.16 shows a continuously variable reactor connected in the low voltage winding of the step up transformer whose secondary is rated for the full test voltage. C_2 represents the load capacitance.

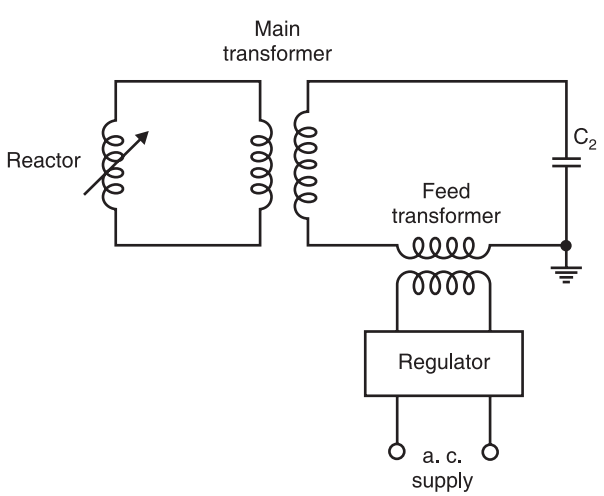

Fig. 2.16 Single transformer/reactor series resonance circuit

If N is the transformation ratio and L is the inductance on the low voltage side of the transformer, then it is reflected with $N^2 L$ value on the secondary side (load side) of the transformer. For certain setting of the reactor, the inductive reactance may equal the capacitive reactance of the circuit, hence resonance will take place. Thus, the reactive power requirement of the supply becomes zero and

it has to supply only the losses of the circuit. However, the transformer has to carry the full load current on the high voltage side. This is a disadvantage of the method. The inductor are designed for high quality factors $Q = \omega L / R$. The feed transformer, therefore, injects the losses of the circuit only.

It has now been possible to manufacture high voltage continuously variable reactors 300 kV per unit using a new technique with split iron core. With this, the testing step up transformer can be omitted as shown in Fig. 2.17. The inductance of these inductors can be varied over a wide range depending upon the capacitance of the load to produce resonance.

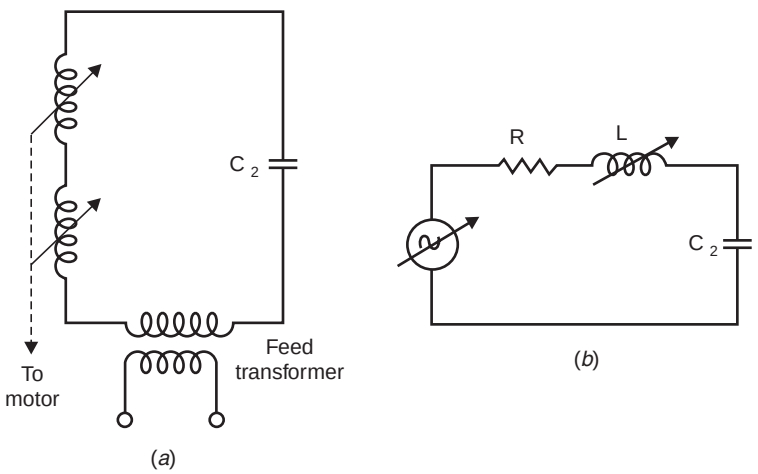

Fig. 2.17 (*a*) Series resonance circuit with variable h.t. reactors (*b*) Equivalent circuit of (a)

Fig. 2.17 (*b*) represents an equivalent circuit for series resonance circuit. Here R is usually of low value. After the resonance condition is achieved, the output voltage can be increased by increasing the input voltage. The feed transformers are rated for nominal current ratings of the reactor.

Under resonance, the output voltage will be

$$V_0 = \frac{V}{R}\frac{1}{\omega C_2}$$

Where V is the supply voltage.

Since at resonance

$$\omega L = \frac{1}{\omega C_2}$$

Therefore $$V_0 = \frac{V}{R}\omega L = VQ$$

where Q is the quality factor of the inductor which usually varies between 40 and 80. This means that with $Q = 40$, the output voltage is 40 times the supply voltage. It also means that the reactive power requirements of the load capacitance in kVA is 40 times the power to be provided by the feed transformer in KW. This results in a relatively small power rating for the feed transformer.

The following are the advantages of series resonance circuit.

(*i*) The power requirements in KW of the feed circuit are (kVA)/*Q* where kVA is the reactive power requirements of the load and *Q* is the quality factor of variable reactor usually greater than 40. Hence, the requirement is very small.

(*ii*) The series resonance circuit suppresses harmonics and interference to a large extent. The near sinusoidal wave helps accurate partial discharge of measurements and is also desirable for measuring loss angle and capacitance of insulating materials using Schering Bridge.

(*iii*) In case of a flashover or breakdown of a test specimen during testing on high voltage side, the resonant circuit is detuned and the test voltage collapses immediately. The short circuit current is limited by the reactance of the variable reactor. It has proved to be of great value as the weak part of the isolation of the specimen does not get destroyed. In fact, since the arc flash over has very small energy, it is easier to observe where exactly the flashover is occurring by delaying the tripping of supply and allowing the recurrence of flashover.

(*iv*) No separate compensating reactors (just as we have in case of test transformers) are required. This results in a lower overall weight.

(*v*) When testing SF_6 switchgear, multiple breakdowns do not result in high transients. Hence, no special protection against transients is required.

(*vi*) Series or parallel connections of several units is not at all a problem. Any number of units can be connected in series without bothering for the impedance problem which is very severely associated with a cascaded test transformer. In case the test specimen requires large current for testing, units may be connected in parallel without any problem.

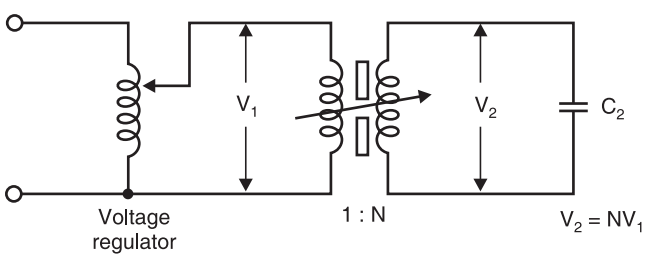

Fig. 2.18 Parallel resonance system

Fig. 2.18 shows schematic of a typical parallel resonant systems. Here the variable reactor is incorporated into the high voltage transformer by introducing a variable air gap in the core of the transformer. With this connection, variation in load capacitance and losses cause variation in input current only. The output voltage remains practically constant. Within the units of single stage design, the parallel resonant method offers optimum testing performance.

In an attempt to take advantage of both the methods of connections, *i.e.*, series and parallel resonant systems, a third system employing series parallel connections was tried. This is basically a modification of a series resonant system to provide most of the characteristics of the parallel system. Fig. 2.19. shows a schematic of a typical series parallel method.

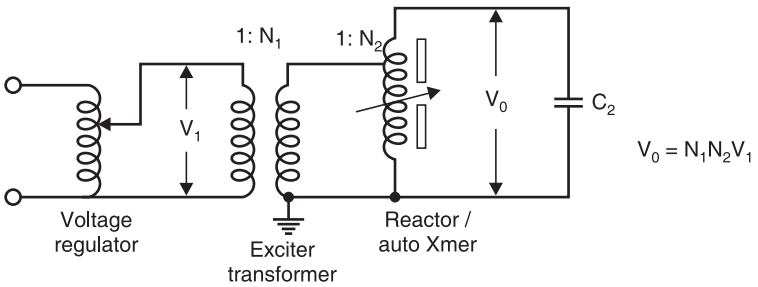

Fig. 2.19 Series-parallel resonant system

Here the output voltage is achieved by auto transformer action and parallel compensation is achieved by the connection of the reactor. It has been observed that during the process of tuning for most of the loads, there is a certain gap opening that will result in the parallel connected test system going into uncontrolled over voltaging of the test sample and if the test set is allowed to operate for a long time, excessive heating and damage to the reactor would result.

Also, it has been observed experimentally that complete balance of ampere turns takes place when the system operates under parallel resonance condition. Under all other settings of the variable reactor, an unbalance in the ampere turns will force large leakage flux into the surrounding metallic tank and clamping structure which will cause large circulating currents resulting in hot spots which will affect adversely the dielectric strength of oil in the tank.

In view of the above considerations, it has been recommended not to go in for series-parallel resonant mode of operation for testing purpose. If a single stage system upto 300 kV using the resonance test voltage is required, parallel resonant system must be adopted. For test voltage exceeding 300 kV, the series resonant method is strongly recommended.

The specific weight of a cascaded test transformer varies between 10 and 20 kg/kVA whereas for a series resonant circuit with variable high voltage reactors it lies between 3 and 6 kg/kVA.

With the development of static frequency convertor, it has now been possible to reduce the specific weight still further. In order to obtain resonance in the circuit a choke of constant magnitude can be used and as the load capacitance changes the source frequency should be changed. Fig. 2.20 shows a schematic diagram of a series resonant circuit with variable frequency source.

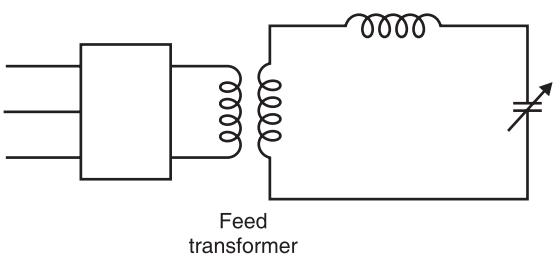

Fig. 2.20 Schematic diagram of series resonant circuit with variable frequency sources

The frequency convertor supplies the losses of the testing circuit only which are usually of the order of 3% of the reactive power of the load capacitor as the chokes can be designed for very high quality factors.

A word of caution is very important, here in regard to testing of test specimen having large capacitance. With a fixed reactance, the frequency for resonance will be small as compared to normal frequency. If the voltage applied is taken as the normal voltage the core of the feed transformer will get saturated as *V*/*f* then becomes large and the flux in the core will be large. So, a suitable voltage must be applied to avoid this situation.

With the static frequency convertor circuits the specific weight has come down to 0.5 kg/kVA.

It is to be noted that whereas the series resonant systems are quite popular for testing cables and highly loss free capacitive loads, cascaded transformers are more common in high voltage laboratories for testing equipment in *MV* range and also for relatively high loads.

EXAMPLES

Example 2.1. *A ten stage Cockraft-Walton circuit has all capacitors of 0.06 μF. The secondary voltage of the supply transformer is 100 kV at a frequency of 150 Hz. If the load current is 1 mA, determine (i) voltage regulation (ii) the ripple (iii) the optimum number of stages for maximum output voltage (iv) the maximum output voltage.*

Solution: Given $C = 0.06$ μF, $I = 1$ mA, $f = 150$ Hz

$n = 10$

Voltage drop $$V = \frac{I}{fC}\left(\frac{2}{3}n^3 + \frac{n^2}{2} + \frac{n}{6}\right) = \frac{I}{fC}\left(\frac{2}{3}n^3 + \frac{n^2}{2}\right)$$

$$= \frac{1\times10^{-3}}{150\times0.06\times10^{-6}}\left(\frac{2}{3}\times10^3 + \frac{10^2}{2}\right)$$

$$= \frac{10^3}{3.0\times3}(666.6 + 50) = \frac{717\times10^3}{3\times3} = 80 \text{ kV}$$

Therefore, percentage voltage regulation

$$\frac{80\times100}{2\times10\times100} = 4\%$$

(*ii*) The ripple voltage $\delta V = \frac{I}{fC}\frac{n(n+1)}{2}$

$$= \frac{1\times10^{-3}\times55}{150\times0.06\times10^{-6}} = 6.1 \text{ kV}$$

$\therefore$ % ripple $$= \frac{6.1\times100}{2\times10\times100}$$

$$= 0.3\% \quad \textbf{Ans.}$$

(*iii*) Optimum no. of stages $$= \sqrt{\frac{V_{max}\, fC}{I}}$$

$$= \sqrt{\frac{100\times150\times0.06\times10^{-6}\times10^3}{10^{-3}}} = 30 \quad \textbf{Ans.}$$

(*iv*) The maximum output voltage

$$= 30 \times \frac{4}{3} \times V_{max}$$

$$= 30 \times \frac{4}{3} \times 100 = 4000 \text{ KV} \quad \textbf{Ans.}$$

Example 2.2. *A 100 kVA 250 V/200 kV feed transformer has resistance and reactance of 1% and 5% respectively. This transformer is used to test a cable at 400 kV at 50 Hz. The cable takes a charging current of 0.5 A at 400 kV. Determine the series inductance required. Assume 1% resistance of the inductor. Also determine input voltage to the transformer. Neglect dielectric loss of the cable.*

Solution: The circuit is drawn in Fig. Ex. 2.2

The resistance and reactance of the transformer are

$$\frac{1}{100} \times \frac{200^2}{0.1} \text{ 4 K}\Omega$$

$$\frac{5}{100} \times \frac{200^2}{0.1} \text{ 20 K}\Omega$$

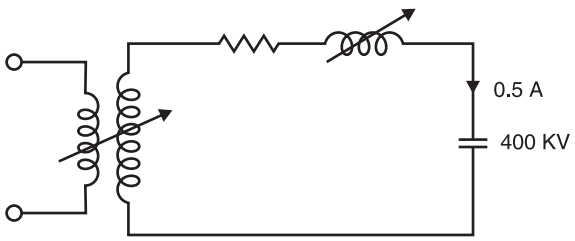

Fig. Ex. 2.2

The resistance of the inductor is also 4 KΩ.

The capacitive reactance of capacitor (Test Specimen)

$$= \frac{400}{0.5} = 800 \text{ K}\Omega$$

For resonance $X_L = X_C$

Inductive reactance of transformer is 20 KΩ . Therefore, additional inductive reactance required will be

$$800 - 20 = 780 \text{ K}\Omega$$

The inductance required $= \dfrac{780 \times 1000}{314} = 2484$ H

Total resistance of the circuit = 8 KΩ

under resonance condition the supply voltage

(Secondary voltage) $= IR = 0.5 \times 8 = 4$ kV

Therefore, primary voltage $= 4 \times \dfrac{250}{200} = 5$ volts **Ans.**

PROBLEMS

2.1. Explain and compare the performance of half wave rectifier and voltage doubler circuits for generation of high d.c. voltages.

2.2. Define ripple voltage. Show that the ripple voltage in a rectifier circuit depends upon the load current and the circuit parameters.

2.3. Explain with neat sketches Cockroft-Walton voltage multiplier circuit. Explain clearly its operation when the circuit is (*i*) unloaded (*ii*) loaded.

2.4. Derive an expression for ripple voltage of a multistage Cockroft-Walton Circuit.

2.5. Derive an expression for the voltage output under load condition. Hence, deduce the condition for optimal number of stage if a maximum value of output voltage is desired.

2.6. Describe with neat diagram the principle of operation and application of a symmetrical cascaded rectifier.

2.7. Explain clearly the basic principle of operation of an electrostatic generator. Describe with neat diagram the principle of operation, application and limitations of Van de Graf generator.

2.8. What is a cascaded transformer? Explain why cascading is done? Describe with neat diagram a three stage cascaded transformer. Label the power ratings of various stages of the transformer.

2.9. Draw equivalent circuit of a 3-stage cascaded transformer and determine the expression for short circuit impedance of the transformer. Hence deduce an expression for the short-circuit impedance of an *n*-stage cascaded transformer.

2.10. Explain with neat diagram the basic principle of reactive power compensation is high voltage a.c. testing of insulating materials.

2.11. Explain with neat diagram the principle of operation of (*i*) series (*ii*) parallel resonant circuits for generating high a.c. voltages. Compare their performance.

2.12. Explain the series-parallel resonant circuit and discuss its advantages and disadvantages.

REFERENCES

Graggs J.D. and Meek J.M., *High Voltage laboratory Technique*, Buttrworth, London 1954.

Enge H.A., *Cascade Transformer High Voltage Generator,* US Patent No. 3596, 167 July, 1971.

Reid R., High Voltage Resonant Testing, *IEEE PES Winter Meeting, 1974 Conf. Paper 74.*

Kuffel E., Zaengl W.S., *High Voltage Engineering Fundamentals,* Pergamon Press, 1984.

Word Berry H. *et al.,* A Comparative Analysis of Resonant Power Supply Design Technique for High Voltage Testing, *Fifth International Symposium on High Voltage Engineering,* Branscheweig 24–28 Aug. 1987. FRG.

DC voltage test set 2000 kV, 10 mA for testing power cables, including a HV measuring resistor and automatic grounding system (foreground)

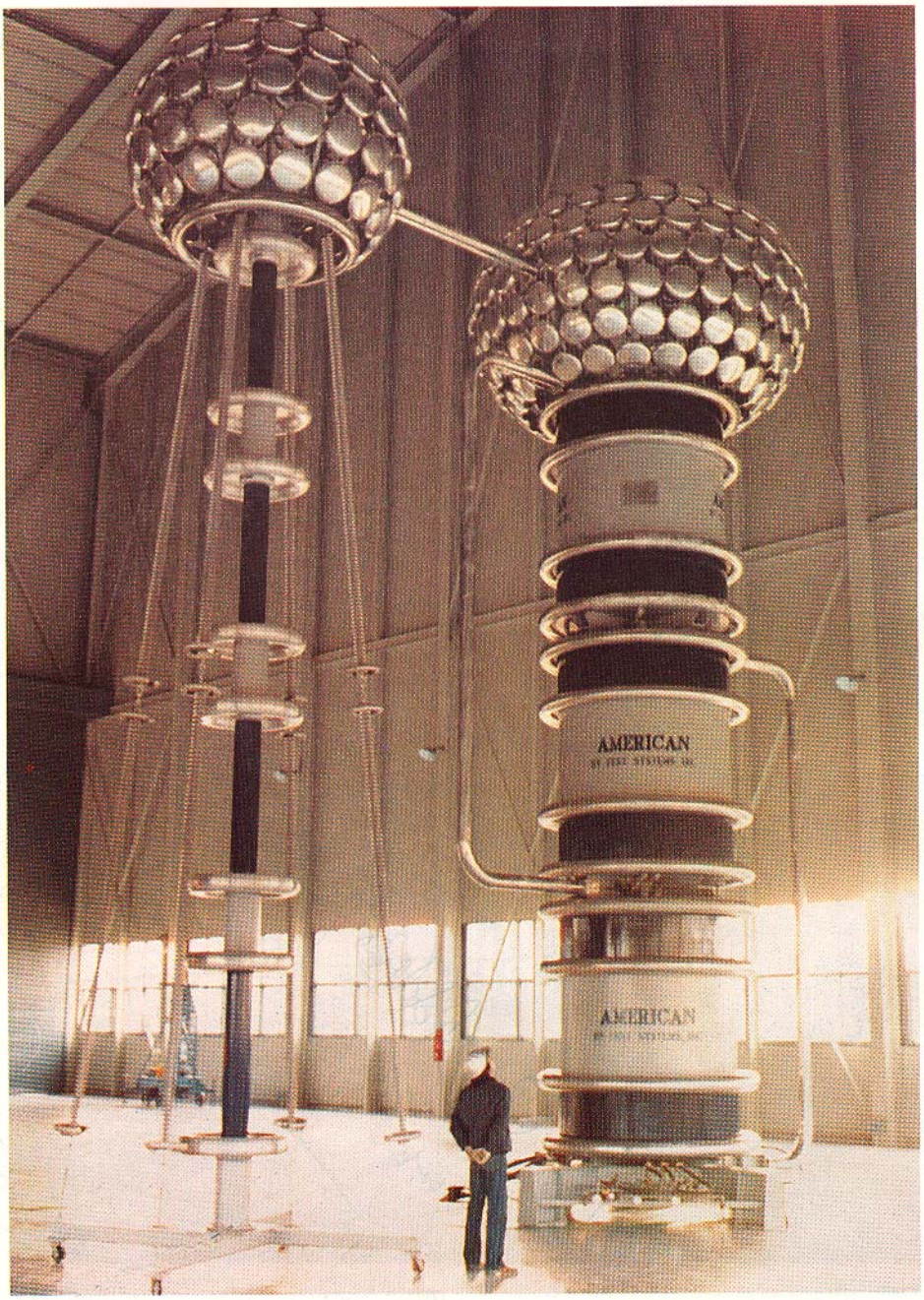

Cascaded serie resonant test system 3 x 350 kV, for the testing of power cables, with AC voltage divider (left)

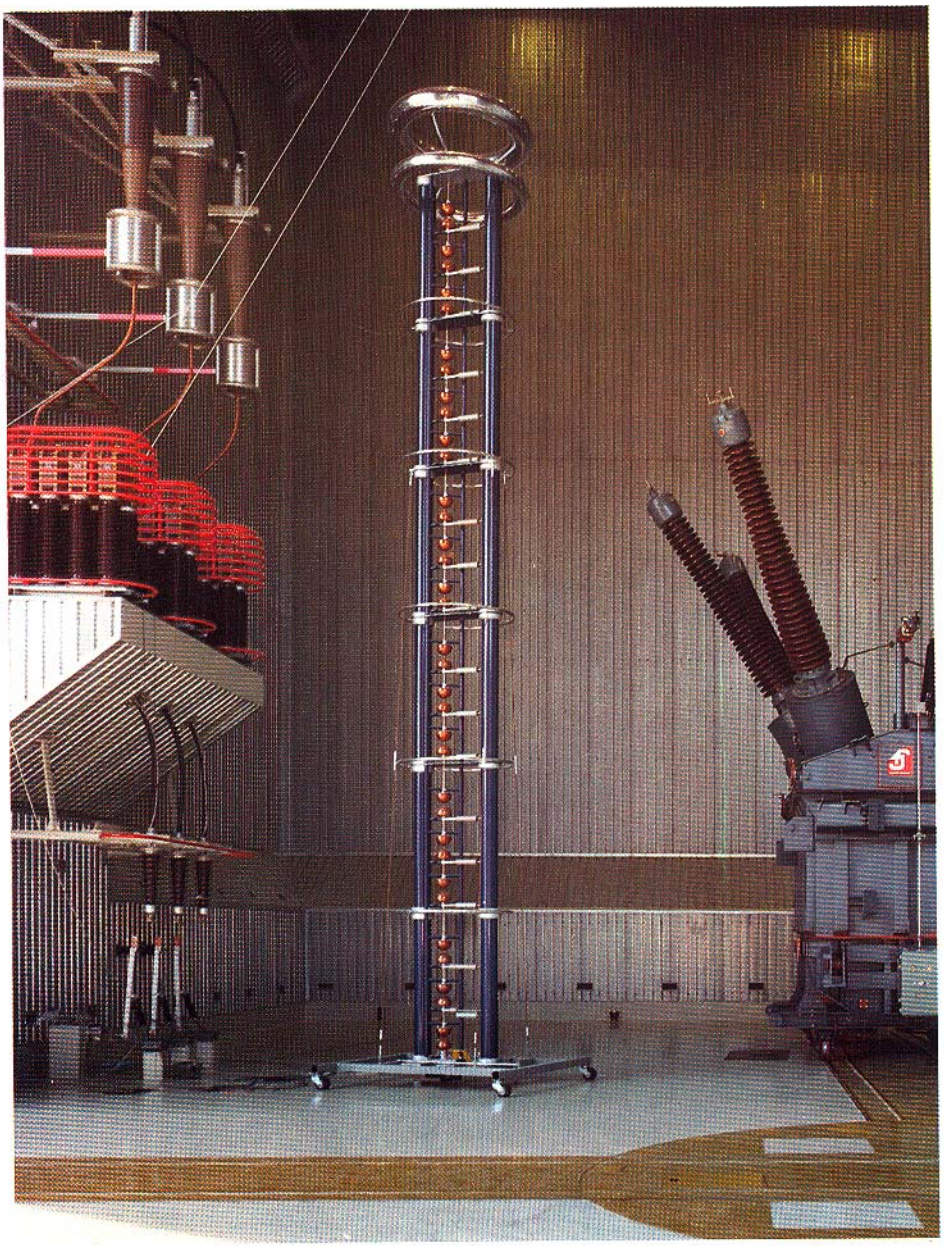

Triggered impulse chopping gap 3600 kV for impulse testing of power transformers

Large outdoor impulse voltage dividers, damped capacitive type with large top electrode for ultra-high switching impulse voltages

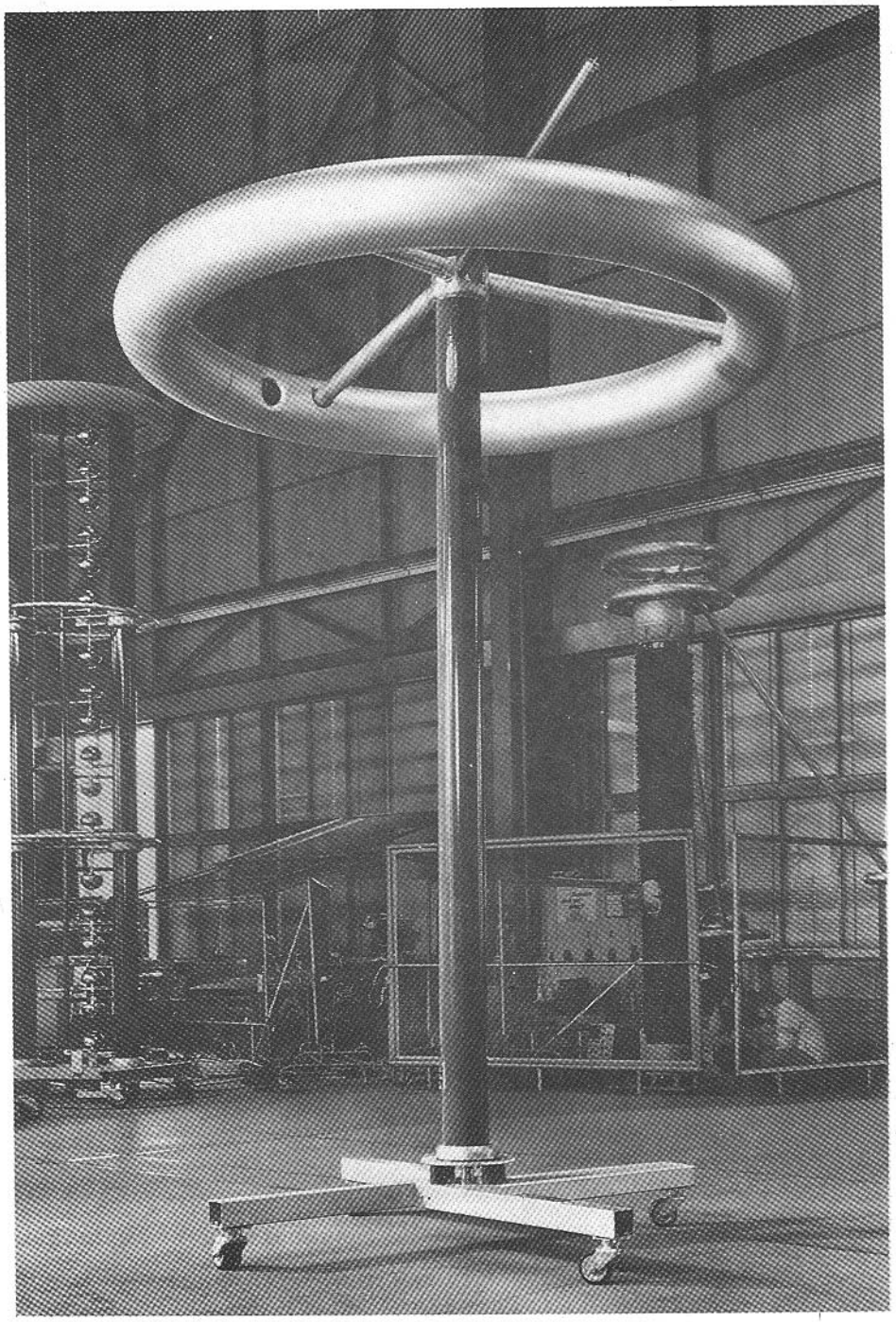

Resistive impulse voltage divider 1800 kV

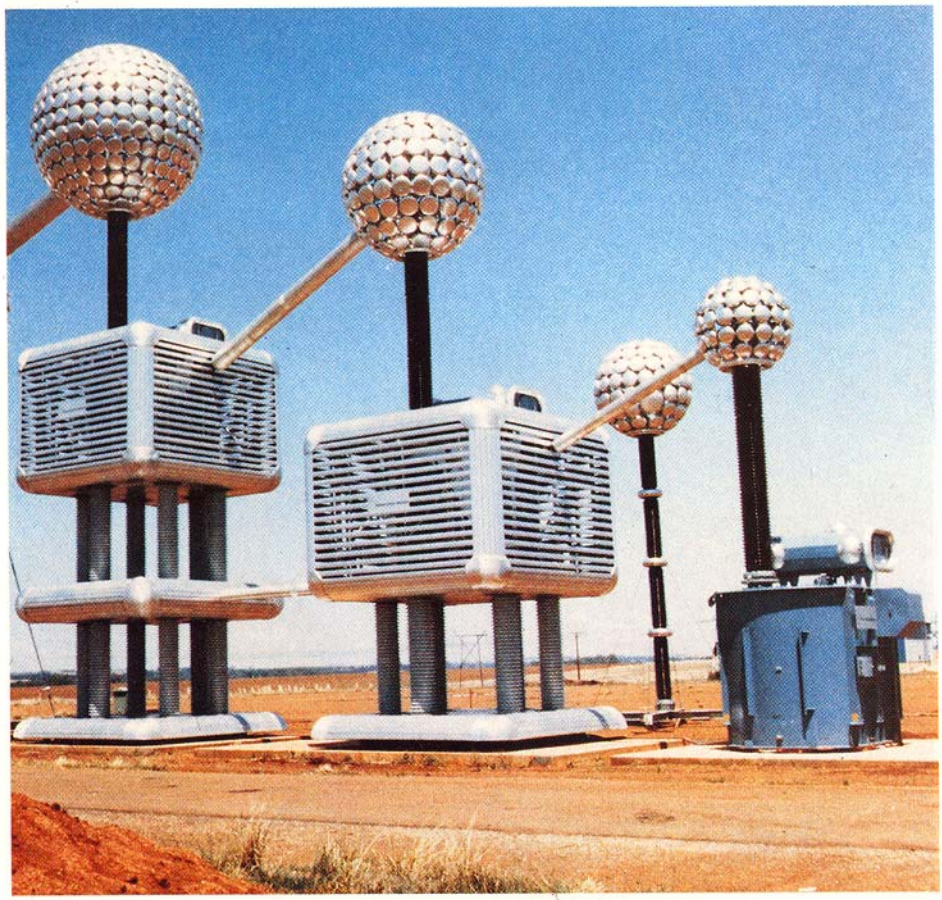

Three-stage cascade transformer 3 x 600 kV, 2 A cont. outdoor type with AC voltage divider 1500 kV

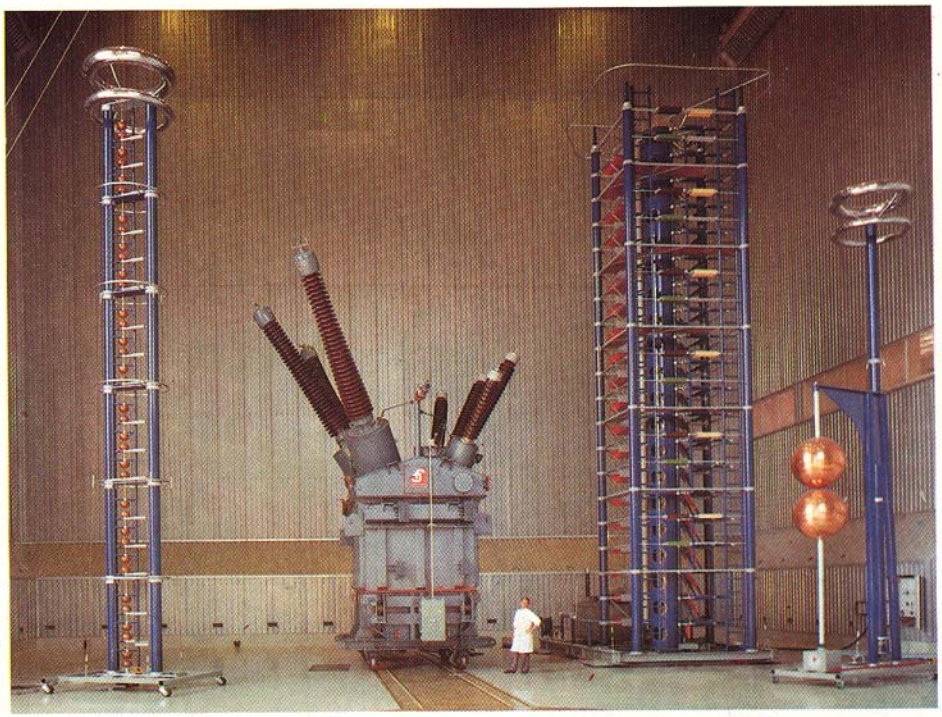

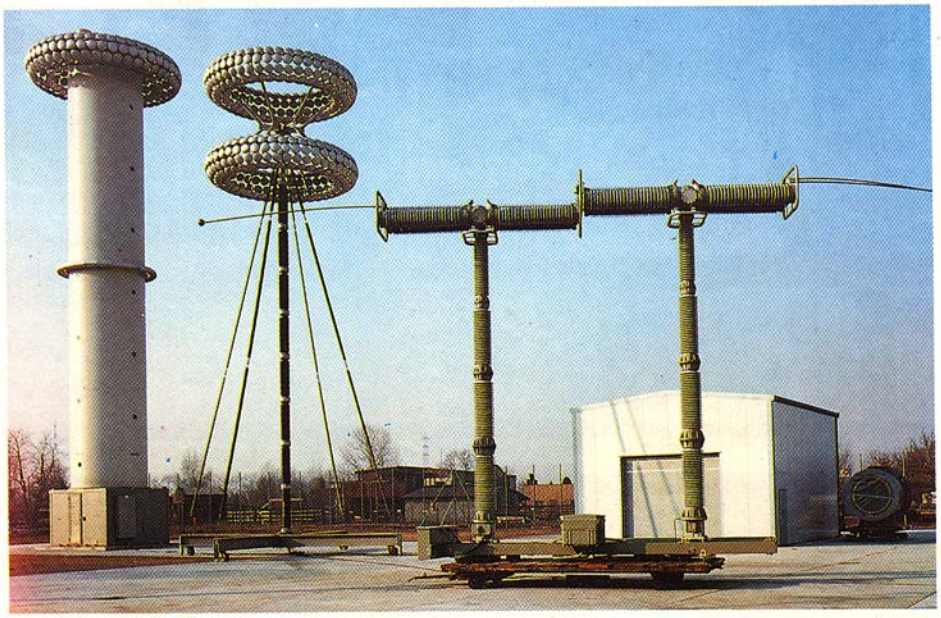

Large impulse voltage generators

Above: Indoor 4000 kV

Below: Outdoor 6400 kV shown together with typical test objects

Above: Large power transformer (center)

Below: Power circuit breakers (foreground right)

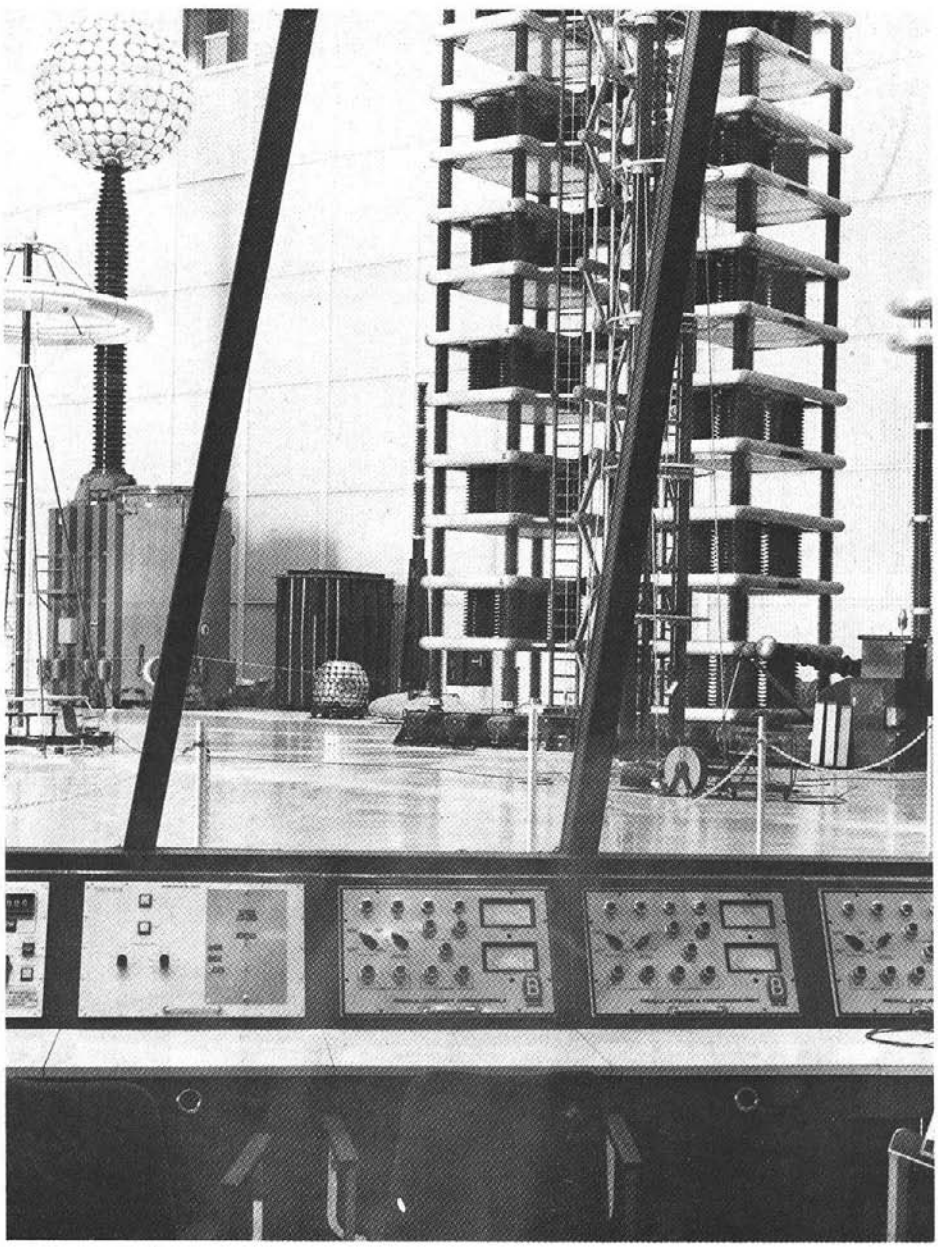

View from the control room at IREQ

3 Generation of Impulse Voltages and Currents

3.1 DEFINITIONS: IMPULSE VOLTAGE

An impulse voltage is a unidirectional voltage which, without appreciable oscillations, rises rapidly to a maximum value and falls more or less rapidly to zero Fig. 3.1. The maximum value is called the peak value of the impulse and the impulse voltage is specified by this value. Small oscillations are tolerated, provided that their amplitude is less than 5% of the peak value of the impulse voltage. In case of oscillations in the wave shape, a mean curve should be considered.

If an impulse voltage develops without causing flash over or puncture, it is called a full impulse voltage; if flash over or puncture occur, thus causing a sudden collapse of the impulse voltage, it is called a chopped impulse voltage. A full impulse voltage is characterised by its peak value and its two time intervals, the wave front and wave tail time intervals defined below:

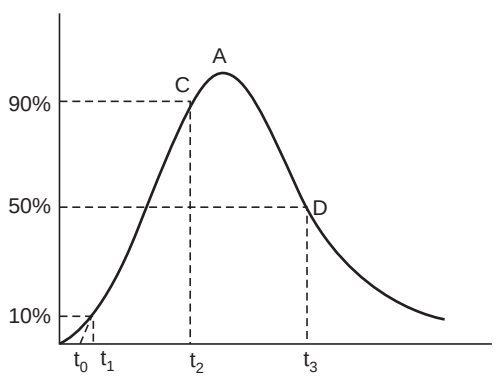

Fig. 3.1 Full impulse wave

The wave front time of an impulse wave is the time taken by the wave to reach to its maximum value starting from zero value. Usually it is difficult to identify the start and peak points of the wave and, therefore, the wave front time is specified as 1.25 times $(t_2 - t_1)$, where t_2 is the time for the wave to reach to its 90% of the peak value and t_1 is the time to reach 10% of the peak value. Since $(t_2 - t_1)$ represents about 80% of the wave front time, it is multiplied by 1.25 to give total wave front time. The point where the line *CB* intersects the time axis is referred to be the nominal starting point of the wave.

The nominal wave tail time is measured between the nominal starting point t_0 and the point on the wave tail where the voltage is 50% of the peak value *i.e.* wave fail time is expressed as $(t_3 - t_0)$.

The nominal steepness of the wave front is the average rate of rise of voltage between the points on the wave front where the voltage is 10% and 90% of the peak value respectively.

The standard wave shape specified in BSS and ISS is a 1/50 micro sec. wave *i.e.* a wave front of 1 micro sec. and a wave tail of 50 micro sec. A tolerance of not more than ±50% on the duration of the

wave front and 20% on the time to half value on the wave tail is allowed. The wave is completely specified as 100 kV, 1/50 micro sec. where 100 kV is the peak value of the wave.

The wave shape recommended by the American Standard Association is 1.5/40 micro sec. with permissible variations of 0.5 micro sec. on the wave front and ±10 micro sec. on the wave tail. Here wave front time is taken as 1.67 times the time taken by the wave to rise from 30% to 90% of its peak value and wave tail time is computed as in BSS or ISS *i.e.* it is given as $(t_3 - t_0)$ Fig. 3.1.

Chopped Wave

If an impulse voltage is applied to a piece of insulation and if a flash over or puncture occurs causing sudden collapse of the impulse voltage, it is called a chopped impulse voltage. If chopping takes place on the front part of the wave, it is known as front chopped wave, Fig. 3.2 (*a*) else, it is known simply as a chopped wave, Fig. 3.2 (*b*). Again, if chopping takes place on the front, it is specified by the peak value corresponding to the chopped value and its nominal steepness is the rate of rise of voltage measured between the points where the voltage is 10% and 90% respectively of the voltage at the instant of chopping. However, a wave chopped on the tail is specified on the lines of full wave.

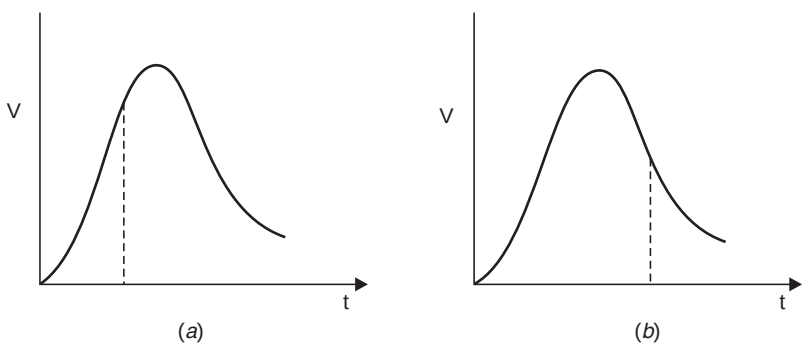

Fig. 3.2 Chopped waves. (*a*) Front chopped wave (*b*) Chopped wave

Impulse Flash Over Voltage

Whenever an impulse voltage is applied to an insulating medium of certain thickness, flash over may or may not take place. If out of a total of say ten applications of impulse voltage about 5 of them flash over then the probability of flash over with that peak voltage of the impulse voltage is 50%. Therefore, a 50 per cent impulse flash over voltage is the peak value of that impulse flash over voltage which causes flash over of the object under test for about half the number of applications of impulses. However, it is to be noted that the flash over occurs at an instant subsequent to the attainment of the peak value. The flash over also depends upon the polarity, duration of wave front and wave tails of the applied impulse voltages.

If the flash over occurs more than 50% of the number of applications, it is defined as impulse flash over voltage in excess of 50%.

The impulse flash over voltage for flash over on the wave front is the value of the impulse voltage at the instant of flash over on the wave front.

Impulse Puncture Voltage

The impulse puncture voltage is the peak value of the impulse voltage which causes puncture of the material when puncture occurs on the wave tail and is the value of the voltage at the instant of puncture when puncture occurs on the wave front.

Impulse Ratio for Flash Over

The impulse ratio for flash over is the ratio of impulse flash over voltage to the peak value of power frequency flash over voltage.

The impulse ratio is not a constant for any particular object, but depends upon the shape and polarity of the impulse voltage, the characteristics of which should be specified when impulse ratios are quoted.

Impulse Ratio for Puncture

The impulse ratio for puncture is the ratio of the impulse puncture voltage to the peak value of the power frequency puncture voltage.

3.2 IMPULSE GENERATOR CIRCUITS

Fig. 3.3 represents an exact equivalent circuit of a single stage impulse generator along with a typical load.

C_1 is the capacitance of the generator charged from a d.c. source to a suitable voltage which causes discharge through the sphere gap. The capacitance C_1 may consist of a single capacitance, in which case the generator is known as a single stage generator or alternatively if C_1 is the total capacitance of a group of capacitors charged in parallel and then discharged in series, it is then known as a multistage generator.

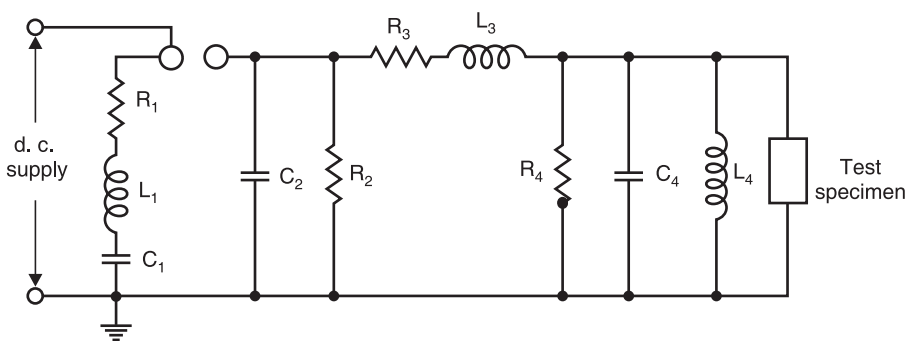

Fig. 3.3 Exact equivalent circuit of a single stage impulse generator with a typical load

L_1 is the inductance of the generator and the leads connecting the generator to the discharge circuit and is usually kept as small as possible. The resistance R_1 consists of the inherent series resistance of the capacitances and leads and often includes additional lumped resistance inserted within the generator for damping purposes and for output waveform control. L_3, R_3 are the external elements which may be connected at the generator terminal for waveform control. R_2 and R_4 control the duration of the wave. However, R_4 also serves as a potential divider when a CRO is used for measurement purposes. C_2 and C_4

represent the capacitances to earth of the high voltage components and leads. C_4 also includes the capacitance of the test object and of any other load capacitance required for producing the required wave shape. L_4 represents the inductance of the test object and may also affect the wave shape appreciably.

Usually for practical reasons, one terminal of the impulse generator is solidly grounded. The polarity of the output voltage can be changed by changing the polarity of the d.c. charging voltage.

For the evaluation of the various impulse circuit elements, the analysis using the equivalent circuit of Fig. 3.3 is quite rigorous and complex. Two simplified but more practical forms of impulse generator circuits are shown in Fig. 3.4 (*a*) and (*b*).

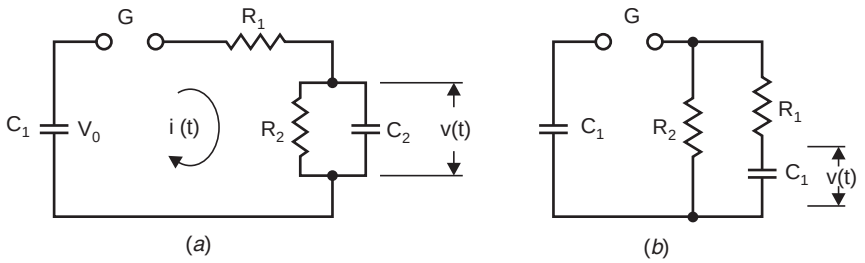

Fig. 3.4 Simplified equivalent circuit of an impulse generator

The two circuits are widely used and differ only in the position of the wave tail control resistance R_2. When R_2 is on the load side of R_1 (Fig. *a*) the two resistances form a potential divider which reduces the output voltage but when R_2 is on the generator side of R_1 (Fig. *b*) this particular loss of output voltage is absent.

The impulse capacitor C_1 is charged through a charging resistance (not shown) to a d.c. voltage V_0 and then discharged by flashing over the switching gap with a pulse of suitable value. The desired impulse voltage appears across the load capacitance C_2. The value of the circuit elements determines the shape of the output impulse voltage. The following analysis will help us in evaluating the circuit parameters for achieving a particular wave shape of the impulse voltage.

3.3 ANALYSIS OF CIRCUIT 'a'

Refer to Fig. 3.4 (*a*). After the gap sparks over, let the current in the generator circuit be $i\,(t)$ at any time t. Using Laplace transform, the impedance of the circuit is

$$Z\,(S) = R_1 + \frac{1}{C_1 s} + \frac{R_2}{R_2 C_2 s + 1}$$

$$= \frac{R_1 R_2 C_1 C_2 s^2 + \left(R_1 C_1 + R_2 C_2 + R_2 C_1\right) s + 1}{C_1 s \left(R_2 C_2 s + 1\right)}$$

$$I\,(s) = \frac{V_0}{sZ(s)} = \frac{V_0}{s} \frac{C_1 s\left(R_2 C_2 s + 1\right)}{R_1 R_2 C_1 C_2 C_2 s^2 + \left(R_1 C_1 + R_2 C_2 + R_2 C_1\right) s + 1}$$

and

$$v(s) = I(s)\,.\,\frac{R_2}{R_2 C_2 s + 1}$$

$$= V_0 R_2 C_1 \frac{1}{R_1 R_2 C_1 C_2 s^2 + (R_1 C_1 + R_2 C_2 + R_2 C_1)s + 1}$$

$$= \frac{V_0 R_2 C_1}{R_1 R_2 C_1 C_2} \cdot \frac{1}{s^2 + \dfrac{R_1 C_1 + R_2 C_2 + R_2 C_1}{R_1 R_2 C_1 C_2} s + \dfrac{1}{R_1 R_2 C_1 C_2}}$$

The roots of the expression in the denominator are

$$\frac{1}{2}\left[\frac{-(R_1 C_1 + R_2 C_2 + R_2 C_1)}{R_1 R_2 C_1 C_2} \pm \sqrt{\left(\frac{R_1 C_1 + R_2 C_2 + R_2 C_1}{R_1 R_2 C_1 C_2}\right)^2 - \frac{4}{R_1 R_2 C_1 C_2}}\right]$$

Let $$\alpha = \frac{R_1 C_1 + R_2 C_2 + R_2 C_1}{2 R_1 R_2 C_1 C_2}$$

and $$\beta = \frac{1}{2}\sqrt{\left(\frac{R_1 C_1 + R_2 C_2 + R_2 C_1}{R_1 R_2 C_1 C_2}\right)^2 - \frac{4}{R_1 R_2 C_1 C_2}}$$

Therefore, the roots are $(-\alpha + \beta)$ and $(-\alpha - \beta)$. The expression for voltage can be rewritten as

$$v(s) = \frac{1}{(s + \alpha - \beta)(s + \alpha + \beta)} \cdot \frac{V_0}{R_1 C_2}$$

Finding the partial fractions of the expression

$$\frac{1}{(s + \alpha - \beta)(s + \alpha + \beta)} = \frac{A}{s + \alpha - \beta} + \frac{B}{(s + \alpha + \beta)}$$

$$= \frac{As + A\alpha + A\beta + Bs + B\alpha - B\beta}{(s + \alpha - \beta)(s + \alpha + \beta)}$$

Comparing the coefficients $A + B = 0$ or $A = -B$ and $A\alpha + A\beta + B\alpha - B\beta = 1$ or $A\alpha + A\beta - A\alpha + A\beta = 1$ or $2A\beta = 1$ or

$$A = \frac{1}{2\beta} \quad \text{and} \quad B = -\frac{1}{2\beta}$$

Substituting these value of A and B, we have

$$v(s) = \frac{V_0}{R_1 C_2} \cdot \frac{1}{2\beta}\left[\frac{1}{s + (\alpha - \beta)} - \frac{1}{s + (\alpha + \beta)}\right]$$

Taking inverse Laplace transform of the voltage transform

$$v(s) = \frac{V_0}{2\beta R_1 C_2}[e^{-(\alpha - \beta)t} - e^{-(\alpha + \beta)t}] \tag{3.1}$$

Let $$V_n = \frac{V_0}{2\beta R_1 C_2}$$

$\therefore$ $$v(t) = V_n [e^{-(\alpha - \beta)t} - e^{-(\alpha + \beta)t}] \tag{3.2}$$

Let t_1 be the wave front time and t_2 the wave tail time, then both α and β must have unique values irrespective of the particular circuit used.

At time t_1, the shope of the wave is zero, therefore, t_1 can be obtained from the relation $dv(t)/dt = 0$

i.e,
$$\frac{dv(t)}{dt} = V_n[-(\alpha-\beta)e^{-(\alpha-\beta)t} + (\alpha+\beta)e^{-(\alpha+\beta)t}] = 0$$

or
$$\frac{\alpha+\beta}{\alpha-\beta} = e^{2\beta t_1}$$

or
$$2\beta t_1 = 1\text{n}\ \frac{\alpha+\beta}{\alpha-\beta}$$

or
$$t_1 = \frac{1}{2\beta}\,1\text{n}\,\frac{\alpha+\beta}{\alpha-\beta} \tag{3.3}$$

and the peak value of the voltage is then given by

$$v_m(t) = V_n[e^{-(\alpha-\beta)t_1} - e^{-(\alpha+\beta)t_1}] \tag{3.4}$$

To obtain t_2, substitute $t = t_2$ in equation (3.1) and the voltage is half of what it is when $t = t_1$ in the same equation *i.e.*

$$V_n[e^{-(\alpha-\beta)t_2} - e^{-(\alpha+\beta)t_2}] = \frac{V_n}{2}[e^{-(\alpha-\beta)t_1} - e^{-(\alpha+\beta)t_1}]$$

Let $t_2 = Kt_1$ where K is a constant, then

$$V_n[e^{-(\alpha-\beta)Kt_1} - e^{-(\alpha+\beta)Kt_1}] = \frac{V_n}{2}[e^{-(\alpha-\beta)t_1} - e^{-(\alpha+\beta)t_1}] \tag{3.5}$$

From equations (3.3) and (3.5) it is possible to obtain desired values of α and β for a required wave shape *i.e.* values of t_1 and K. Calculations can be simplified by the fact that in practice the second term on the left side of equation (3.5) is usually much smaller than the first term and can, therefore, be neglected.

Therefore, we have

$$e^{-(\alpha-\beta)Kt_1} = \frac{1}{2}[e^{-(\alpha-\beta)t_1} - e^{-(\alpha+\beta)t_1}]$$

or
$$2e^{-(\alpha-\beta)Kt_1} = e^{-(\alpha-\beta)t_1} - e^{-(\alpha+\beta)t_1}$$

Multiplying by $e^{(\alpha-\beta)t_1}$ both sides, we have

$$2e^{-(\alpha-\beta)(K-1)t_1} = 1 - e^{-2\beta t_1}$$

or
$$\alpha-\beta = \frac{2}{t_1(K-1)}.\ln\left(\frac{2}{1-e^{-2\beta t_1}}\right) \tag{3.6}$$

If $2\beta t_1 > 4$ equation (3.6) reduced to

$$\alpha-\beta = \frac{0.7}{t_1(K-1)} \tag{3.7}$$

With this assumption the results are found to be within 2% error.

Using equations (3.5) and (3.7) approximate values of α and β can be evaluated. The values of α and β corresponding to some typical waveforms are given below and have been obtained by using equations (3.5) and (3.6).

Table 3.1

Values of α and β for typical wave form

Wave	α	β
0.5/5	4.080	3.922
1/5	1.557	1.366
1/10	2.040	1.961
1.5/40	1.776	1.757
1/50	3.044	3.029

Table 3.2

Calculation for a 1/50 micro sec. wave

Time in micro sec.	$e^{-0.015t}$	$e^{-6.073t}$	*(2) – (3)*	*1.01749(4)*
0.0	1.0	1.0	0.00	0.0
0.1	0.998501	0.5448199	0.45368	0.4616148
0.2	0.9970045	0.2968287	0.7001757	0.71242
0.3	0.9955101	0.1617181	0.8337919	0.8483749
0.4	0.9940179	0.0881072	0.9059106	0.9217549
0.5	0.992528	0.0480026	0.9445253	0.961045
0.6	0.9910403	0.0261557	0.9648875	0.9817633
0.8	0.9880717	0.0077628	0.9803088	0.9974577
1.0	0.9851119	0.002342	0.9828076	1.0000
1.1	0.9836353	0.0012554	0.9823798	0.995616
1.2	0.982116	0.00068396	0.981477	0.998643
2.0	0.9704455	5.3095×10^{-6}	0.970445	0.987418
10.0	0.8607079	0.0	0.8607079	0.87576
50	0.4723665	0.0	0.4723665	0.4806281
48	0.4867522	0.0	0.4867522	0.49526
47	0.4941085	0.0	0.4941085	0.5627

It is to be noted that if values of α and β as given above are used, time is to be taken in microseconds.

Table 3.2 generates values for an 1/50 micro sec. impulse wave using equation (3.2) and values of α and β as in Table 3.1.

$$v(t) = V_n[e^{-(\alpha-\beta)t} - e^{-(\alpha+\beta)t}]$$
$$= V_n\,[e^{-(3.044-3.029)} - e^{-6.073t}]$$

$$= V_n [e^{-0.015t} - e^{-6.073t}]$$

Let p.u. $V_n = 1.01749$

From the first and the last column of the Table 3.2 it is clear that for $t = 1.0$ micro sec. the voltage is maximum and for $t = 50$ micro sec. it is almost 50% of the maximum value.

For certain impulse generator, the impulse capacitance C_1 is fixed whereas, the load capacitance C_2 will vary depending upon the equipment to be tested. The ratio of these capacitance C_1/C_2 plays an important role in the design of the impulse generator. Now

$$\alpha^2 - \beta^2 = \frac{1}{4}\left(\frac{1}{R_1C_1} + \frac{1}{R_2C_2} + \frac{1}{R_1C_2}\right)^2 - \frac{1}{4}\left(\frac{1}{R_1C_1} + \frac{1}{R_2C_2} + \frac{1}{R_1C_2}\right)^2 + \frac{1}{R_1R_2C_1C_2}$$

$$= \frac{1}{R_1R_2C_1C_2}$$

or
$$\frac{1}{R_1C_2} = R_2C_1 (\alpha^2 - \beta^2) \tag{3.8}$$

Substituting this value of $1/R_1C_2$ in equation (3.1) we have

$$v(t) = V_0R_2C_1 \frac{\alpha^2 - \beta^2}{2\beta} [e^{-(\alpha - \beta)t} - e^{-(\alpha + \beta)t}] \tag{3.9}$$

Let
$$\gamma = \frac{C_1}{C_2}$$

Since
$$\alpha = \frac{1}{2}\left[\frac{1}{R_1C_1} + \frac{1}{R_2C_2} + \frac{1}{R_1C_2}\right]$$

and
$$\alpha^2 - \beta^2 = \frac{1}{R_1R_2C_1C_2}$$

Therefore,
$$\alpha = \frac{1}{2}\left[(\alpha^2 - \beta^2) R_2C_2 + \frac{1}{R_2C_2} + R_2C_1 (\alpha^2 - \beta^2)\right]$$

$$= \frac{1}{2}\left[(\alpha^2 - \beta^2) \frac{R_2C_1}{\gamma} + \frac{\gamma}{R_2C_1} = R_2C_1(\alpha^2 - \beta^2)\right]$$

$$= \frac{1}{2}\left[\left(\frac{\gamma + 1}{\gamma}\right)(\alpha^2 - \beta^2) R_2C_1 + \frac{\gamma}{R_2C_1}\right]$$

Multiplying the equation by R_2C_1/γ and rearranging, we have

$$\left(\frac{R_2C_1}{\gamma}\right)^2 (\gamma + 1)(\alpha^2 - \beta^2) - 2\alpha\frac{R_2C_1}{\gamma} + 1 = 0$$

or
$$\left(\frac{R_2C_1}{\gamma}\right)^2 - \frac{2\alpha}{(\gamma + 1)(\alpha^2 - \beta^2)} \frac{R_2C_1}{\gamma} + \frac{1}{(\gamma + 1)(\alpha^2 - \beta^2)} = 0$$

Therefore,

$$\frac{R_2C_1}{\gamma} = \frac{\alpha}{(\gamma + 1)(\alpha^2 - \beta^2)} \pm \left[\left\{\frac{\alpha}{(\gamma + 1)(\alpha^2 - \beta^2)}\right\}^2 - \frac{1}{(\gamma + 1)(\alpha^2 - \beta^2)}\right]^{1/2}$$

or
$$R_2 = \frac{1}{C_1}\left[\frac{\alpha \pm \sqrt{\alpha^2 - (\gamma+1)(\alpha^2-\beta^2)}}{\frac{\gamma+1}{\gamma}(\alpha^2-\beta^2)}\right] \tag{3.10}$$

From equation (3.10) it is clear that for a given wave shape (certain value of α and β) resistance R_2 depends upon the ratio γ. Similarly, value of R_1 can also be derived to be

$$R_1 = \frac{1}{C_1}\left[\frac{\gamma+1}{\alpha \pm \sqrt{\alpha^2 - (\gamma+1)(\alpha^2-\beta^2)}}\right] \tag{3.11}$$

From equations (3.10) and (3.11) it is again clear that R_1 and R_2 will be physically realisable only if

$$\alpha^2 - (\gamma+1)(\alpha^2-\beta^2) \geq 0$$

or
$$\alpha^2 \geq (\gamma+1)(\alpha^2-\beta^2)$$

or
$$\frac{\alpha^2}{\alpha^2-\beta^2} \leq \gamma+1$$

or
$$\frac{\beta^2}{\alpha^2-\beta^2} \geq \gamma$$

or
$$\gamma \leq \frac{\beta^2}{\alpha^2-\beta^2} \tag{3.12}$$

This shows that in order to realise a given wave shape, certain values of R_1 and R_2 are required and these values will depend upon the ratio C_1/C_2. In order that R_1 and R_2 are physically realisable resistance, the ratio C_1/C_2 must not exceed certain value. This ratio can be evaluated for different wave shapes by choosing the typical values of α and β from Table 3.1 for these wave shapes. The values are listed in Table 3.3.

Table 3.3

Wave	*Max. value of*
0.5/5	12.166
1/5	3.342
1/40	12.166
1.5/40	45.988
1/50	100.717

Table 3.4 gives approximate value of the capacitances and γ of different types of equipments assuming an average value of C_1 as 25 nF.

Using Tables 3.1 and 3.4 and the equations (3.10) and (3.11) values of wave front (R_1) and wave tail resistance R_2 can be evaluated for different impulse waves and equipments to the impulse tested.

Table 3.4
Approximate capacitance of some equipments

Equipment	*Capacitance*	γ
Line insulators, pin insulators	25 pF	1000
Bushings	150 to 400 pF	62.5
Current transformers	200 to 600 pF	41.67
Power transformers upto 1 MVA	1000 to 2000 pF	12.5
Power transformers upto 50 MVA	10,000 pF	2.5
Power transformers above 100 MVA	30,000 pF	0.83
Cable samples for 10 m length	2500 pF	10.0
Experimental set up measuring upto 100 KV	100 pF	250
Capacitor, leads for a.c. test voltage upto 1000 KV	1000 pF	25

As is said earlier the voltage efficiency of circuit '*a*' is inferior to that of circuit '*b*' therefore, we leave the study of circuit '*a*' here and take up circuit '*b*' and analyse it in detail.

3.4 ANALYSIS OF CIRCUIT 'b'

Refer to Fig. 3.4 (*b*). The equivalent circuit after the gap *G* flashes over is given in Fig. 3.5.

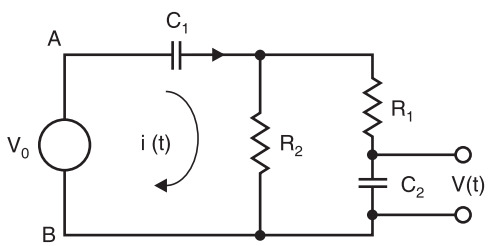

Fig. 3.5 Equivalent of Fig. 3.4 (*b*)

The equivalent transform impedance as seen between points *AB*

$$Z(s) = \frac{1}{C_1 s} + \frac{R_2(1/C_2 s + R_1)}{R_1 + R_2 + 1/C_2 s}$$

$$= \frac{1}{C_1 s} + \frac{R_2\,(R_1 C_2 s + 1)}{(R_1 + R_2) C_2 s + 1}$$

$$= \frac{(R_1 + R_2)\,C_2 s + 1 + R_1 R_2 C_1 C_2 s^2 + R_2 C_1 s}{R_1 C_1 C_2 s^2 + R_2 C_1 C_2 s^2 + C_1 s}$$

$$= \frac{(R_1 C_2 + R_2 C_2 + R_2 C_1) s + R_1 R_2 C_1 C_2 s^2 + 1}{C_1 s[(R_1 C_2 + R_2 C_2) s + 1]}$$

$$I(s) = \frac{V_0}{s} \cdot \frac{C_1 s\,[(R_1 C_2 + R_2 C_2)\,s + 1]}{R_1 R_2 C_1 C_2 s^2 + (R_1 C_2 + R_2 C_2 + R_2 C_1)\,s + 1}$$

Therefore,
$$v(s) = I(s)\,\frac{R_2 \,.\, 1/C_2 s}{(R_1 + R_2) + 1/C_2 s} = I(s) \,.\, \frac{R_2}{(R_1 + R_2)\,C_2 s + 1}$$

$$= \frac{V_0}{s}\,\frac{C_1 s\,[(R_1 + R_2)\,C_2 s + 1]\,R_2}{[R_1 R_2 C_1 C_2 s^2 + (R_1 C_2 + R_2 C_2 + R_2 C_1)\,s + 1][(R_1 + R_2)]}$$

$$= \frac{V_0}{s}\,\frac{R_2 C_1 s}{R_1 R_2 C_1 C_2 s^2 + (R_1 C_2 + R_2 C_2 + R_2 C_1)\,s + 1}$$

Dividing the numerator and denominator by $R_1R_2C_1C_2$, we have

$$v(s) = \frac{V_0}{R_1C_2}\left[\frac{1}{s^2 + \left(\frac{1}{R_2C_1} + \frac{1}{R_1C_1} + \frac{1}{R_1C_2}\right)s + \frac{1}{R_1R_2C_1C_2}}\right] \tag{3.13}$$

Let $$\alpha = \frac{1}{2}\left[\frac{1}{R_2C_1} + \frac{1}{R_1C_1} + \frac{1}{R_1C_2}\right]$$

and $$\beta = \frac{1}{2}\left[\left(\frac{1}{R_2C_1} + \frac{1}{R_1C_1} + \frac{1}{R_1C_2}\right)^2 - \frac{4}{R_1R_2C_1C_2}\right]^{1/2}$$

Equation (3.13) can be rewritten as

$$v(s) = \frac{V_0}{R_1C_2}\frac{1}{(s+\alpha-\beta)(s+\alpha+\beta)}$$

$$v(t) = \frac{V_0}{2R_1C_2\beta}\left[e^{-(\alpha-\beta)t} - e^{-(\alpha+\beta)t}\right] \tag{3.14}$$

Let $\gamma = C_1/C_2$ and working on the similar lines as for the circuit '*a*', we have

$$R_2 = \frac{1}{C_1}\left[\frac{\alpha \pm \sqrt{-\alpha^2 - \frac{1+\gamma}{\gamma}(\alpha^2-\beta^2)}}{\frac{1+\gamma}{\gamma}(\alpha^2-\beta^2)}\right] \tag{3.15}$$

and $$R_1 = \frac{1}{C_1}\left[\frac{1+\gamma}{\alpha \pm \sqrt{\alpha^2 - \frac{1+\gamma}{\gamma}(\alpha^2-\beta^2)}}\right] \tag{3.16}$$

Again, in order that, R_1 and R_2 are physically realisable

$$\alpha^2 - \frac{1+\gamma}{\gamma}(\alpha^2-\beta^2) \geq 0$$

or $$\alpha^2 \geq \frac{1+\gamma}{\gamma}(\alpha^2-\beta^2)$$

or $$\frac{\alpha^2}{\alpha^2-\beta^2} \geq \frac{1+\gamma}{\gamma}$$

or $$\frac{\alpha^2}{\alpha^2-\beta^2} - 1 \geq \frac{1}{\gamma}$$

or $$\gamma \geq \frac{\alpha^2-\beta^2}{\beta^2} \tag{3.17}$$

This shows that γ has a lower limit given by inequality (3.17). Table 3.5 gives values of γ for different wave shapes in order that R_1 and R_2 could be physically realisable for those wave shapes. Values of α and β required in (3.17) are obtained from Table 3.1.

Table 3.5 shows that for a given wave shape if the ratio $\gamma = C_1/C_2$ exceeds the corresponding value given in this table, there exists physically realisable values of R_1 and R_2 to obtain that wave shape.

Table 3.5

Wave shape	*Minimum value of* γ
0.5/5	0.0821943
1/5	0.2991994
1/10	0.0821943
1.5/40	0.0217447
1/50	0.0099287

Table 3.6
Value of R_1 as obtained from (3.16)

Wave shape	*Value of* γ					
	0.83	2.5	10	12.5	41.67	62.5
0.5/5	9.3827	17.6	55.1	67.59	213.41	317.5
1/5	27.629	49.31	151.6	185.8	584.9	875
1/10	19.51	31.11	117.18	137.57	433.9	645.5
1.5/40	20.86	39.71	124.6	152.68	482.6	718.2
1/50	6.039	11.48	72.45	88.92	281.02	418

Table 3.7
Value of R_2 as obtained from (3.15)

Wave shape	*Value of* γ					
	0.83	2.5	10	12.5	41.67	62.5
0.5/5	111.6	178.79	228.9	233.3	146.3	246
1/5	86.16	145.27	189	194.8	204.16	256
1/10	121	197	253.7	258.1	273.3	275.5
1.5/40	948	1501	1914	1948	2055	2071
1/50	1274	2011	2561	2609	2572	2775

Again comparing Tables 3.4 and 3.5 it is clear that for most of the equipments to be tested the value of γ is much greater than the minimum required and, therefore, this is yet another advantage of circuit '*b*' over circuit '*a*' where one has to be cautious for selection of R_1 and R_2 for some shapes.

Tables (3.6) and (3.7) respectively give the value of R_1 and R_2 for some typical wave shapes and values for ratio C_1/C_2 with C_1 = 25 nF.

Again if γ is large Equations (3.15) and (3.16) reduce to

$$R_2 = \frac{1}{C_1} \cdot \frac{1}{\alpha - \beta} \tag{3.18}$$

and

$$R_2 = \frac{1}{C_1(\alpha + \beta)} + \frac{\gamma}{C_1(\alpha + \beta)} \tag{3.19}$$

From Tables (3.6) (3.7) and equations (3.18) and (3.19) it is clear that when $\gamma \geq 10$ value of R_2 is almost constant for a given wave shape and different values of γ *i.e.* for a given wave, the value of wave tail resistance is constant if the load capacitance is such that $C_1/C_2 \geq 10$. However, the situation is different for wave front resistance R_1. Its variation is a straight line one with variation in the ratio C_1/C_2.

While calculating R_1 using equation (3.16) we have neglected the inductance of the system which will always be present and hence there will be oscillations on the waveform as the generator discharges and hence the tolerances on the wave front time ± 0.5 μ sec. must be taken into account. Neglecting the position of the wave tail resistance in Fig. (3.4) which has no effect on wave front time, and assuming an inductance L in series with the circuit an approximate equivalent circuit for determining the wave front resistance is given in Fig. 3.6.

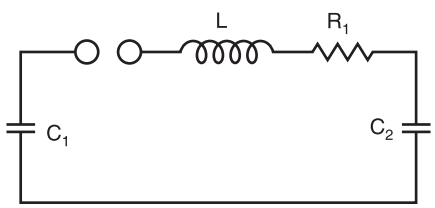

Fig. 3.6 Circuit for calculation of wave front resistance R_1

The circuit thus reduces to a simple damped series resonant circuit and the critical resistance R_1 for the circuit to be non-oscillatory is given by

$$R_1 = 2\sqrt{L/C} \tag{3.20}$$

where

$$\frac{1}{C} = \frac{1}{C_1} + \frac{1}{C_2}$$

Equation (3.20) is in general suitable for predicting the limiting values for the front resistance R_1.

From Tables (3.6) and (3.7) it is clear that for a given wave shape and γ, the inequality $R_2C_1 >> R_1C_2$ holds good.

Corresponding to the wave front time t_1 equation (3.14) becomes

$$V_{\max}(t_1) = \frac{V_0}{2R_1C_2\beta}[e^{-(\alpha-\beta)t_1} - e^{-(\alpha+\beta)t_1}]$$

We define here the voltage efficiency of the generator or utilization factor of the generator as the ratio of the peak value of the output voltage $V_{\max}(t_1)$ the charging voltage V_0 and is denoted as

$$\eta = \frac{V_{\max}(t_1)}{V_0} = \frac{1}{2R_1C_2\beta}[e^{(\alpha-\beta)t_1} - e^{-(\alpha+\beta)t_1}]$$

Here

$$\alpha = \frac{1}{2}\left[\frac{1}{R_2C_1} + \frac{1}{R_1C_2} + \frac{1}{R_1C_1}\right]$$

and

$$\beta = \frac{1}{2}\left[\left(\frac{1}{R_2C_1} + \frac{1}{R_1C_1} + \frac{1}{R_1C_2}\right)^2 - \frac{4}{R_1R_2C_1C_2}\right]^{1/2}$$

When $R_2C_1 >> R_1C_2$, neglecting $1/R_2C_1$

We have $$\alpha = \frac{1}{2R_1}\left[\frac{1}{C_2} + \frac{1}{C_1}\right] = \frac{C_1 + C_2}{2C_1C_2R_1} \approx \beta$$

Neglecting the term $\frac{1}{R_2C_1}$ and $\frac{4}{R_1R_2C_1C_2}$.

Therefore, $$\eta = \frac{v_{\max}(t_1)}{V_0} = \frac{2C_1C_2R_1}{2R_1C_2(C_1 + C_2)} \approx \frac{C_1}{C_1 + C_2}$$

Here the term $e^{-(\alpha+\beta)t_1}$ is neglected as compared to $e^{-(\alpha-\beta)t_1}$

$$\eta = \frac{1}{1 + \frac{C_2}{C_1}} \tag{3.21}$$

Therefore, higher the generator capacitance the higher is the voltage efficiency of the generator. The impulse energy transformed during a discharge is given by

$$W = \frac{1}{2}C_1V_0^2 \tag{3.22}$$

With inductive loads the capacitance of generator must be large enough to prevent oscillations on the tail of the impulse wave. The minimum permissible capacitance is given by

$$C_1 = \frac{8t_2^2}{L} \tag{3.23}$$

where t_2 = Wave tail time in micro sec. L_2 = Inductance of the test object in Henry and C_1, the capacitance in *pF*.

In case of a 3-phase power transformer with *MVA* rating as *M* and *V* the rated voltage in kV, *Z* the percentage impedance, the minimum value of generator capacitance should be

$$C_1 = \frac{M \times 10^8}{ZV^2}\ \mu F \tag{3.24}$$

The impulse voltage is applied to one phase and the other two phases are grounded, the secondary terminals are short-circuited.

3.5 MULTISTAGE IMPULSE GENERATOR CIRCUIT

In order to obtain higher and higher impulse voltage, a single stage circuit is inconvenient for the following reasons:

(*i*) The physical size of the circuit elements becomes very large.

(*ii*) High d.c. charging voltage is required.

(*iii*) Suppression of corona discharges from the structure and leads during the charging period is difficult.

(*iv*) Switching of vary high voltages with spark gaps is difficult.

In 1923 E. Marx suggested a multiplier circuit which is commonly used to obtain impulse voltages with as high a peak value as possible for a given d.c. charging voltage.

Depending upon the charging voltage available and the output voltage required a number of identical impulse capacitors are charged in parallel and then discharged in series, thus obtaining a multiplied total charging voltage corresponding to the number of stages. Fig. 3.7 shows a 3-stage impulse generator circuit due to Marx employing '*b*' circuit connections. The impulse capacitors C_1 are charged to the charging voltage V_0 through the high charging resistors R_c in parallel. When all the gaps G break down, the C_1' capacitances are connected in series so that C_2 is charged through the series connection of all the wave front resistances R_1' and finally all C_1' and C_2 will discharge through the resistors R_2' and R_1'. Usually $R_c >> R_2 >> R_1$.

If in Fig. 3.7 the wave tail resistors R_2' in each stage are connected in parallel to the series combination of R_1', G and C_1', an impulse generator of type circuit '*a*' is obtained.

In order that the Marx circuit operates consistently it is essential to adjust the distances between various sphere gaps such that the first gap G_1 is only slightly less than that of G_2 and so on. If is also necessary that the axes of the gaps G be in the same vertical plane so that the ultraviolet radiations due to spark in the first gap G, will irradiate the other gaps. This ensures a supply of electrons released from the gap electrons to initiate breakdown during the short period when the gaps are subjected to overvoltages.

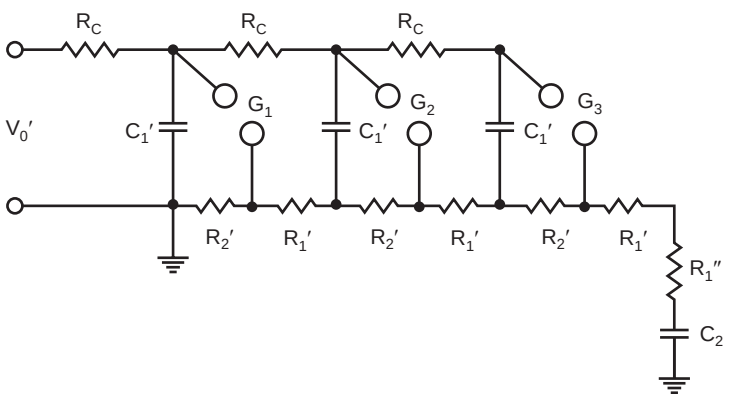

Fig. 3.7 A 3-stage Marx impulse generator in circuit '*b*' connections.

The wave front control resistance can have three possible locations (*i*) entirely within the generator (*ii*) entirely outside the generator (*iii*) partly within and partly outside the generator.

The first arrangement is unsatisfactory as the inductance and capacitance of the external leads and the load form an oscillatory circuit which requires to be damped by an external resistance. The second arrangement is also unsatisfactory as a single external front resistance will have to withstand, even though for a very short time, the full rated voltage and therefore, will turn out to be inconveniently long and would occupy much space. A compromise between the two is the third arrangement as shown in Fig. 3.7 and thus both the "space economy" and damping of oscillations are taken care of.

It can be seen that Fig. 3.7 can be reduced to the single stage impulse generator of Fig. 3.4 (*b*). After the generator has fired, the total discharge capacitance C_1 may be given as

$$\frac{1}{C_1} \sum^{n} \frac{1}{C_1'}$$

the equivalent front resistance

$$R_1 = \sum^{n} R_1' + R_1''$$

and the equivalent tail control resistance

$$R_2 = \sum^{n} R_2'$$

where n is the number of stages.

Goodlet has suggested another circuit shown in Fig. 3.8, for generation of impulse voltage where the load is earthed during the charging period, without the necessity for an isolating gap. The impulse output voltage has the same polarity as the charging voltage is case of Marx circuit, it is reversed in case of Goodlet circuit. Also, on discharge, both sides of the first spark gap are raised to the charging voltage in the Marx circuit but in case of Goodlet circuit they attain earth potential.

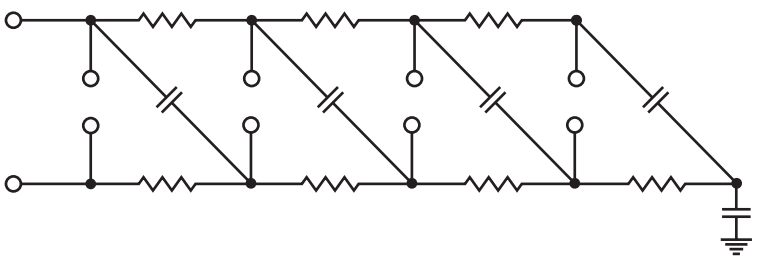

Fig. 3.8 Basic goodlet circuit

3.6 CONSTRUCTION OF IMPULSE GENERATOR

An impulse generator requires a d.c. power supply for charging the impulse capacitance C_1 of the generator. The supply consists of a step up transformer and rectifier. The charging times should not be less than 3 to 10 seconds as every application of voltage will leave behind preionising effects, so a time should be allowed between two successive applications so that the prestressing effects within the insulations do not influence the breakdown strength. These days thyristorized controlled d.c. supply for charging is available.

The resistors may be made up of wire, liquid or composite (carbon etc.) resistive materials. The liquid and carbon resistors even though have high heat capacity, these are invariably not used especially for wave front and tail control resistances as these are highly unstable *i.e.* their value is not constant and may change with various factors. Therefore, non-inductive wire would resistors are used for this purpose even though these are relatively costly. It is found that for most of the circuits if the time constant of those resistances is less than 0.1 micro se. they are considered quite satisfactory from the view point of oscillation in the circuit. These resistors should be placed in such a way that they can be exchanged and replaced easily as they must be charged as per the requirement of a particular wave shape.

The layout of an impulse generator is mainly decided by the type of capacitors used. Oil paper insulated capacitors having low inductance and high rate of discharge are normally employed. The material oil is often replaced by special fluids which are having higher permittivity to reduce the size of the capacitor for the same capacitance. Some of the designs use oil impregnated capacitors in insulating containers. These capacitors have the dielectric assembled in an insulating cylinder of porcelain or varnished paper with plane metal plates. An advantage of this form of capacitor is that successive stages of capacitors can be built up in vertical columns, each stage being separated from the adjacent one by supports of the same form as the capacitors but without the dielectric. Recently, modular constructions with simple capacitor units within insulating cylinders or vessels or within metal tanks

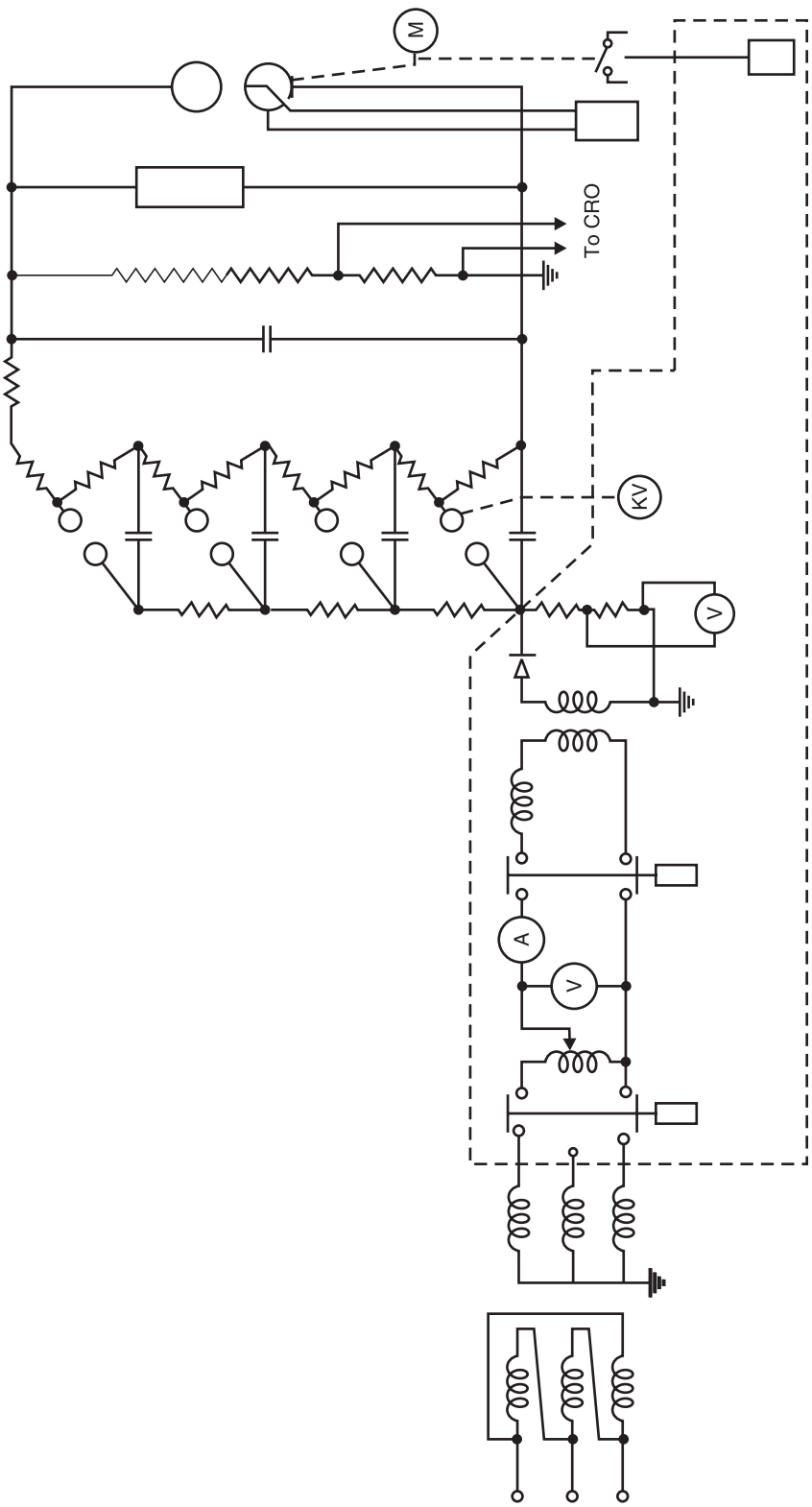

Fig. 3.9 Impulse generator circuit

and bushings have been recommended, are in use. These designs were made possible due to the use of high dielectric fluids (*e.g.* SF_6) which could reduce the size of the capacitors significantly.

The coupling sphere gaps are arranged one above the other on horizontal arms and the setting of the gaps is adjusted by a remotely controlled motor in conjunction with an indicator. This arrangement with mutual irradiation ensures a perfect cascading of the spark gaps. They are normally incapsulated in a chimney provided with dust free and dry air. The use of proper gas mixtures gives good switching performance.

The impulse generator should have a device to earth the capacitors when it is not in operation. The d.c. capacitors can build up high voltages after a short time of short circuit due to the relaxation phenomenon. A series protective resistance should be included in this earthing device to avoid too high discharge currents.

The front and tail resistors are fixed to the generator frame by means of resistor carriers of bakelised paper tubes. The charging resistors are fixed along the sphere gap column. All leads and electrodes within the generator should be dimensioned properly to avoid too heavy corona discharges during the charging period.

A typical impulse generator circuit giving all details is shown in Fig. 3.9.

3.7 TRIGGERING AND SYNCHRONISATION OF THE IMPULSE GENERATOR

Impulse generators are normally operated in conjunction with cathode ray oscillographs for measurement and for studying the effect of impulse waves on the performance of the insulations of the equipments. Since the impulse waves are of shorter duration, it is necessary that the operation of the generator and the oscillograph should be synchronised accurately and if the wave front of the wave is to be recorded accurately, the time sweep circuit of the oscillograph should be initiated at a time slightly before the impulse wave reaches the deflecting plates.

If the impulse generator itself initiates the sweep circuit of the oscillograph, it is then necessary to connect a delay cable between the generator or the potential divider and the deflecting plates of the oscilloscope so that the impulse wave reaches the plates at a controlled time after the sweep has been tripped. However, the use of delay cable leads to inaccuracies in measurement. For this reason, some tripping circuits have been developed where the sweep circuit is operated first and then after a time of about 0.1 to 0.5 μ sec. the generator is triggered.

One of the methods involves the use of a three-sphere gap in the first stage of the generator as shown in Fig. 3.10. The spacing between the spheres is so adjusted that the two series gaps are able to withstand the charging voltage of the impulse generator. A high resistance is connected between the outer spheres and its centre point is connected to the control sphere so that the voltage between the outer spheres is equally divided between the two gaps. If the generator is now charged to a voltage slightly less than the breakdown voltage of the gaps, the breakdown can be achieved at any instant by applying an impulse of either polarity and of a peak voltage not less than one fifth of the charging voltage to the control sphere.

The operation is explained as follows. The switch *S* is closed which initiates the sweep circuit of the oscillograph. The same impulse is applied to the grid of the thyratron tube. The inherent time delay of the thyratron ensures that the sweep circuit begins to operate before the start of the high voltage impulse.

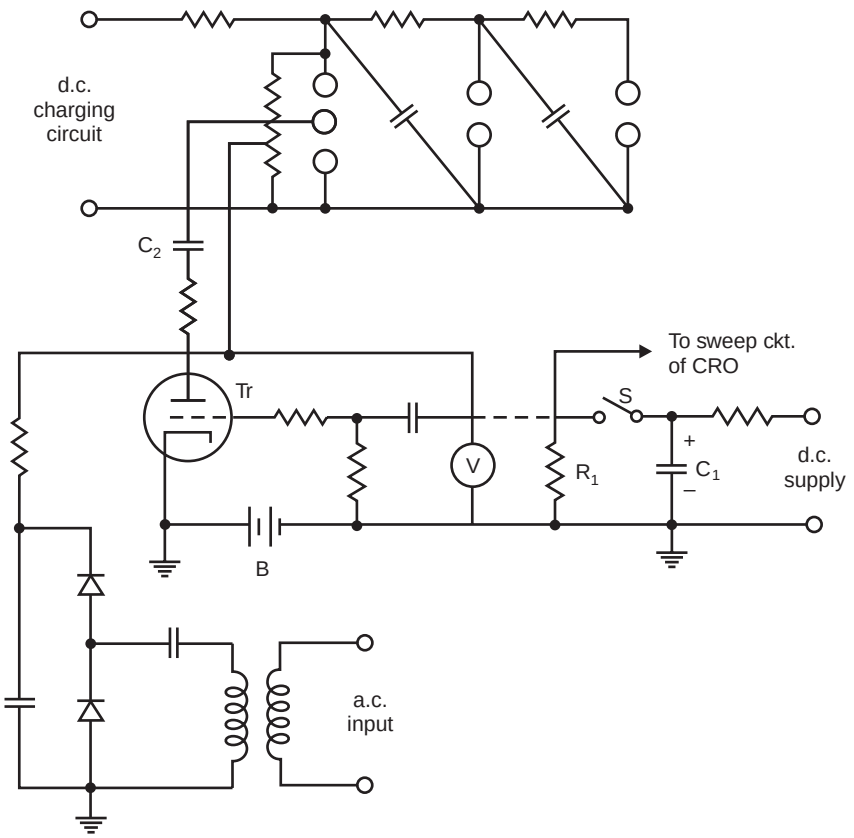

Fig. 3.10 Circuit for synchronisation

A further delay can be introduced if required by means of a capacitance-resistance circuit R_1C_1. The tripping impulse is applied through the capacitor C_2. During the chargnig period of the generator the anode of the thyratron tube is held at a positive potential of about 20 kV. The grid is held at negative potential with the help of battery *B* so that it does not conduct during the charging period. As the switch *S* is closed, the trigger pulse is applied to the grid of the thyratron tube which conducts and a negative impulse of 20 kV is applied to the central sphere which triggers the impulse generator.

Fig. 3.11 shows a trigatron gap which is used as the first gap of the impulse generator and consists essentially of a three-electrode gap. The high voltage electrode is a sphere and the earthed electrode may be a sphere, a semi-sphere or any other configuration which gives homogeneous electric field. A small hole is drilled into the earthed electrode into which a metal rod projects. The annular gap between the rod and the surrounding hemisphere is about 1 mm. A glass tube is fitted over the rod electrode and is surrounded by a metal foil which is connected to the earthed hemisphere. The metal rod or trigger electrode forms the third electrode, being essentially at the same potential as the drilled electrode, as it is connected to it through a high resistance, so that the control or tripping pulse can be applied between these two electrodes. When a tripping pulse is applied to the rod, the field is distorted in the main gap and the latter breaks down at a voltage appreciably lower than that required to cause its breakdown in the absence of the tripping pulse. The function of the glass tube is to promote corona discharge round the rod as this causes photoionisation in the annular gap and the main gap and consequently facilitates their rapid breakdown.

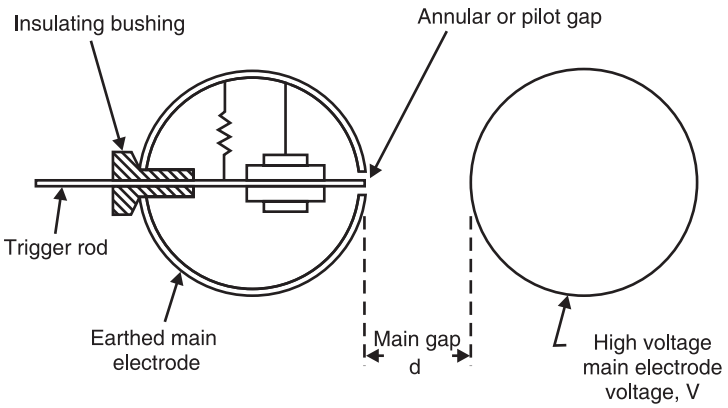

Fig. 3.11 The trigatron spark gap

For single stage or multi-stage impulse generators the trigatron gaps have been found quite satisfactory and these require a tripping voltage of about 5 kV of either polarity. The tripping circuits used today are commercially available and provide in general two or three tripping pulses of lower amplitudes. Fig. 3.12 shows a typical tripping circuit. The capacitor C_1 is charged through a high resistance R_1. As the remotely controlled switch S is closed, a pulse is applied to the sweep circuit of the oscillograph through the capacitor C_3. At the same time the capacitor C_2 is charged up and a triggering pulse is applied to the trigger electrode of the trigatron. The requisite delay in triggering the generator can be provided by suitably adjusting the values of R_2 and C_2. The residual charge on C_2 can be discharged through a high resistance R_3. These days lasers are also used for tripping the spark gap.

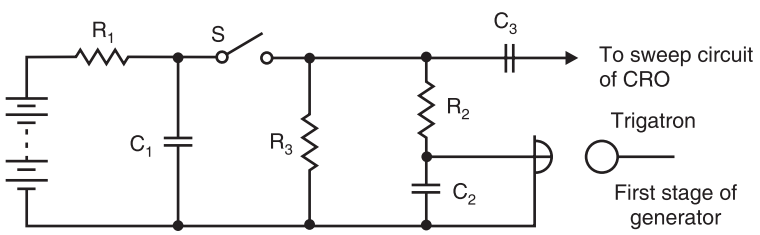

Fig. 3.12 A typical tripping circuit of a trigatron

The trigatron also has a phase shifting circuit associated with it so as to synchronise the initiation time with an external alternating voltage. Thus, it is possible to combine high alternating voltage tests with a superimposed impulse wave of adjustable phase angle.

The trigatron is designed so as to prevent the overcharging of the impulse capacitors in case of an accidental failure of triggering. An indicating device shows whether the generator is going to fire correctly or not. An additional feedback circuit provides for a safe wave chopping and oscillograph release, independent of the emitted control pulse.

3.8 IMPULSE CURRENT GENERATION

The impulse current wave is specified on the similar lines as an impulse voltage wave. A typical impulse current wave is shown in Fig. 3.13.

High current impulse generators usually consist of a large number of capacitors connected in parallel to the common discharge path. A typical impulse current generator circuit is shown in Fig. 3.14.

The equivalent circuit of the generator is shown in Fig. 3.15 and approximates to that of a capacitance C charged to a voltage V_0 which can be considered to discharge through an inductance L and a resistance R. In practice both L and R are the effective inductance and resistance of the leads, capacitors and the test objects.

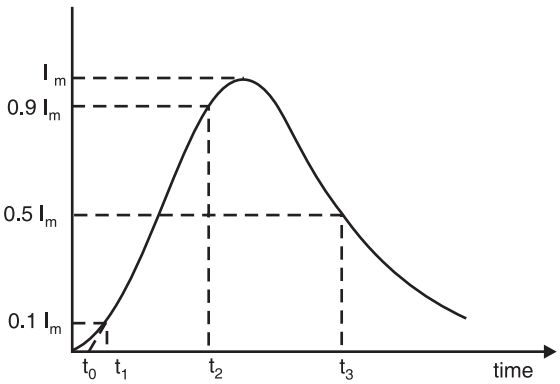

Fig. 3.13 A typical impulse current wave

3.8.1 Analysis of Impulse Current Generator Refer to Fig. 3.15

After the gap S is triggered, the Laplace transform current is given as

$$I(s) = \frac{V_0}{s}\frac{1}{R + sL + 1/Cs}$$

$$= \frac{V}{L}\cdot\frac{1}{s^2 + R/Ls + 1/LC}$$

$$= \frac{V}{L}\cdot\frac{1}{(s+\alpha)^2 + \omega^2}$$

where $\alpha = \dfrac{R}{2L}$ and $\omega = \left(\dfrac{1}{LC} - \dfrac{R^2}{4L^2}\right)^{1/2}$

or $$\omega = \frac{1}{\sqrt{LC}}\left(1 - \frac{R^2C}{4L}\right)^{1/2} = \frac{1}{\sqrt{LC}}(1 - \nu^2)^{1/2}$$

where $$\nu = \frac{R}{2}\sqrt{\frac{C}{L}}$$

Taking the inverse Laplace we have the current

$$i(t) = \frac{V}{\omega L}e^{-\alpha t}\sin\omega t \qquad (3.25)$$

For current $i(t)$ to be maximum $\dfrac{di(t)}{dt} = 0$

$$\frac{di(t)}{dt} = \frac{V}{\omega L}\left[\omega e^{-\alpha t}\cos\omega t - \alpha e^{-\alpha t}\sin\omega t\right] = 0$$

$$= \frac{V}{\omega L}e^{-\alpha t}\left[\omega\cos\omega t - \alpha\sin\omega t\right] = 0$$

or $$\frac{\omega}{\sqrt{\alpha^2 + \omega^2}}\cos\omega t - \frac{\alpha}{\sqrt{\alpha^2 + \omega^2}}\sin\omega t = 0$$

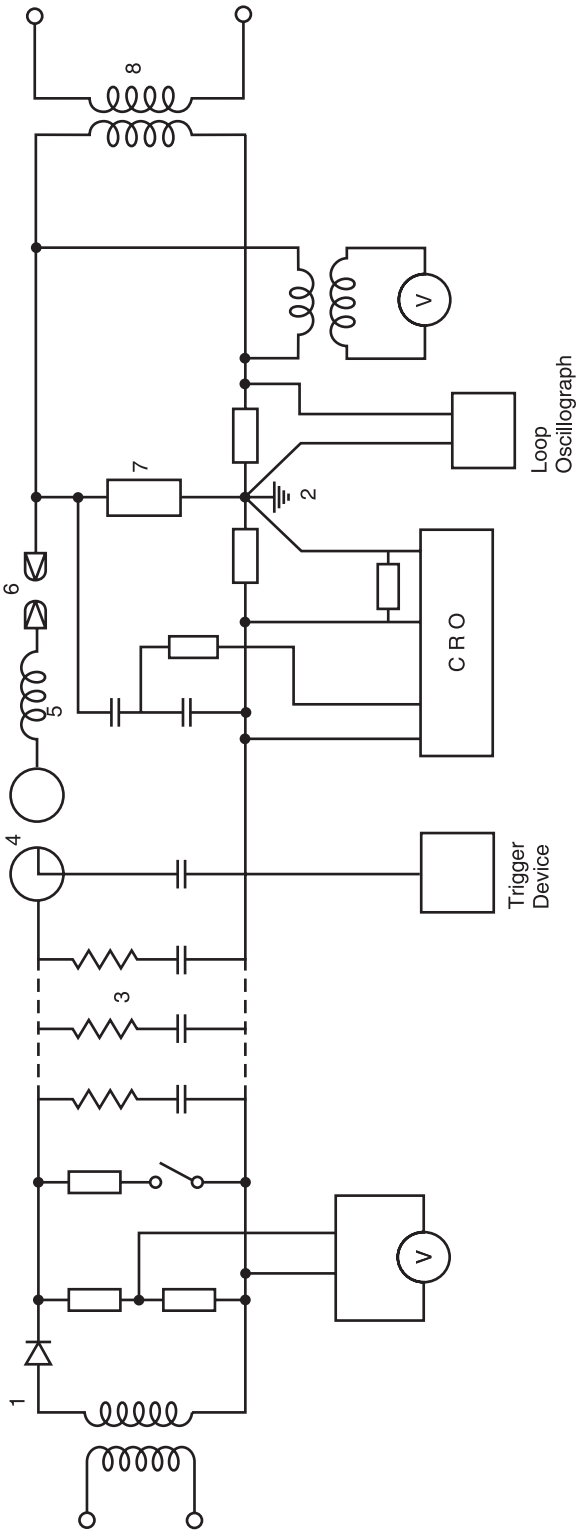

Fig. 3.14 A typical impulse current generator circuit. 1. Charging unit 2. Earthing device 3. Capacitors with damping resistors 4. Firing sphere gap. 5. Reactor coil 6. Protective sphere gap 7. Test specimen (LA) 8. Test transformer for power frequency.

or $\sin\theta\cos\omega t - \cos\theta\sin\omega t = 0$

or $\sin(\theta - \omega t) = 0$

or $\omega t = \theta$

or $t_{max} = \dfrac{\theta}{\omega}$

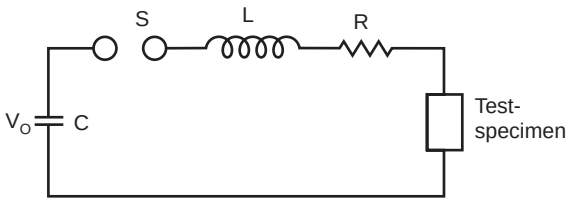

Fig. 3.15

where t_{max} is the time when the first maximum value of current occurs and

$$\theta = \sin^{-1}\frac{\omega}{\sqrt{\alpha^2 + \omega^2}}$$

$$= \sin^{-1}\frac{\omega}{\left[\dfrac{R_2}{4L^2} + \dfrac{1}{LC} - \dfrac{R^2}{4L^2}\right]^{1/2}}$$

$$= \sin^{-1}\sqrt{LC\,\omega}$$

or $$t_{max} = \frac{\sin^{-1}\sqrt{LC\omega}}{\omega} = \frac{\sin^{-1}\sqrt{LC}\,.\,\dfrac{1}{\sqrt{LC}}(1-\nu^2)^{1/2}}{\dfrac{1}{\sqrt{LC}}(1-\nu^2)^{1/2}}$$

or $$t_{max} = \sqrt{LC}(1-\nu^2)^{-1/2}\sin^{-1}(1-\nu^2)^{1/2} = \sqrt{LC}.\frac{\sin^{-1}(1-\nu^2)^{1/2}}{(1-\nu^2)^{1/2}}$$

Substituting the value of $t = t_{max}$ in (3.25) the first maximum value of current is given as

$$I_{max} = \frac{V_0\sqrt{LC}}{(1-\nu^2)^{1/2}L}\,.\,\mathrm{Exp}\left[-\frac{R\sqrt{LC}\,\sin^{-1}(1-\nu^2)^{1/2}}{2L\qquad(1-\nu^2)^{1/2}}\right]$$

$$\sin\left\{\frac{(1-\nu^2)^{1/2}}{\sqrt{LC}}\,.\,\sqrt{LC}\,(1-\nu^2)^{-1/2}\,\sin^{-1}(1-\nu^2)^{1/2}\right\}$$

$$= \frac{V_0}{(1-\nu^2)^{1/2}}\cdot\sqrt{\frac{C}{L}}\,.\,\mathrm{Exp}\left[\frac{-\nu\sin^{-1}(1-\nu^2)^{1/2}}{(1-\nu^2)^{1/2}}\right].\sin\left\{\sin^{-1}(1-\nu^2)^{1/2}\right\}$$

$$= V_0\sqrt{\frac{C}{L}\,\mathrm{Exp}\left[\frac{-\nu\sin^{-1}(1-\nu^2)^{1/2}}{(1-\nu^2)^{1/2}}\right]} \qquad (3.26)$$

Equation (3.26) can be rewritten as

$$I_{max} = V_0\sqrt{\frac{C}{L}}f(\nu) = \sqrt{\frac{2W}{L}}f(\nu)$$

where $$W = \frac{1}{2}CV_0^2$$

the initial energy stored by the generator.

If $R = 0$, $\nu = 0$ then from equation (3.26) it is clear that $I = V_0\sqrt{C/L}$ and from equation 3.25

$$i(t) = V_0\sqrt{\frac{C}{L}}\sin\frac{t}{\sqrt{LC}}$$

Fig. 3.16 shows the current response for different values of ν

From equation it is clear that for maximum value of current the inductance of the circuit should be low for a given initial energy W. The usual value of f (ν) without adding damping elements varies between 0.85 and 0.95.

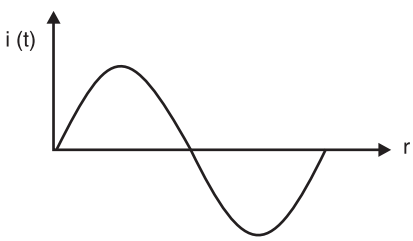

Fig. 3.16 Current response of circuit in Fig. 3.15

Unidirectional impulse can be produced by damping with additional resistance. However, this results in reduced peak value of current *e.g.* the value of the current during critical damping ($R = 2\sqrt{L/C}$) is about 0.368 times its value when no damping ($R = 0$) is present. It has been found that an approximately unidirectional wave form can be obtained by the use of a non-linear damping resistance in the circuit with a reduction of I_m to only about 0.7 times and the $V_0\sqrt{C/L}$. The effective inductance of the unit can be reduced by sub-dividing the capacitance C into groups of smaller units.

In a typical design several capacitor units connected in parallel are placed around the test object in horse-shoe shape with the minimum diameter. The conductors between the capacitors and the test objects are to be as short as possible and are placed in narrow parallel lines. As an alternative, co-axial cables can also be used as these have inherently very low inductance.

Normally on long high voltage transmission lines square wave impulse current are propagated during discharge of these lines. These waves can be generated by simulating artificial lines with the help of capacitor connected in series with choke. The number of elements is inversely proportional to the ripple tolerated on the square wave.

EXAMPLES

Example 3.1. *A ten-stage impulse generator has 0.250 μF condensers. The wave front and wave tail resistances are 75 ohms and 2600 respectively. If the load capacitance is 2.5 nF, determine the wave front and w ave tail times of the impulse wave.*

Solution: In general

$$t_1 = \frac{1}{2\beta}\ln\frac{\alpha+\beta}{\alpha-\beta}$$

and

$$\alpha - \beta = \frac{0.7}{t_1(K-1)} \text{ where } K = \frac{t_2}{t_1}$$

For circuit '*b*'

$$\alpha = \frac{1}{2}\left[\frac{1}{R_2C_1} + \frac{1}{R_1C_1} + \frac{1}{R_1C_2}\right]$$

and $$\beta = \frac{1}{2}\left[4\alpha^2 - \frac{4}{R_1 R_2 C_1 C_2}\right]^{1/2}$$

In the given problem

$$R_1 = 75 \text{ ohms}, R_2 = 2600 \text{ ohms}, C_1 = \frac{250}{10} = 25 \text{ nF}$$

and $$C_2 = 2.5 \text{ nF}$$

$$\therefore \quad \alpha = \frac{10^9}{2}\left[\frac{1}{2600 \times 25} + \frac{1}{75 \times 25} + \frac{1}{75 \times 2.5}\right]$$

$$\approx \frac{10^9}{2}\left[\frac{1}{75 \times 25} + \frac{1}{75 \times 2.5}\right]$$

$$\approx \frac{10^9}{2}\,[5.333 \times 10^{-4} + 5.333 \times 10^{-3}]$$

$$\approx \frac{10^9}{2} \times 5.8663 \times 10^{-3}$$

$$\approx 2.933 \times 10^6$$

Now $$\frac{4 \times 10^{18}}{75 \times 2600 \times 25 \times 2.5} = 3.282 \times 10^{11}$$

$$\therefore \quad \beta = 2.9189 \times 10^6$$

$$t_1 = \frac{1}{2 \times 2.9189} \ln \frac{2.933 + 2.9189}{2.933 - 2.9189}$$

$$= 0.1713 \ln \frac{5.8519}{0.0141}$$

$$= 1.03 \ \mu \text{ sec.}$$

$$0.0141 = \frac{0.7}{1.03\,(K - 1)}$$

$$K - 1 = 48.07$$

$$K = 49.07$$

or $$t_2 = 50.5 \ \mu \text{ sec.} \quad \textbf{Ans.}$$

Approximate values of wave front and wave tail times can be obtained as follows:

The approximate circuit during charging of load capacitance by the generator capacitance is a follows:

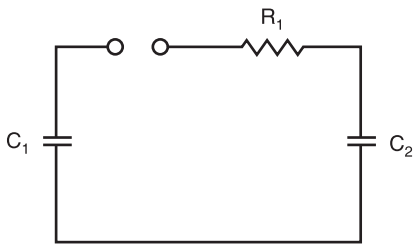

Here R_2 is neglected and the time taken for charging to peak value is approximately three times the time constant of the circuit. During charging C_1 and C_2 are in series. Therefore,

$$t_1 = 3\,\frac{C_1 C_2}{C_1 + C_2} R_1$$

During discharge C_1 and C_2 are in parallel and R_1 and R_2 in series. Hence the time for 50% discharge is approximately given as

$$t_2 = 0.7\ (R_1 + R_2)\ (C_1 + C_2)$$

Using these formulae, we have

$$t_1 = 3 \times \frac{25 \times 2.5 \times 10^{-18}}{27.5 \times 10^{-9}} \times 75$$

$$= 511 \times 10^{-9} \text{ sec.}$$

$$= 0.511\ \mu \text{ sec.}$$

and $$t_2 = 0.7\ (2675)\ (27.5) \times 10^{-9}$$

$$= 51.5\ \mu \text{ sec.}$$

On comparison with the values obtained through exact formulate it is found that whereas wave tail time is more or less same, the wave front time as calculated through approximate formula is quite erroneous.

Example 3.2. *A 12-stage impulse generator has capacitors each rated at 0.3 μF, 150 kV. The capacitance of the test specimen is 400 pF. Determine the wave front and wave tail resistance to produce at 1.2/50 μ sec. impulse wave. Also determine the maximum output voltage if the charging voltage is 125 kV.*

Solution: Using the approximate formulae, we have

$$t_1 = 1.2 \times 10^{-6} = 3\ R_1 \frac{C_1 C_2}{C_1 + C_2}$$

where $$C_1 = \frac{0.3}{12} = 0.025\ \mu\text{F} = 25\ \text{nF}$$

$$1.2 \times 10^{-6} = 3\ R_1 \frac{25 \times 0.4}{25.4} \times 10^{-9}$$

$$R_1 = 1016\ \Omega$$

$$50 \times 10^{-6} = 0.7\ (1016 + R_2)\ (25.4) \times 10^{-9}$$

$$R_2 + 1016 = 2812$$

$$R_2 = 1796\ \Omega$$

Alternative:

$$t_1 = \frac{1}{2\beta} \ln \frac{\alpha + \beta}{\alpha - \beta}$$

$$\frac{\alpha + \beta}{\alpha - \beta} = e^{2\beta t_1}$$

and $$\alpha - \beta = \frac{0.7}{(50 - t_1)}$$

$$\alpha - \beta = \frac{0.7}{48.8} = 0.014344$$

Since $\gamma = \frac{C_1}{C_2} = 62.5$ and is a large value

$$R_1 \approx \frac{1}{C_1} \cdot \frac{1}{\alpha - \beta} = \frac{1}{25 \times 10^{-3} \times 0.014344}$$

$$= 2788\ \Omega$$

Since $\alpha \approx \beta$

$$t_1 = \frac{2}{2\alpha} \ln\left(\frac{2\alpha}{0.014344}\right)$$

$$2.4\ \alpha = \ln 139\ \alpha$$

After a few trials say $\alpha = 2.43$

LHS = 5.832 and RHS = 5.82

Therefore $\alpha \approx 2.43$

$\therefore$ $\beta = 2.415656$

$$R_1 = \frac{1}{C_1} \cdot \frac{1}{\alpha + \beta} + \frac{1}{C_1} \cdot \frac{62.5}{\alpha + \beta}$$

$$= \frac{1}{25 \times 10^{-3}} \left[\frac{1}{4.8456} + \frac{62.5}{4.8456}\right]$$

$$R_1 = \frac{1}{25 \times 10^{-3}} \left(\frac{63.5}{4.8456}\right) = 534\ \Omega$$

From the result it is clear that the approximate formulae are really approximate and, therefore, they give only some idea of the final exact results. The maximum output voltage is given by

$$\frac{V_0}{2 R_1 C_2 \beta} [e^{-(\alpha - \beta)t_1} - e^{-(\alpha + \beta)t_1}]$$

where $V_0 = 125 \times 12 = 1500$ KV $[e^{-0.014344 \times 1.2} - e^{-4.8456 \times 1.2}]$

$\therefore$ $$\nu_{max}(t) = \frac{1500}{2 \times 524 \times 0.4 \times 10^{-3} \times 2.41565}$$

$$= 1481 \times 0.983$$

$$= 1455\ \text{kV} \quad \textbf{Ans.}$$

Example 3.3. *An impulse current generator has total capacitance of 15 μF, the charging voltage 125 KV, the circuit inductance 2 mH and the dynamic resistance 1 ohm. Determine the peak current and wave shape of the wave.*

Solution: The maximum value of current is given as

$$I_{max} = V_0 \sqrt{\frac{C}{L}}\, e\, \frac{-\nu \sin^{-1}(1 - \nu^2)^{1/2}}{(1 - \nu^2)^{1/2}}$$

where $$\nu = \frac{R}{2} \sqrt{\frac{C}{L}}$$

$$= \frac{1}{2} \sqrt{\frac{15 \times 10^{-6}}{2 \times 10^{-3}}}$$

$$= 4.33 \times 10^{-2}$$

Now $$e^{\frac{-\nu \sin^{-1}(1-\nu^2)^{1/2}}{(1-\nu^2)^{1/2}}} = e^{-0.0433 \times 1.526}$$

$$= 0.936$$

$\therefore$ $$I_{max} = 125 \times 8.66 \times 10^{-2} \times 0.936$$

$$= 10.13 \text{ KA}$$ Ans.

Now $$t_1 = \sqrt{LC}\, \frac{\sin^{-1}(1-\nu^2)^{1/2}}{(1-\nu^2)^{1/2}}$$

$$= \sqrt{2 \times 10^{-3} \times 15 \times 10^{-6}} \times 1.5267$$

$$= 2.6 \times 10^{-4}$$

$$= 260\ \mu \text{ sec.}$$

The general expression for current

$$i(t) = V_0 \sqrt{\frac{C}{L}}\, e^{-\alpha t} \sin \frac{t}{\sqrt{LC}}$$

$$i(t_2) = 5.06 = 125 \times 8.66 \times 10^{-2}\, e^{-t_2/2000} \sin \frac{t_2}{\sqrt{15 \times 2000}}$$

or $$0.46 = e^{-t_2/2000} \sin \frac{t_2}{173.2}$$

After a few trials say $t_2 = 1275\ \mu$ sec.

$$\text{RHS} = 0.5286 \sin \frac{1275}{173.2}$$

$$= 0.5286 \times 0.883$$

$$= 0.466$$

Therefore, time to 50% value is 1275 μ sec. **Ans.**

PROBLEMS

3.1. Define the terms (*i*) Impulse voltages; (*ii*) Chopped wave; (*iii*) Impulse flash over voltage; (*iv*) Impulse puncture voltage; (*v*) Impulse ratio for flash over; (*vi*) Impulse ratio for puncture.

3.2. Draw a neat exact equivalent circuit of an Impulse Generator and indicate the significance of each parameter being used.

3.3. Draw and compare the two simplified equivalent circuits of the impulse generator circuits (*a*) and (*b*).

3.4. Give complete analysis of circuit '*a*' and show that the wave front and wave tail resistances are physically realisable only under certain condition. Derive the condition.

3.5. Give complete analysis of circuit '*b*' and derive the condition for physical realisation of wave front and wave tail resistances.

3.6. Derive an expression for voltage efficiency of a single stage impulse generator.

3.7. Describe the construction, principle of operation and application of a multistage Marx's Surge Generator.

3.8. Explain the Goodlet circuit of impulse voltage generation and compare its performance with that of Marx'x Circuit.

3.9. Describe the construction of various components used in the development of an impulse generator.

3.10. Explain with neat diagram triggering and synchronisation of the impulse generator with the CRO.

3.11. Draw a typical impulse current generator circuit and explain its operation and application.

3.12. Draw a neat diagram of a high current generator circuit (equivalent circuit) and through analysis of the circuit show how the wave form can be controlled.

4 Measurement of High Voltages and Currents

4.1 INTRODUCTION

Transient measurements have much in common with measurements of steady state quantities but the short-lived nature of the transients which we are trying to record introduces special problems. Frequently the transient quantity to be measured is not recorded directly because of its large magnitudes *e.g.* when a shunt is used to measure current, we really measure the voltage across the shunt and then we assume that the voltage is proportional to the current, a fact which should not be taken for granted with transient currents. Often the voltage appearing across the shunt may be insufficient to drive the measuring device; it requires amplification. On the other hand, if the voltage to be measured is too large to be measured with the usual meters, it must be attenuated. This suggests an idea of a measuring system rather than a measuring device.

Measurements of high voltages and currents involves much more complex problems which a specialist, in common electrical measurement, does not have to face. The high voltage equipments have large stray capacitances with respect to the grounded structures and hence large voltage gradients are set up. A person handling these equipments and the measuring devices must be protected against these over voltages. For this, large structures are required to control the electrical fields and to avoid flash over between the equipment and the grounded structures. Sometimes, these structures are required to control heat dissipation within the circuits. Therefore, the location and layout of the equipments is very important to avoid these problems. Electromagnetic fields create problems in the measurements of impulse voltages and currents and should be minimised.

The chapter is devoted to describing various devices and circuits for measurement of high voltages and currents. The application of the device to the type of voltages and currents is also discussed.

4.2 SPHERE GAP

Sphere gap is by now considered as one of the standard methods for the measurement of peak value of d.c., a.c. and impulse voltages and is used for checking the voltmeters and other voltage measuring devices used in high voltage test circuits. Two identical metallic spheres separated by certain distance form a sphere gap. The sphere gap can be used for measurement of impulse voltage of either polarity provided that the impulse is of a standard wave form and has wave front time at least 1 micro sec. and wave tail time of 5 micro sec. Also, the gap length between the sphere should not exceed a sphere radius. If these conditions are satisfied and the specifications regarding the shape, mounting, clearances

of the spheres are met, the results obtained by the use of sphere gaps are reliable to within ±3%. It has been suggested in standard specification that in places where the availability of ultraviolet radiation is low, irradiation of the gap by radioactive or other ionizing media should be used when voltages of magnitude less than 50 kV are being measured or where higher voltages with accurate results are to be obtained.

In order to understand the importance of irradiation of sphere gap for measurement of impulse voltages especially which are of short duration, it is necessary to understand the time-lag involved in the development of spark process. This time lag consists of two components—(*i*) The statistical time-lag caused by the need of an electron to appear in the gap during the application of the voltage. (*ii*) The formative time lag which is the time required for the breakdown to develop once initiated.

The statistical time-lag depends on the irradiation level of the gap. If the gap is sufficiently irradiated so that an electron exists in the gap to initiate the spark process and if the gap is subjected to an impulse voltage, the breakdown will take place when the peak voltage exceeds the d.c. breakdown value. However, if the irradiation level is low, the voltage must be maintained above the d.c. breakdown value for a longer period before an electron appears. Various methods have been used for irradiation *e.g.* radioactive material, ultraviolet illumination as supplied by mercury arc lamp and corona discharges.

It has been observed that large variation can occur in the statistical time-lag characteristic of a gap when illuminated by a specified light source, unless the cathode conditions are also precisely specified.

Irradiation by radioactive materials has the advantage in that they can form a stable source of irradiation and that they produce an amount of ionisation in the gap which is largely independent of the gap voltage and of the surface conditions of the electrode. The radioactive material may be placed inside high voltage electrode close behind the sparking surface or the radioactive material may form the sparking surface.

The influence of the light from the impulse generator spark gap on the operation of the sphere gaps has been studied. Here the illumination is intense and occurs at the exact instant when it is required, namely, at the instant of application of the voltage wave to the sphere gap.

The formative time lag depends mainly upon the mechanism of spark growth. In case of secondary electron emission, it is the transit time taken by the positive ion to travel from anode to cathode that decides that formative time lag. The formative time-lag decreases with the applied over voltage and increase with gap length and field non-uniformity.

Specifications on Spheres and Associated Accessories

The spheres should be so made that their surfaces are smooth and their curvatures as uniform as possible. The curvature should be measured by a spherometer at various positions over an area enclosed by a circle of radius 0.3 D about the sparking point where D is the diameter of the sphere and sparking points on the two spheres are those which are at minimum distances from each other.

For smaller size, the spheres are placed in horizontal configuration whereas large sizes (diameters), the spheres are mounted with the axis of the sphere gaps vertical and the lower sphere is grounded. In either case, it is important that the spheres should be so placed that the space between spheres is free from external electric fields and from bodies which may affect the field between the spheres (Figs. 4.1 and 4.2).

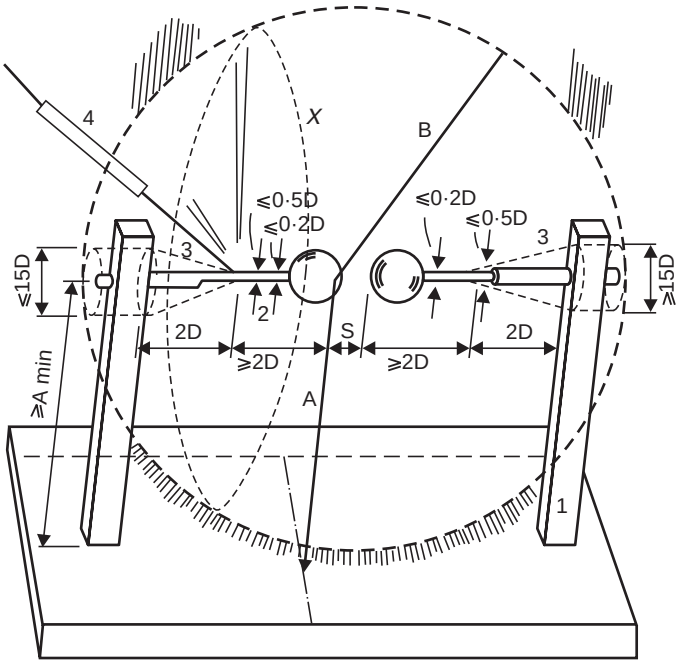

Fig. 4.1

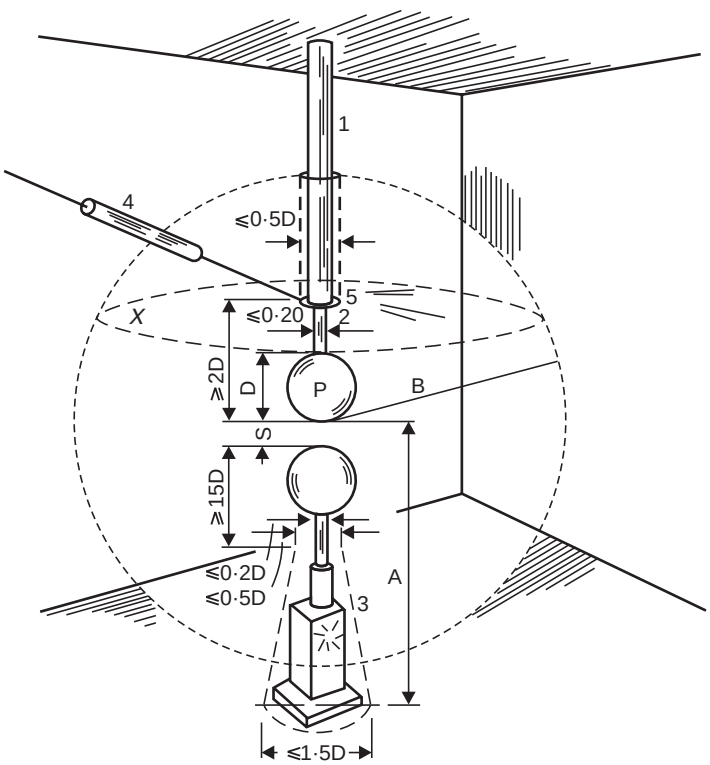

Fig. 4.2

According to BSS 358: 1939, when one sphere is grounded, the distance from the sparking point of the high voltage sphere to the equivalent earth plane to which the earthed sphere is connected should lie within the limits as given in Table 4.1.

Table 4.1

Height of sparking point of high voltage sphere above the equivalent earth plane.

***S* = Sparking point distance**

Sphere Diameter		*S < 0.5 D*		*S > 0.5 D*	
D		*Maxm. Height*	*Min. Height*	*Maxm. Height*	*Min. Height*
Upto	25 cms.	7 D	10 S	7 D	5 D
	50 cms.	6 D	8 S	6 D	4 D
	75 cms.	6 D	8 S	6 D	4 D
	100 cms.	5 D	7 S	5 D	3.5 D
	150 cms.	4 D	6 S	4 D	3 D
	200 cms.	4 D	6 S	4 D	3 D

In order to avoid corona discharge, the shanks supporting the spheres should be free from sharp edges and corners. The distance of the sparking point from any conducting surface except the shanks should be greater than

$$\left(25 + \frac{V}{3}\right) \text{cms}$$

where V is the peak voltage is kV to be measured. When large spheres are used for the measurement of low voltages the limiting distance should not be less than a sphere diameter.

It has been observed that the metal of which the spheres are made does not affect the accuracy of measurements MSS 358: 1939 states that the spheres may be made of brass, bronze, steel, copper, aluminium or light alloys. The only requirement is that the surfaces of these spheres should be clean, free from grease films, dust or deposited moisture. Also, the gap between the spheres should be kept free from floating dust particles, fibres etc.

For power frequency tests, a protective resistance with a value of $1\Omega/V$ should be connected in between the spheres and the test equipment to limit the discharge current and to prevent high frequency oscillations in the circuit which may otherwise result in excessive pitting of the spheres. For higher frequencies, the voltage drop would increase and it is necessary to have a smaller value of the resistance. For impulse voltage the protective resistors are not required. If the conditions of the spheres and its associated accessories as given above are satisfied, the spheres will spark at a peak voltage which will be close to the nominal value shown in Table 4.2. These calibration values relate to a temperature of 20°C and pressure of 760 mm Hg. For a.c. and impulse voltages, the tables are considered to be accurate within ±3% for gap lengths upto 0.5 *D*. The tables are not valid for gap lengths less than 0.05 *D* and impulse voltages less than 10 kV. If the gap length is greater than 0.5 *D*, the results are less accurate and are shown in brackets.

Table 4.2

Sphere gap with one sphere earthed

Peak value of disruptive discharge voltages (50% for impulse tests) are valid for (*i*) alternating voltages (*ii*) d.c. voltage of either polarity (*iii*) negative lightning and switching impulse voltages

Sphere Gap Spacing mm	*Voltage KV Peak Sphere dia in cm.*						
	12.5	25	50	75	100	150	200
10	31.7						
20	59.0						
30	85	86					
40	108	112					
50	129	137	138	138	138	138	
75	167	195	202	203	203	203	203
100	(195)	244	263	265	266	266	266
125	(214)	282	320	327	330	330	330
150		(314)	373	387	390	390	390
175		(342)	420	443	443	450	450
200		(366)	460	492	510	510	510
250		(400)	530	585	615	630	630
300			(585)	665	710	745	750
350			(630)	735	800	850	855
400			(670)	(800)	875	955	975
450			(700)	(850)	945	1050	1080
500			(730)	(895)	1010	1130	1180
600				(970)	(1110)	1280	1340
700				(1025)	(1200)	1390	1480
800					(1260)	1490	1600
900					(1320)	1580	1720
1000					(1360)	1660	1840
1100						1730	1940
1200						1800	2020
1300						1870	2100
1400						1920	2180
1500						1960	2250
1600							2320
1700							2370
1800							2410
1900							2460
2000							2490

Due to dust and fibre present in the air, the measurement of d.c. voltages is generally subject to larger errors. Here the accuracy is within ±5% provided the spacing is less than 0.4 *D* and excessive dust is not present.

The procedure for high voltage measurement using sphere gaps depends upon the type of voltage to be measured.

Table 4.3

Sphere Gap with one sphere grounded
Peak values of disruptive discharge voltages (50% values).
Positive lightning and switching impulse voltages

Sphere Gap	*Peak Voltage kV Sphere dia in cms*						
Spacing mm	12.5	25	50	75	100	150	200
10	31.7						
20	59	59					
30	85.5	86					
40	110	112					
50	134	138	138	138	138	138	138
75	(181)	199	203	202	203	203	203
100	(215)	254	263	265	266	266	266
125	(239)	299	323	327	330	330	330
150		(337)	380	387	390	390	390
175		(368)	432	447	450	450	450
200		(395)	480	505	510	510	510
250		(433)	555	605	620	630	630
300			(620)	695	725	745	760
350			(670)	770	815	858	820
400			(715)	(835)	900	965	980
450			(745)	(890)	980	1060	1090
500			(775)	(940)	1040	1150	1190
600				(1020)	(1150)	(1310)	1380
700				(1070)	(1240)	(1430)	1550
750				(1090)	(1280)	(1480)	1620
800					(1310)	(1530)	1690
900					(1370)	(1630)	(1820)
1000					(1410)	(1720)	1930
1100						(1790)	(2030)
1200						(1860)	(2120)

For the measurement of a.c. or d.c. voltage, a reduced voltage is applied to begin with so that the switching transient does not flash over the sphere gap and then the voltage is increased gradually till the gap breaks down. Alternatively the voltage is applied across a relatively large gap and the spacing is

then gradually decreased till the gap breaks down. Corresponding to this gap the value of peak voltage can be read out from the calibration tables. However, it is reminded that the calibration tables values correspond to 760 mm Hg pressure and 20°C temperature. Any deviation from the value, a correction factor will have to be used to get the correct value of the voltage being measured.

For the measurement of 50% impulse disruptive discharge voltages, the spacing of the sphere gap or the charging voltage of the impulse generator is adjusted in steps of 3% of the expected disruptive voltage. Six applications of the impulse should be made at each step and the interval between two applications is 5 seconds. The value giving 50% probability to disruptive discharge is preferably obtained by interpolation between at least two gap or voltage settings, one resulting in two disruptive discharges or less out of six applications and the other in four disruptive discharges or more out of again six applications.

Another method, simple though less accurate, is to adjust the settings such that four to six disruptive discharges are obtained in a series of ten successive applications.

The breakdown voltage of a sphere gap increases with increase in pressure and decreases with increase in temperature. The value of disruptive voltages as given in Tables 4.2 and 4.3 correspond to 760 mm Hg pressure and 20°C. For small variation in temperatures and pressures, the disruptive voltage is closely proportional to the relative air density. The relative air density δ is given by

$$\delta = \frac{293b}{760\,(273 + t)}$$

where b and t are the atmospheric conditions (pressure in mm of Hg and temperature in °C respectively) during measurement. The disruptive voltage V is given $V = K_d V_0$

Where V_0 is the disruptive voltage as given in the Tables 4.2 and 4.3 and K_d is a correction factor given in Table 4.4. K_d is a slightly non-linear function of δ a result explained by Paschen's law.

Table 4.4

Air density correction factor K_d

δ	0.70	0.75	0.8	0.85	0.90	0.95	1.0	1.05	1.10
K_d	0.72	0.76	0.81	0.86	0.90	0.95	1.0	1.05	1.09

Some of the other factors which influence the breakdown value of air are discussed here.

Influence of Nearby Earthed Objects

The influence of nearby earthed object on the direct voltage breakdown of horizontal gaps was studied by Kuffel and Husbands. They surrounded the gap by a cylindrical metal cage and found that the breakdown voltage reduced materially especially when the gap length exceeded a sphere radius. The experiments were conducted on 6.25 and 12.5 cm. diameter spheres when the radius of the surrounding metal cylinder (B) was varied from 12.6 D to 4 D. The observation corresponding to 12.6 D was taken as a reference. The reduction in the breakdown voltage for a given S/D fitted closely into an empirical relation of the form.

$$\Delta V = m \ln \frac{B}{D} + C$$

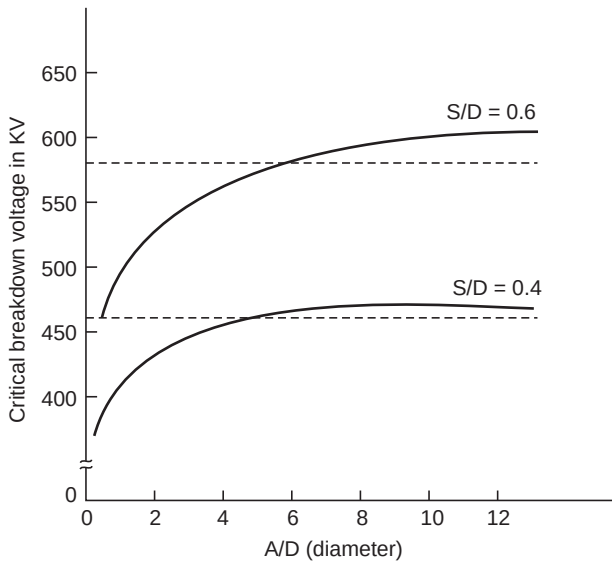

Fig. 4.3 Breakdown voltage as a function of *A*/*D*

Where ΔV = per cent reduction in voltage in the breakdown voltage from the value when the clearance was 12.6 *D*, and *m* and *C* are the factors dependent on the ratio *S/D*.

Fiegel and Keen have studied the influence of nearby ground plane on impulse breakdown voltage of a 50 cm diameter sphere gap using 1.5/40 micro sec. negative polarity impulse wave. Fig. 4.3 shows the breakdown voltage as a function of *A*/*D* for various values of *S/D*. The voltage values were corrected for relative air density.

It is observed that the voltage increases with increase in the ratio *A/D*. The results have been compared with those given in Table 4.2 and represented in Fig. 4.3 by dashed lines. The results also agree with the recommendation regarding the minimum and maximum values of *A/D* as given in Table 4.1.

Influence of Humidity

Kuffel has studied the effect of the humidity on the breakdown voltage by using spheres of 2 cms to 25 cms diameters and uniform field electrodes. The effect was found to be maximum in the region 0.4 mm Hg. and thereafter the change was decreased. Between 4–17 mm Hg. the relation between breakdown voltage and humidity was practically linear for spacing less than that which gave the maximum humidity effect. Fig. 4.4 shows the effect of humidity on the breakdown voltage of a 25 cm diameter sphere with spacing of 1 cm when a.c. and d.c voltages are applied. It can be seen that

(*i*) The a.c. breakdown voltage is slightly less than d.c. voltage.

(*ii*) The breakdown voltage increases with the partial pressure of water vapour.

It has also been observed that

(*i*) The humidity effect increases with the size of spheres and is largest for uniform field electrodes.

(*ii*) The voltage change for a given humidity change increase with gap length.

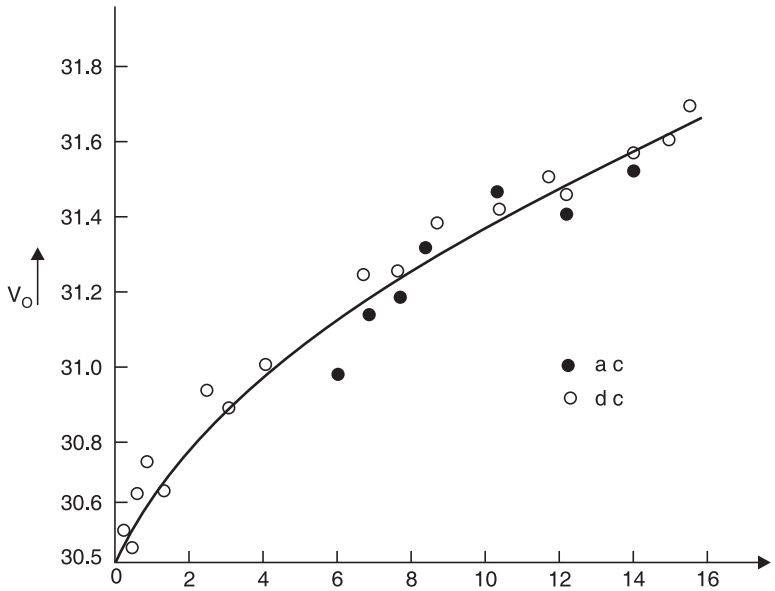

Fig. 4.4 Breakdown voltage humidity relation for a.c. and d.c. for 1.0 cm gap between 25 cms diameter spheres

The increase in breakdown voltage with increase in partial pressure of water vapour and this increase in voltage with increase in gap length is due to the relative values of ionisation and attachment coefficients in air. The water particles readily attach free electrons, forming negative ions. These ions therefore slow down and are unable to ionise neutral molecules under field conditions in which electrons will readily ionise. It has been observed that within the humidity range of 4 to 17 g/m^3 (relative humidity of 25 to 95% for 20°C temperature) the relative increase of breakdown voltage is found to be between 0.2 to 0.35% per gm/m^3 for the largest sphere of diameter 100 cms and gap length upto 50 cms.

Influence of Dust Particles

When a dust particle is floating between the gap this results into erratic breakdown in homogeneous or slightly inhomogenous electrode configurations. When the dust particle comes in contact with one electrode under the application of d.c. voltage, it gets charged to the polarity of the electrode and gets attracted by the opposite electrode due to the field forces and the breakdown is triggered shortly before arrival. Gaps subjected to a.c. voltages are also sensitive to dust particles but the probability of erratic breakdown is less. Under d.c. voltages erratic breakdowns occur within a few minutes even for voltages as low as 80% of the nominal breakdown voltages. This is a major problem, with high d.c. voltage measurements with sphere gaps.

4.3 UNIFORM FIELD SPARK GAPS

Bruce suggested the use of uniform field spark gaps for the measurements of a.c., d.c. and impulse voltages. These gaps provide accuracy to within 0.2% for a.c. voltage measurements an appreciable

improvement as compared with the equivalent sphere gap arrangement. Fig. 4.5 shows a half-contour of one electrode having plane sparking surfaces with edges of gradually increasing curvature.

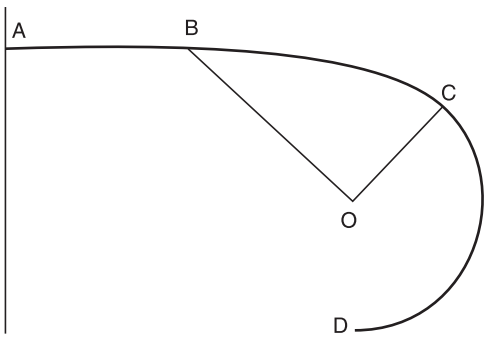

Fig. 4.5 Half contour of uniform spark gap

The portion *AB* is flat, the total diameter of the flat portion being greater than the maximum spacing between the electrodes. The portion *BC* consists of a sine curve based on the axes *OB* and *OC* and given by $XY = CO \sin (BX/BO \cdot \pi/2)$. *CD* is an arc of a circle with centre at *O*.

Bruce showed that the breakdown voltage *V* of a gap of length *S* cms in air at 20°C and 760 mm Hg. pressure is within 0.2 per cent of the value given by the empirical relation.

$$V = 24.22S + 6.08\sqrt{S}$$

This equation, therefore, replaces Tables 4.2 and 4.3 which are necessary for sphere gaps. This is a great advantage, that is, if the spacing between the spheres for breakdown is known the breakdown voltage can be calculated.

The other advantages of uniform field spark gaps are

(*i*) No influence of nearby earthed objects

(*ii*) No polarity effect.

However, the disadvantages are

(*i*) Very accurate mechanical finish of the electrode is required.

(*ii*) Careful parallel alignment of the two electrodes.

(*iii*) Influence of dust brings in erratic breakdown of the gap. This is much more serious in these gaps as compared with sphere gaps as the highly stressed electrode areas become much larger.

Therefore, a uniform field gap is normally not used for voltage measurements.

4.4 ROD GAPS

A rod gap may be used to measure the peak value of power frequency and impulse voltages. The gap usually consists of two 1.27 cm square rod electrodes square in section at their end and are mounted on insulating stands so that a length of rod equal to or greater than one half of the gap spacing overhangs the inner edge of the support. The breakdown voltages as found in American standards for different gap lengths at 25° C, 760 mm Hg. pressure and with water vapour pressure of 15.5 mm Hg. are reproduced here.

Gap length in Cms.	*Breakdown Voltage KV peak*	*Gap Length in cms.*	*Breakdown Voltage KV peak*
2	26	80	435
4	47	90	488
6	62	100	537
8	72	120	642
10	81	140	744
15	102	160	847
20	124	180	950
25	147	200	1054
30	172	220	1160
35	198		
40	225		
50	278		
60	332		
70	382		

The breakdown voltage is a rod gap increases more or less linearly with increasing relative air density over the normal variations in atmospheric pressure. Also, the breakdown voltage increases with increasing relative humidity, the standard humidity being taken as 15.5 mm Hg.

Because of the large variation in breakdown voltage for the same spacing and the uncertainties associated with the influence of humidity, rod gaps are no longer used for measurement of a.c. or impulse voltages. However, more recent investigations have shown that these rods can be used for d.c. measurement provided certain regulations regarding the electrode configurations are observed. The arrangement consists of two hemispherically capped rods of about 20 mm diameter as shown in Fig. 4.6.

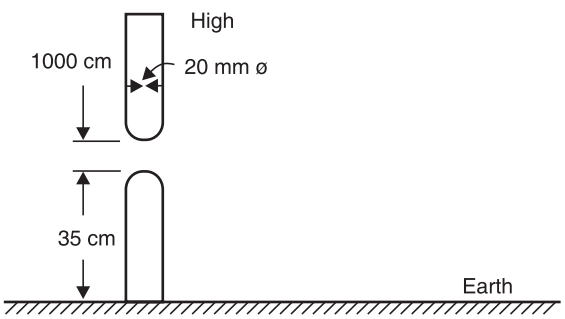

Fig. 4.6 Electrode arrangement for a rod gap to measure HVDC

The earthed electrode must be long enough to initiate positive breakdown streamers if the high voltage rod is the cathode. With this arrangement, the breakdown voltage will always be initiated by positive streamers for both the polarities thus giving a very small variation and being humidity dependent. Except for low voltages (less than 120 kV), where the accuracy is low, the breakdown voltage can be given by the empirical relation.

$$V = \delta\,(A + BS)\,4\,\sqrt{5.1\times10^{-2}\,(h+8.65)}\ \text{kV}$$

where h is the absolute humidity in gm/m^3 and varies between 4 and 20 gm/m^3 in the above relation. The breakdown voltage is linearly related with the gap spacing and the slope of the relation B = 5.1 kV/cm and is found to be independent of the polarity of voltage. However constant A is polarity dependent and has the values

A = 20 kV for positive polarity

= 15 kV for negative polarity of the high voltage electrode.

The accuracy of the above relation is better than ±20% and, therefore, provides better accuracy even as compared to a sphere gap.

4.5 ELECTROSTATIC VOLTMETER

The electric field according to Coulomb is the field of forces. The electric field is produced by voltage and, therefore, if the field force could be measured, the voltage can also be measured. Whenever a voltage is applied to a parallel plate electrode arrangement, an electric field is set up between the plates. It is possible to have uniform electric field between the plates with suitable arrangement of the plates. The field is uniform, normal to the two plates and directed towards the negative plate. If A is the area of the plate and E is the electric field intensity between the plates ε the permittivity of the medium between the plates, we know that the energy density of the electric field between the plates is given as,

$$W_d = \frac{1}{2}\,\varepsilon\,E^2$$

Consider a differential volume between the plates and parallel to the plates with area A and thickness dx, the energy content in this differential volume Adx is

$$dW = W_d\,Adx = \frac{1}{2}\varepsilon E^2\,Adx$$

Now force F between the plates is defined as the derivative of stored electric energy along the field direction *i.e.*,

$$F = \frac{dW}{dx} = \frac{1}{2}\,\varepsilon\,E^2 A$$

Now $E = V/d$ where V is the voltage to be measured and d the distance of separation between the plates. Therefore, the expression for force

$$F = \frac{1}{2}\,\varepsilon\,\frac{V^2 A}{d^2}$$

Since the two plates are oppositely charged, there is always force of attraction between the plates. If the voltage is time dependant, the force developed is also time dependant. In such a case the mean value of force is used to measure the voltage. Thus

$$F = \frac{1}{T}\int_0^T F(t)dt = \frac{1}{T}\int\frac{1}{2}\,\varepsilon\,\frac{V^2(t)}{d^2}\,A\,dt = \frac{1}{2}\,\frac{\varepsilon A}{d^2}\cdot\frac{1}{T}\int V^2(t)dt = \frac{1}{2}\,\varepsilon A\,\frac{V_{rms}^2}{d^2}$$

Electrostatic voltmeters measure the force based on the above equations and are arranged such that one of the plates is rigidly fixed whereas the other is allowed to move. With this the electric field gets disturbed. For this reason, the movable electrode is allowed to move by not more than a fraction of a millimetre to a few millimetres even for high voltages so that the change in electric field is negligibly small. As the force is proportional to square of V_{rms}, the meter can be used both for a.c. and d.c. voltage measurement.

The force developed between the plates is sufficient to be used to measure the voltage. Various designs of the voltmeter have been developed which differ in the construction of electrode arrangement and in the use of different methods of restoring forces required to balance the electrostatic force of attraction. Some of the methods are

(*i*) Suspension of moving electrode on one arm of a balance.

(*ii*) Suspension of the moving electrode on a spring.

(*iii*) Pendulous suspension of the moving electrode.

(*iv*) Torsional suspension of moving electrode.

The small movement is generally transmitted and amplified by electrical or optical methods. If the electrode movement is minimised and the field distribution can exactly be calculated, the meter can be used for absolute voltage measurement as the calibration can be made in terms of the fundamental quantities of length and force.

From the expression for the force, it is clear that for a given voltage to be measured, the higher the force, the greater is the precision that can be obtained with the meter. In order to achieve higher force for a given voltage, the area of the plates should be large, the spacing between the plates (d) should be small and some dielectric medium other than air should be used in between the plates. If uniformity of electric field is to be maintained an increase in area A must be accompanied by an increase in the area of the surrounding guard ring and of the opposing plate and the electrode may, therefore, become unduly large specially for higher voltages. Similarly the gap length cannot be made very small as this is limited by the breakdown strength of the dielectric medium between the plates. If air is used as the medium, gradients upto 5 kV/cm have been found satisfactory. For higher gradients vacuum or SF_6 gas has been used.

The greatest advantage of the electrostatic voltmeter is its extremely low loading effect as only electric fields are required to be set up. Because of high resistance of the medium between the plates, the active power loss is negligibly small. The voltage source loading is, therefore, limited only to the reactive power required to charge the instrument capacitance which can be as low as a few picofarads for low voltage voltmeters.

The measuring system as such does not put any upper limit on the frequency of supply to be measured. However, as the load inductance and the measuring system capacitance form a series resonance circuit, a limit is imposed on the frequency range. For low range voltmeters, the upper frequency is generally limited to a few MHz.

Fig. 4.7 shows a schematic diagram of an absolute electrostatic voltmeter. The hemispherical metal dome D encloses a sensitive balance B which measures the force of attraction between the movable disc which hangs from one of its arms and the lower plate P. The movable electrode M hangs with a clearance of above 0.01 cm, in a central opening in the upper plate which serves as a guard ring. The

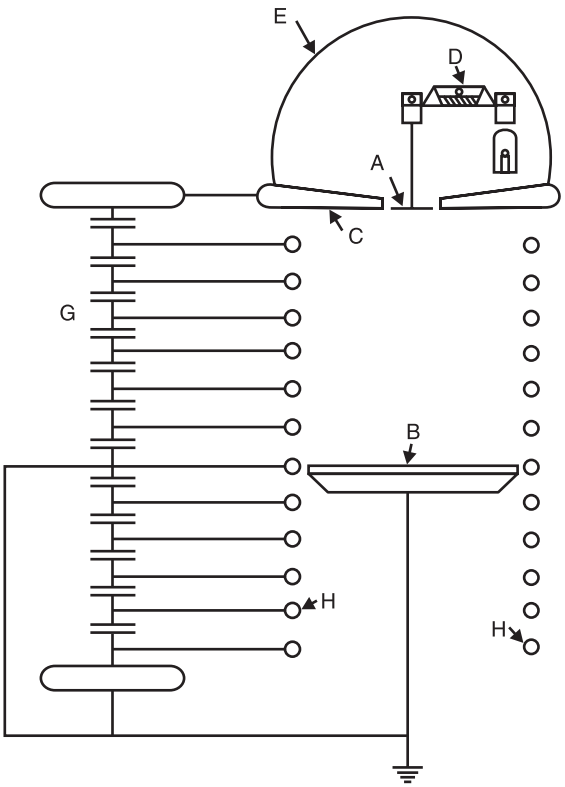

Fig. 4.7 Schematic diagram of electrostatic voltmeter

diameter of each of the plates is 1 metre. Light reflected from a mirror carried by the balance beam serves to magnify its motion and to indicate to the operator at a safe distance when a condition of equilibrium is reached. As the spacing between the two electrodes is large (about 100 cms for a voltage of about 300 kV), the uniformity of the electric field is maintained by the guard rings *G* which surround the space between the discs *M* and *P.* The guard rings *G* are maintained at a constant potential in space by a capacitance divider ensuring a uniform spatial potential distribution. When voltages in the range 10 to 100 kV are measured, the accuracy is of the order of 0.01 per cent.

Hueter has used a pair of sphares of 100 cms diameter for the measurement of high voltages utilising the electrostatic attractive force between them. The spheres are arranged with a vertical axis and at a spacing slightly greater than the sparking distance for the particular voltage to be measured. The upper high voltage sphere is supported on a spring and the extension of spring caused by the electrostatic force is magnified by a lamp-mirror scale arrangement. An accuracy of 0.5 per cent has been achieved by the arrangement.

Electrostatic voltmeters using compressed gas as the insulating medium have been developed. Here for a given voltage the shorter gap length enables the required uniformity of the field to be maintained with electrodes of smaller size and a more compact system can be evolved.

One such voltmeter using SF_6 gas has been used which can measure voltages upto 1000 kV and accuracy is of the order of 0.1%. The high voltage electrode and earthed plane provide uniform electric field within the region of a 5 cm diameter disc set in a 65 cm diameter guard plane. A weighing balance

arrangement is used to allow a large damping mass. The gap length can be varied between 2.5, 5 and 10 cms and due to maximum working electric stress of 100 kV/cm, the voltage ranges can be selected to 250 kV, 500 kV and 100 kV. With 100 kV/cm as gradient, the average force on the disc is found to be 0.8681 N equivalent to 88.52 gm wt. The disc movements are kept as small as 1 μm by the weighing balance arrangement.

The voltmeters are used for the measurement of high a.c. and d.c. voltages. The measurement of voltages lower than about 50 volt is, however, not possible, as the forces become too small.

4.6 GENERATING VOLTMETER

Whenever the source loading is not permitted or when direct connection to the high voltage source is to be avoided, the generating principle is employed for the measurement of high voltages, A generating voltmeter is a variable capacitor electrostatic voltage generator which generates current proportional to the voltage to be measured. Similar to electrostatic voltmeter the generating voltmeter provides loss free measurement of d.c. and a.c. voltages. The device is driven by an external constant speed motor and does not absorb power or energy from the voltage measuring source. The principle of operation is explained with the help of Fig. 4.8. *H* is a high voltage electrode and the earthed electrode is subdivided into a sensing or pick up electrode *P,* a guard electrode *G* and a movable electrode *M,* all of which are at the same potential. The high voltage electrode *H* develops an electric field between itself and the electrodes *P, G* and *M.* The field lines are shown in Fig. 4.8. The electric field density σ is also shown. If electrode *M* is fixed and the voltage *V* is changed, the field density σ would change and thus a current $i\,(t)$ would flow between *P* and the ground.

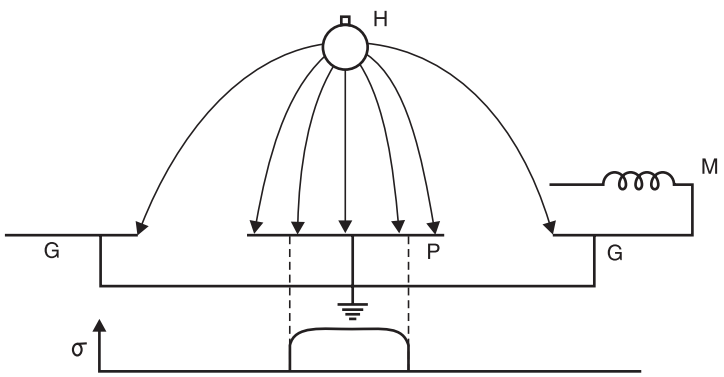

Fig. 4.8 Principle of generating voltmeter

$$i\,(t) = \frac{dq(t)}{dt} = \frac{d}{dt}\left[\int \sigma\,(a)da\right]$$

Where $\sigma\,(a)$ is the electric field density or charge density along some path and is assumed constant over the differential area *da* of the pick up electrode. In this case $\sigma\,(a)$ is a function of time also and $\int da$ the area of the pick up electrode *P* exposed to the electric field.

However, if the voltage *V* to be measured is constant (d.c voltage), a current $i(t)$ will flow only if it is moved *i.e.* now $\sigma\,(a)$ will not be function of time but the charge *q* is changing because the area of the pick up electrode exposed to the electric field is changing. The current $i(t)$ is given by

$$i(t) = \frac{d}{dt}\int_{A(t)} \sigma(a)da = \varepsilon \frac{d}{dt}\int_{A(t)} E(a)da$$

where $\sigma(a) = \varepsilon E(a)$ and ε is the permittivity of the medium between the high voltage electrode and the grounded electrode. The integral boundary denotes the time varying exposed area.

The high voltage electrode and the grounded electrode in fact constitute a capacitance system. The capacitance is, however, a function of time as the area A varies with time and, therefore, the charge $q(t)$ is given as

$$q(t) = C(t)V(t)$$

and

$$i(t) = \frac{dq}{dt} C(t) \frac{dV(t)}{dt} + V(t) \frac{dC(t)}{dt}$$

For d.c. voltages $\dfrac{dV(t)}{dt} = 0$

Hence $$i(t) = V \frac{dC(t)}{dt}$$

If the capacitance varies linearly with time and reaches its peak value C_m is time $T_c/2$ and again reduces to zero linearly in time $T_c/2$, the capacitance is given as

$$C(t) = 2 \frac{C_m}{T_c} t$$

For a constant speed of n rpm of synchronous motor which is varying the capacitance, time T_c is given by $T_c = 60/n$.

Therefore $$I = 2C_m V \frac{n}{60} = \frac{n}{30} C_m V$$

If the capacitance C varies sinusoidally between the limits C_0 and $(C_0 + C_m)$ then

$$C = C_0 + C_m \sin wt$$

and the current i is then given as

$$i(t) = i_m \cos wt \text{ where } i_m = VC_m\omega$$

Here ω is the angular frequency of variation of the capacitance. If ω is constant, the current measured is proportional to the voltage being measured. Generally the current is rectified and measured by a moving coil meter. Generating voltmeters can be used for a.c. voltage measurement also provided the angular frequency ω is the same or equal to half that of the voltage being measured. Fig 4.9 shows the variations of C as a function of time together with a.c. voltage, the frequency of which is twice the frequency of $C(t)$.

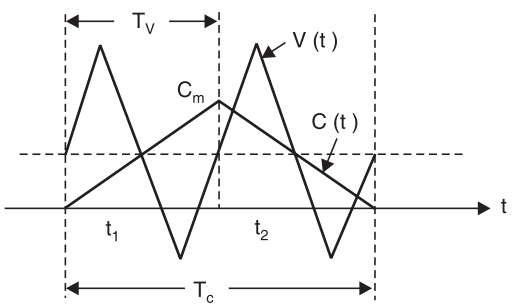

Fig. 4.9 Capacitance and voltage variation

It can be seen from Fig. 4.9 that whatever be the phase relation between voltage and the capacitance, over one cycle variation of the voltage is same (*e.g.* $V(t_1) - V(t_2)$) and the rate of change of

capacitance over the period T_v is equal to C_m/T_v. Therefore, the instantaneous value of current $i(t) = C_m f_v V(t)$ where $f_v = 1/T_v$ the frequency of voltage.

Since $f_v = 2f_c$ and $f_c = 60/n$ we obtain

$$I(t) = n/30\ C_m V(t)$$

Fig. 4.10 shows a schematic diagram of a generating voltmeter which employs rotating vanes for variation of capacitance. The high voltage electrode is connected to a disc electrode D_3 which is kept at a fixed distance on the axis of the other low voltage electrodes D_2, D_1, and D_0. The rotor D_0 is driven at a constant speed by a synchronous motor at a suitable speed. The rotor vanes of D_0 cause periodic change in capacitance between the insulated disc D_2 and the high voltage electrode D_3. The number and shape of vanes are so designed that a suitable variation of capacitance (sinusodial or linear) is achieved. The a.c. current is rectified and is measured using moving coil meters. If the current is small an amplifier may be used before the current is measured.

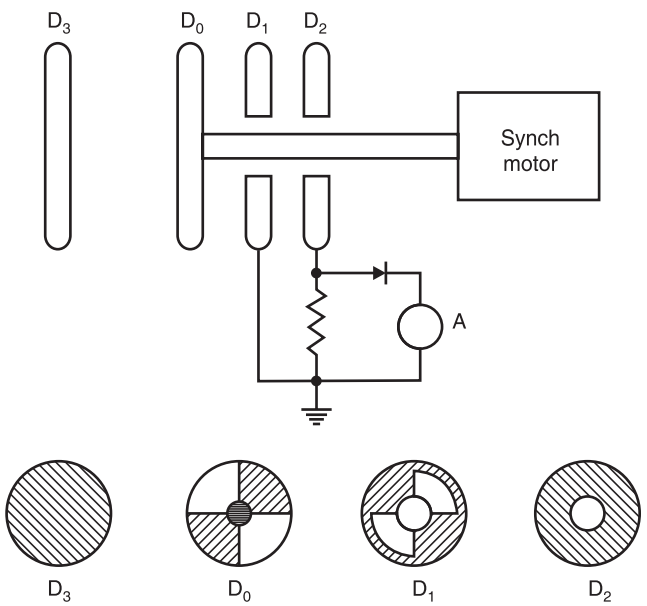

Fig. 4.10 Schematic diagram of generating voltmeter

Generating voltmeters are linear scale instruments and applicable over a wide range of voltages. The sensitivity can be increased by increasing the area of the pick up electrode and by using amplifier circuits.

The main advantages of generating voltmeters are (*i*) scale is linear and can be extrapolated (*ii*) source loading is practically zero (*iii*) no direct connection to the high voltage electrode.

However, they require calibration and construction is quite cumbersome.

The breakdown of insulating materials depends upon the magnitude of voltage applied and the time of application of voltage. However, if the peak value of voltage is large as compared to breakdown strength of the insulating material, the disruptive discharge phenomenon is in general caused by the instantaneous maximum field gradient stressing the material. Various methods discussed so far can measure peak voltages but because of complex calibration procedures and limited accuracy call for

more convenient and more accurate methods. A more convenient though less accurate method would be the use of a testing transformer wherein the output voltage is measured and recorded and the input voltage is obtained by multiplying the output voltage by the transformation ratio. However, here the output voltage depends upon the loading of the secondary winding and wave shape variation is caused by the transformer impedances and hence this method is unacceptable for peak voltage measurements.

4.7 THE CHUBB-FORTESCUE METHOD

Chubb and Fortescue suggested a simple and accurate method of measuring peak value of a.c. voltages. The basic circuit consists of a standard capacitor, two diodes and a current integrating ammeter (MC ammeter) as shown in Fig. 4.11 (*a*).

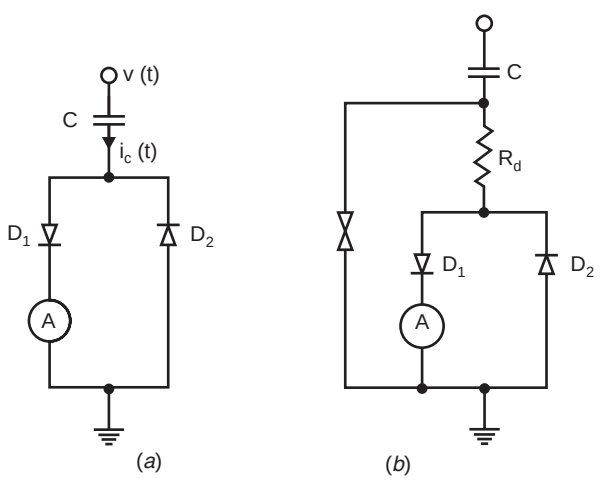

Fig. 4.11 (*a*) Basic circuit (*b*) Modified circuit

The displacement current $i_c(t)$, Fig. 4.12 is given by the rate of change of the charge and hence the voltage $V(t)$ to be measured flows through the high voltage capacitor C and is subdivided into positive and negative components by the back to back connected diodes. The voltage drop across these diodes can be neglected (1 *V* for *Si* diodes) as compared with the voltage to be measured. The measuring instrument (M.C. ammeter) is included in one of the branches. The ammeter reads the mean value of the current.

$$I = \frac{1}{T}\int_{t_1}^{t_2} C\frac{dv(t)}{dt}.dt = \frac{C}{T}.2V_m = 2V_m fC \text{ or } V_m = \frac{I}{2fC}$$

The relation is similar to the one obtained in case of generating voltmeters. An increased current would be obtained if the current reaches zero more than once during one half cycle. This means the wave shapes of the voltage would contain more than one maxima per half cycle. The standard a.c. voltages for testing should not contain any harmonics and, therefore, there could be very short and rapid voltages caused by the heavy predischarges, within the test circuit which could introduce errors in measurements. To eliminate this problem filtering of a.c. voltage is carried out by introducing a damping resistor in between the capacitor and the diode circuit, Fig. 4.11 (*b*).

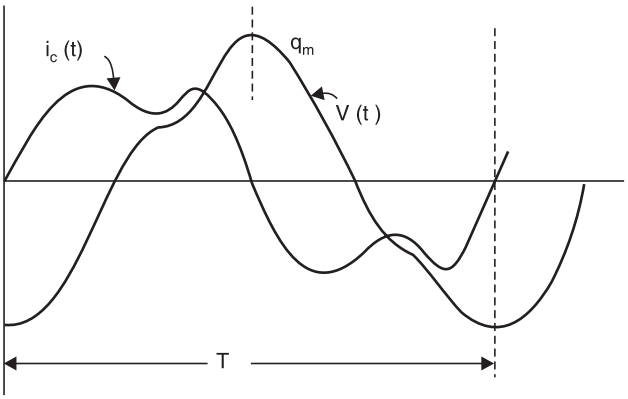

Fig. 4.12

Also, if full wave rectifier is used instead of the half wave as shown in Fig. 4.11, the factor 2 in the denominator of the above equation should be replaced by 4. Since the frequency *f*, the capacitance *C* and current *I* can be measured accurately, the measurement of symmetrical a.c. voltages using Chubb and Fortescue method is quite accurate and it can be used for calibration of other peak voltage measuring devices.

Fig. 4.13 shows a digital peak voltage measuring circuit. In contrast to the method discussed just now, the rectified current is not measured directly, instead a proportional analog voltage signal is derived which is then converted into a proportional medium frequency for using a voltage to frequency convertor (Block A in Fig. 4.13). The frequency ratio f_m/f is measured with a gate circuit controlled by the a.c. power frequency (supply frequency *f*) and a counter that opens for an adjustable number of period $\Delta t = p/f$. The number of cycles *n* counted during this interval is

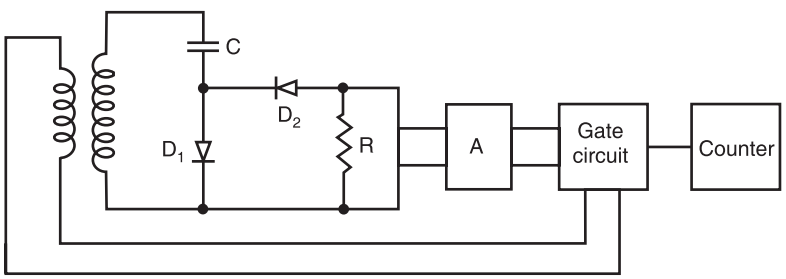

Fig. 4.13 Digital peak voltmeter

$$n = \Delta t f_m = \frac{p}{f} fm$$

where *p* is a constant of the instrument.

Let $$A = \frac{f_m}{Ri_c} = \frac{f_m}{R2V_m fC} = \frac{f_m}{f} \cdot \frac{1}{2RV_m C}$$

Therefore, $$n = p\, 2ARV_m C$$

where *A* represents the voltage to frequency conversion factor.

Thus the indicator can be calibrated to read V_m directly by selecting suitable values of A, p and R.

The voltmeter is found to given an accuracy of 0.35%.

4.7.1 Peak Voltmeters with Potential Dividers

Passive circuits are not very frequently used these days for measurement of the peak value of a.c. or impulse voltages. The development of fully integrated operational amplifiers and other electronic circuits has made it possible to sample and hold such voltages and thus make measurements and, therefore, have replaced the conventional passive circuits. However, it is to be noted that if the passive circuits are designed properly, they provide simplicity and adequate accuracy and hence a small description of these circuits is in order. Passive circuits are cheap, reliable and have a high order of electromagnetic compatibility. However, in contrast, the most sophisticated electronic instruments are costlier and their electromagnetic compatibility (EMC) is low.

The passive circuits cannot measure high voltages directly and use potential dividers preferably of the capacitance type.

Fig. 4.14 shows a simple peak voltmeter circuit consisting of a capacitor voltage divider which reduces the voltage V to be measured to a low voltage V_m.

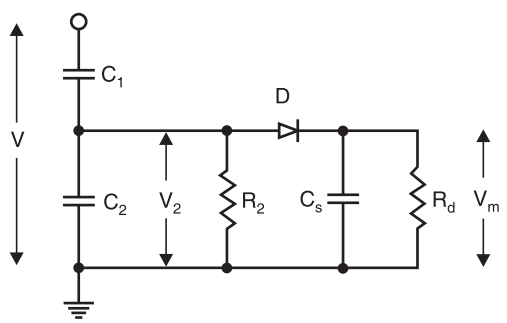

Fig. 4.14 Peak voltmeter

Suppose R_2 and R_d are not present and the supply voltage is V. The voltage across the storage capacitor C_s will be equal to the peak value of voltage across C_2 assuming voltage drop across the diode to be negligibly small. The voltage could be measured by an electrostatic voltmeter or other suitable voltmeters with very high input impedance. If the reverse current through the diode is very small and the discharge time constant of the storage capacitor very large, the storage capacitor will not discharge significantly for a long time and hence it will hold the voltage to its value for a long time. If now, V is decreased, the voltage V_2 decreases proportionately and since now the voltage across C_2 is smaller than the voltage across C_s to which it is already charged, therefore, the diode does not conduct and the voltage across C_s does not follow the voltage across C_2. Hence, a discharge resistor R_d must be introduced into the circuit so that the voltage across C_s follows the voltage across C_2. From measurement point of view it is desirable that the quantity to be measured should be indicated by the meter within a few seconds and hence R_d is so chosen that $R_d C_s \approx 1$ sec. As a result of this, following errors are introduced. With the connection of R_d, the voltage across C_s will decrease continuously even when the input voltage is kept constant. Also, it will discharge the capacitor C_2 and the mean potential of $V_2(t)$ will gain a negative d.c. component. Hence a leakage resistor R_2 must be inserted in parallel with C_2 to equalise these unipolar discharge currents. The second error corresponds to the voltage shape across the storage capacitor which contains ripple and is due to the discharge of the capacitor C_s. If the input impedance of the measuring device is very high, the ripple is independent of the meter being used. The error is approximately proportional to the ripple factor and is thus frequency dependent as the discharge time-constant cannot be changed. If $R_d C_s = 1$ sec, the discharge error amounts to 1% for 50 Hz and 0.33%.

for 150 Hz. The third source of error is related to this discharge error. During the conduction time (when the voltage across C_s is lower than that across C_2 because of discharge of C_s through R_d) of the diode the storage capacitor C_s is recharged to the peak value and thus C_s becomes parallel with C_2. If discharge error is e_d, recharge error e_r is given by

$$e_r = 2e_d \frac{C_s}{C_1 + C_2 + C_s}$$

Hence C_s should be small as compared with C_2 to keep down the recharge error.

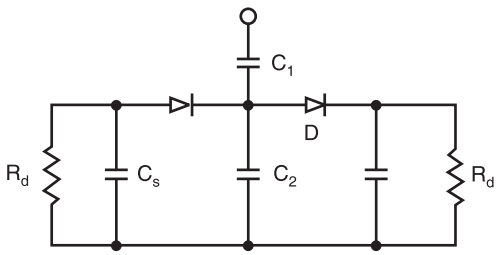

Fig. 4.15 Modified peak voltmeter circuit

It has also been observed that in order to keep the overall error to a low value, it is desirable to have a high value of R_2. The same effect can be obtained by providing an equalising arm to the low voltage arm of the voltage divider as shown in Fig. 4.15. This is accomplished by the addition of a second network comprising diode, C_s and R_d for negative polarity currents to the circuit shown in Fig. 4.14. With this, the d.c. currents in both branches are opposite in polarity and equalise each other. The errors due to R_2 are thus eliminated.

Rabus developed another circuit shown in Fig. 4.16. to reduce errors due to resistances. Two storage capacitors are connected by a resistor R_s within every branch and both are discharged by only one resistance R_d.

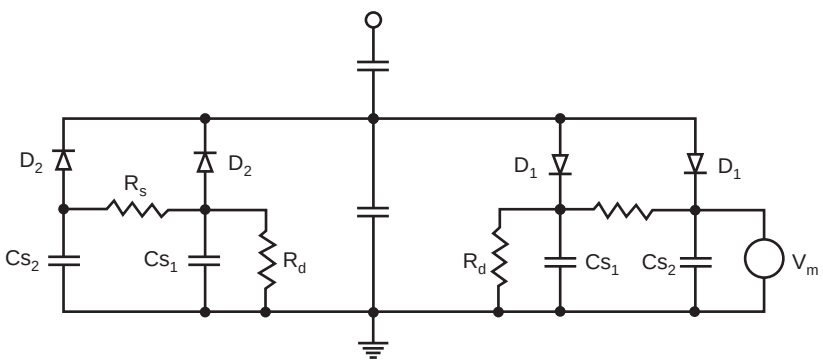

Fig. 4.16 Two-way booster circuit designed by Rabus

Here because of the presence of R_s, the discharge of the storage capacitor C_{s2} is delayed and hence the inherent discharge error e_d is reduced. However, since these are two storage capacitors within one branch, they would draw more charge from the capacitor C_2 and hence the recharge error e_r would increase. It is, therefore, a matter of designing various elements in the circuit so that the total sum of all the errors is a minimum. It has been observed that with the commonly used circuit elements in the voltage dividers, the error can be kept to well within about 1% even for frequencies below 20 Hz.

The capacitor C_1 has to withstand high voltage to be measured and is always placed within the test area whereas the low voltage arm C_2 including the peak circuit and instrument form a measuring unit located in the control area. Hence a coaxial cable is always required to connect the two areas. The cable capacitance comes parallel with the capacitance C_2 which is usually changed in steps if the

voltage to be measured is changed. A change of the length of the cable would, thus, also require recalibration of the system. The sheath of the coaxial cable picks up the electrostatic fields and thus prevents the penetration of this field to the core of the conductor. Also, even though transient magnetic fields will penetrate into the core of the cable, no appreciable voltage (extraneous of noise) is induced due to the symmetrical arrangement and hence a coaxial cable provides a good connection between the two areas. Whenever, a discharge takes place at the high voltage end of capacitor C_1 to the cable connection where the current looks into a change in impedance a high voltage of short duration may be built up at the low voltage end of the capacitor C_1 which must be limited by using an over voltage protection device (protection gap). These devices will also prevent complete damage of the measuring circuit if the insulation of C_1 fails.

4.8 IMPULSE VOLTAGE MEASUREMENTS USING VOLTAGE DIVIDERS

If the amplitudes of the impulse voltage is not high and is in the range of a few kilovolts, it is possible to measure them even when these are of short duration by using CROS. However, if the voltages to be measured are of high magnitude of the order of magavolts which normally is the case for testing and research purposes, various problems arise. The voltage dividers required are of special design and need a thorough understanding of the interaction present in these voltage dividing systems. Fig. 4.17 shows a layout of a voltage testing circuit within a high voltage testing area. The voltage generator *G* is connected to a test object—*T* through a lead *L*.

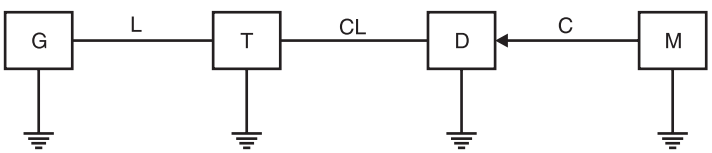

Fig. 4.17 Basic voltage testing circuit

These three elements form a voltage generating system. The lead *L* consists of a lead wire and a resistance to damp oscillation or to limit short-circuit currents if of the test object fails. The measuring system starts at the terminals of the test object and consists of a connecting lead *CL* to the voltage divider *D*. The output of the divider is fed to the measuring instrument (CRO etc.) *M*. The appropriate ground return should assure low voltage drops for even highly transient phenomena and keep the ground potential of zero as far as possible.

It is to be noted that the test object is a predominantly capacitive element and thus this forms an oscillatory circuit with the inductance of the load. These oscillations are likely to be excited by any steep voltage rise from the generator output, but will only partly be detected by the voltage divider. A resistor in series with the connecting leads damps out these oscillations. The voltage divider should always be connected outside the generator circuit towards the load circuit (Test object) for accurate measurement. In case it is connected within the generator circuit, and the test object discharges (chopped wave) the whole generator including voltage divider will be discharged by this short circuit at the test object and thus the voltage divider is loaded by the voltage drop across the lead *L*. As a result, the voltage measurement will be wrong.

Yet for another reason, the voltage divider should be located away from the generator circuit. The dividers cannot be shielded against external fields. All objects in the vicinity of the divider which

may acquire transient potentials during a test will disturb the field distribution and thus the divider performance. Therefore, the connecting lead *CL* is an integral part of the potential divider circuit.

In order to avoid electromagnetic interference between the measuring instrument *M* and *C* the high voltage test area, the length of the delay cable should be adequately chosen. Very short length of the cable can be used only if the measuring instrument has high level of electromagnetic compatibility (EMC). For any type of voltage to be measured, the cable should be co-axial type. The outer conductor provides a shield against the electrostatic field and thus prevents the penetration of this field to the inner conductor. Even though, the transient magnetic fields will penetrate into the cable, no appreciable voltage is induced due to the symmetrical arrangement. Ordinary coaxial cables with braided shields may well be used for d.c. and a.c. voltages. However, for impulse voltage measurement double shielded cables with predominently two insulated braided shields will be used for better accuracy.

During disruption of test object, very heavy transient current flow and hence the potential of the ground may rise to dangerously high values if proper earthing is not provided. For this, large metal sheets of highly conducting material such as copper or aluminium are used. Most of the modern high voltage laboratories provide such ground return along with a Faraday Cage for a complete shielding of the laboratory. Expanded metal sheets give similar performance. At least metal tapes of large width should be used to reduce the impedance.

4.8.1 Voltage Divider

Voltages dividers for a.c., d.c. or impulse voltages may consist of resistors or capacitors or a convenient combination of these elements. Inductors are normally not used as voltage dividing elements as pure inductances of proper magnitudes without stray capacitance cannot be built and also these inductances would otherwise form oscillatory circuit with the inherent capacitance of the test object and this may lead to inaccuracy in measurement and high voltages in the measuring circuit. The height of a voltage divider depends upon the flash over voltage and this follows from the rated maximum voltage applied. Now, the potential distribution may not be uniform and hence the height also depends upon the design of the high voltage electrode, the top electrode. For voltages in the megavolt range, the height of the divider becomes large. As a thumb rule following clearances between top electrode and ground may be assumed.

2.5 to 3 metres/MV for d.c. voltages.

2 to 2.5 m/MV for lightning impulse voltages.

More than 5 m/MV rms for a.c. voltages.

More than 4 m/MV for switching impulse voltage.

The potential divider is most simply represented by two impedances Z_1 and Z_2 connected in series and the sample voltage required for measurement is taken from across Z_2, Fig. 4.18.

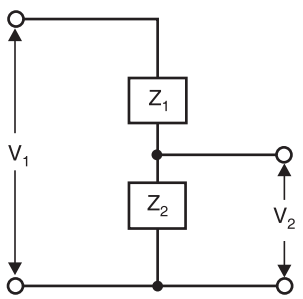

Fig. 4.18 Basic diagram of a potential divider circuit

If the voltage to be measured is V_1 and sampled voltage V_2, then

$$V_2 = \frac{Z_2}{Z_1 + Z_2} V_1$$

If the impedances are pure resistances

$$V_2 = \frac{R_2}{R_1 + R_2} V_1$$

and in case pure capacitances are used

$$V_2 = \frac{C_1}{C_1 + C_2} V_1$$

The voltage V_2 is normally only a few hundred volts and hence the value of Z_2 is so chosen that V_2 across it gives sufficient deflection on a CRO. Therefore, most of the voltage drop is available across the impedance Z_1 and since the voltage to be measured is in megavolt the length of Z_1 is large which result in inaccurate measurements because of the stray capacitances associated with long length voltage dividers (especially with impulse voltage measurements) unless special precautions are taken. On the low voltage side of the potential dividers where a screened cable of finite length has to be employed for connection to the oscillograph other errors and distortion of wave shape can also occur.

Resistance Potential Dividers

The resistance potential dividers are the first to appear because of their simplicity of construction, less space requirements, less weight and easy portability. These can be placed near the test object which might not always be confined to one location.

The length of the divider depends upon two or three factors. The maximum voltage to be measured is the first and if height is a limitation, the length can be based on a surface flash over gradient in the order of 3–4 kV/cm irrespective of whether the resistance R_1 is of liquid or wirewound construction. The length also depends upon the resistance value but this is implicitly bound up with the stray capacitance of the resistance column, the product of the two (RC) giving a time constant the value of which must not exceed the duration of the wave front it is required to record.

It is to be noted with caution that the resistance of the potential divider should be matched to the equivalent resistance of a given generator to obtain a given wave shape.

Fig. 4.19 (*a*) shows a common form of resistance potential divider used for testing purposes where the wave front time of the wave is less than 1 micro sec.

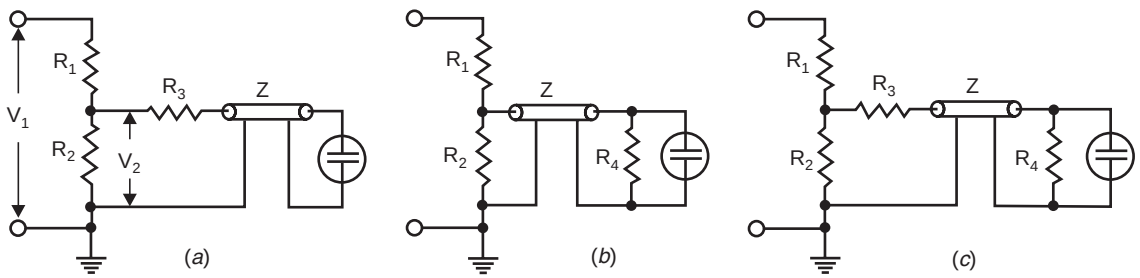

Fig. 4.19 Various forms of resistance potential dividers recording circuits (*a*) Matching at divider end (*b*) Matching at Oscillograph end (*c*) Matching at both ends of delay cable

Here R_3, the resistance at the divider end of the delay cable is chosen such that $R_2 + R_3 = Z$ which puts an upper limit on R_2 *i.e.*, $R_2 < Z$. In fact, sometimes the condition for matching is given as

$$Z = R_3 + \frac{R_1 R_2}{R_1 + R_2}$$

But, since usually $R_1 >> R_2$, the above relation reduces to $Z = R_3 + R_2$. From Fig. 4.19 (*a*), the voltage appearing across R_2 is

$$V_2 = \frac{Z_1}{Z_1 + R_1} V_1$$

where Z_1 is the equivalent impedance of R_2 in parallel with $(Z + R_3)$, the surge impedance of the cable being represented by an impedance Z to ground.

Now $$Z_1 = \frac{(Z + R_3)R_2}{R_2 + Z + R_3} = \frac{(Z + R_3)R_2}{2Z}$$

Therefore, $$V_2 = \frac{(Z + R_3)R_2}{2Z} \frac{V_1}{Z_1 + R_1}$$

However, the voltage entering the delay cable is

$$V_3 = \frac{V_2}{Z + R_3} Z = \frac{Z}{Z + R_3} \frac{(Z + R_3)R_2}{2Z} \cdot \frac{V_1}{Z_1 + R_1} = V_1 \frac{R_2}{2(Z_1 + R_1)}$$

As this voltage wave reaches the CRO end of the delay cable, it suffers reflections as the impedance offered by the CRO is infinite and as a result the voltage wave transmitted into the CRO is doubled. The CRO, therefore, records a voltage

$$V_3' = \frac{R_2}{Z_1 + R_1} V_1$$

The reflected wave, however, as it reaches the low voltage arm of the potential divider does not suffer any reflection as $Z = R_2 + R_3$ and is totally absorbed by $(R_2 + R_3)$.

Since R_2 is smaller than Z and Z_1 is a parallel combination of R_2 and $(R_3 + Z)$, Z_1 is going to be smaller than R_2 and since $R_1 >> R_2$, R_1 will be much greater than Z_1 and, therefore to a first approximation $Z_1 + R_1 \approx R_1$.

Therefore, $$V_3' = \frac{R_2}{R_1} V_1 \approx \frac{R_2}{R_1 + R_2} V_1 \text{ as } R_2 << R_1$$

Fig. 4.19 (*b*) and (*c*) are the variants of the potential divider circuit of Fig. 4.19 (*a*). The cable matching is done by a pure ohmic resistance $R_4 = Z$ at the end of the delay cable and, therefore, the voltage reflection coefficient is zero *i.e.* the voltage at the end of the cable is transmitted completely into R_4 and hence appears across the CRO plates without being reflected. As the input impedance of the delay cable is $R_4 = Z$, this resistance is a parallel to R_2 and forms an integral part of the divider's low voltage arm. The voltage of such a divider is, therefore, calculated as follows:

Equivalent impedance

$$= R_1 + \frac{R_2 Z}{R_2 + Z} = \frac{R_1(R_2 + Z) + R_2 Z}{(R_2 + Z)}$$

Therefore, Current $$I = \frac{V_1(R_2 + Z)}{R_1(R_2 + Z) + R_2 Z}$$

and voltage $$V_2 = \frac{IR_2 Z}{R_2 + Z} = \frac{V_1(R_2 + Z)}{R_1(R_2 + Z) + R_2 Z} \frac{R_2 Z}{R_2 + Z}$$

$$= \frac{R_2 Z}{R_1(R_2 + Z) + R_2 Z} V_1$$

or voltage ratio $$\frac{V_2}{V_1} = \frac{R_2 Z}{R_1(R_2 + Z) + R_2 Z}$$

Due to the matching at the CRO end of the delay cable, the voltage does not suffer any reflection at that end and the voltage recorded by the CRO is given as

$$V_2 = \frac{R_2 Z\, V_1}{R_1(R_2 + Z) + R_2 Z} = \frac{R_2 Z V_1}{(R_1 + R_2)Z + R_1 R_2} = \frac{R_2 V_1}{(R_1 + R_2) + \dfrac{R_1 R_2}{Z}}$$

Normally for undistorted wave shape through the cable

$$Z \approx R_2$$

Therefore,

$$V_2 = \frac{R_2}{2R_1 + R_2} V_1$$

For a given applied voltage V_1 this arrangement will produce a smaller deflection on the CRO plates as compared to the one in Fig. 4.19 (*a*).

The arrangement of Fig. 4.19 (*c*) provides for matching at both ends of the delay cable and is to be recommended where it is felt necessary to reduce to the minimum irregularities produced in the delay cable circuit. Since matching is provided at the CRO end of the delay cable, therefore, there is no reflection of the voltage at that end and the voltage recorded will be half of that recorded in the arrangement of Fig. 4.19 (*a*) *viz*.

$$V_2 = \frac{R_2}{2(R_1 + R_2)} V_1$$

It is desirable to enclose the low voltage resistance (*s*) of the potential dividers in a metal screening box. Steel sheet is a suitable material for this box which could be provided with a detachable close fitting lid for easy access. If there are two low voltage resistors at the divider position as in Fig. 4.19 (*a*) and (*c*), they should be contained in the screening box, as close together as possible, with a removable metallic partition between them. The partition serves two purposes (*i*) it acts as an electrostatic shield between the two resistors (*ii*) it facilitates the changing of the resistors. The lengths of the leads should be short so that practically no inductance is contributed by these leads. The screening box should be fitted with a large earthing terminal. Fig. 4.20 shows a sketched cross-section of possible layout for the low voltage arm of voltage divider.

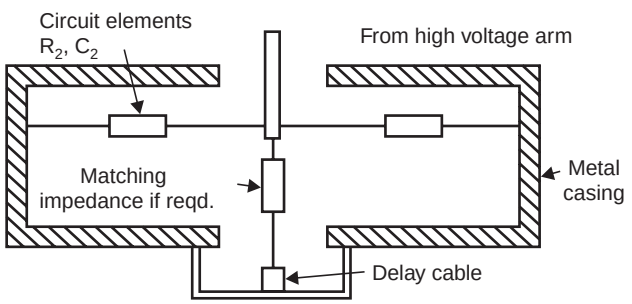

Fig. 4.20 Cross-section of low voltage arm of a voltage divider

Capacitance Potential Dividers

Capacitance potential dividers are more complex than the resistance type. For measurement of impulse voltages not exceeding 1 MV capacitance dividers can be both portable and transportable. In general, for measurement of 1 MV and over, the capacitance divider is a laboratory fixture. The capacitance dividers are usually made of capacitor units mounted one above the other and bolted together. It is this failure which makes the small dividers portable. A screening box similar to that described earlier can be used for housing both the low voltage capacitor unit C_2 and the matching resistor if required.

The low voltage capacitor C_2 should be non-inductive. A form of capacitor which has given excellent results is of mica and tin foil plate, construction, each foil having connecting tags coming out at opposite corners. This ensures that the current cannot pass from the high voltage circuit to the delay cable without actually going through the foil electrodes. It is also important that the coupling between the high and low voltage arms of the divider be purely capacitive. Hence, the low voltage arm should contain one capacitor only; two or more capacitors in parallel must be avoided because of appreciable inductance that would thus be introduced. Further, the tappings to the delay cable must be taken off as close as possible to the terminals of C_2. Fig. 4.21 shows variants of capacitance potential dividers.

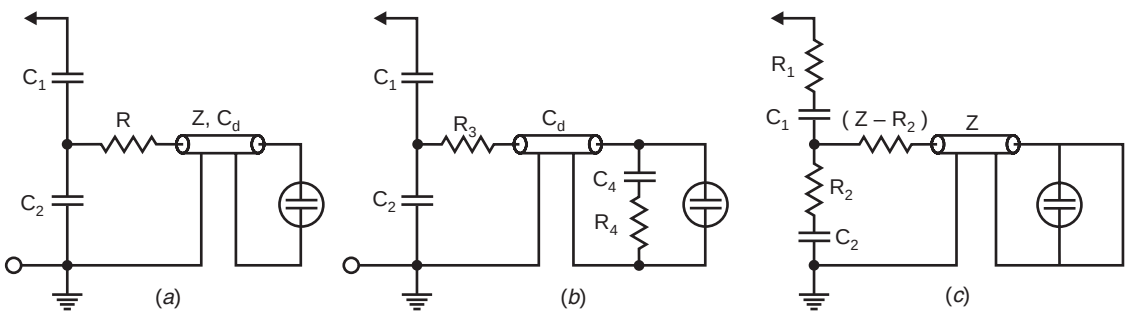

Fig. 4.21 Capacitor dividers (*a*) Simple matching (*b*) Compensated matching (*c*) Damped capacitor divider simple matching

For voltage dividers in Fig. (*b*) and (*c*), the delay cable cannot be matched at its end. A low resistor in parallel to C_2 would load the low voltage arm of the divider too heavily and decrease the output voltage with time. Since R and Z form a potential divider and $R = Z$, the voltage input to the cable will be half of the voltage across the capacitor C_2. This halved voltages travels towards the open end of the cable (CRO end) and gets doubled after reflection. That is, the voltage recorded by the CRO is equal to the voltage across the capacitor C_2. The reflected wave charges the cable to its final voltage magnitude and is absorbed by R (*i.e.* reflection takes place at R and since $R = Z$, the wave is completely absorbed as coefficient of voltage reflection is zero) as the capacitor C_2 acts as a short circuit for high frequency waves. The transformation ratio, therefore, changes from the value:

$$\frac{C_1 + C_2}{C_1}$$

for very high frequencies to the value

$$\frac{C_1 + C_2 + C_d}{C_1}$$

for low frequencies.

However, the capacitance of the delay cable C_d is usually small as compared with C_2.

For capacitive divider an additional damping resistance is usually connected in the lead on the high voltage side as shown in Fig. 4.21 (*c*). The performance of the divider can be improved if damping resistor which corresponds to the aperiodic limiting case is inserted in series with the individual element of capacitor divider. This kind of damped capacitive divider acts for high frequencies as a resistive divider and for low frequencies as a capacitive divider. It can, therefore, be used over a wide range of frequencies *i.e.* for impulse voltages of very different duration and also for alternating voltages.

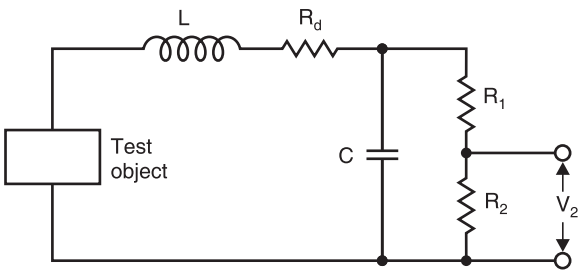

Fig. 4.22 Simplified diagram of a resistance potential divider

Fig. 4.22 shows a simplified diagram of a resistance potential divider after taking into considerations the lead in connection as the inductance and the stray capacitance as lumped capacitance. Here L represents the loop inductance of the lead-in connection for the high voltage arm. The damping resistance R_d limits the transient overshoot in the circuit formed by test object, L, R_d and C. Its value has a decided effect on the performance of the divider. In order to evaluate the voltage transformation of the divider, the low voltage arm voltage V_2 resulting from a square wave impulse V_1 on the *hv* side must be investigaged. The voltage V_2 follows curve 2 in Fig. 4.23 (*a*) in case of aperiodic damping and curve 2 in Fig. 4.23 (*b*) in case of sub-critical damping. The total area between curves 1 and 2 taking into consideration the polarity, is described as the response time.

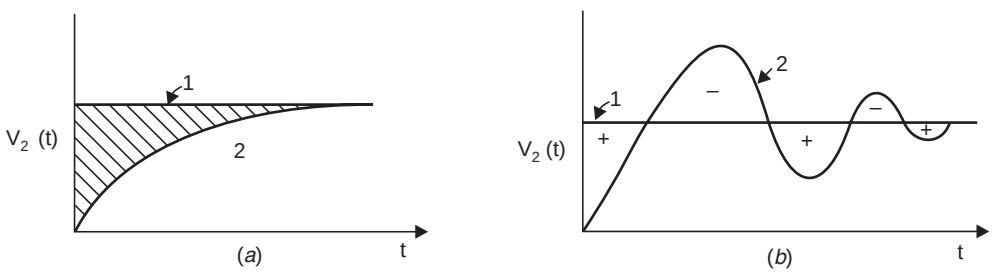

Fig. 4.23 The response of resistance voltage divider

With subcritical damping, even though the response time is smaller, the damping should not be very small. This is because an undesirable resonance may occur for a certain frequency within the passing frequency band of the divider. A compromise must therefore be realised between the short rise time and the rapid stabilization of the measuring system. According to IEC publication No. 60 a maximum overshoot of 3% is allowed for the full impulse wave, 5% for an impulse wave chopped on the front at times shorter than 1 micro sec. In order to fulfill these requirements, the response time of the divider must not exceed 0.2 micro sec. for full impulse waves 1.2/50 or 1.2/5 or impulse waves chopped on the

tail. If the impulse wave is chopped on the front at time shorter than 1 micro sec the response time must be not greater than 5% of the time to chopping.

4.8.2 Klydonograph or Surge Recorder

Since lightning surges are infrequent and random in nature, it is necessary to instal a large number of recording devices to obtain a reasonable amount of data regarding these surges produced on transmission lines and other equipments. Some fairly simple devices have been developed for this purpose. Klydonograph is one such device which makes use of the patterns known as Litchenberg figures which are produced on a photographic film by surface corona discharges.

The Klydonograph (Fig. 4.24) consists of a rounded electrode resting upon the emulsion side of a photographic film or plate which is kept on the smooth surface of an insulating material plate backed by a plate electrode. The minimum critical voltage to produce a figure is about 2 kV and the maximum voltage that can be recorded is about 20 kV, as at higher voltages spark overs occurs which spoils the film. The device can be used with a potential divider to measure higher voltages and with a resistance shunt to measure impulse current.

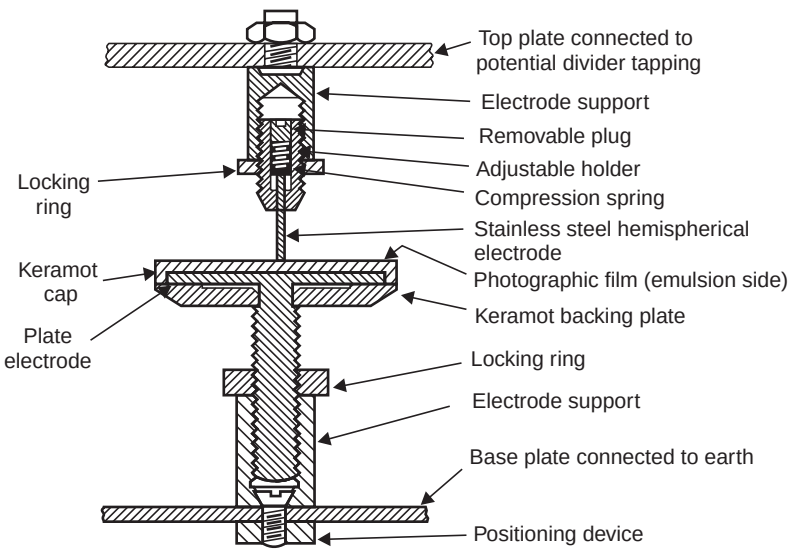

Fig. 4.24 Klydonograph

There are characteristic differences between the figures for positive and negative voltages. However, for either polarity the radius of the figure (if it is symmetrical) or the maximum distance from the centre of the figure to its outside edge (if it is unsymmetrical) is a function only of the applied voltage. The oscillatory voltages produce superimposed effects for each part of the wave. Thus it is possible to know whether the wave is unidirectional or oscillatory. Since the size of the figure for positive polarity is larger, it is preferable to use positive polarity figures. This is particularly desirable in case of measurement of surges on transmission lines or other such equipment which are ordinarily operating on a.c. voltage and the alternating voltage gives a black band along the centre of the film caused by superposition of positive and negative figures produced on each half cycle. For each surge voltage it is possible to obtain both positive and negative polarity figures by connecting pairs of electrodes in parallel, one pair with a high voltage point and an earthed plate and the other pair with a high voltage plate and an earthed point.

Klydonograph being a simple and inexpensive device, a large number of elements can be used for measurement. It has been used in the past quite extensively for providing statistical data on magnitude, polarity and frequency of voltage surges on transmission lines even though its accuracy of measurement is only of the order of 25 per cent.

4.9 MEASUREMENT OF HIGH D.C., AND IMPULSE CURRENTS

High currents are used in power system for testing circuit breakers, cables lightning arresters etc. and high currents are encountered during lightning discharges, switching transients and shunt faults. These currents require special techniques for their measurements.

High Direct Currents

Low resistance shunts are used for measurement of these currents. The voltage drop across the shunt resistance is measured with the help of a millivoltmeter. The value of the resistance varies usually between 10 microohm and 13 milliohm. This depends upon the heating effect and the loading permitted in the circuit. The voltage drop is limited to a few millivolts usually less than 1 V. These resistances are oil immersed and are made as three or four terminal resistances to provide separate terminals for voltage measurement for better accuracy.

Hall Generators

Hall effect (Fig. 4.25) is used to measure very high direct current. Whenever electric current flows through a metal plate placed in a magnetic field perpendicular to it, Lorenz force will deflect the electrons in the metal structure in a direction perpendicular to the direction of both the magnetic field and the flow of current. The charge displacement results in an e.m.f. in the perpendicular direction called the Hall voltage. The Hall voltage is proportional to the current I, the magnetic flux density B and inversely proportional to the plate thickness d *i.e.*,

$$V_H = R\frac{BI}{d}$$

where R is the Hall coefficient which depends upon the material of the plate and temperature of the plate. For metals the Hall coefficient is very small and hence semiconductor materials are used for which the Hall coefficient is high.

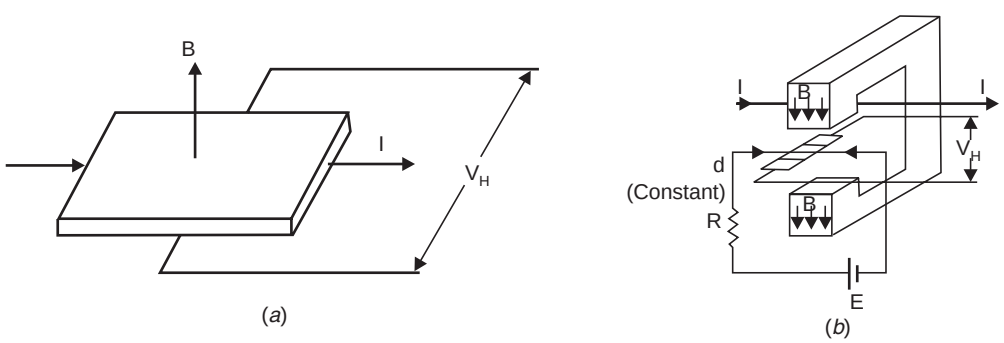

Fig. 4.25 Hall generator

When large d.c. currents are to be measured the current carrying conductor is passed through an iron cored magnetic circuit (Fig. 4.25 (*b*)). The magnetic field intensity produced by the conductor in the air gap at a depth *d* is given by

$$H = \frac{1}{2\pi d}$$

The Hall element is placed in the air gap and a small constant d.c. current is passed through the element. The voltage developed across the Hall element is measured and by using the expression for Hall voltage the flux density *B* is calculated and hence the value of current *I* is obtained.

High Power Frequency Currents

High Power frequency currents are normally measured using current transformers as use of low resistance shunts involves unnecessary power loss. Besides, the current transformers provide isolation from high voltage circuits and thus it is safer to work on *HV* circuits Fig. 4.26 shows a scheme for current measurements using current transformers and electro-optical technique.

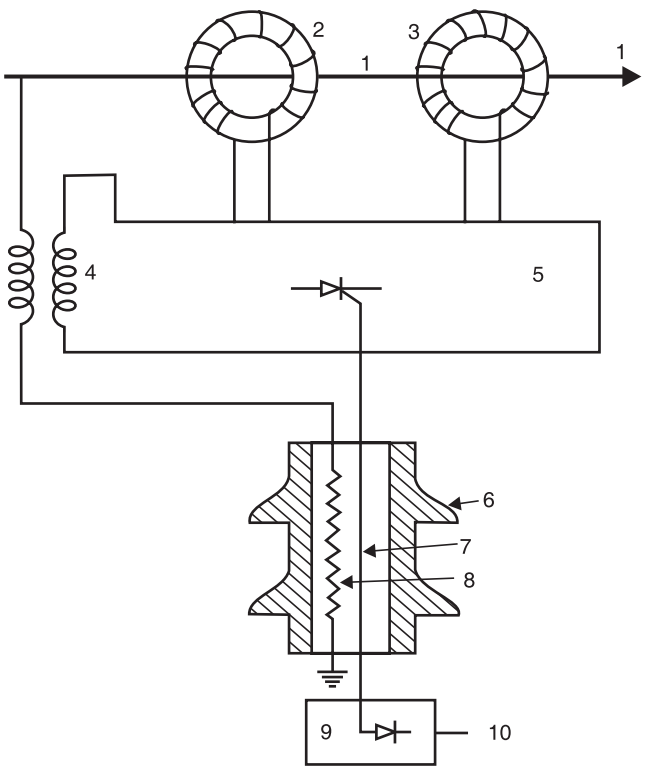

Fig. 4.26 Current transformers and electro-optical system for high a.c. current measurements

A voltage signal proportional to the current to be measured is produced and is transmitted to the ground through the electro-optical device. Light pulses proportional to the voltage signal are transmitted by a glass optical fibre bundle to a photodetector and converted back into an analog voltage signal. The required power for the signal convertor and optical device are obtained from suitable current and voltage transformers.

High Frequency and Impulse Currents

In power system the amplitude of currents may vary between a few amperes to a few hundred kiloamperes and the rate of rise of currents can be as high as $10^{10}A$/sec and the rise time can vary between a few micro seconds to a few macro seconds. Therefore, the device to be used for measuring such currents should be capable of having a good frequency response over a very wide frequency band. The methods normally employed are—(*i*) resistive shunts; (*ii*) elements using induction effects; (*iii*) Faraday and Hall effect devices. With these methods the accuracy of measurement varies between 1 to 10%. Fig. 4.27 shows the circuit diagram of the most commonly used method for high impulse current measurement. The voltage across the shunt resistance *R* due to impulse current *i*(*t*) is fed to the oscilloscope through a delay cable *D*. The delay cable is terminated through an impedance *Z* equal to the surge impedance of the cable to avoid reflection of the voltage to be measured and thus true measurement of the voltage is obtained. Since the dimension of the resistive element is large, it will have residual inductance *L* and stray capacitance *C*. The inductance could be neglected at low frequencies but at higher frequencies the inductive reactance would be comparable with the resistance of the shunt. The effect of inductance and capacitance above 1 MHz usually should be considered. The resistance values range between 10 micro ohm to a few milliohms and the voltage drop is of the order of few volts. The resistive shunts used for measurements of impulse currents of large duration is achieved only at considerable expense for thermal reasons. The resistive shunts for impulse current of short duration can be built with rise time of a few nano seconds of magnitude. The resistance element can be made of parallel carbon film resistors or low inductance wire resistors of parallel resistance wires or resistance foils.

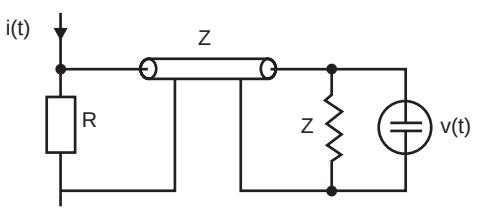

Fig. 4.27 Circuit for high impulse current measurement

Assuming the stray capacitance to be negligibly small the voltage drop across the shunt in complex frequency domain may be written as

$$V(s) = I(s)[R + Ls]$$

It is to be noted that in order to have flat frequency response of the resistive element the stray inductance and capacitance associated with the element must be made as small as possible. In order to minimise the stray field effects following designs of the resistive elements have been suggested and used

1. Bifilar flat strip shunt.
2. Co-axial tube or Park's shunt
3. Co-axial squirrel cage shunt.

The bifilar flat strip shunts suffer from stray inductance associated with the resistance element and its potential leads are linked to a small part of the magnetic flux generated by the current that is being measured. In order to eliminate the problems associated with the bifilar shunts, coaxial shunts were developed (Fig. 4.28). Here the current enters the inner cylinder of the shunt element and returns through an outer cylinder. The space between the two cylinders is occupied by air which acts like a perfacts insulator. The voltage drop across the element is measured between the potential pick up point

and the outer case. The frequency response of this element is almost a flat characteristic upto about 1000 MHz and the response time is a few nanoseconds. The upper frequency limit is governed by the skin effect in the sensitive element.

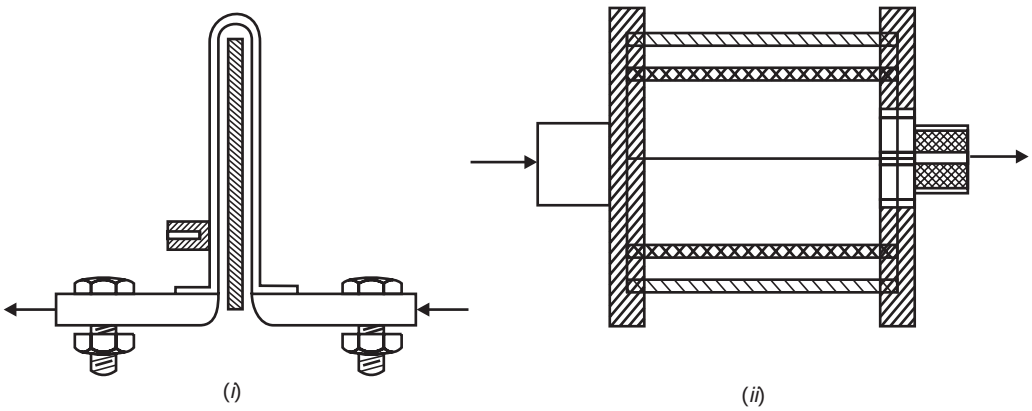

Fig. 4.28 (*i*) Bifilar flat strip; (*ii*) Co-axial squirrel cage

Squirrel cage shunts are high ohmic shunts which can dissipate larger energies as compared to coaxial shunts which are unsuitable due to their limitation of heat dissipation, larger wall thickness and the skin effect. Squirrel cage shunt consists of thick metallic rods or strips placed around the periphery of a cylinder and the structure resembles the rotor construction of a double squirrel cage induction motor. The step response of the element is peaky and, therefore, a compensating network is used in conjunction with the element to improve its frequency response. Rise times less than 8 *n* sec and band width of 400 MHz have been obtained with these shunts.

Elements using Induction Effects

If the current to be measured is flowing through a conductor which is surrounded by a coil as shown in Fig. 4.29, and M is the mutual inductance between the coil and the conductor, the voltage across the coil terminals will be:

$$v(t) = M \frac{di}{dt}$$

Usually the coil is wound on a non-magnetic former in the form of a toroid and has a large number of turns, to have sufficient voltage induced which could be recorded. The coil is wound criss-cross to reduce the leakage inductance. If M is the number of turns of the coil, A the coil area and l_m its mean length, the mutual inductance is given by

$$M = \frac{\mu_0 NA}{l}$$

Usually an integrating circuit RC is employed as shown in Fig. 4.29 to obtain the output voltage proportional to the current to be measured. The output voltage is given by

$$v_0(t) = \frac{1}{RC}\int_0^t v(t)dt = \frac{1}{RC}\int M \frac{di}{dt} . dt = \frac{M}{RC}\int di = \frac{M}{RC} i(t)$$

or

$$v(t) = \frac{RC}{M} v_0(t)$$

Integration of $v(t)$ can be carried out more elegantly by using an appropriately wired operational amplifier. The frequency response of the Rogowski coil is flat upto 100 MHz but beyond that it is affected by the stray electric and magnetic fields and also by the skin effect.

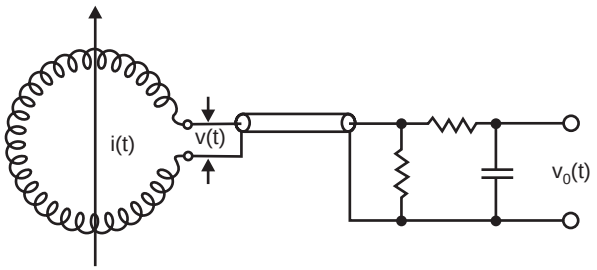

Fig. 4.29 Rogowski coil for high impulse current measurements

Magnetic Links

These are used for the measurement of peak magnitude of the current flowing in a conductor. These links consist of a small number of short steel strips on high retentivity. The link is mounted at a known distance from the current carrying conductor. It has been found through experiments that the remanant magnetism of the link after impulse current of 0.5/5 micro sec shape passes through the conductor is same as that caused by a direct current of the same peak value. Measurement of the remanance possessed by the link after the impulse current has passed through the conductor enables to calculate the peak value of the current. For accurate measurements, it is usual to mount two or more links at different distances from the same conductor. Because of its relative simplicity, the method has been used for measurement of lightning current especially on transmission towers.

It is to be noted that the magnetic links help in recording the peak value of the impulse current but gives no information regarding the wave shape of the current. For this purpose, an instrument called Fulcronograph has been developed which consists of an aluminium wheel round the rim of which are slots containing magnetic links of sufficient length to project on both sides of the wheel. As the wheel is rotated, the links pass successively through a pair of narrow coils through which flows the current to be measured. The current at the instant during which a particular link traverses the coil, can be determined by a subsequent measurement of the residual flux in the link and, therefore, a curve relating the variation of current with time can be obtained. The time scale is governed by the speed of rotation of the wheel.

Hall Generators

The high amplitude a.c. and impulse currents can be measured by Hall Generator described earlier. For the Hall Generator, though a constant control current flows which is permeated by the magnetic field of the current to be measured, the Hall voltage is directly proportional to the measuring current. This method became popular with the development of semi-conductor with sufficient high value of Hall constant. The band width of such devices is found to be about 50 MHz with suitable compensating devices and feedback.

Faraday Generator or Magneto Optic Method

These methods of current measurement use the rotation of the plane of polarisation in materials by the magnetic field which is proportional to the current (Faraday effect). When a linearly polarised light

beam passes through a transparent crystal in the presence of a magnetic field, the plane of polarisation of the light beam undergoes relation. The angle of rotation is given by

$$\theta = \alpha\, Bl$$

where α = A constant of the cyrstal which is a function of the wave length of the light.

B = Magnetic flux density due to the current to be measured in this case.

l = Length of the crystal.

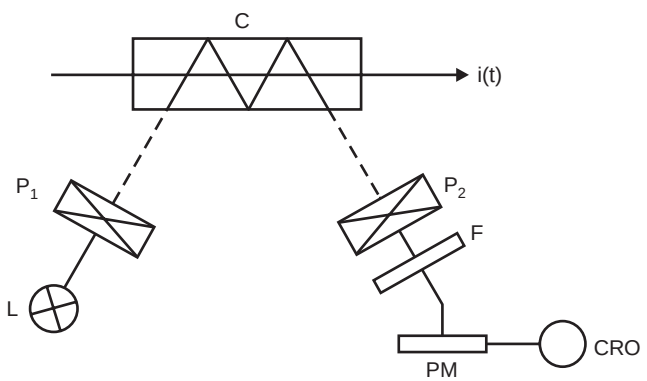

Fig. 4.30 Magneto-optical method

Fig. 4.30 shows a schematic diagram of Magneto-optic method. Crystal C is placed parallel to the magnetic field produced by the current to be measured. A beam of light from a stabilised light source is made incident on the crystal C after it is passed through the polariser P_1. The light beam undergoes rotation of its plane of polarisation. After the beam passes through the analyser P_2, the beam is focussed on a photomultiplier, the output of which is fed to a CRO. The filter F allows only the monochromatic light to pass through it. Photoluminescent diodes too, the momentary light emission of which is proportional to the current flowing through them, can be used for current measurement. The following are the advantages of the method (*i*) It provides isolation of the measuring set up from the main current circuit. (*ii*) It is insensitive to overloading. (*iii*) As the signal transmission is through an optical system no insulation problem is faced. However, this device does not operate for d.c. current.

EXAMPLES

Example 4.1. *Determine the breakdown voltage for air gaps of 2 mm and 15 mm lengths under uniform field and standard atmospheric conditions. Also, determine the voltage if the atmospheric pressure is 750 mm Hg and temperature 35°C.*

Solution: According to empirical formula which holds good at standard atmospheric conditions

$$V_b = 24.22\, S + 6.08\sqrt{S}$$

where S is the gap length in cms.

(*i*) When $S = 0.2$ cm

$$V = 24.22 \times 0.2 + 6.08\sqrt{0.2} = 7.56 \text{ kV}$$ **Ans.**

(*ii*) When $S = 1.5$ cms

$$V_b = 24.22 \times 1.5 + 6.08\sqrt{1.5} = 36.33 + 7.446 = 43.776 \text{ kV} \quad \textbf{Ans.}$$

The air density correction factor

$$= \frac{3.92\,b}{273+t} = \frac{3.92 \times 75}{273+35} = 0.9545 \quad \textbf{Ans.}$$

Therefore, voltage for 2 mm gap will be 7.216 kV and for 15 mm gap it will be 41.78 kV.

Example 4.2. *An absolute electrostatic voltmeter has a movable circular plate 8 cms in diameter. If the distance between the plates during a measurement is 4 mm, determine the potential difference when the force of attraction is 0.2 gm wt.*

Solution: Area of plate $\frac{\pi}{4} \times 8^2 = 16\,\pi$ sq. cm

Spacing between the plates $d = 4$ mm

Force of attraction $= \frac{1}{2}\varepsilon \frac{V^2}{d^2} A$

$$0.2 \times 10^{-3} \times 9.8 = \frac{1}{2} \times \frac{1}{36\,\pi} \times 10^{-9} \frac{V^2}{16 \times 10^{-6}} \times 16\,\pi \times 10^{-4}$$

$$1.96 \times 10^{-3} = \frac{1}{72} \times 10^{-7}\, V^2$$

of $V = 1188$ volts. **Ans.**

Example 4.3. *An electrostatic voltmeter has two parallel plates. The movable plate is 10 cm in diameter. With 10 kV between the plates the pull is 5×10^{-3} N. Determine the change in capacitance for a movement of 1 mm of movable plate.*

Solution: $$5 \times 10^{-3} = \frac{1}{2} \cdot \frac{1}{36\,\pi} \times 10^{-9} \times \frac{18^8}{d^2} 25\pi \times 10^{-4}$$

or $d = 26.35$ mm.

Therefore, change in capacitance

$$\frac{10^3}{36} \times 10^{-9} \times 25\,\pi \times 10^{-4} \left(\frac{1}{26.35} - \frac{1}{27.35} \right) = 0.0959 \text{ pF} \quad \textbf{Ans.}$$

Example 4.4. *A generating voltmeter is required to measure voltage between 15 kV to 250 kV. If the indicating meter reads a minimum current of 2* μ*A and maximum of 35* μ*A,* determine the capacitance of the generating voltmeter. Assume that the speed of driving synchronous motor is 1500 rpm.

Solution:

$$I_{rms} = \frac{VC_m w}{\sqrt{2}}$$

$$2 \times 10^{-6} = \frac{15 \times 1000 \times C_m}{\sqrt{2}} \times \frac{2\pi \times 1500}{60}$$

$$C_m = 12 \times 10^{-7} \times 10^{-6} = 1.5 \text{ pF} \quad \textbf{Ans.}$$

At 250 kV, the current indicated will be

$$2 \times \frac{250}{15} = 33.3\,\mu\text{A} \quad \textbf{Ans.}$$

Example 4.5. *A peak reading voltmeter is required to measure voltage upto 150 kV. The peak voltmeter uses an RC circuit, a microammeter and a capacitance potential divider. The potential divider has a ratio of 1200 : 1 and the micrometer can read upto 10 μA. Determine the value of R and C if the time constant of RC circuit is 8 secs.*

Solution: The voltage across the low voltage arm of the potential divider,

$$= \frac{150 \times 1000}{1200} = 125 \text{ volts.}$$

The same voltage appears across the resistance.

Therefore $$R = \frac{V}{I} = \frac{125}{10 \times 10^{-6}} = 12.5\,\text{M}\Omega$$

Since the time constant of the *RC* circuit is 8 sec.

$$C = \frac{8}{12.5 \times 10^6} = 0.64\,\mu\text{F} \quad \textbf{Ans.}$$

Example 4.6. *A Rogowski coil is required to measure impulse current of 8 kA having rate of change of current of 10^{10} A/sec. The voltmeter is connected across the integrating circuit which reads 8 volts for full scale deflection. The input to the integrating circuit is from the Rogowski Coil. Determine the mutual inductance of coil R and C of the integrating circuit.*

Solution: $$i(t) = \frac{RC}{M} V_0\,(t)$$

$$8 \times 10^3 = \frac{RC}{M} \times 8$$

or $$\frac{RC}{M} = 10^3$$

Time taken for the current wave to reach to maximum value

$$= \frac{8 \times 1000}{10^{10}} = 8 \times 10^{-7} \text{ sec.}$$

This is for 1/4th of a cycle. Therefore for one cycle, the time is

$$T = 32 \times 10^{-7}$$

$\therefore$ $$f = \frac{1}{T} = \frac{1}{32 \times 10^{-7}} = \frac{10^7}{32} \text{ Hz}$$

For proper integration

$$\frac{1}{CR} = \frac{f}{5} = \frac{10^7}{32 \times 5} = \frac{10^6}{16}$$

or $$CR = \frac{16}{10^6}$$

Also since $$\frac{CR}{M} = 10^3$$

$$M = \frac{CR}{10^3} = \frac{16}{10^6} \times \frac{1}{10^3} = 16 \text{ nH} \quad \textbf{Ans.}$$

Taking $$R = 8 \times 10^3\ \Omega \quad \textbf{Ans.}$$

$$C = \frac{16}{10^6} \frac{1}{8 \times 10^3} = 2 \text{ nF} \quad \textbf{Ans.}$$

PROBLEMS

4.1. What are the requirements of a sphere gap for measurement of high voltages? Discuss the disadvantages of sphere gap for measurements.

4.2. Explain clearly the procedure for measurement of (*i*) impulse; (*ii*) a.c. high voltages using sphere gap.

4.3. Discuss the effect of (*i*) nearby earthed objects (*ii*) humidity and (*iii*) dust particles on the measurements using sphere gaps.

4.4. Describe the construction of a uniform field spark gap and discuss its advantages and disadvantages for high voltage measurements.

4.5. Explain with neat diagram how rod gaps can be used for measurement of high voltages. Compare its performance with a sphere gap.

4.6. Explain with neat diagram the principle of operation of an Electrostatic Voltmeter. Discuss its advantages and limitations for high voltage measurements.

4.7. Draw a neat schematic diagram of a generating voltmeter and explain its principle of operation. Discuss its application and limitations.

4.8. Draw Chubb-Fortescue Circuit for measurement of peak value of a.c. voltages discuss its advantages over other methods.

4.9. Discuss the problems associated with peak voltmeter circuits using passive elements. Draw circuit developed by Rabus and explain how this circuit overcomes these problems.

4.10. What are the problems associated with measurement of very high impulse voltages? Explain how these can be taken care of during measurements.

4.11. Discuss and compare the performance of (*i*) resistance (*ii*) capacitance potential dividers for measurement of impulse voltages.

4.12. Discuss various resistance potential dividers and compare their performance of measurement of impulse voltages.

4.13. Discuss various capacitance, potential dividers and compare their performance for measurement of impulse voltages.

4.14. Draw a simplified equivalent circuit of a resistance potential divider and discuss its step response.

4.15. Discuss various methods of measuring high d.c. and a.c. currents.

4.16. Discuss various methods of measuring high impulse currents.

4.17. What is Rogowski Coil? Explain with a neat diagram its principle of operation for measurement of high impulse currents.

5 High Voltage Testing of Electrical Equipment

Man has been power hungry since time-immemorial. In modern times the world has seen phenomenal increase in demand for energy, of which an important component is that of electrical energy. The production of electrical energy in big plants under the most economic condition makes it necessary that more and more energy be transported over longer and longer distances. Therefore, transmission at extra high voltages and the erection of systems which may extend over whole continents has become the most urgent problems to be solved in the near future. The very fast development of systems is followed by studies of equipment and the service conditions they have to fulfill. These conditions will also determine the values for testing at alternating, impulse and d.c. voltages under specific conditions.

As we go for higher and higher operating voltages (say above 1000 kV) certain problems are associated with the testing techniques. Some of these are:

(*i*) Dimension of high voltage test laboratories.

(*ii*) Characteristics of equipment for such laboratories.

(*iii*) Some special aspects of the test techniques at extra high voltages.

The dimensions of laboratories for test equipments of 750 kV and above are fixed by the following main considerations:

(*i*) Figures (values) of test voltages under different conditions.

(*ii*) Sizes of the test of equipments in a.c., d.c. and impulse voltages.

(*iii*) Distances between the objects under high voltage during the test period and the earthed surroundings such as floors, walls and roofs of the buildings. The problems associated with the characteristics of the equipments used for testing are summarised here.

In alternating voltage system, a careful choice of the characteristics of the testing transformer is essential. It is known that the flash over voltage of the insulator in air or in any insulating fluid depends upon the capacitance of the supply system. This is due to the fact that a voltage drop may not maintain preliminary discharges or breakdown. It is, therefore, suggested that a capacitance of at least 1000 pF must be connected across the insulator to obtain the correct flash over or puncture voltage and also under breakdown condition (a virtual short circuit) the supply system should be able to supply at least 1 amp for clean and 5 amp for polluted insulators at the test voltage.

There are some difficult problems with impulse testing equipments also especially when testing large power transformers or large reactors or large cables operating at very high voltages. The equivalent capacitance of the impulse generator is usually about 40 nano farads independent of the operating voltage which gives a stored energy of about $1/2 \times 40\ \ 10^{-9} \times 36 \times 10^{9} = 720$ KJ for 6 MV generators

which is required for testing equipments operating at 150 kV. It is not at all difficult to pile up a large number of capacitances to charge them in parallel and then discharge in series to obtain a desired impulse wave. But the difficulty exists in reducing the internal reactance of the circuit so that a short wave front with minimum oscillation can be obtained. For example for a 4 MV circuit the inductance of the circuit is about 140 μH and it is impossible to test an equipment with a capacitance of 5000 pF with a front time of 1.2 μ sec. and less than 5% overshoot on the wave front.

Cascaded rectifiers are used for high voltage d.c. testing. A careful consideration is necessary when test on polluted insulation is to be performed which requires currents of 50 to 200 mA but extremely predischarge streamer of 0.5 to 1 amp during milliseconds occur. The generator must have an internal reactance in order to maintain the test voltage without too high a voltage drop.

5.1 TESTING OF OVERHEAD LINE INSULATORS

Various types of overhead line insulators are (*i*) Pin type (*ii*) Post type (*iii*) String insulator unit (*iv*) Suspension insulator string (*v*) Tension insulator.

Arrangement of Insulators for Test

String insulator unit should be hung by a suspension eye from an earthed metal cross arm. The test voltage is applied between the cross arm and the conductor hung vertically down from the metal part on the lower side of the insulator unit.

Suspension string with all its accessories as in service should be hung from an earthed metal cross arm. The length of the cross arm should be at least 1.5 times the length of the string being tested and should be at least equal to 0.9 m on either side of the axis of the string. No other earthed object should be nearer to the insulator string then 0.9 m or 1.5 times the length of the string whichever is greater. A conductor of actual size to be used in service or of diameter not less than 1 cm and length 1.5 times the length of the string is secured in the suspension clamp and should lie in a horizontal plane. The test voltage is applied between the conductor and the cross arm and connection from the impulse generator is made with a length of wire to one end of the conductor. For higher operating voltages where the length of the string is large, it is advisable to sacrifice the length of the conductor as stipulated above. Instead, it is desirable to bend the ends of the conductor over in a large radius.

For tension insulators the arrangement is more or less same as in suspension insulator except that it should be held in an approximately horizontal position under a suitable tension (about 1000 Kg.).

For testing pin insulators or line post insulators, these should be mounted on the insulator pin or line post shank with which they are to be used in service. The pin or the shank should be fixed in a vertical position to a horizontal earthed metal cross arm situated 0.9 m above the floor of the laboratory. A conductor of 1 cm diameter is to be laid horizontally in the top groove of the insulator and secured by at least one turn of tie-wire, not less than 0.3 cm diameter in the tie-wire groove. The length of the wire should be at least 1.5 times the length of the insulator and should over hang the insulator at least 0.9 m on either side in a direction at right angles to the cross arm. The test voltage is applied to one end of the conductor.

High voltage testing of electrical equipment requires two types of tests: (*i*) Type tests, and (*ii*) Routine test. Type tests involves quality testing of equipment at the design and development level *i.e.* samples of the product are taken and are tested when a new product is being developed and designed or

an old product is to be redesigned and developed whereas the routine tests are meant to check the quality of the individual test piece. This is carried out to ensure quality and reliability of individual test objects.

High voltage tests include (*i*) Power frequency tests and (*ii*) Impulse tests. These tests are carried out on all insulators.

(*i*) 50% dry impulse flash over test.

(*ii*) Impulse withstand test.

(*iii*) Dry flash over and dry one minute test.

(*iv*) Wet flash over and one minute rain test.

(*v*) Temperature cycle test.

(*vi*) Electro-mechanical test.

(*vii*) Mechanical test.

(*viii*) Porosity test.

(*ix*) Puncture test.

(*x*) Mechanical routine test.

The tests mentioned above are briefly described here.

(*i*) The test is carried out on a clean insulator mounted as in a normal working condition. An impulse voltage of 1/50 μ sec. wave shape and of an amplitude which can cause 50% flash over of the insulator, is applied, *i.e.* of the impulses applied 50% of the impulses should cause flash over. The polarity of the impulse is then reversed and procedure repeated. There must be at least 20 applications of the impulse in each case and the insulator must not be damaged. The magnitude of the impulse voltage should not be less than that specified in standard specifications.

(*ii*) The insulator is subjected to standard impulse of 1/50 μ sec. wave of specified value under dry conditions with both positive and negative polarities. If five consecutive applications do not cause any flash over or puncture, the insulator is deemed to have passed the impulse withstand test. If out of five, two applications cause flash over, the insulator is deemed to have filed the test.

(*iii*) Power frequency voltage is applied to the insulator and the voltage increased to the specified value and maintained for one minute. The voltage is then increased gradually until flash over occurs. The insulator is then flashed over at least four more times, the voltage is raised gradually to reach flash over in about 10 seconds. The mean of at least five consecutive flash over voltages must not be less than the value specified in specifications.

(*iv*) If the test is carried out under artificial rain, it is called wet flash over test. The insulator is subjected to spray of water of following characteristics:

Precipitation rate	3 ± 10% mm/min.
Direction	45° to the vertical
Conductivity of water	100 micro siemens ± 10%

Temperature of water Ambient +15°C

The insulator with 50% of the one-min. rain test voltage applied to it, is then sprayed for two minutes, the voltage raised to the one minute test voltage in approximately 10 sec. and maintained there for one minute. The voltage is then increased gradually till flash over occurs and the insulator is then

flashed at least four more times, the time taken to reach flash over voltage being in each case about 10 sec. The flash over voltage must not be less than the value specified in specifications.

(*v*) The insulator is immersed in a hot water bath whose temperature is 70° higher than normal water bath for *T* minutes. It is then taken out and immediately immersed in normal water bath for *T* minutes. After *T* minutes the insulator is again immersed in hot water bath for *T* minutes. The cycle is repeated three times and it is expected that the insulator should withstand the test without damage to the insulator or glaze. Here $T = (15 + W/1.36)$ where *W* is the weight of the insulator in kgs.

(*vi*) The test is carried out only on suspension or tension type of insulator. The insulator is subjected to a 2½ times the specified maximum working tension maintained for one minute. Also, simultaneously 75% of the dry flash over voltage is applied. The insulator should withstand this test without any damage.

(*vii*) This is a bending test applicable to pin type and line-post insulators. The insulator is subjected to a load three times the specified maximum breaking load for one minute. There should be no damage to the insulator and in case of post insulator the permanent set must be less than 1%. However, in case of post insulator, the load is then raised to three times and there should not be any damage to the insulator and its pin.

(*viii*) The insulator is broken and immersed in a 0.5% alcohol solution of fuchsin under a pressure of 13800 kN/m^2 for 24 hours. The broken insulator is taken out and further broken. It should not show any sign of impregnation.

(*ix*) An impulse over voltage is applied between the pin and the lead foil bound over the top and side grooves in case of pin type and post insulator and between the metal fittings in case of suspension type insulators. The voltage is 1/50 μ sec. wave with amplitude twice the 50% impulse flash over voltage and negative polarity. Twenty such applications are applied. The procedure is repeated for 2.5, 3, 3.5 times the 50% impulse flash over voltage and continued till the insulator is punctured. The insulator must not puncture if the voltage applied is equal to the one specified in the specification.

(*x*) The string in insulator is suspended vertically or horizontally and a tensile load 20% in excess of the maximum specified working load is applied for one minute and no damage to the string should occur.

5.2 TESTING OF CABLES

High voltage power cables have proved quite useful especially in case of HV d.c. transmission. Underground distribution using cables not only adds to the aesthetic looks of a metropolitan city but it provides better environments and more reliable supply to the consumers.

Preparation of Cable Sample

The cable sample has to be carefully prepared for performing various tests especially electrical tests. This is essential to avoid any excessive leakage or end flash overs which otherwise may occur during testing and hence may give wrong information regarding the quality of cables. The length of the sample cable varies between 50 cms to 10 m. The terminations are usually made by shielding the ends of the cable with stress shields so as to relieve the ends from excessive high electrical stresses.

A cable is subjected to following tests:

(*i*) Bending tests.

(*ii*) Loading cycle test.

(*iii*) Thermal stability test.

(*iv*) Dielectric thermal resistance test.

(*v*) Life expectancy test.

(*vi*) Dielectric power factor test.

(*vii*) Power frequency withstand voltage test.

(*viii*) Impulse withstand voltage test.

(*ix*) Partial discharge test.

(*i*) It is to be noted that a voltage test should be made before and after a bending test. The cable is bent round a cylinder of specified diameter to make one complete turn. It is then unwound and rewound in the opposite direction. The cycle is to be repeated three times.

(*ii*) A test loop, consisting of cable and its accessories is subjected to 20 load cycles with a minimum conductor temperature 5°C in excess of the design value and the cable is energized to 1.5 times the working voltage. The cable should not show any sign of damage.

(*iii*) After test as at (*ii*), the cable is energized with a voltage 1.5 times the working voltage for a cable of 132 kV rating (the multiplying factor decreases with increases in operating voltage) and the loading current is so adjusted that the temperature of the core of the cable is 5°C higher than its specified permissible temperature. The current should be maintained at this value for six hours.

(*iv*) The ratio of the temperature difference between the core and sheath of the cable and the heat flow from the cable gives the thermal resistance of the sample of the cable. It should be within the limits specified in the specifications.

(*v*) In order to estimate life of a cable, an accelerated life test is carried out by subjecting the cable to a voltage stress higher than the normal working stress. It has been observed that the relation between the expected life of the cable in hours and the voltage stress is given by

$$g = \frac{K}{n\sqrt{t}}$$

where K is a constant which depends on material and n is the life index depending again on the material.

(*vi*) High Voltage Schering Bridge is used to perform dielectric power factor test on the cable sample. The power factor is measured for different values of voltages *e.g.* 0.5, 1.0, 1.5 and 2.0 times the rated operating voltages. The maximum value of power factor at normal working voltage does not exceed a specified value (usually 0.01) at a series of temperatures ranging from 15°C to 65°C. The difference in the power factor between rated voltage and 1.5 times the rated voltage and the rated voltage and twice the rated voltage does not exceed a specified value. Sometimes the source is not able to supply charging current required by the test cable, a suitable choke in series with the test cable helps in tiding over the situation.

(*vii*) Cables are tested for power frequency a.c. and d.c. voltages. During manufacture the entire cable is passed through a higher voltage test and the rated voltage to check the continuity of the cable. As a routine test the cable is subjected to a voltage 2.5 times the working voltage for 10 min without damaging the insulation of the cable. HV d.c. of 1.8 times the rated d.c. voltage of negative polarity for 30 min. is applied and the cable is said to have withstood the test if no insulation failure takes place.

(*viii*) The test cable is subjected to 10 positive and 10 negative impulse voltage of magnitude as specified in specification, the cable should withstand 5 applications without any damage. Usually, after

the impulse test, the power frequency dielectric power factor test is carried out to ensure that no failure occurred during the impulse test.

(*ix*) Partial discharge measurement of cables is very important as it gives an indication of expected life of the cable and it gives location of fault, if any, in the cable.

When a cable is subjected to high voltage and if there is a void in the cable, the void breaks down and a discharge takes place. As a result, there is a sudden dip in voltage in the form of an impulse. This impulse travels along the cable as explained in detail in Chapter VI. The duration between the normal pulse and the discharge pulse is measured on the oscilloscope and this distance gives the location of the void from the test end of the cable. However, the shape of the pulse gives the nature and intensity of the discharge.

In order to scan the entire length of the cable against voids or other imperfections, it is passed through a tube of insulating material filled with distilled water. Four electrodes, two at the end and two in the middle of the tube are arranged. The middle electrodes are located at a stipulated distance and these are energized with high voltage. The two end electrodes and cable conductor are grounded. As the cable is passed between the middle electrode, if a discharge is seen on the oscilloscope, a defect in this part of the cable is stipulated and hence this part of the cable is removed from the rest of the cable.

5.3 TESTING OF BUSHINGS

Bushings are an integral component of high voltage machines. A bushing is used to bring high voltage conductors through the grounded tank or body of the electrical equipment without excessive potential gradients between the conductor and the edge of the hole in the body. The bushing extends into the surface of the oil at one end and the other end is carried above the tank to a height sufficient to prevent breakdown due to surface leakage.

Following tests are carried out on bushings:

(*i*) *Power Factor Test*

The bushing is installed as in service or immersed in oil. The high voltage terminal of the bushing is connected to high voltage terminal of the Schering Bridge and the tank or earth portion of the bushing is connected to the detector of the bridge. The capacitance and p.f. of the bushing is measured at different voltages as specified in the relevant specification and the capacitance and p.f. should be within the range specified.

(*ii*) *Impulse Withstand Test*

The bushing is subjected to impulse waves of either polarity and magnitude as specified in the standard specification. Five consecutive full waves of standard wave form (1/50 μ sec.) are applied and if two of them cause flash over, the bushing is said to be defective. If only one flash over occurs, ten additional applications are made. If no flash over occurs, bushing is said to have passed the test.

(*iii*) *Chopped Wave and Switching Surge Test*

Chopped wave and switching surge of appropriate duration tests are carried out on high voltage bushings. The procedure is identical to the one given in (*ii*) above.

(*iv*) *Partial Discharge Test*

In order to determine whether there is deterioration or not of the insulation used in the bushing, this test is carried out. The procedure is explained in detail in Chapter-VI. The shape of the discharge is an

indication of nature and severity of the defect in the bushing. This is considered to be a routine test for high voltage bushings.

(*v*) *Visible Discharge Test at Power Frequency*

The test is carried out to ascertain whether the given bushing will give rise to ratio interference or not during operation. The test is carried out in a dark room. The voltage as specified is applied to the bushing (IS 2099). No discharge other than that from the grading rings or arcing horns should be visible.

(*vi*) *Power Frequency Flash Over or Puncture Test*

(*Under Oil*): The bushing is either immersed fully in oil or is installed as in service condition. This test is carried out to ascertain that the internal breakdown strength of the bushing is 15% more than the power frequency momentary dry withstand test value.

5.4 TESTING OF POWER CAPACITORS

Power capacitors is an integral part of the modern power system. These are used to control the voltage profile of the system. Following tests are carried out on shunt power capacitors (IS 2834):

(*i*) *Routine Tests*

Routine tests are carried out on all capacitors at the manufacturer's premises. During testing, the capacitor should not breakdown or behave abnormally or show any visible deterioration.

(*ii*) *Test for Output*

Ammeter and Voltmeter can be used to measure the kVAr and capacitance of the capacitor. The kVAr calculated should not differ by more than –5 to +10% of the specified value for capacitor units and 0 to 10% for capacitors banks.

The a.c. supply used for testing capacitor should have frequency between 40 Hz to 60 Hz, preferably as near as possible to the rated frequency and the harmonics should be minimum.

(*iii*) *Test between Terminals*

Every capacitor is subjected to one of the following two tests for 10 secs:

(*a*) D.C. test; the test voltage being $V_t = 4.3\ V_0$

(*b*) A.C. test $V_t = 2.15\ V_0$, where V_0 is the rms value of the voltage between terminals which in the test connection gives the same dielectric stress in the capacitor element as the rated voltage V_n gives in normal service.

(*iv*) *Test between Line Terminals and Container (For capacitor units)*

An a.c. voltage of value specified in column 2 of Table 5.1 is applied between the terminals (short circuited) of the capacitor unit and its container and is maintained for one minute, no damage to the capacitor should be observed.

Figures with single star represent values corresponding to reduced insulation level (Effectively grounded system) and with double star full insulation level (non-effectively grounded system).

Table 5.1
Power frequency and impulse test voltages
(Between terminals and the container)

System Voltage kV (rms)	*Power Frequency Test Voltage kV (rms)*	*Impulse Test Voltage kV (peak)*
12	28	75
24	50	125
36	70	170
72.5	140	325
145	230*	550*
	275**	650**
245	395*	900*
	460**	1050**

(*v*) *IR Test*

The insulation resistance of the test capacitor is measured with the help of a megger. The megger is connected between one terminal of the capacitor and the container. The test voltage shall be d.c. voltage not less than 500 volts and the acceptable value of IR is more than 50 megohms.

(*vi*) *Test for efficiency of Discharge Device*

In order to provide safety to personnel who would be working on the capacitors, it is desirable to connect very high resistance across the terminals of the capacitor so that they get discharged in about a few seconds after the supply is switched off. The residual capacitor voltage after the supply voltage is switched off should reduce to 50 volts in less than one minute of the capacitor is rated upto 650 volts and 5 minutes if the capacitor is rated for voltage more than 650 volts.

A d.c. voltage $\sqrt{2}$ × rms rated voltage of the capacitor is applied across the parallel combination of R and C where C is the capacitance of the capacitor under test and R is the high resistance connected across the capacitor. The supply is switched off and the fall in voltage across the capacitor as a function of time is recorded. If C is in microfarads and R in ohms, the time to discharge to 50 volts can be calculated from the formula

$$t = 2.3 \times 10^{-6}\, CR\, (\log_{10} V - 1.7) \text{ secs}$$

where V is the rated rms voltage of the capacitor in volts.

Type Tests

The type tests are carried out only once by the manufacturer to prove that the design of capacitor complies with the design requirements:

(*i*) *Dielectric Loss Angle Test (p.f. test)*

High voltage schering bridge is used to measure dielectric power factor. The voltage applied is the rated voltage and at temperatures 27°C ± 2°C. The value of the loss angle tan δ should not be more than 10% the value agreed to between the manufacturer and the purchaser and it should not exceed 0.0035 for mineral oil impregnants and 0.005 for chlorinated impregnants.

(*ii*) *Test for Capacitor Loss*

The capacitor loss includes the dielectric loss of the capacitor and the V^2/R loss in the discharge resistance which is permanently connected. The dielectric loss can be evaluated from the loss angle as obtained in the previous test and V^2/R loss can also be calculated. The total power loss should not be more than 10% of the value agreed to between the manufacturer and consumer.

(*iii*) *Stability Test*

The capacitor is placed in an enclosure whose temperature is maintained at ±2°C above the maximum working temperature for 48 hours. The loss angle is measured after 16 hours, 24 hours and 48 hours using High voltage Schering Bridge at rated frequency and at voltage 1.2 times the rated voltage. If the respective values of loss angle are tan δ_1, tan δ_2 and tan δ_3, these values should satisfy the following relations (anyone of them):

(*a*) $\tan \delta_1 + \tan \delta_2 \leq 2 \tan \delta_2 < 2.1 \tan \delta_1$

or (*b*) $\tan \delta_1 \geq \tan \delta_2 \geq \tan \delta_3$

(*iv*) *Impulse voltage test between terminal and container*

The capacitor is subjected to impulse voltage of 1/50 μ sec. Wave and magnitude as stipulated in column 3 of Table 5.1. Five impulses of either polarity should be applied between the terminals (joined together) and the container. It should withstand this voltage without causing any flash overs.

5.5 TESTING OF POWER TRANSFORMERS

Transformer is one of the most expensive and important equipment in power system. If it is not suitably designed its failure may cause a lengthy and costly outage. Therefore, it is very important to be cautious while designing its insulation, so that it can withstand transient over voltage both due to switching and lightning. The high voltage testing of transformers is, therefore, very important and would be discussed here. Other tests like temperature rise, short circuit, open circuit etc. are not considered here. However, these can be found in the relevant standard specification.

Partial Discharge Test

The test is carried out on the windings of the transformer to assess the magnitude of discharges. The transformer is connected as a test specimen similar to any other equipment as discussed in Chapter-VI and the discharge measurements are made. The location and severity of fault is ascertained using the travelling wave theory technique as explained in Chapter VI. The measurements are to be made at all the terminals of the transformer and it is estimated that if the apparent measured charge exceeds 10^4 picocoulombs, the discharge magnitude is considered to be severe and the transformer insulation should be so designed that the discharge measurement should be much below the value of 10^4 pico-coulombs.

Impulse Testing of Transformer

The impulse level of a transformer is determined by the breakdown voltage of its minor insulation (Insulation between turn and between windings), breakdown voltage of its major insulation (insulation between windings and tank) and the flash over voltage of its bushings or a combination of these. The impulse characteristics of internal insulation in a transformer differs from flash over in air in two main respects. Firstly the impulse ratio of the transformer insulation is higher (varies from 2.1 to 2.2) than that of bushing (1.5 for bushings, insulators etc.). Secondly, the impulse breakdown of transformer

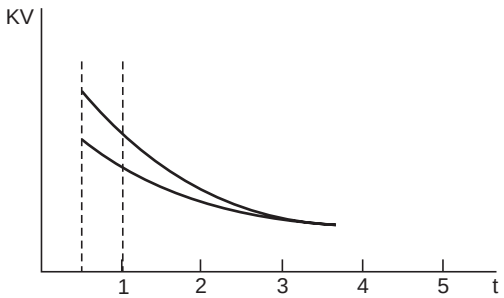

Fig. 5.1 Volt time curve of typical major insulation in transformer

insulation in practically constant and is independent of time of application of impulse voltage. Fig. 5.1 shows that after three micro seconds the flash over voltage is substantially constant. The voltage stress between the turns of the same winding and between different windings of the transformer depends upon the steepness of the surge wave front. The voltage stress may further get aggravated by the piling up action of the wave if the length of the surge wave is large. In fact, due to high steepness of the surge waves, the first few turns of the winding are overstressed and that is why the modern practice is to provide extra insulation to the first few turns of the winding. Fig. 5.2 shows the equivalent circuit of a transformer winding for impulse voltage.

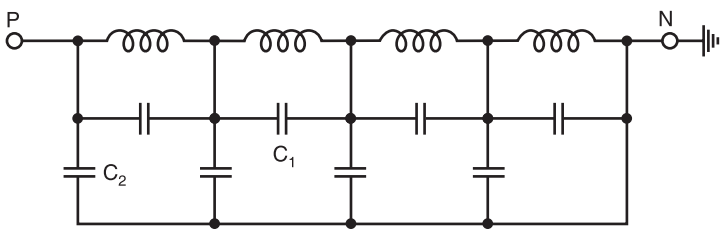

Fig. 5.2 Equivalent circuit of a transformer for impulse voltage

Here C_1 represents inter-turn capacitance and C_2 capacitance between winding and the ground (tank). In order that the minor insulation will be able to withstand the impulse voltage, the winding is subjected to chopped impulse wave of higher peak voltage than the full wave. This chopped wave is produced by flash over of a rod gap or bushing in parallel with the transformer insulation. The chopping time is usually 3 to 6 micro seconds. While impulse voltage is applied between one phase and ground, high voltages would be induced in the secondary of the transformer. To avoid this, the secondary windings are short-circuited and finally connected to ground. The short circuiting, however, decreases the impedance of the transformer and hence poses problem in adjusting the wave front and wave tail timings of wave. Also, the minimum value of the impulse capacitance required is given by

$$C_0 = \frac{P \times 10^8}{Z \times V^2} \mu F$$

where P = rated MVA of the transformer Z = per cent impedance of transformer. V = rated voltage of transformer.

Fig. 5.3 shows the arrangement of the transformer for impulse testing. CRO forms an integral part of the transformer impulse testing circuit. It is required to record to wave forms of the applied voltage and current through the winding under test.

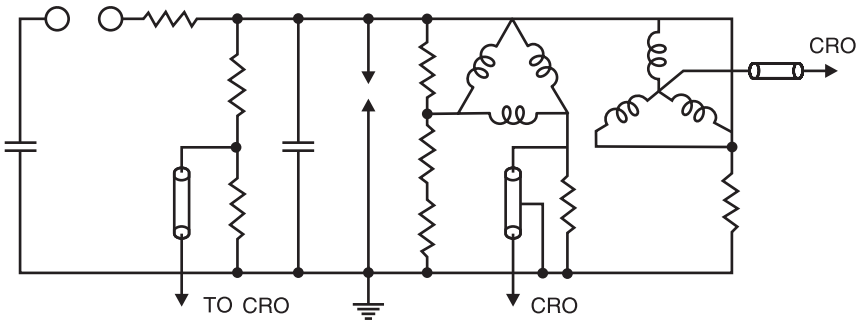

Fig. 5.3 Arrangement for impulse testing of transformer

Impulse testing consists of the following steps:

(*i*) Application of impulse of magnitude 75% of the Basic Impulse Level (BIL) of the transformer under test.

(*ii*) One full wave of 100% of BIL.

(*iii*) Two chopped wave of 115% of BIL.

(*iv*) One full wave of 100% BIL and

(*v*) One full wave of 75% of BIL.

During impulse testing the fault can be located by general observation like noise in the tank or smoke or bubble in the breather.

If there is a fault, it appears on the Oscilloscope as a partial of complete collapse of the applied voltage.

Study of the wave form of the neutral current also indicated the type of fault. If an arc occurs between the turns or form turn to the ground, a train of high frequency pulses are seen on the oscilloscope and wave shape of impulse changes. If it is a partial discharge only, high frequency oscillations are observed but no change in wave shape occurs.

The bushing forms an important and integral part of transformer insulation. Therefore, its impulse flash over must be carefully investigated. The impulse strength of the transformer winding is same for either polarity of wave whereas the flash over voltage for bushing is different for different polarity. The manufacturer, however, while specifying the impulse strength of the transformer takes into consideration the overall impulse characteristic of the transformer.

5.6 TESTING OF CIRCUIT BREAKERS

An equipment when designed to certain specification and is fabricated, needs testing for its performance. The general design is tried and the results of such tests conducted on one selected breaker and are thus applicable to all others of identical construction. These tests are called the type tests. These tests are classified as follows:

1. Short circuit tests:
   (*i*) Making capacity test.
   (*ii*) Breaking capacity test.
   (*iii*) Short time current test.
   (*iv*) Operating duty test

2. Dielectric tests:
   (*i*) Power frequency test:
      (*a*) One minute dry withstand test.
      (*b*) One minute wet withstand test.
   (*ii*) Impulse voltage dry withstand test.
3. Thermal test.
4. Mechanical test

Once a particular design is found satisfactory, a large number of similar C.Bs. are manufactured for marketing. Every piece of C.B. is then tested before putting into service. These tests are known as routine tests. With these tests it is possible to find out if incorrect assembly or inferior quality material has been used for a proven design equipment. These tests are classified as (*i*) operation tests, (*ii*) millivoltdrop tests, (*iii*) power frequency voltage tests at manufacturer's premises, and (*iv*) power frequency voltage tests after erection on site.

We will discuss first the type tests. In that also we will discuss the short circuit tests after the other three tests.

Dielectric Tests

The general dielectric characteristics of any circuit breaker or switchgear unit depend upon the basic design *i.e.* clearances, bushing materials, etc. upon correctness and accuracy in assembly and upon the quality of materials used. For a C.B. these factors are checked from the viewpoint of their ability to withstand over voltages at the normal service voltage and abnormal voltages during lightning or other phenomenon.

The test voltage is applied for a period of one minute between (*i*) phases with the breaker closed, (*ii*) phases and earth with C.B. open, and (*iii*) across the terminals with breaker open. With this the breaker must not flash over or puncture. These tests are normally made on indoor switchgear. For such C.Bs the impulse tests generally are unnecessary because it is not exposed to impulse voltage of a very high order. The high frequency switching surges do occur but the effect of these in cable systems used for indoor switchgear are found to be safely withstood by the switchgear if it has withstood the normal frequency test.

Since the outdoor switchgear is electrically exposed, they will be subjected to over voltages caused by lightning. The effect of these voltages is much more serious than the power frequency voltages in service. Therefore, this class of switchgear is subjected in addition to power frequency tests, the impulse voltage tests.

The test voltage should be a standard 1/50 μ sec wave, the peak value of which is specified according to the rated voltage of the breaker. A higher impulse voltage is specified for non-effectively grounded system than those for solidly grounded system. The test voltages are applied between (*i*) each pole and earth in turn with the breaker closed and remaining phases earthed, and (*ii*) between all terminals on one side of the breaker and all the other terminals earthed, with the breaker open. The specified voltages are withstand values *i.e.* the breaker should not flash over for 10 applications of the wave. Normally this test is carried out with waves of both the polarities.

The wet dielectric test is used for outdoor switchgear. In this, the external insulation is sprayed for two minutes while the rated service voltage is applied; the test overvoltage is then maintained for 30 seconds during which no flash over should occur. The effect of rain on external insulation is partly beneficial, insofar as the surface is thereby cleaned, but is also harmful if the rain contains impurities.

Thermal Tests

These tests are made to check the thermal behaviour of the breakers. In this test the rated current through all three phases of the switchgear is passed continuously for a period long enough to achieve steady state conditions. Temperature readings are obtained by means of thermocouples whose hot junctions are placed in appropriate positions. The temperature rise above ambient, of conductors, must normally not exceed 40°C when the rated normal current is less than 800 amps and 50°C if it is 800 amps and above.

An additional requirement in the type test is the measurement of the contact resistances between the isolating contacts and between the moving and fixed contacts. These points are generally the main sources of excessive heat generation. The voltage drop across the breaker pole is measured for different values of d.c. current which is a measure of the resistance of current carrying parts and hence that of contacts.

Mechanical Tests

A C.B. must open and close at the correct speed and perform such operations without mechanical failure. The breaker mechanism is, therefore, subjected to a mechanical endurance type test involving repeated opening and closing of the breaker. B.S. 116: 1952 requires 500 such operations without failure and with no adjustment of the mechanism. Some manufacture feel that as many as 20,000 operations may be reached before any useful information regarding the possible causes of failure may be obtained. A resulting change in the material or dimensions of a particular component may considerably improve the life and efficiency of the mechanism.

Short Circuit Tests

These tests are carried out in short circuit testing stations to prove the ratings of the C.Bs. Before discussing the tests it is proper to discuss about the short circuit testing stations.

There are two types of testing stations; (*i*) field type, and (*ii*) laboratory type.

In case of field type stations the power required for testing is directly taken from a large power system. The breaker to be tested is connected to the system. Whereas this method of testing is economical for high voltage C.Bs. it suffers from the following drawbacks:

1. The tests cannot be repeatedly carried out for research and development as it disturbs the whole network.
2. The power available depends upon the location of the testing stations, loading conditions, installed capacity, etc.
3. Test conditions like the desired recovery voltage, the RRRV etc. cannot be achieved conveniently.

In case of laboratory testing the power required for testing is provided by specially designed generators. This method has the following advantages:

1. Test conditions such as current, voltage, power factor, restriking voltages can be controlled accurately.
2. Several indirect testing methods can be used.
3. Tests can be repeated and hence research and development over the design is possible.

The limitations of this method are the cost and the limited power availability for testing the breakers.

Short Circuit Test Plants

The essential components of a typical test plant are represented in Fig. 5.4. The short-circuit power is supplied by specially designed short-circuit generators driven by induction motors. The magnitude of voltage can be varied by adjusting excitation of the generator or the transformer ratio. A plant master-breaker is available to interrupt the test short circuit current if the test breaker should fail. Initiation of the short circuit may be by the master breaker, but is always done by a making switch which is specially designed for closing on very heavy currents but never called upon to break currents. The generator winding may be arranged for either star or delta connection according to the voltage required; by further dividing the winding into two sections which may be connected in series or parallel, a choice of four voltages is available. In addition to this the use of resistors and reactors in series gives a wide range of current and power factors. The generator, transformer and reactors are housed together, usually in the building accommodating the test cells.

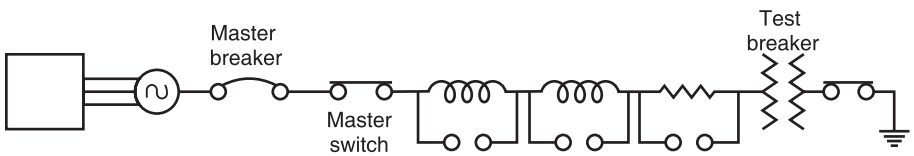

Fig. 5.4 Schematic diagram of a typical test plant

Generator

The short circuit generator is different in design from the conventional power station. The capacity of these generators may be of the order of 2000 MVA and very rigid bracing of the conductors and coil ends is necessary in view of the high electromagnetic forces possible. The limiting factor for the maximum output current is the electromagnetic force. Since the operation of the generator is intermittent, this need not be very efficient. The reduction of ventilation enables the main flux to be increased and permits the inclusion of extra coil end supports. The machine reactance is reduced to a minimum.

Immediately before the actual closing of the making switch the generator driving motor is switched out and the short circuit energy is taken from the kinetic energy of the generator set. This is done to avoid any disturbance to the system during short circuit. However, in this case it is necessary to compensate for the decrement in generator voltage corresponding to the diminishing generator speed during the test. This is achieved by adjusting the generator field excitation to increase at a suitable rate during the short circuit period.

Resistors and Reactors

The resistors are used to control the p.f. of the current and to control the rate of decay of d.c. component of current. There are a number of coils per phase and by combinations of series and parallel connections, desired value of resistance and/or reactance can be obtained.

Capacitors

These are used for breaking line charging currents and for controlling the rate of re-striking voltage.

Short Circuit Transformers

The leakage reactance of the transformer is low so as to withstand repeated short circuits. Since they are in use intermittently, they do not pose any cooling problem. For voltage higher than the generated

voltages, usually banks of single phase transformers are employed. In the short circuit station at Bhopal there are three single phase units each of 11 kV/76 kV. The normal rating is 30 MVA but their short circuit capacity is 475 MVA.

Master C.Bs.

These breakers are provided as back up which will operate, should the breaker under test fail to operate. This breaker is normally air blast type and the capacity is more than the breaker under test. After every test, it isolates the test breaker from the supply and can handle the full short circuit of the test circuit.

Make Switch

The make switch is closed after other switches are closed. The closing of the switch is fast, sure and without chatter. In order to avoid bouncing and hence welding of contacts, a high air pressure is maintained in the chamber. The closing speed is high so that the contacts are fully closed before the short circuit current reaches its peak value.

Test Procedure

Before the test is performed all the components are adjusted to suitable values so as to obtain desired values of voltage, current, rate of rise of restriking voltage, p.f. etc. The measuring circuits are connected and oscillograph loops are calibrated.

During the test several operations are performed in a sequence in a short time of the order of 0.2 sec. This is done with the help of a drum switch with several pairs of contacts which is rotated with a motor. This drum when rotated closes and opens several control circuits according to a certain sequence. In one of the breaking capacity tests the following sequence was observed:

(*i*) After running the motor to a speed the supply is switched off.

(*ii*) Impulse excitation is switched on.

(*iii*) Master C.B. is closed.

(*iv*) Oscillograph is switched on.

(*v*) Make switch is closed.

(*vi*) C.B. under test is opened.

(*vii*) Master C.B. is opened.

(*viii*) Exciter circuit is switched off.

The circuit for direct test is shown in Fig. 5.5

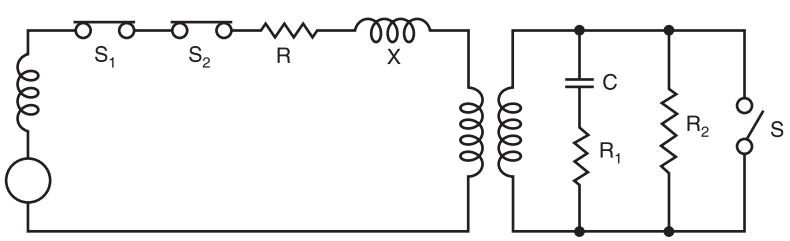

Fig. 5.5 Circuit for direct testing

Here X_G = generator reactance, S_1 and S_2 are master and make switches respectively. R and X are the resistance and reactance for limiting the current and control of p.f., T is the transformer, C, R_1 and R_2 is the circuit for adjusting the restriking voltage.

For testing, breaking capacity of the breaker under test, master and breaker under test are closed first. Short circuit is applied by closing the making switch. The breaker under test is opened at the desired moment and breaking current is determined from the oscillograph as explained earlier.

For making capacity test the master and the make switches are closed first and short circuit is applied by closing the breaker under test. The making current is determined from the oscillograph as explained earlier.

For short-time current test, the current is passed through the breaker for a short-time say 1 second and the oscillograph is taken as shown in Fig. 5.6.

From the oscillogram the equivalent r.m.s. value of short-time current is obtained as follows:

The time interval 0 to T is divided into 10 equal parts marked as 0, 1, 2 ..., 9, 10. Let the r.m.s. value of currents at these instants be I_0, I_1, I_2, ..., I_9, I_{10} (asymmetrical values). From these values, the r.m.s. value of short-time current is calculated using Simpson formula.

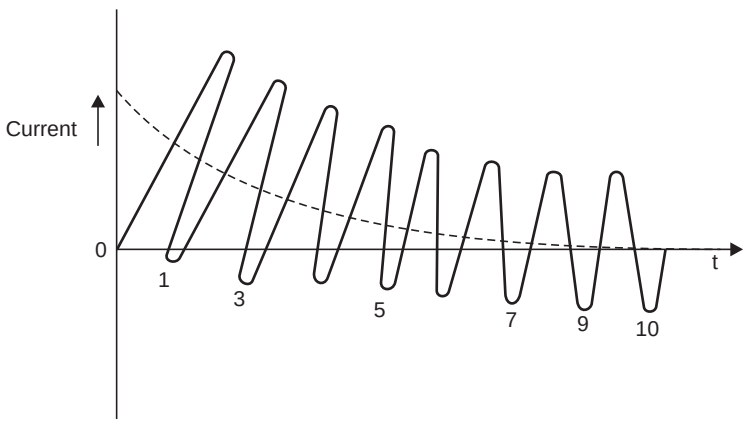

Fig. 5.6 Determination of short-time current

$$I = \sqrt{\frac{1}{3}[K_0^2 + 4(I_1^2 + I_3^2 + I_5^2 + \ldots + I_9^2) + 2(I_2^2 + I_4^2 + \ldots + I_{10}^2)]}$$

Operating duty tests are performed according to standard specification unless the duty is marked on the rating plate of the breaker. The tests according to specifications are:

(*i*) B—3′—B—3′—B at 10% of rated symmetrical breaking capacity;

(*ii*) B—3′—B—3′—B at 30% of rated symmetrical breaking capacity;

(*iii*) B—3′—B—3′—B at 60% of rated symmetrical breaking capacity;

(*iv*) B—3′—MB—3′—MB at not less than 100% of rated symmetrical breaking capacity and not less than 100% of rated making capacity. Test duty (*iv*) may be performed as two separate duties as follows:

(*a*) M—3′—M (Make test);

(*b*) B—3′—B—3′—B (Break test)

(*v*) B—3′—B—3′—B at not less than 100% rated asymmetrical breaking capacity.

Here B and M represent breaking and making operations respectively. MB denotes the making operation followed by breaking operation without any international time-lag.3′ denotes the time in minutes between successive operations of an operating duty.

5.7 TEST VOLTAGE

For different transmission voltages, the test voltages required are given in the following Tables:

Table 5.2

Test voltages for a.c. equipments

System nominal voltage (rms)	*Power frequency withstand voltage (rms)*	*Impulse withstand voltage*	*Switching surge withstand voltage*
400	520	1425	875
525	670	1800	1100
765	960	2300	1350
1100	1416	2800	1800
1500	1920	3500	2200

Table 5.3

Test voltages for d.c. equipments

Normal voltage	*D.C. withstand voltage kV*	*Impulse withstand voltage kV*	*Switching surge withstand voltage kV*
± 400 KV	800	1350	1000
± 600 KV	1200	1900	1500
± 800 KV	1600	2300	2000

Table 5.4

Test voltages required for different system voltage (a.c. system)

Nominal voltage KV (rms)	*Power frequency voltage kV (rms)*	*Impulse withstand voltage kV*	*Switching surge voltage kV*
400	800	2400	1150
765	1000	3000	1750
1100	1400	3700	2300
1500	1900	4600	2800

If the insulation requirements for a particular operating voltage are required to be studied in a research and development laboratory, the voltage levels required in the laboratory are given in Tables 5.4 and 5.5.

Table 5.5

Test voltages required for different d.c. system voltages

Nominal voltage kV	*D.C. voltage kV*	*Impulse withstand voltage kV*	*Switching surge voltage kV*
± 400	800	1750	1300
± 600	1200	2500	2000
± 800	1600	3000	2600

Table 5.6 shows approximate dimension of the testing equipment and the equipment to be tested.

Table 5.6

Approximate dimensions of the testing equipment and the equipment to be tested

Nominal voltage of the equipment kV (rms)	*A.C. transformer height (m)*	*Impulse generator height (m)*	*Dimension of Test-object*
400	10	6	7 × 2 × 11
765	15	8	11 × 2 × 17
1100	18	12	17 × 2 × 24
1500	22	15	28 × 2 × 38

Table 5.7 shows some of the very important high voltage laboratories in the world.

Table 5.7

High voltage laboratories in the world

Location	*Dimension*	*Power frequency Test Voltage MV*	*Impulse Test Voltage MV*	*Switching Surge Voltage MV*
Australia		1.5	8.0	–
Bharat Heavy Elect. Bhopal, India	67 × 35 × 35	1.5	3.6	2.0
CESI-Milan, Italy	150 × 75 × 55	2.3	4.8 (200 KJ)	3.0
College of Engineering, Guindy, Madras	25 × 15 × 15	0.3	1.2	–
College of Engineering, Jabalpur (MP)	33 × 26 × 30	0.5	1.4 (16 KJ)	–
College of Engineering, Kakinada, AP	20 × 12 × 8	0.5	1.4 (16 KJ)	–

Electricity DC, France	65 × 65 × 45	2.5	7.2 (1010 KJ)	6.0
Hydro-Quebec Montreal, Canada	82 × 68 × 50	2.5	6.4 (400 KJ)	6.0
Indian Instt. of Science, Bangalore	37.5 × 25 × 19	1.05	3.0 (50 KJ)	1.6
Indian Instt. of Technology, Madras	28 × 10 × 9.7	0.80	1.5 (36 KJ)	–
Russia	115 × 80 × 60	3.0	8.0	–
Technical University Darmstadt, W. Germany	32 × 25 × 21	1.2	3.2	–
Technical University Munich, W. Germany	34 × 23 × 19	1.2	3.0	–

PROBLEMS

5.1. Explain the procedure for testing string insulator.
5.2. Describe the arrangement of insulators for performing various tests.
5.3. List out various tests to be carried out on insulator and give a brief account of each test.
5.4. Write a short note on the cable sample preparation before it is subjected to various tests.
5.5. List out various tests to be carried out on a cable and give a brief account of each test.
5.6. Explain briefly various tests to be carried out on a bushing.
5.7. Explain the function of discharge device used in a power capacitor and explain the test for efficacy of this device.
5.8. Explain the procedure for performing (*i*) IR test (*ii*) Stability test and (*iii*) Partial discharge test.
5.9. Explain briefly impulse testing of power transformer.
5.10. Describe various tests to be carried out on C.B.

6 Nondestructive Insulation Test Techniques

All electrical appliances are insulated with gaseous or liquid or solid or a suitable combination of these materials. The insulation is provided between live parts or between live part and grounded part of the appliance. The materials may be subjected to varying degrees of voltages, temperatures and frequencies and it is expected of these materials to work satisfactorily over these ranges which may occur occasionally in the system. The dielectric losses must be low and the insulation resistance high in order to prevent thermal breakdown of these materials. The void formation within the insulating materials must be avoided as these deteriorate the dielectric materials.

When an insulating material is subjected to a voltage for investigation, it is usually not possible to draw conclusion regarding the cause of breakdown from the knowledge of the breakdown voltage particularly in solid materials. Earlier, the quality of insulation was judged, mainly by the insulation resistance and its dielectric strength. However, these days high voltage equipments and installations are subjected to various tests. These tests should also yield information regarding the life expectancy and the long term stability of the insulating materials.

One of the possible testing procedure is to over-stress insulation with high a.c. and/ or d.c. or surge voltages. However, the disadvantage of the technique is that during the process of testing the equipment may be damaged if the insulation is faulty. For this reason, following non-destructive testing methods that permit early detection for insulation faults are used:

(*i*) Measurement of the insulation resistance under d.c. voltages.

(*ii*) Determination of loss factor tan δ and the capacitance C.

(*iii*) Measurement of partial discharges.

6.1 LOSS IN A DIELECTRIC

An ideal dielectric is loss-free and if its relative permittivity is ε_r, its permittivity is given by

$$\varepsilon = \varepsilon_0 \varepsilon_r$$

and ε also known as the dielectric constant is a real number. A real dielectric is always associated with loss. The following are the mechanisms which lead to the loss:

(*i*) Conduction loss P_c by ionic or electronic conduction. The dielectric, has σ as conductivity.

(*ii*) Polarization loss P_p by orientation boundary layer or deformation polarization.

(*iii*) Ionisation loss P_i by partial discharges internal or external zones.

Fig. 6.1 shows an equivalent circuit of a dielectric with loss due to conduction, polarization and partial discharges. An ideal dielectric can be represented by a pure capacitor C_1, conduction losses can be taken into account by a resistor R_0 (σ) in parallel. Polarization losses produce a real component of the displacement current which is simulated by resistor R_1. Pulse partial discharges are simulated by right hand branch. C_3 is the capacitance of the void and S is the spark gap which fires during *PD* discharge and the repeated recharging of C_3 is effected either by a resistor R_2 or a capacitor C_2.

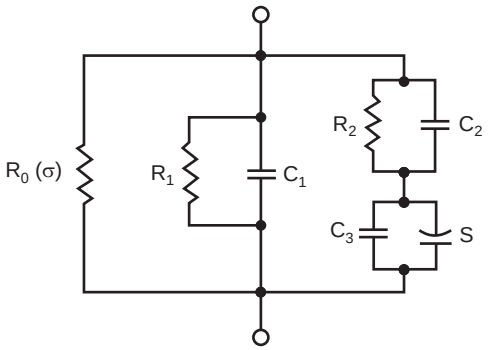

Fig. 6.1 Equivalent circuit of a dielectric

6.2 MEASUREMENT OF RESISTIVITY

When a dielectric is subjected to a steady state static electric field E the current density J_c is given by

$$J_c = \sigma E$$

Assuming a cuboid of the insulating material with thickness d and area A, then

Current $I = J_c A$ and power loss $= VI$

$$= VJ_c A = V \sigma EA = V\sigma \frac{V}{d} A.\frac{d}{d} = \frac{V}{d} \sigma \frac{V}{d} A.d = \sigma E^2 . \text{ Volume.}$$

Therefore, specific dielectric loss = σE^2 Watts/m^3.

The conductivity of the insulating materials viz liquid and solid depends upon the temperature and the moisture contents. The leakage resistance R_0 (σ) of an insulating material is determined by measuring the current when a constant d.c. voltage is applied. Since the current is a function of time as different mechanisms are operating simultaneously. So to measure only the conduction current it is better to measure the current about 1 min after the voltage is switched on. For simple geometries of the specimen (cuboid or cube) specific resistivity ($p = 1/\sigma$) can be calculated from the leakage resistance measured. If I is the conduction current measure and V the voltage applied, the leakage resistance is given by

$$R = \frac{V}{I} = \rho \frac{d}{A}$$

where d is the thickness of the specimen and A is the area of section.

Fig. 6.2. shows a simple arrangement for measurement of resistivity of the insulating material. The d.c. voltage of 100 volt or 1000 volt is applied between electrode 1 and the earth. The measuring electrode 2 is earthed through a sensitive ammeter. The third electrode known as guard ring electrode surrounds the measuring electrode and is directly connected to ground so as to eliminate boundary field effects and surface currents. The width of the guard electrode should be at least twice the thickness of the specimen and the unguarded electrode (1) must extend to the outer edge of the guard electrode. The

gap between electrode 2 and 3 should be as small as possible. A thin metallic foil usually of aluminium or lead of about 20 μm thickness is placed between the electrodes and specimen for better contact. The specific conductivity for most of the insulating material lies in the range of 10^{-16} to 10^{-10} S/cm, which gives currents to be measured of these speciemen to be of the order of picoampers or nanoamperes.

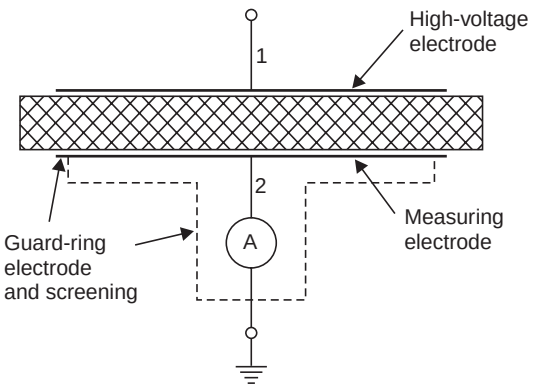

Fig. 6.2 Electrode arrangement to measure the specific resistivity of an insulation specimen

The measuring leads should be appropriately and carefully screened. The measurement of conduction current using d.c. voltage not only provides information regarding specific resistivity of the material but it gives an idea of health of the insulating material. If conduction currents are large, the insulating properties of the material are lost. This method, therefore, has proved very good in the insulation control of large electrical machines during their period of operation.

6.3 MEASUREMENT OF DIELECTRIC CONSTANT AND LOSS FACTOR

Dielectric loss and equivalent circuit

In case of time varying electric fields, the current density J_c using Amperes law is given by

$$J_c = \sigma E + \frac{\partial D}{\partial t} = \sigma E + \varepsilon \frac{\partial E}{\partial t}$$

For harmonically varying fields

$$E = E_m e^{j\omega t}$$

$$\frac{\partial E}{\partial t} = jE_m \omega e^{j\omega t} = j\,\omega\, E$$

Therefore,

$$J_c = \sigma E + j\,\omega\,\varepsilon\, E$$
$$= (\sigma + j\,\omega\,\varepsilon)E$$

In general, in addition to conduction losses, ionization and polarization losses also occur and, therefore, the dielectric constant $\varepsilon = \varepsilon_0\,\varepsilon_r$ is no longer a real quantity rather it is a

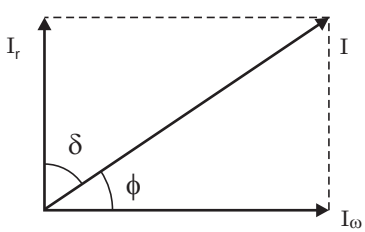

Fig. 6.3 Phasor diagram for a real dielectric material

complex quantity. By definition, the dissipation factor tan δ is the ratio of real component of current I_ω to the reactive component I_r (Fig. 6.3).

$$\tan \delta = \frac{I_\omega}{I_r} = \frac{p_{\text{did}}}{P_r}$$

Here δ is the angle between the reactive component of current and the total current flowing through the dielectric at fundamental frequency. When δ is very small tan δ = δ when δ is expressed in radians and tan δ = sin δ = sin (90 – ϕ) = cos ϕ *i.e.*, tan δ then equals the power factor of the dielectric material.

As mentioned earlier, the dielectric loss consists of three components corresponding to the three loss mechanism.

$$P_{\text{diel}} = P_c + P_p + P_i$$

and for each of these an individual dissipation factor can be given such that

$$\tan \delta = \tan \delta_c + \tan \delta_p + \tan \delta_i$$

If only conduction losses occur then

$$P_{\text{diel}} = P_c = \sigma E^2 Ad = V^2 \omega C \tan \delta = \frac{V^2 \omega \varepsilon_0 \varepsilon_r A}{d} \tan \delta$$

or
$$\sigma E^2 = \frac{V^2}{d^2} \omega \varepsilon_0 \varepsilon_r \tan \delta = E^2 \omega \varepsilon_0 \varepsilon_r \tan \delta$$

or
$$\tan \delta = \frac{\sigma}{\omega \varepsilon_0 \varepsilon_r}$$

This shows that the dissipation factor due to conduction loss alone is inversely proportional to the frequency and can, therefore, be neglected at higher frequencies. However, for supply frequency each loss component will have considerable magnitude.

In order to include all losses, it is customary to refer the existence of a loss current in addition to the charging current by introducing complex permittivity.

$$\varepsilon^* = \varepsilon' - j\, \varepsilon''$$

and the total current I is expressed as

$$I = (j\, \omega \varepsilon' + \omega \varepsilon'') \frac{C_0}{\varepsilon_0} V$$

where C_0 is the capacitance without dielectric material.

or
$$I = j\, \omega\, C_0\, \varepsilon_r^* \,.\, V$$

where
$$\varepsilon_r^* = \frac{(\varepsilon' - j\, \varepsilon'')}{\varepsilon_0} = \varepsilon'_r - j\, \varepsilon_r''$$

ε_r^* is called the complex relative permittivity or complex dielectric constant, ε' and ε_r' are called the permittivity and relative permittivity and ε'' and ε_r'' are called the loss factor and relative loss factor respectively.

The loss tangent

$$\tan \delta = \frac{\varepsilon''}{\varepsilon'} = \frac{\varepsilon_r''}{\varepsilon_r'}$$

The product of the angular frequency and ε'' is equivalent to the dielectric conductivity σ'' *i.e.*, $\sigma'' = \omega\varepsilon''$.

The dielectric conductivity takes into account all the three power dissipative processes including the one which is frequency dependent. Fig. 6.4 shows two equivalent circuits representing the electrical behaviour of insulating materials under a.c. voltages, losses have been simulated by resistances.

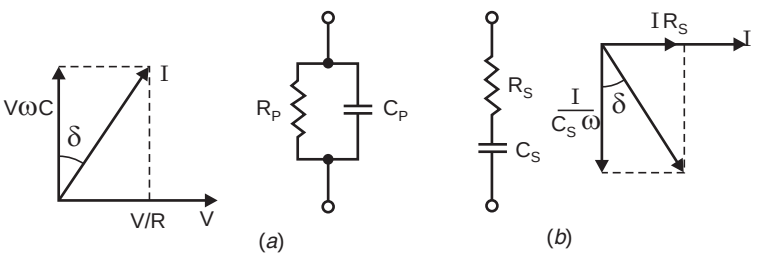

Fig. 6.4 Equivalent circuits for an insulating material

Normally the angle between *V* and the total current in a pure capacitor is 90°. Due to losses, this angle is less than 90°. Therefore, δ is the angle by which the voltage and charging current fall short of the 90° displacement.

For the parallel circuit the dissipation factor is given by

$$\tan \delta = \frac{1}{\omega C_p R_p}$$

and for the series circuit

$$\tan \delta = \omega C_s R_s$$

For a fixed frequency, both the equivalents hold good and one can be obtained from the other. However, the frequency dependence is just the opposite in the two cases and this shows the limited validity of these equivalent circuits.

The information obtained from the measurement of tan δ and complex permittivity is an indication of the quality of the insulating material.

(*i*) If tan δ varies and changes abruptly with the application of high voltage, it shows inception of internal partial discharge.

(*ii*) The effect to frequency on the dielectric properties can be studied and the band of frequencies where dispersion occurs *i.e.*, where that permittivity reduces with rise in frequency can be obtained.

6.4 HIGH VOLTAGE SCHERING BRIDGE

The bridge is widely used for capacity and dielectric loss measurement of all kinds of capacitances, for instance cables, insulators and liquid insulating materials. We know that most of the high voltage equipments have low capacitance and low loss factor. Typical values of these equipments are given in Chapter 3. This bridge is then more suitable for measurement of such small capacitance equipments as the bridge uses either high voltage or high frequency supply. If measurements for such low capacity equipments is carried out at low voltage, the results so obtained are not accurate.

Fig. 6.5 shows a high voltage schering bridge where the specimen has been represented by a parallel combination of R_p and C_p.

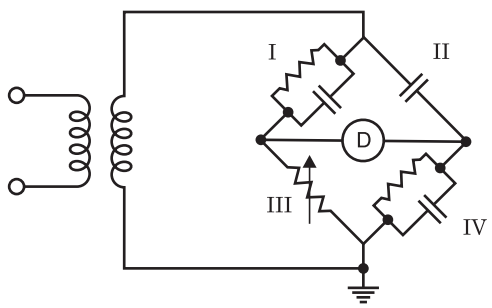

Fig. 6.5 Basic high voltage schering bridge

The special features of the bridge are:

1. High voltage supply, consists of a high voltage transformer with regulation, protective circuitry and special screening. The input voltage is 220 volt and output continuously variable between 0 and 10 kV. The maximum current is 100 mA and it is of 1 kVA capacity.
2. Screened standard capacitor C_s of 100 $pF \pm 5\%$, 10 kV max and dissipation factor tan $\delta = 10^{-5}$. It is a gas-filled capacitor having negligible loss factor over a wide range of frequency.
3. The impedances of arms I and II are very large and, therefore, current drawn by these arms is small from the source and a sensitive detector is required for obtaining balance. Also, since the impedance of arm I and II are very large as compared to III and IV, the detector and the impedances in arm III and IV are at a potential of only a few volts (10 to 20 volts) above earth even when the supply voltage is 10 kV, except of course, in case of breakdown of one of the capacitors of arm I or II in which case the potential will be that of supply voltage. Spark gaps are, therefore, provided to spark over whenever the voltage across arm III or IV exceeds 100 volt so as to provide personnel safety and safety for the null detector.
4. *Null Detector:* An oscilloscope is used as a null detector. The γ–plates are supplied with the bridge voltage V_{ab} and the *x*-plates with the supply voltage *V*. If V_{ab} has phase difference with respect to *V*, an ellipse will appear on the screen (Fig. 6.6). However, if magnitude balance is not reached, an inclined straight line will be observed on the screen. The information about the phase is obtained from the area of the eclipse and the one about the magnitude from the inclination angle. Fig. 6.6*a* shows that both magnitude and phase are balanced and this represents the null point condition. Fig. (6.6*c*) and (*d*) shows that only phase and amplitude respectively are balanced.

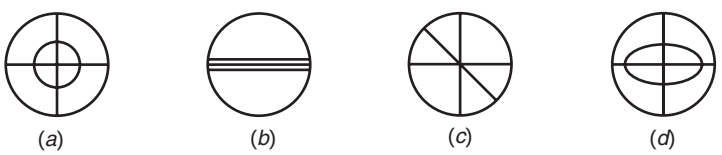

Fig. 6.6 Indications on null detector

The handling of bridge keys allows to meet directly both the phase and the magnitude conditions in a single attempt. A time consuming iterative procedure being used earlier is thus avoided and also with this a very high order of accuracy in the measurement is achieved. The high accuracy is obtained as these null oscilloscopes are equipped with a γ – amplifier of automatically controlled gain. If the impedances are far away from the balance point, the whole screen is used. For nearly obtained balance, it is still almost fully used. As V_{ab} becomes smaller, by approaching the balance point, the gain increases automatically only for deviations very close to balance, the ellipse area shrinks to a horizontal line.

5. *Automatic Guard Potential Regulator:* While measuring capacitance and loss factors using a.c. bridges, the detrimental stray capacitances between bridge junctions and the ground adversely affect the measurements and are the source of error. Therefore, arrangements should be made to shield the measuring system so that these stray capacitances are either neutralised, balanced or eliminated by precise and rigorous calculations. Fig. 6.7 shows various stray capacitance associated with High Voltage Schering Bridge.

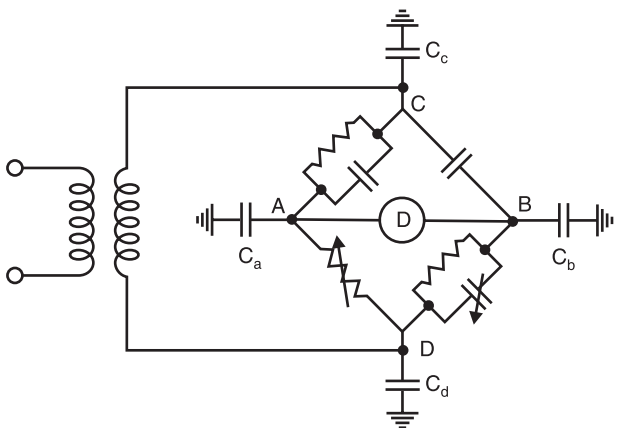

Fig. 6.7 Schering bridge with stray capacitances

C_a, C_b, C_c and C_d are the stray capacitances at the junctions *A*, *B*, *C* and *D* of the bridge. If point *D* is earthed during measurement capacitance C_d is thus eliminated. Since C_c comes across the power supply for earthed bridge, has no influence on the measurement. The effect of other stray capacitances C_a and C_b can be eliminated by use of auxiliary arms, either guard potential regulator or auxiliary branch as suggested by Wagner.

Fig. 6.8 shows the basic principle of Wagner earth to eliminate the effect of stray capacitances C_a and C_b. In this arrangement an additional arm *Z* is connected between the low voltage terminal of the four arm bridge and earth. The stray capacitance *C* between the high voltage terminal of the bridge and the grounded shield and the impedance *Z* together constitute a six arm bridge and a double balancing procedure is required.

Switch *S* is first connected to the bridge point *b* and balance is obtained. At this point *a* and *b* are at the same potential but not necessarily at the ground potential. Switch *S* is now connected to point *C* and by adjusting impedance *Z* balance is again obtained. Under this condition point '*a*' must be at the same potential as earth although it is not permanently at earth potential. Switch *S* is again connected to point *b* and balance is obtained by adjusting bridge parameters. The procedure is repeated till all the three points *a*, *b* and *c* are at the earth potential and thus C_a and C_b are eliminated.

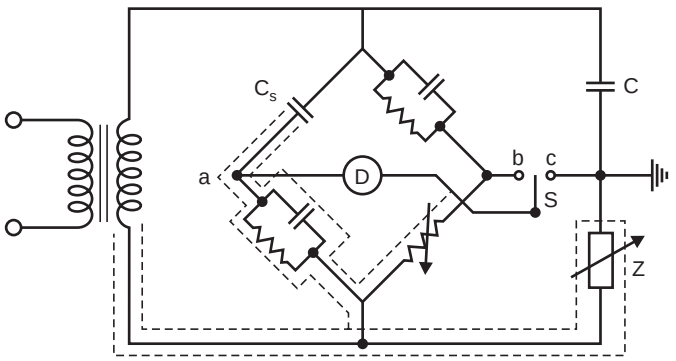

Fig. 6.8 Bridge incorporating Wagner earth

This method is, however, now rarely used. Instead an auxiliary arm using automatic guard potential regulator is used. The basic circuit is shown in Fig. 6.9.

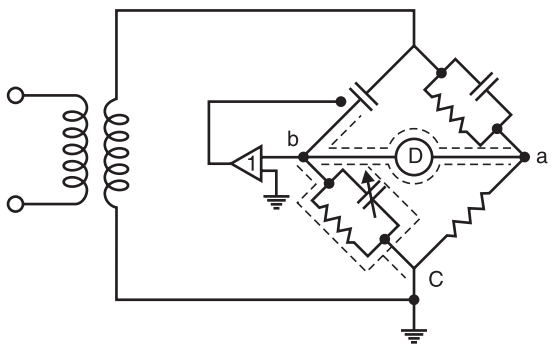

Fig. 6.9 Automatic Wagner earth or automatic guard potential regulator

The guard potential regulator keeps the shield potential at the same value as that of the detector diagonal terminals *a* and *b* for the bridge balance considered. Since potentials of *a*, *b* and shield are held at the same value the stray capacitances are eliminated. During the process of balancing the bridge the points *a* and *b* attain different values of potential in magnitude and phase with respect to ground. As a result, the guard potential regulator should be able to adjust the voltage both in magnitude and phase. This is achieved with a voltage divider arrangement provided with coarse and fine controls, one of them fed with in-phase and the other quadrature component of voltage. The control voltage is then the resultant of both components which can be adjusted either in positive or in negative polarity as desired. The comparison between the shielding potential adjusted by means of the Guard potential regulator and the bridge voltage is made in the null indicator oscilloscope as mentioned earlier. Modifying the potential, it is easy to bring the reading of the null detector to a horizontal straight line which shows a balance between the two voltages both in magnitude and phase.

The automatic guard potential regulator adjusts automatically the guard potential of the bridge making this equal in magnitude and phase to the potential of the point *a* or *b* with respect to ground. The regulator does not use any external source of voltage to achieve this objective. It is rather connected to the bridge corner point between *a* or *b* and *c* and is taken as a reference voltage and this is then transmitted to the guard circuit with unity gain both in magnitude and phase. The shields of the leads to C_s and C_p are not grounded but connected to the output of the regulator which, in fact, is an operational amplifier. The input impedance of the amplifier is more than 1000 Megaohms and the output impedance is less than 0.5 ohm. The high input impedance and very low output impedance of the amplifier does not load the detector and keeps the shield potential at any instant at an artificial ground.

6.4.1 Balancing the Bridge

For ready reference Fig. 6.5 is reproduced here and its phasor diagram under balanced condition is drawn in Fig. 6.10 (*b*)

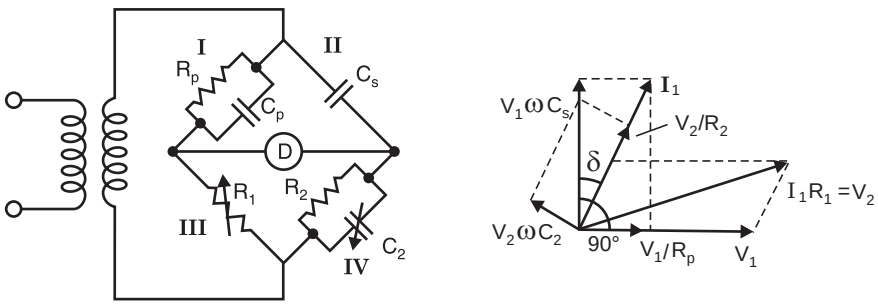

Fig. 6.10 (*a*) Schering bridge (*b*) Phasor diagram

The bridge is balanced by successive variation of R_1 and C_2 until on the oscilloscope (Detector) a horizontal straight line is observed:

At balance $$\frac{Z_I}{Z_{II}} = \frac{Z_{III}}{Z_{IV}}$$

Now $$Z_I = \frac{R_p}{1 + j\,\omega\, C_p R_p}$$

$$Z_{II} = \frac{1}{j\,\omega\, C_s}$$

$$Z_{III} = R_I \text{ and } Z_{IV} = \frac{R_2}{1 + j\,\omega\, C_2 R_2}$$

From balance equation we have

$$\frac{R_p}{R_1\,(1 + i\omega\, C_p R_p)} = \frac{1/j\,\omega\, C_s\,(1 + j\omega\, C_2 R_2)}{R_2}$$

or $$\frac{R_p\,(1 - j\,\omega\, C_p R_p)}{R_1\left(1 + \omega^2 C_p^2 R_p^2\right)} = \frac{1 + j\,\omega\, C_2 R_2}{j\,\omega\, C_s R_2}$$

or $$\frac{R_p}{R_1\left(1 + \omega^2 C_p^2 R_p^2\right)} - \frac{j\,\omega\, C_p R_p^2}{R_1\left(1 + \omega^2 C_p^2 R_p^2\right)} = -\frac{j}{\omega C_s R_2} + \frac{C_2}{C_s}$$

Equating real part, we have

$$\frac{R_p}{R_1\left(1 + \omega^2 C_p^2 R_p^2\right)} = \frac{C_2}{C_s}$$

and equating imaginary part, we have

$$\frac{\omega\, C_p R_p^2}{R_1\left(1 + \omega^2\, C_p^2 R_p^2\right)} = \frac{1}{\omega C_s R_2}$$

Now tan δ from the phasor diagram

$$\tan \delta = \frac{V_1/R_p}{V_1 \omega C_p} = \frac{1}{\omega C_p R_p} = \frac{V_2\ \omega\ C_2}{V_2/R_2} = \omega C_2 R_2$$

Also $$\cos \delta = \frac{V_1 \omega C_p}{V_1 \sqrt{\left(1/R_p^2\right) + \omega^2 C_p^2}}$$

or $$\cos^2 \delta = \frac{\omega^2 C_p^2 R_p^2}{1 + \omega^2 C_p^2 R_p^2}$$

or $$\frac{\omega C_p R_p}{1 + \omega^2 C_p^2 R_p^2} = \cos^2 \delta \,.\, \frac{1}{\omega\ C_p R_p} = \frac{R_1}{\omega\ C_s R_2 R_p}$$

or $$C_p = \cos^2 \delta\ C_s \frac{R_2}{R_1}$$

Since δ is usually very small cos δ = 1

Therefore $$C_p \approx C_s \frac{R_2}{R_1}$$

and $$\tan \delta_p = \omega\ C_2 R_2$$

and since $$\frac{1}{\omega\ C_p R_p} = \omega\ C_2 R_2$$

or $$\omega^2 C_p R_p C_2 R_2 = 1$$

or $$R_p = \frac{1}{\omega^2 R_2 C_2 C_p} \approx \frac{R_1}{\omega^2 R_2 C_2 C_s R_2} \approx \frac{R_1}{\omega^2 C_2 C_s R_2^2}$$

If, however, the specimen is replaced by *a* series equivalent circuit, then at balance

$$Z_I = R_s - \frac{j}{\omega C_s}$$

and the equation becomes

$$\frac{R_s - j/\omega C_s}{R_1} = \frac{1 + j\,\omega C_2 R_2}{j\,\omega C_s' R_2}$$

or $$\frac{R_s}{R_1} - \frac{j}{\omega\ C_s R_1} = -\frac{j}{\omega C_s' R_2} + \frac{C_2}{C_s'}$$

Equating real parts, we have

$$\frac{R_s}{R_1} = \frac{C_2}{C_s'}$$

or $$R_s = R_1 \frac{C_2}{C_s'}$$

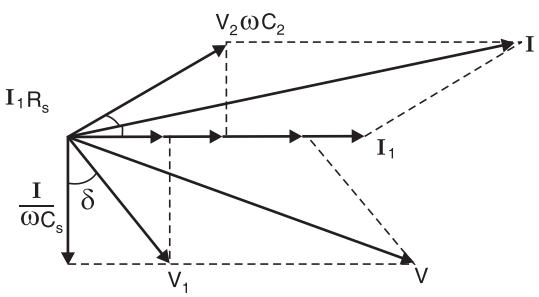

Fig. 6.11 Phasor diagram of S.B. for series equivalent of specimen

Similarly equating imaginary part, we have

$$\omega C_s R_1 = \omega C_s' R_2$$

or

$$C_s = C_s' \frac{R_2}{R_1}$$

To find out tan δ, we draw the phasor diagram of the bridge circuit (Fig. 6.11).

$$\tan \delta_s = \frac{I_1 R_s}{I_1/\omega C_s} = \omega C_s R_s$$

6.5 MEASUREMENT OF LARGE CAPACITANCE

In order to measure a large capacitance, the resistance R_1 should be able to carry large value of current and resistance R_1 should be of low value. To achieve this, a shunt of S ohm is connected across R_1 as shown in Fig. 6.12. It is desirable to connect a fixed resistance R in series with variable resistance R_1 so as to protect R_1 from excessive current, should it accidentally be set to a very low value.

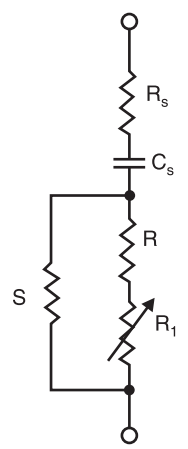

Fig. 6.12 Shunt arrangement for measurement of large capacitance

We know that under balanced condition for series equivalent representation of specimen

$$C_s = C_s' \frac{R_2}{R_1}$$

But here R_1 is to be replaced by the equivalent of $(R + R_1) \parallel S$.

or

$$\frac{(R + R_1) S}{R + R_1 + S}$$

or

$$\frac{1}{R_{eq}} = \frac{R + R_1 + S}{(R + R_1) S}$$

Therefore,

$$C_s = C_s' R_2 \cdot \frac{R + R_1 + S}{(R + R_1) S} \cdot \frac{R_1}{R_1} = C_s' \frac{R_2}{R_1} \cdot \frac{R_1 (R + R_1 + S)}{(R + R_1) S}$$

usually $R << R_1$

Therefore

$$C_s = C_s' \frac{R_2}{R_1} \frac{R_1 (R + R_1 + S)}{R_1 S} = C_s' \frac{R_2}{R_1} \left[\frac{R}{S} + \frac{R_1}{S} + 1 \right]$$

and

$$\tan \delta = \omega C_s' R_2 . R/R_1$$

If circuit elements of Schering bridge are suitably designed, the bridge principle can be used upto to 100 kHz of frequency. However, common schering bridge can be used upto about 10 kHz only.

6.6 SCHERING BRIDGE METHOD FOR GROUNDED TEST SPECIMEN

A dielectric material which is to be tested, one side of this is usually grounded *e.g.* underground cables or bushings with flanges grounded to the tank of a transformer etc. There are two well known methods

used for such measurement. One is the inversion of a Schering bridge shown in Fig. 6.13 with the operator, ratio arms and null detector inside a Faraday Cage at high potential. The system requires the cage to be insulated for the full test voltage and with suitable design may be used upto maximum voltage available. However, there are difficulties in inverting physically the standard capacitor and it becomes necessary to mount it on a platform insulated for full voltage.

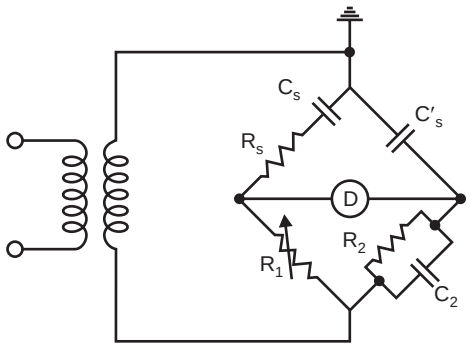

Fig. 6.13 Inverted Schering bridge

Second method requires grounding of detector as shown in Fig. 6.14. In this arrangement, stray capacitances of the high voltage terminal C_q and of the source, leads etc. come in parallel with the test object. Hence, balancing is carried out in two steps: First step: The test specimen is disconnected and the capacitance C_q and loss factor tan δ_q are measured. Second step: The test object is connected in the bridge and new balance is obtained. The second balance gives net capacitance of the parallel combination *i.e.*,

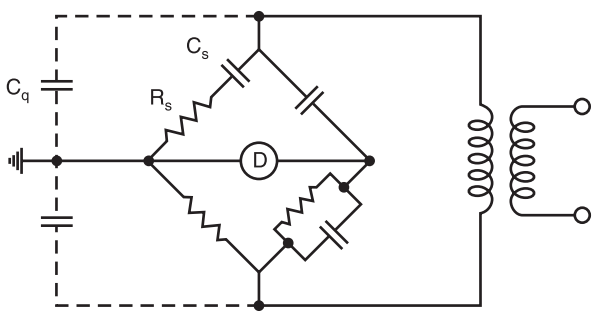

Fig. 6.14 Grounded specimen

$$C_s' = C_s + C_q$$

and
$$\tan \delta_q' = \frac{C_s \tan \delta_s + C_q \tan \delta_q}{C_s + C_q}$$

Hence the capacitance and loss factor of the specimen are

$$C_s = C_s'' - C_q$$

and
$$\tan \delta_s = \frac{C_s'' \tan \delta'' - C_q \tan \delta_q}{C_s}$$

If the stray capacitances are large as compared to the capacitance of the specimen, the accuracy of measurement is poor.

6.7 SCHERING BRIDGE FOR MEASUREMENT OF HIGH LOSS FACTOR

If the loss factor tan δ of a specimen is large, the bridge arm containing resistance R_2 is modified. Resistance R_2 is made as a slide wire alongwith a decade resistor and a fixed capacitance C_2 is connected across the resistance R_2 as shown in Fig. 6.15 (*a*). This modification can be used for test specimen having loss factor of the order of 1.0. If it is more than one and upto 10 or greater C_2, R_2 arm is not made a parallel combination, rather it is made a series combination as shown in Fig. 6.15 (*b*) Here, of course R_2 is made variable.

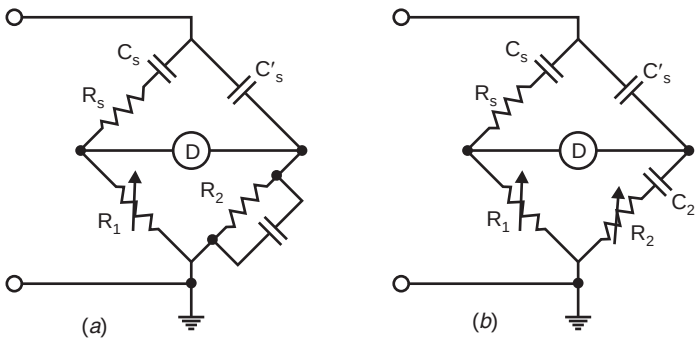

Fig. 6.15 Schering bridges for large loss factor

6.8 TRANSFORMER RATIO ARM BRIDGE

For measurement of various parameters like resistance, inductance, capacitance, usually four arm bridges are used. For high frequency measurements, the arm with high resistances leads to difficulties due to their residual inductance, capacitance and skin effect. Also if length of the leads is large, shielding is difficult. Hence at high frequencies the transformer ratio arm bridge which eliminates at least two arms, are preferred. These bridges provide more accurate results for small capacitance measurements. There are two types of transformer ratio arm bridges (*i*) Voltage ratio; (*ii*) Current ratio. The voltage ratio type is used for high frequency low voltage application. Fig. 6.16 shows schematic diagram of a voltage ratio arm bridge. Assuming ideal transformer, under balance condition:

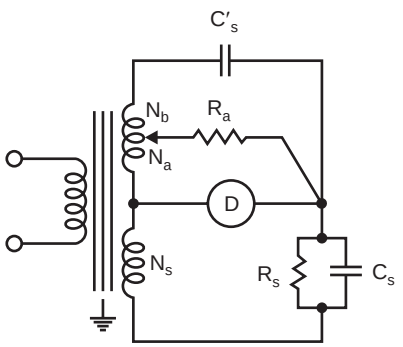

Fig. 6.16 Transformer voltage ratio arm bridge

$$\frac{V_b}{V_s} = \frac{N_b}{N_s} = \frac{C_s}{C_s'} \text{ and } \frac{R_s}{R_a} = \frac{N_s}{N_a}$$

However, in practical situation due to the presence of magnetising current and the load currents, the voltage ratio slightly differs from the turns ratio and therefore, the method involves certain errors. The errors are classified as ratio error and load error which can be calculated before hand for a transformer. A typical bridge has a useful range from a fraction of a *pF* to about 100 μ*F* and is accurate over a wide range of frequency from 100 Hz to 100 kHz, the accuracy being better than ± 0.5%.

The current ratio arm bridge is used for high voltage low frequency applications. The main advantage of the method is that the test specimen is subjected to full system voltage. Fig. 6.17 shows schematic diagram of the bridge. The main component of the bridge is a three winding current transformer with very low losses and leakage (core of high permeability). The transformer is carefully shielded against stray magnetic fields and protected against mechanical vibrations.

The main feature of the arrangement is that under balance condition, there is no net *mmf* across the windings 1 and 2. Also the stray capacitances between the windings and the screened low voltage leads does not enter in the balance expression as there is no voltage developed between them. This feature makes this bridge possible to use long leads without using Wagner's earth. The sensitivity of the bridge is higher than that of the Schering bridge. The balance is obtained by varying N_1, N_2 and R.

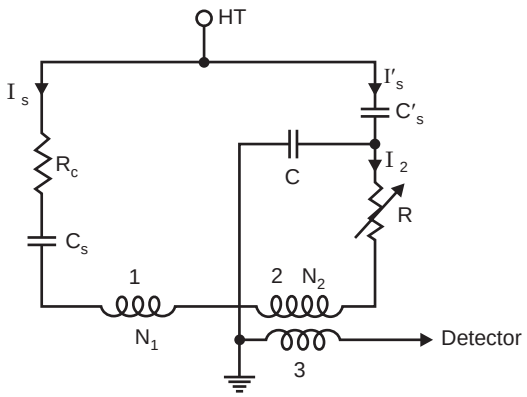

Fig. 6.17 Transformer current ratio arm bridge

Under balance condition, the voltage across the detector coil is zero and

$$I_s N_1 = I_2 N_2$$

Voltage across the *R*-*C* arm is

$$V = \frac{I_s' R}{1 + j\omega CR}$$

Current I_2 through coil 2 is

$$I_2 = \frac{I_s' \dfrac{1}{j\,\omega C}}{R + \dfrac{1}{j\,\omega c}} = \frac{I_s'}{1 + J\omega CR}$$

Now total impedance of the branch consisting of C_s' and R and C.

$$Z = \left[\frac{1}{j\,\omega C_s'} + \frac{R}{1 + j\omega\, CR}\right]$$

Therefore, if unity voltage is applied, the current through this branch.

$$I_s' = \frac{1}{\dfrac{1}{j\,\omega C_s'} + \dfrac{R}{1 + j\,\omega CR}} = \frac{j\,\omega C_s'(1 + j\,\omega CR)}{1 + j\,\omega CR + j\,\omega C_s' R}$$

or
$$I_2 = \frac{j\,\omega C_s'(1 + j\,\omega CR)}{1 + j\,\omega R(C + C_s')} \cdot \frac{1}{1 + j\,\omega CR} = \frac{j\,\omega C_s'}{1 + j\,\omega R(C + C_s')}$$

Now again with unity voltage

$$I_s = \frac{1}{R_s + \dfrac{1}{j\,\omega C}} = \frac{j\,\omega C_s'}{1 + j\,\omega C_s R_s}$$

$$\frac{I_s}{I_2} = \frac{[1 + j\,\omega R(C + C_s')]C_s}{(1 + j\,\omega C_s R_s)C_s'} = \frac{N_2}{N_1}$$

Therefore, $$\frac{C_s}{C_s'} = \frac{N_2}{N_1}$$

or $$C_s = C_s' \frac{N_2}{N_1}$$

and $$\tan \delta_s = \omega R (C_s' + C)$$

6.9 PARTIAL DISCHARGES

Partial discharge is defined as localised discharge process in which the distance between two electrodes is only partially bridged *i.e.,* the insulation between the electrodes is partially punctured. Partial discharges may originate directly at one of the electrodes or occur in a cavity in the dielectric. Some of the typical partial discharges are: (*i*) Corona or gas discharge. These occur due to non-uniform field on sharp edges of the conductor subjected to high voltage especially when the insulation provided is air or gas or liquid Fig. 6.18 (*a*). (*ii*) Surface discharges and discharges in laminated materials on the interfaces of different dielectric material such as gas/solid interface as gas gets over stressed ε_r times the stress on the solid material (where ε_r is the relative permittivity of solid material) and ionization of gas results Fig. 6.18 (*b*) and (*c*). (*iii*) Cavity discharges: When cavities are formed in solid or liquid insulating materials the gas in the cavity is over stressed and discharges are formed Fig. 6.18 (*d*) (*iv*). Treeing Channels: High intensity fields are produced in an insulating material at its sharp edges and this deteriorates the insulating material. The continuous partial discharges so produced are known as Treeing Channels Fig. 6.18 (*e*).

External Partial Discharge

External partial discharge is the process which occurs external to the equipment e.g. on overhead lines, on armature etc.

Internal Partial Discharge

Internal paratial discharge is a process of electrical discharge which occurs inside a closed system (discharge in voids, treeing etc). This kind of classification is essential for the PD measuring system as external discharges can be nicely distinguished from internal discharges. Partial discharge measurement have been used to assess the life expectancy of insulating materials. Even though there is no well defined relationship, yet it gives sufficient idea of the insulating properties of the material. Partial discharges on insulation can be measured not only by electrical methods but by optical, acoustic and chemical method also. The measuring principles are based on energy conversion process associated with electrical discharges such as emission of electromagnetic waves, light, noise or formation of chemical compounds. The oldest and simplest but less sensitive is the method of listening to hissing sound coming out of partial discharge. A high value of loss factor tan δ is an indication of occurrence of partial discharge in the material. This is also not a reliable measurement as the additional losses generated due to application of high voltage are localised and can be very small in comparison to the volume losses resulting from polarization process. Optical methods are used only for those materials which are transparent and thus not applicable for all materials. Acoustic detection methods using ultrasonic transducers have, however, been used with some success. The most modern and the most accurate methods are the electrical methods. The main objective here is to separate impulse currents associated with PD from any other phenomenon.

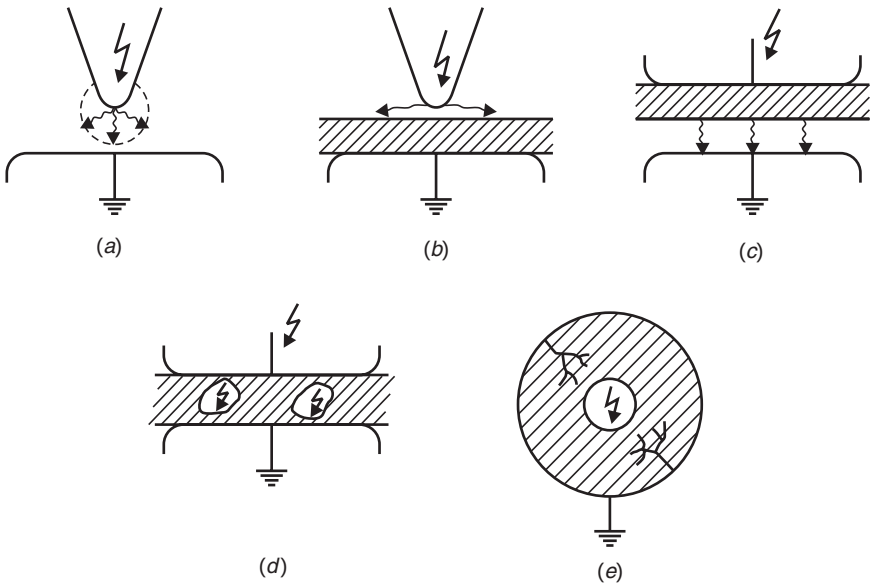

Fig. 6.18 Various partial discharges

6.9.1 The Partial Discharge Equivalent Circuit

If there are any partial discharges in a dielectric material, these can be measured only across its terminal. Fig. 6.19 shows a simple capacitor arrangement in which a gas filled void is present. The partial discharge in the void will take place as the electric stress in the void is ε_r times the stress in the rest of the material where ε_r is the relative permittivity of the material. Due to geometry of the material, various capacitances are formed as shown in Fig. 6.19 (*a*). Flux lines starting from electrode and terminating at the void will form one capacitance C_{b1} and similarly C_{b2} between electrode *B* and the cavity. C_c is the capacitance of the void. Similarly C_{a1} and C_{a2} are the capacitance of healthy portions of the dielectric on the two sides of the void. Fig. 6.19 (*b*) shows the equivalent of 6.19 (*a*) where $C_a = C_{a1} + C_{a2}$, and $C_b = C_{b1}C_{b2}/(C_{b1} + C_{b2})$ and C_c is the cavity capacitance. In general $C_a >> C_b >> C_c$.

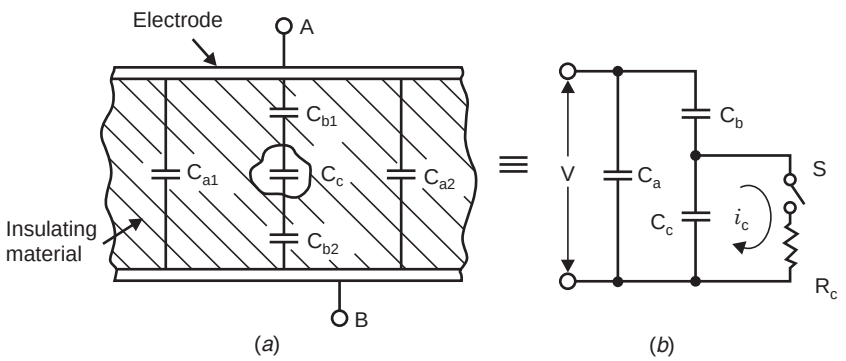

Fig. 6.19. (*a*) Dielectric material with a cavity (*b*) Equivalent circuit

Closing of switch *S* is equivalent to simulating partial discharge in the void as the voltage V_c across the void reaches breakdown voltage. The discharge results into a current $i_c(t)$ to flow. Resistor R_c simulates the finite value of current $i_c(t)$.

Suppose voltage V is applied across the electrode A and B and the sample is charged to this voltage and source is removed. The voltage V_c across the void is sufficient to breakdown the void. It is equivalent to closing switch S in Fig. 6.19 (b). As a result, the current $i_c(t)$ flows which releases a charge $\Delta q_c = \Delta V_c C_c$ which is dispersed in the dielectric material across the capacitance C_b and C_a. Here ΔV_c is the drop in the voltage V_c as a result of discharge. The equivalent circuit during redistribution of charge Δq_c is shown in Fig. 6.20.

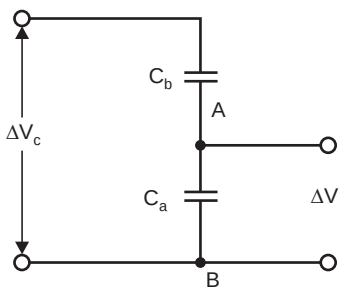

Fig. 6.20 Equivalent of 6.19 (a) after discharge

The voltage as measured across AB will be

$$\Delta V = \frac{C_b}{C_a + C_b} \Delta V_c = \frac{C_b}{C_a + C_b} \frac{\Delta q_c}{C_c}$$

Ordinarily ΔV_c is in kV whereas ΔV is a few volts since the ratio C_b/C_a is of the order of 10^{-4} to 10^{-3}. The voltage drop ΔV even though can be measured but as C_b and C_c are normally not known neither ΔV_c nor Δq_c can be obtained. Also since V is in kV and ΔV is in volts the ratio $\Delta V/V$ is very small $\approx 10^{-3}$, therefore the detection of $\Delta V/V$ is a tedious task.

Suppose, that the test object remains connected to the voltage source Fig. 6.21. Here C_k is the coupling capacitor. Z is the impedance consisting either only of the lead impedance of or lead impedance and PD-free inductor or filter which decouples the coupling capacitor and the test object from the source during discharge period only, when very high frequency current pulse $i_c(t)$ circulate between C_k and C_t. C_t is the total equipment capacitance of the test specimen.

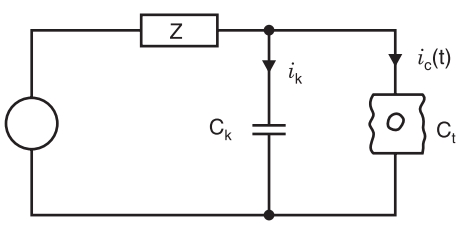

Fig. 6.21

It is to be noted that Z offers high impedance to circular current (impulse currents) and, therefore, these are limited only to C_k and C_t. However, supply frequency displacement currents continue to flow through C_k and C_t and wave shapes of currents through C_k and C_t are shown in Fig. 6.22.

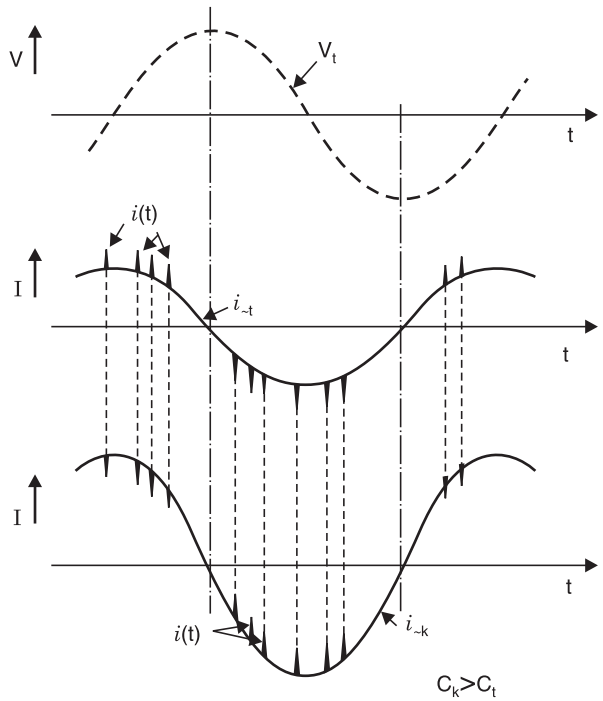

Fig. 6.22 Current wave forms in C_k and C_t.

It is interesting to find that pulse currents in C_k and C_t have exactly same location but opposite polarities and these are of the same magnitude. Therefore, one can say that these pulse currents are not supplied by the source but are due to local partial discharges. The amplitude of pulses depends upon the voltage applied and the number of pulses depends upon the number of voids. The larger the number of faults the higher the number of pulses over a half cycle.

During discharge, the voltage across the test object C_t falls by an amount ΔV and during this period C_k stores the energy and release the charge between C_k and C_t thus compensating the drop ΔV. The equivalent capacitance of the test specimen is $C_t \approx C_a + C_b$ assuming C_c to be negligibly small. If $C_k >> C_t$, the charge transfer is given by

$$q = \int i\,(t)\,dt \approx (C_a + C_b)\,\Delta V$$

Now
$$\Delta V = \frac{C_b}{C_a + C_b}\,\Delta V_c$$

and
$$\Delta V = \frac{q}{C_a + C_b}$$

Therefore,
$$\frac{q}{C_a + C_b} = \frac{C_b}{C_a + C_b}\,\Delta V_c$$

or
$$q = C_b\,\Delta V_C$$

Here q is known as apparent charge as it is not equal to the charge locally involved *i.e.* $C_c\,\Delta V_c$. This charge q is, however, more realistic than calculating ΔV, as q is independent of C_a whereas ΔV depends upon C_a.

In practice the condition $C_k >> C_t$ is never satisfied as the C_k will over load the supply and also it will be uneconomical. However, if C_k is slightly greater than C_t, the sensitivity of measurement is reduced as the compensating current $i_c(t)$ becomes small. If C_t is comparable to C_k and ΔV is the drop in voltage of C_t as a result of discharge, the transfer of charge between C_t and C_k will result into common voltage $\Delta V'$.

$$\Delta V' = \frac{C_t \Delta V + C_k . O}{C_t + C_k} = \frac{C_t \Delta V}{C_t + C_k} = \frac{q}{C_t + C_k}$$

$\Delta V'$ is the net rise in voltage of the parallel combination of C_k and C_t and, therefore, the charge q_m transferred to C_t from C_k will be

$$q_m = C_k \Delta V'$$

The charge q_m is known as measurable charge. The ratio of measurable charge to apparent charge is, therefore, given as

$$\frac{q_m}{q} = \frac{C_k}{C_t + C_k}$$

In order to have high sensitivity of measurements *i.e.*, high q_m/q it is clear that C_k should be large compared to C_t. But we know that there are disadvantages in having large value of C_k. Therefore, this method of measurement of *PD* has limited applications.

The measurement of *PD* current pulses provides important information concerning the discharge processes in a test specimen. The time response of an electric discharge depends mainly on the nature of fault and design of insulating material. The shape of the circular current is an indication of the physical discharge process at the fault location in the test object. The principle of measurement of *PD* current is shown in Fig. 6.23.

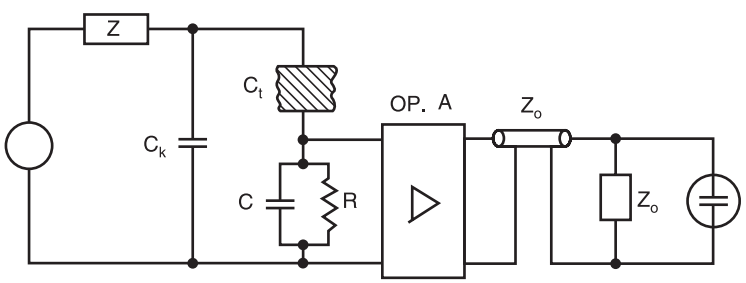

Fig. 6.23 Principle of pulse current measurement

Here C indicates the stray capacitance between the lead of C_t and the earth, the input capacitance of the amplifier and other stray capacitances. The function of the high pass amplifier is to suppress the power frequency displacement current $i_k(t)$ and $I_c(t)$ and to further amplify the short duration current pulses. Thus the delay cable is electrically disconnected from the resistance R. Suppose during a partial discharge a short duration pulse current $\delta(t)$ is produced and results in apparent charge q on C_t which will be redistributed between C_t, C and C_k . The circuit for the same is given in Fig. 6.24.

Potential across C_t $= \dfrac{q}{C_t + \dfrac{CC_k}{C + C_k}}$

Therefore, voltage across C will be

$$v = \frac{q}{C_t + \dfrac{CC_k}{C + C_k}} \cdot \frac{C_k}{C + C_k} = \frac{q}{C_t\,(C + C_k) + CC_k} \cdot C_k$$

$$= \frac{qC_k}{CC_t + C_kC_t + CC_k} = \frac{q}{C + C_t\left(1 + \dfrac{C}{C_k}\right)}$$

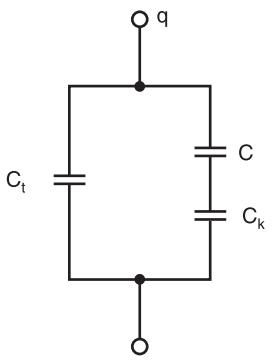

Fig. 6.24 Equivalent of 6.23 after discharge

and because of resistance R the expression for voltage across R will be

$$v(t) = \frac{q}{C + C_t\left(1 + \dfrac{C}{C_k}\right)} e^{-t/\tau}$$

where $$\tau = \left(C + \frac{C_tC_k}{C_t + C_k}\right) R$$

The wave shape of the voltage pulse is shown in Fig. 6.25.

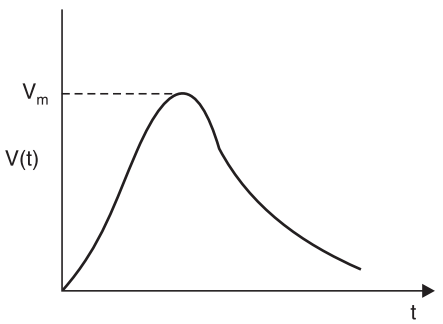

Fig. 6.25 Wave shape of voltage across R

The voltage across the resistance R indicates a fast rise and is followed by an exponential decay with time constant τ. The circuit elements have thus deferred the original current wave shape especially the wave tail side of the wave and therefore, the measurement of the pulse current $i(t)$ is a difficult task.

Also, the PD pulse currents get corrupted due to various interferences present in the system. The power frequency displacement current $i_k(t)$ and $i_t(t)$ are major sources of interference as these currents vary from a few *mA* to several amperes. Higher harmonics in the supply and pulse current in the thyristorized control circuits are always present which will interfere with the *PD* currents. On load taps in a transformer, carbon brushes in a generator are yet other sources of noise in the circuits. Mainly interferences can be classified as follows:–

(*i*) *Pulse shaped noise signals:* These are due to impulse phenomenon similar to *PD* currents.

(*ii*) *Harmonic signals:* These are mainly due to power supply and thyristorised controllers.

We are taking apparent charge as the index level of the partial discharges which is integration of *PD* pulse currents. Therefore, continuous alternating current of any frequency would disturb the integration process of the measuring circuit and hence it is important that these currents (other than *PD*

currents) must be suppressed before the mixture of currents is passed through the integrating circuit. The solution to the problem is obtained by using filter circuits which may be completely independent of integrating circuits.

Fig. 6.26 shows two different ways in which the measuring impedance Z_m can be connected in the circuit.

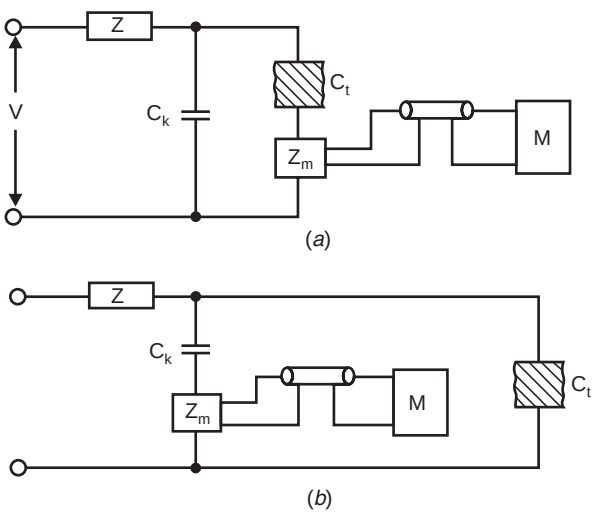

Fig. 6.26

In Fig. 6.26 (*a*) Z_m is connected in series with C_t and provides better sensitivity as the PD currents excited from C_t would be better picked up by measuring circuit Z_m. However, the disadvantage is that in case of puncture of the test specimen the measuring circuit would also be damaged. Specifically for this reason, the second arrangement in which Z_m is connected between the ground terminal of C_k and the ground and is the circuit most commonly used.

As is mentioned earlier, according to international standards the level of partial discharges is judged by quantity of apparent charge measured. The apparent charge is obtained by integration of the circular current $i_c(t)$. This operation is carried out on the PD pulses using 'wide band' and 'narrow band', measuring systems. These are basically band pass filters with amplifying action. If we examine the frequency spectrum of the pulse current, it will be clear why band pass filters are suitable for integrating PD pulse currents.

We know that for a non-periodic pulse current $i(t)$, the complex frequency spectrum of the current is given by Fourier transform as

$$I(j\,\omega) = \int_{-\infty}^{\infty} i(t)\, e^{-j\omega t}\, dt$$

Let $i(t) = I_0 e^{-t/\tau}$ as an approximation to actual PD pulse current

$$I(j\,\omega) = \int_0^{\infty} I_0 e^{-t/\tau} e^{-j\omega t}\, dt = I_0 \int_0^{\infty} e^{-(1/\tau + j\omega)t}\, dt$$

$$= -\frac{I_0}{1/\tau + j\omega}\left[e^{-(1/\tau + j\omega)t}\right]_0^{\infty}$$

$$= -\frac{I_0\tau}{1 + j\omega\tau}[0 - 1] = \frac{I_0\tau}{1 + j\omega\tau}$$

The amplitude $|I(j\omega)| = \dfrac{I_0\tau}{\sqrt{1+\omega^2\tau^2}}$

and phase angle $-\tan^{-1}\dfrac{\omega\tau}{1}$

Fig. 6.27 (*a*) shows the PD current pulse and 6.27 (*b*) shows the amplitude $I(j\omega)$ vs. frequency plot.

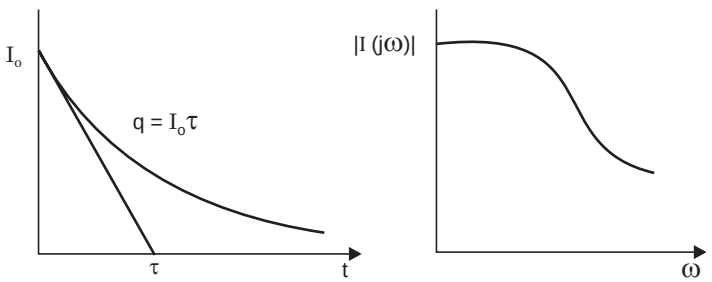

Fig. 6.27 (*a*) PD current pulse (*b*) Frequency spectrum of the pulse current

Here the current is approximated by an exponentially decaying curve and, therefore, neither $i(t)$ nor $I(j\omega)$ vanish and so a new measure of "pulse width" is required. The time constant τ is a measure of the width of $i(t)$, a line tangent to $i(t)$, a line tangent to $i(t)$ at $t = 0$ intersects the line $i = 0$ at $t = \tau$ as shown in Fig. 6.27 (*a*).

From the above expression and Fig. 6.27 (*b*) it is clear that as $\omega \to 0$ $I(j\omega) \to I_0\tau$ which means that the d.c. content of the frequency spectrum equals the apparent charge in the pulse current. Therefore, the frequency spectrum of *PD* pulses current contains complete information concerning the apparent charge in the low frequency range. In order to have proper integration of the pulse current, the time constant τ of the pulse should be greater than the time constant of the measuring circuit or the band width (upper cut off frequency) of the measuring system should be much lower than that of the spectrum of the pulse currents to be measured.

6.9.2 Wide-Band Circuit

Fig. 6.28 shows the principle of wide band circuits.

The coupling impedance Z_m is a parallel combination of R, L and C whose quality factor is low. The complex impedance Z_m is given as

$$\frac{1}{Z_m} = \frac{1}{R} + \frac{1}{j\omega L} + j\omega C$$

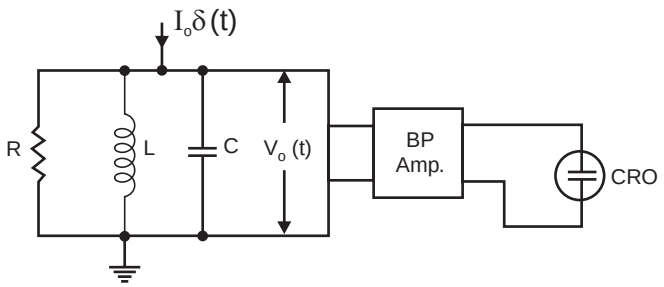

Fig. 6.28 PD measuring circuitc wide band

or
$$Z_m = \frac{j\omega RL}{j\omega L + R - RLC\omega^2} = \frac{R}{1 - j\dfrac{R}{\omega L} + jRC\omega}$$

$$|Z_m| = \frac{R}{\left[1 + \left(\dfrac{R}{\omega L} - RC\omega\right)^2\right]^{1/2}} = \frac{R}{\left[1 + \dfrac{R^2}{\omega^2 L}\left(1 - \dfrac{\omega^2}{\omega_0^2}\right)^2\right]^{1/2}}$$

$$= \frac{R}{\left[1 + R^2\,\dfrac{C}{L}\cdot\dfrac{1}{CL\,\omega^2}\left(1 - \dfrac{\omega^2}{\omega_0^2}\right)^2\right]^{1/2}} = \frac{R}{\left[1 + Q^2\,\dfrac{\omega_0^2}{\omega^2}\,\dfrac{\omega^2}{\omega_0^2}\left(1 - \dfrac{\omega^2}{\omega_0^2}\right)^2\right]^{1/2}}$$

$$= \frac{R}{\left[1 + Q^2\left(\dfrac{\omega_0}{\omega} - \dfrac{\omega}{\omega_0}\right)^2\right]^{1/2}} = \frac{R}{\left[1 + Q^2\left(\dfrac{f_0}{f} - \dfrac{f}{f_0}\right)^2\right]^{1/2}}$$

Where $Q = \dfrac{R}{\sqrt{L/C}}$ and $f_0 = \dfrac{1}{2\pi\sqrt{LC}}$ Where $C = C_s + C_c + \dfrac{C_t C_k}{C_t + C_k}$

C_s is the stray capacitance, C_c the capacitance of the delay cable.

The measuring impedance Z_m is the impedance of a band pass filter which suppresses harmonic currents depending upon the selected circuit quality factor Q, below and above the resonance frequency f_0 *i.e.*, Z_m will suppress all frequency currents below and above its resonance frequency. The alternate is – 20 *dB* per decade if $Q = 1$ and can be greatly increased.

Also, the measuring circuit Z_m performs integration of the PD pulse currents $i(t) = I_0\,\delta(t)$.

The voltage $v_0(t)$ as shown in Fig. 6.28 can be obtained by writing nodal equation

$$\frac{V_0(s)}{R} + \frac{V_0(s)}{sL} + V_0(s)\,Cs = I_0$$

$$V_0(s) = \frac{RsLI_0}{RLCs^2 + sL + R} = \frac{I_0 s/C}{s^2 + \dfrac{s}{RC} + \dfrac{1}{LC}}$$

$$= \frac{I_0 s/C}{\left(s + \frac{1}{2RC}\right)^2 + \frac{1}{LC} - \frac{1}{(4R^2C^2)}} = \frac{I_0 s/C}{(s+\alpha)^2 + \beta^2}$$

where $$\alpha = \frac{1}{2RC} \text{ and } \beta = \sqrt{\frac{1}{LC} - \alpha^2}$$

Therefore, $$V_0(s) = \frac{q}{C} \cdot \left[\frac{s}{(s+\alpha)^2 + \beta^2}\right]$$

$$V_0(s) = \frac{q}{C}\frac{s}{(s+\alpha)^2 + \beta^2} = \frac{q}{C}\left[\frac{s+\alpha}{(s+\alpha)^2 + \beta^2} - \frac{\alpha}{(s+\alpha)^2 + \beta^2}\right]$$

$$= \frac{q}{C}\left[\frac{s+\alpha}{(s+\alpha)^2 + \beta^2} - \frac{\alpha}{\beta} \cdot \frac{\beta}{(s+\alpha)^2 + \beta^2}\right]$$

$$= \frac{q}{C}\left[e^{-\alpha t}\cos\beta t - \frac{\alpha}{\beta} e^{-\alpha t}\sin\beta t\right]$$

$$= \frac{q}{C} e^{-\alpha t}\left[\cos\beta t - \frac{\alpha}{\beta}\sin\beta t\right]$$

The above equation shows a damped oscillatory output voltage where amplitude is proportional to the charge q. The charge due to the pulse $i(t)$ is actually stored by the capacitor C instantaneously but due to the presence of inductance and resistance, Oscillations are produced. If these oscillations are not damped, the resolution time of the filter will be large and proper integration will not take place especially of the subsequent current pulses. There is a possibility of over lapping and the results obtained will be erroneous. The resolution time as is said earlier should be smaller than the time constant τ of the current pulse [$i\ (t)\ I_0 e^{-t/\tau}$]. The resolution time or decay time depends upon the Q-factor and resonance frequency f_0 of the measuring impedance Z_m. Let $Q = 1 = R/\sqrt{LC}$. Therefore $R = \sqrt{L/C}$ and

$$\alpha = \frac{1}{2\sqrt{(L/C)}.C} = \frac{\omega_0}{2} = \pi f_0$$

Suppose the resolution time is

$$T = \frac{1}{f_0} \text{ and } f_0 = 100 \text{ kHz}$$

The resolution time is about 10 μ sec and for higher values of Q, T will be still larger. The resonance frequency is also affected by the coupling capacitance C_k and the capacitance C_t of the test specimen as these contribute to the formation of C. Therefore, the $R\ L\ C$ circuit should be chosen or selected according to the test specimen so that a desired resonance frequency is obtained. The desired central frequency f_0 or a band width around f_0 is decided by the band pass amplifier connected to this resonant circuit. These amplifiers are designed for typically lower and upper cut off frequencies

(– 3 *dB*) between 150 kHz and 100 kHz. This band of frequency is chosen as it is much higher than the power supply frequency and also the frequency which are not used by broadcasting stations. The resolution time becomes less than 10 μ sec. and hence proper integration of the current pulse is made possible. However, the main job of the amplifier is to increase the sensitivity of the whole measuring system. The time dependency of the output voltage v_0 (t) can be seen on the oscilloscope. In the usual ellipse representation, the individual pulse v_0 (t) are practically only recognizable on vertical lines of different heights as one rotation of the ellipse corresponds to one period of the supply system 20 m sec. for 50 Hz and 16.7 m sec. for 60 Hz supplies. Fig. 6.29.

The magnitude of the individual discharge is quantified by comparing the pulse crest value with the one obtained from the calibration circuit as shown in Fig. 6.30. The calibration circuit consists of a voltage step generator V_0 and a series capacitor C_0. The charge q is simulated with no normal voltage applied to the PD testing circuit. It is possible to suggest the location of the partial discharges in an insulating material by looking at the display on the CRO screen.

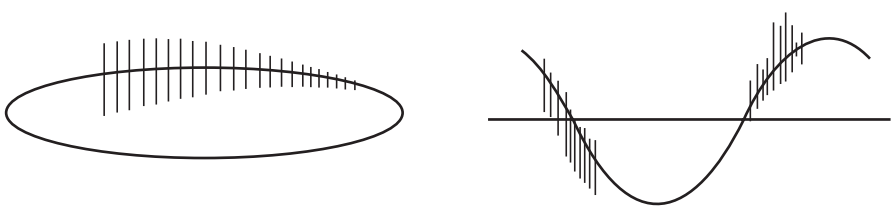

Fig. 6.29

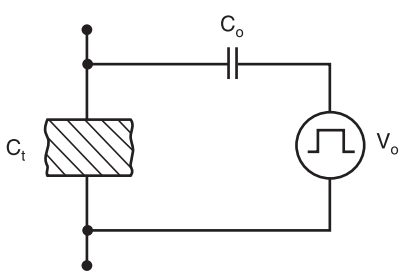

Fig. 6.30 Circuit for calibration of the oscilloscope

6.9.3 Narrow Band PD-Detection Circuit

A narrow band PD detection circuit is basically a very sensitive measurement receiver circuit with a continuously variable measuring or centre frequency f_m in the range of approximately 50 kHZ to several MHz. The nomenclature to narrow-band is justified as the band width of the filter amplifier is typically only 9 kHz. However, if special circumstances demand, the band width may be slightly made wider or narrower than 9 kHz.

Fig. 6.31 shows a narrow band PD measuring circuit.ℑ

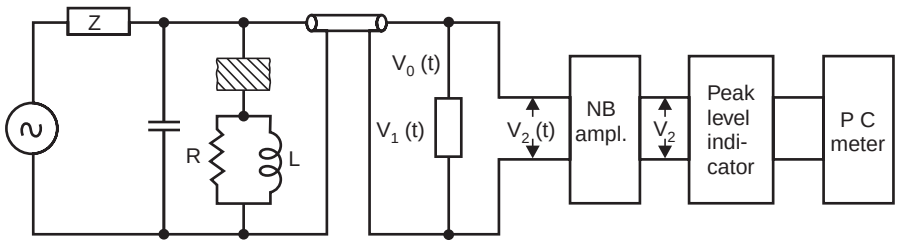

Fig. 6.31 Basic narrow band PD measuring circuit

Parallel combination of R and L constitute the measuring impedance Z_m. The measuring impedance acts as a high pass and high frequency PD currents pulses $i\,(t)$ are decoupled from the test circuit. Whereas in wide band circuits the measuring impedance $Z_m\,(R \parallel L \parallel C)$ performs integration operation on the input Dirac delta current $i(t)$, no integration is carried out by Z_m in the narrow band circuit. A low resistance rating of the measuring impedance Z_m prevents that the series connection of C_k and C_t attenuates high frequency components of PD signals. Since the delay cable is terminated with Z_0 which is the surge impedance of the cable itself the capacitance C_c of the cable does not play any role.

Assuming that the parallel combination of R and L is so chosen that L does not perform integrating operation on the input signal $i(t) = I_0\,\delta\,(t)$, the voltage $v_1(t)$ at the input of the narrow band amplifier is proportional to the PD impulse current $i(t)$ *i.e.*,

$$v_1\,(t) = I_0\,\delta\,(t)\,R_m$$

Again, assuming that $i\,(t) = I_0\,e^{-t/\tau}$ as in Fig. 6.27, we have

$$v_1\,(t) = I_0 e^{-t/\tau}\,R_m$$

$$V_1\,(j\,\omega) = \frac{I_0\,\tau\,R_m}{1 + j\,\omega\,\tau} = \frac{V_0\,\tau}{1 + j\,\omega\,\tau}$$

where $$R_m = \frac{RZ_0}{R + Z_0}$$

The time constant of the circuit $T = R_m C$

where $$C = \frac{C_t C_k}{C_t + C_k}$$

Let $$S_0 = V_0\,\tau$$

The quantity S_0 contains the information concerning the individual pulse charge q and is referred to as the integral signal amplitude and is represented in Fig. 6.32.

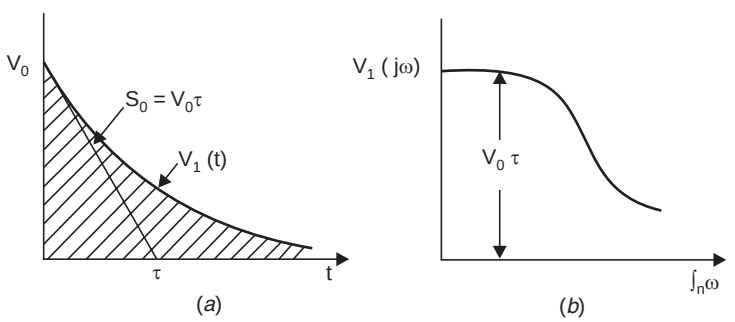

Fig. 6.32 (*a*) Approximate voltage impulse (*b*) Its frequency response

The input voltage to the narrow band amplifier is, therefore, represented as

$$v_1(t) = V_0 e^{-t/\tau}$$

Fig. 6.32 (*b*) shows impulse response of the measuring impedance circuit. This voltage impulse now is the input to the narrow band amplifier. So our objective now is to find the impulse response of the amplifier. However, the impulse response of any network is the transfer function of the network itself.

Assume an idealised transfer function of a narrow band amplifier as shown in Fig. 6.33 (*a*) with constant magnitude G_0, mid band angular frequency ω_m and an angular band width $\Delta\omega$. For such an ideal narrow band pass amplifier, the phase shift can be assumed to be linear function of angular frequency especially within the band pass response.

We also know that there is an inherent time delay between the impulse excitation and the response output of the network. Let this delay be t_0. The output response of the narrow band receiver is given by

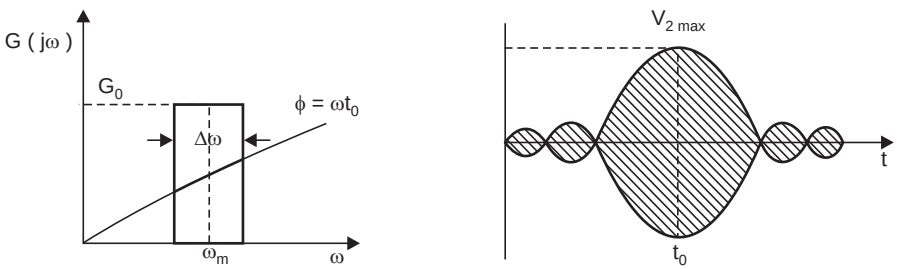

Fig. 6.33 (*a*) Idealised transfer function of narrow band receiver
(*b*) Impulse response of (*a*)

$$V_2(j\omega) = G(j\omega)\, V_1(j\omega)$$

and since $v_1(t) = S_0\,\delta(t);\ V_1(j\omega) = S_0$

$$G(j\omega) = G_0 e^{-j\omega t_0}$$

Therefore

$$v_2(t) = \frac{1}{\pi}\int_{\omega_m - \frac{\Delta\omega}{2}}^{\omega_m + \frac{\Delta\omega}{2}} S_0 G_0 e^{-j\omega t_0}\, e^{j\omega t}\, d\omega$$

$$= \frac{S_0 G_0}{\pi}\left[\frac{e^{j\omega(t-t_0)}}{j^{(t-t_0)}}\right]_{\omega_m - \Delta\omega/2}^{\omega_m + \Delta\omega/2}$$

$$v_2(t) = \frac{S_0 G_0}{\pi}\left[\frac{e^{j(\omega_m + \Delta\omega/2)(t-t_0)} - e^{j(\omega_m - \Delta\omega/2)(t-t_0)}}{j(t-t_0)}\right]$$

$$= \frac{S_0 G_0}{\pi}.\,\Delta\omega e^{j\omega_m (t-t_0)}\left[\frac{e^{j\Delta\omega(t-t_0)/2} - e^{-j\Delta\omega(t-t_0)/2}}{[2j\,(t-t_0)/2]\,\Delta\omega}\right]$$

$$= \frac{S_0 G_0}{\pi}\,\Delta\omega e^{j\omega_m (t-t_0)}\, Si\,\frac{\Delta\omega(t-t_0)}{2}$$

Neglecting the imaginary component, we have

$$v_2(t) = \frac{S_0 G_0}{\pi}\,\Delta\omega Si\left[\frac{\Delta\omega(t-t_0)}{2}\right]\cos\omega_m (t-t_0)$$

$$= 2S_0G_0\Delta f Si\left[\frac{\Delta\omega(t-t_0)}{2}\right]\cos\omega_m\,(t-t_0)$$

$$= V_{2\max}\,Si\left[\frac{\Delta\omega(t-t_0)}{2}\right]\cos\omega_m\,(t-t_0)$$

Fig. 6.33 (*b*) shows the plot of the above equation. It is clear that the impulse response of the narrow band pass receiver is an oscillatory one whose main frequency is given by f_m and the amplitudes are given by S_i function which is the envelope of the oscillations. The maximum value $V_{2max} = 2S_0G_0\,\Delta f$ where Δf is the idealised band width of the amplifier. There are two main disadvantages of the narrow band amplifier:

(*i*) If $\Delta\omega << \omega_m$, the positive and negative peak values of the response are equal and hence the polarity of the input pulse can't be detected.

(*ii*) The duration of the response is quite long.

Ideally, after the first current zero of the response

$$\frac{\sin x}{x}$$

the amplitude should decrease to very low value for proper measurements. If we redraw Fig. 6.33 (*b*) with normalised value of $v_2(t)$ along ordinate and abscissa $\Delta f\,(t - t_0)$ we obtain the variation as shown in Fig. 6.34.

We know the response as shown in Fig. 6.32 or 6.33 is that of an ideal distortion free system. However, the pulse response of a real filter does not show such pronounced oscillation outside of $\Delta f(t - t_0)$, $= \pm 1$ *i.e.,* in a real system after the first current zero of the response

$$\frac{\sin x}{x}$$

the oscillations reduce to negligibly small values.

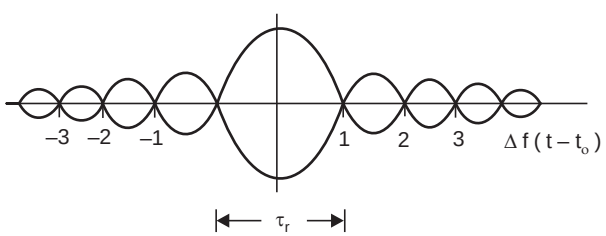

Fig. 6.34

The response time, therefore, is defined as

$$\tau_r = \frac{2}{\Delta f}$$

For a typical value $\Delta f = 9$ kHz, the response time $\tau_r = 220\ \mu$ sec. which is a much longer period as compared to in case of a wide band amplifier circuit. τ_r is the resolution time of the circuit and should be of the same order as that of the time constant of the input pulse for accurate measurement otherwise it leads to overlapping of pulses and the measurement becomes erroneous.

The first peak of the response is an indication of the charge q of the PD current pulses and can be detected by a peak level detector (pc meter). Fig. 6.31.

The narrow band PD detectors use radio interference voltage (RIV) meters for measurement of apparent charge. The main component of an RIV meter is a selective voltmeter of high sensitivity which can be tuned within the frequency range of interest. The selectivity may be reached by a narrow band pass filter characteristic and thus RIV is primarily a super-heterodyne type receiver, though a straight type narrow band receiver may also be considered as a high quality linear amplifier with a band pass filter characteristic and of sufficient amplification to give high sensitivity. The mid band frequency f_m should be continuously variable and f_m should be treated as a resonance frequency f_0 as this is suggested in the IEC recommendations for PD measurements.

Table 6.1 below gives comparison between the wide band and narrow band receiver circuits for measurement of PD current pulses.

Table 6.1

Comparison between wide band and narrow band PD measuring circuits

		Wide Band	*Narrow Band*
1.	Bandwidth	f_2–f_1 = 150 to 200 kHz	Δf = 9 kHz
2.	Centre frequency	Fixed f_0 = 80 – 150 kHz	Variable f_m = 50 kHz to 2 MHz
3.	Pulse resolution time	Small about 15 μ sec.	Large about 220 μ sec.
4.	Pulse polarity	Detectable	Not detectable
5.	Noise susceptibility	Relatively high as no. of interference sources increases with band width	Low due to selective measurements through variable centre frequency.
6.	Maximum admissible PD pulse width	Approx 1 μ sec.	Depends upon f_m in
7.	Indication of measured value	Directly in pC	Directly in pC

Table above shows relative merits and demerits of the two circuits. However, in practical situations, a system that can be switched over between wide band and narrow band should prove to be more versatile and useful.

6.10 BRIDGE CIRCUIT

Fig. 6.35 shows a bridge circuit used to suppress parasitic interference signals effectively. The circuit mainly consists of two individually balanceable measuring conductances *GA* and *GB* which are inserted into the ground conductors of capacitors C_k and C_t. The bridge can be balanced by a calibration generator when it is not energized. The calibration generator is connected between ground, the high voltage common terminal of the C_k and C_t in order to simulate external interference signals.

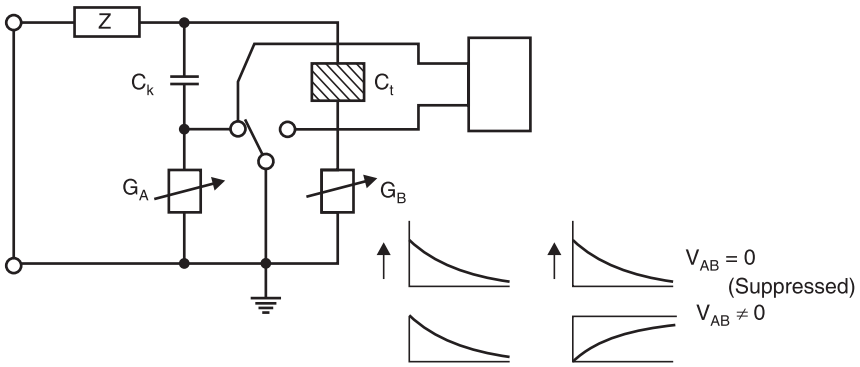

Fig. 6.35 Basic principle of bridge circuit

The setting of the conductances *GA* and *GB* for balance depends upon the capacitances C_k and C_t. However, in order to have high sensitivity of the bridge, the conductances should be as low as possible. The practical limit is given by the current carrying capacity of the individual components in the bridge arms *GA* and *GB*. If the conductances are not of proper value, the current pulses are so long ($\tau = C_k/GA = C_t/GB$) that these would involve errors in measurements. Sometimes the instruction manual suggests suitable values of *GA* and *GB* for the purpose.

If V_A and V_B are of the same magnitude and having the same polarity, the measuring instrument shows zero deflection. When an external signal occurs, this will induce same current-I in both the circuit branches which in turn would cause same voltage drops across *GA* and *GB* and hence the measuring instruments would read zero. However, if there is partial discharge in C_t, circular current $i(t)$ will flow and the polarity of V_A and V_B will now be opposed and the differential voltage V_{AB} will be indicated by the meter. The measuring instrument can be of either wide band or narrow band type. With this circuit, it is possible to obtain interference suppression factors varying from 1:20 to 1:1000 depending upon the construction of capacitances C_t and C_k and the type of source of interference. If the capacitances C_t and C_k are identical, interference suppression factors of 1:1000 can be achieved as the entire arrangement is then symmetrical. The test object should be placed close to each other so that the interference effect is identical. Under highly unfavourable condition e.g. PD testing of outdoor switch gear where an ambient noise level exists because of corona discharges and radio interferences, the effective interference suppression factors may be only around 1: 20. Also if the values of C_t and C_k differ materially, lower interference suppression factor is then expected as the bridge will have to be balanced over a large frequency range and the bridge has then less accuracy of measurement. However, the narrow band measuring system makes it possible to measure with a variable centre frequency at which the bridge circuit achieves maximum interference suppression.

6.11 OSCILLOSCOPE AS PD MEASURING DEVICE

Oscilloscope is an integral and indispensable component of a PD measuring system. An indicating meter e.g. a pC meter and RIV meter can give quantity of charge, whether the charge is as a result of partial discharge or due to external interferences, cannot be estimated. This problem can be solved only if the output wave form is studied on the Oscilloscope. Whether the origin of the discharges is from within the test object or not, can frequently be determined based on the typical patterns. If it is ascertained from the patterns that the discharge is from the test object, the magnitude of the apparent charge should be measured with pC meters or RIV meters. The peak value of the integrated pulse current is the

desired apparent charge q. These signals are normally superposed on the a.c. test voltage for observation on the Oscilloscope. Depending upon the preferences either sine or elliptical shapes can be selected. One complete rotation of the ellipse or one complete cycle of sine wave equals 20 m sec. of duration. Since the duration of these current pulses to be measured is a few microsecond, these pulses when seen on the power frequency wave, look like vertical lines of varying heights superimposed on the power frequency waves.

Whenever calibration facility exists in the PD test circuit, the calibration curve of known charge appears on the screen. The calibration pulse can be shifted entirely along the ellipse or sine curve of the power supply and the signal to be measured can be compared with the calibration pulse.

6.12 RECURRENT SURGE GENERATOR

The power transformers, the power transmission lines and rotating machines are exposed to lightning surges and, therefore, these should be impulse tested during their design and development stages. The surge voltage distribution along the transformer winding is very important to know especially for the design of its high voltage insulation. For such purposes it is not desirable to subject the winding to its full withstand voltage rather low impulse voltage should be used to avoid risk of damage to the winding during test and to reduce the cost of test apparatus. Therefore, low voltage test impulses having the same wave form as the standard high voltage surges and to which transformers respond in more or less a linear fashion have been suggested. The low voltage impulses are synchronised with the recurrent time base of a CRO so that what is observed on the screen of the CRT is an apparently steady state and the distribution of voltage along the transformer winding can be studied.

Fig. 6.36 shows a schematic diagram of recurrent generator developed by Rohats. The arrangement of elements R_1, R_2 and C_2 is similar to that of circuit '*a*' of Fig. 3.4 R_1 controls the wave front time and R_2 the wave tail time.

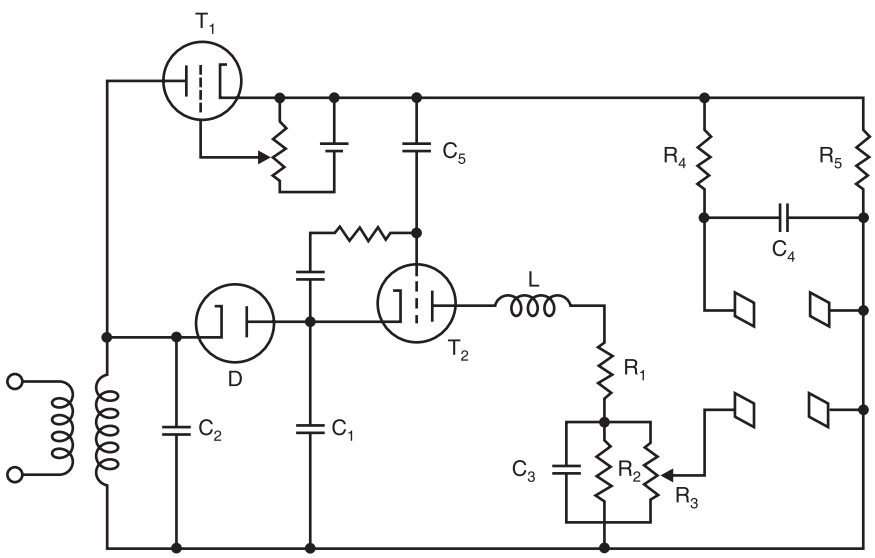

Fig. 6.36 Basic circuit of recurrent surge generator

When T_1 conducts, it charges the capacitance C_4 through R_4 which gives deflection on the time axis of the CRO. At the same time a positive impulse is fed through C_5 to the grid of T_2 which conducts. C_1 which was charged in the previous half cycle, starts discharging through L, R_1, R_2 and C_2. A part of the output across R_3 is fed into the deflection plates of CRO. The time base is adjusted with the resistance R_4.

During the past many years, many circuits have been developed. One of the most modern recurrent surge generators is shown in Fig. 6.37.

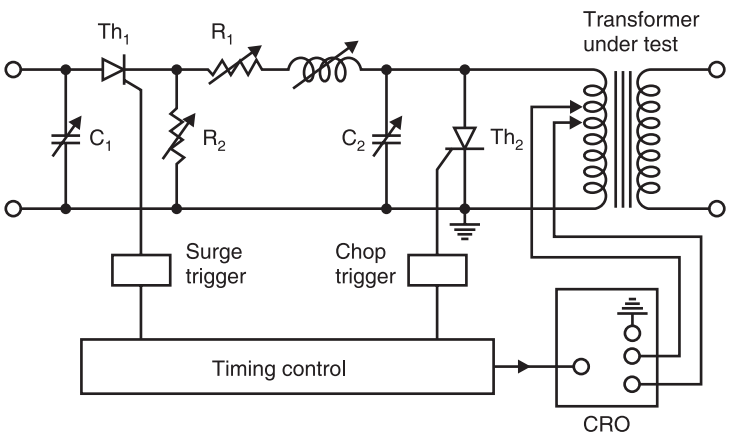

Fig. 6.37 Recurrent surge generator circuit

In this circuit both the full impulse wave and chopped impulse waves can be obtained by controlling the firing of thyristor Th_1 and Th_2 through surge trigger circuit and chop trigger circuits respectively. The wave front time and wave till timings are controlled using R_1 and R_2 respectively. C_1 corresponds to the total impulse capacitance and C_2 the load capacitance. The impulse generation sequence is repeated and synchronised with the mains frequency. The impulse can also be trigged manually in a non-recurrent manner. In case the impulse circuit elements R_1, R_2 L are insufficient, additional external resistance can be connected.

Fig. 6.37 shows arrangement of recurrent surge generator for measurement of inter turn potential of the transformer winding. Similarly the potential at any point of the winding can also be studied.

EXAMPLES

Example 6.1: *A 20 kV, 50 Hz Schering bridge has a standard capacitance of 106 μF. In a test on a bakelite sheet balance was obtained with a capacitance of 0.35 μF in parallel with a non-inductive resistance of 318 ohms, the non-inductive resistance in the remaining arm of the bridge being 130 ohms. Determine the equivalent series resistance and capacitance and the p.f. of the specimen.*

Solution: Here $C'_s = 106\ \mu F$, $C_2 = 0.35\ \mu F$

$R_2 = 318$ ohms and $R_1 = 130$ ohms.

Since $$R_s = R_1 \frac{C_2}{C'_s} = 130 \times \frac{0.35}{106} = 0.429 \text{ ohm}$$ **Ans.**

and $$C_s = C'_s \frac{R_2}{R_1} = 106 \times \frac{318}{130} = 259\ \mu\text{F} \quad \textbf{Ans.}$$

$$\tan \delta_s = \omega C_s R_s = 314 \times 259 \times 10^{-6} \times 0.429$$
$$= 3.5 \times 10^4 \times 10^{-6} = 0.035 \quad \textbf{Ans.}$$

Since $$\tan \delta = \sin \delta = \cos (90 - \delta)$$
$$= \cos \phi = 0.035 \quad \textbf{Ans.}$$

Example 6.2. *Determine p.f. and the equivalent parallel resistance and capacitance of the rest specimen of example 6.1*

Solution: For parallel equivalent

$$C_p = C_s \frac{R_2}{R_1}$$

Here C_s is the standard capacitance

$$C_p = 106 \times \frac{318}{130} = 259\ \mu F \quad \textbf{Ans.}$$

$$R_p = \frac{R_1}{\omega^2 C_2 C_s R_2^2}$$

$$R_p = \frac{130}{314^2 \times 0.35 \times 106 \times 10^{-12} \times 318^2}$$

$$= 351 \text{ ohms} \quad \textbf{Ans.}$$

$$\tan \delta = \frac{1}{314 \times 351 \times 259 \times 10^{-6}}$$

$$= \frac{1}{28.54} = 0.035 \quad \textbf{Ans.}$$

Example 6.3. *A 33 kV, 50 Hz high voltage Schering bridge is used to test a sample of insulation. The various arms have the following parameters on balance. The standard capacitance 500 pF, the resistive branch 800 ohm and branch with parallel combination of resistance and capacitance has values 180 ohms and 0.15 μF. Determine the value of the capacitance of this sample its parallel equivalent loss resistance, the p.f. and the power loss under these test conditions.*

Solution: Given $C_s = 500$ pF

$R_1 = 800$ ohm

$R_2 = 180$ ohm

$C_2 = 0.15\ \mu$F

Now $$C_p = C_s \frac{R_2}{R_1} = 500 \times 10^{-12} \times \frac{180}{800} = 112.5 \text{ pF}$$

$$R_p = \frac{R_1}{\omega^2 C_2 C_s R_2^2} = \frac{800}{314^2 \times 500 \times 10^{-12} \times 0.15 \times 10^{-6} \times 180^2}$$

$$= \frac{800}{2.3958 \times 10^{11} \times 10^{18}} = 333.9 \times 10^{7} = 3339 \text{ M}\Omega$$

$$\text{p.f.} = \tan \delta_p = \frac{1}{\omega C_p R_p} = \frac{1}{314 \times 112.5 \times 10^{-12} \times 3339 \times 10^{6}}$$

$$= \frac{1}{117.95} \quad 0.008478 \quad \textbf{Ans.}$$

Power loss

$$= \frac{V^2}{R} = \frac{33^2 \times 10^6}{3339 \times 10^6}$$

$$= 0.326 \text{ watts} \quad \textbf{Ans.}$$

Example 6.4. *A length of cable is tested for insulation resistance by the loss of charge method. An electrostatic voltmeter of infinite resistance is connected between the cable conductor and earth forming therewith a joint capacitance of 600 pF. It is observed that after charging the voltage falls from 250 volts to 92 V in one min. Determine the insulation resistance of the cable.*

Solution: The voltage at any time t is given as

$$v = Ve^{-t/CR}$$

where V is the initial voltage

or $$\frac{V}{v} = e^{t/CR}$$

or $$1\text{n} \frac{V}{v} = \frac{t}{CR}$$

or $$\text{R} = \frac{t}{C \, 1\text{n} \frac{V}{v}} = \frac{60}{600 \times 10^{-12} \, 1\text{n} \frac{250}{92}}$$

$$= \frac{60}{600 \times 10^{-12} \times 1}$$

$$= 100{,}000 \text{ M ohms} \quad \textbf{Ans.}$$

Example 6.5. *Following measurements are made to determine the dielectric constant and complex permittivity of a test specimen:*

The air capacitance of the electrode system = 50 pF

The capacitance and loss angle of the electrodes with specimen = 190 pF and 0.0085 respectively.

Solution: The dielectric constant $\varepsilon_r = \frac{190}{50} = 3.8$

Now complex permittivity $\varepsilon = \varepsilon' - j\varepsilon''$

$$= \varepsilon_0 (\varepsilon_r' - j\varepsilon_r'')$$

$$\varepsilon_r' = \varepsilon_r = 3.8$$

$$\tan \delta = \frac{\varepsilon_r''}{\varepsilon_r'} = \frac{\varepsilon_r''}{3.8} = 0.0085$$

or $$\varepsilon_r'' = 0.0323$$

$$\varepsilon = \varepsilon_0 (3.8 - j\, 0.0323)$$

$$= 8.854 \times 10^{-12} (3.8 - j\, 0.0323)$$

$$= (3.36 - j\, 0.0286) \times 10^{-11} \text{ F/m} \quad \textbf{Ans.}$$

Example 6.6. *Determine the specific heat generated in the test specimen due to dielectric loss if the dielectric constant and loss angle of the specimen are 3.8 and 0.0085 respectively. The electric field is 40 kV/cm at 50 Hz.]*

Solution: The specific loss is given by

$$\sigma E^2 \text{ Watts/m}^3$$

where σ is the conductivity of the specimen and E the strength of electric field.

Also we know that

$$\tan \delta = \frac{\sigma}{\omega \varepsilon_0 \varepsilon_r}$$

or $$\sigma = \omega \varepsilon_0 \varepsilon_r \tan \delta$$

Therefore, specific loss is given as

$$\sigma E^2 = \omega \varepsilon_0 \varepsilon_r \tan \delta\, E^2$$

$$= 314 \times 8.854 \times 10^{-12} \times 3.8 \times 0.0085 \times 1600 \times 10^{10}$$

$$= 1436 \text{ Watts/m}^3 \quad \textbf{Ans.}$$

Example 6.7. *A solid dielectric of 1 cm thickness and $\varepsilon_r = 3.8$ has an internal void of 1 mm thickness. If the void is filled with air which breaks down at 21 KV/cm, determine the voltage at which an internal discharge can occur.*

Solution: Refer to Fig. Ex. 6.7

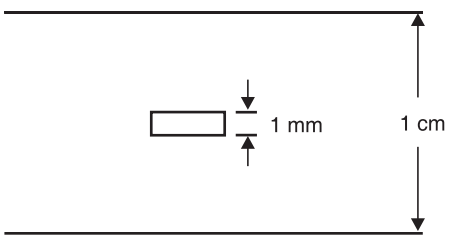

For internal discharge to take place the gradient in void should be 21 kV/cm. Therefore, the gradient in the dielectric slab will be

$$\frac{21}{3.8} = 5.526 \text{ kV/cm.}$$

Therefore, total voltage required to produce these gradient will be

$$= 5.526 \times 0.9 + 21 \times 0.1$$

$$= 4.97 + 2.1$$

$$= 7.07 \text{ kV rms} \quad \textbf{Ans.}$$

PROBLEMS

6.1. What is non-destructive testing of insulating materials? Give very briefly the characteristics of these methods.

6.2. Starting from first principles, develop expression to evolve equivalent circuit of an insulating material.

6.3. Draw a neat diagram of a high voltage schering bridge and describe various features of the bridge.

6.4. Describe the functions of (*i*) Null detector (*ii*) Automatic guard potential regulator used in high voltage Schering bridge.

6.5. Draw a neat diagram of high voltage Schering bridge and analyse it for balanced condition. Draw its phasor diagram. Assume (*i*) Series equivalent (*ii*) Parallel equivalent representation of the insulating material.

6.6. What modifications do you suggest in the basic Schering bridge while measuring large capacitances? Give its analysis. How the expressions for capacitance and loss angle get modified?

6.7. What is an inverted schering bridge? Give its application.

6.8. Explain the operation of high voltage Schering bridge when the test specimen (*i*) is grounded (*ii*) has high loss factor.

6.9. Discuss various types of transformer ratio arm bridges and give their application and advantages.

6.10. Describe with a neat diagram the principle of the operation of transformer current ratio arm bridge. Explain how this is used for measurement of capacitance and loss factor of an insulating material.

6.11. What are partial discharges? Differentiate between internal and external discharges.

6.12. Develop and draw equivalent circuit of insulating material during partial discharge.

6.13. What is apparent charge in relation to partial discharges? Show that the calculation of apparent charge as a measure of partial discharges even though is more realistic than calculation of change in voltage across the electrode, has limited application for partial discharge measurement.

6.14. Explain with neat diagram basic principle of pulse current measurement for estimation of partial discharges.

6.15. Write short note on the measuring impedance circuit for estimation of partial discharges.

6.16. Shows that the d.c. content of the frequency spectrum equals the apparent charge in the pulse current.

6.17. Explain with neat diagrams how wide band circuit can be used for measuring partial discharge.

6.18. "For proper measurement of partial discharge the resolution time of the circuit should be smaller than the time-constant of the current pulse" Why? Explain.

6.19. Explain with neat diagram the Narrow-Band PD-detection circuit.

6.20. Show that the impulse response of narrow-bandpass receiver is an Oscilatory and with main frequency fm and the amplitude is given by signum function. Discuss the limitation of narrow bandpass detector.

6.21. Compare the performance of narrow band and wide band *PD* measuring circuits.

6.22. Explain with neat diagram a bridge circuit used for suppressing interference signals.

6.23. Write a short note on the use of an Oscilloscope as a *PD* measuring device.

6.24. Explain why the Schering bridge is particularly suitable for measurements at high voltages and outline the precautions necessary to avoid errors.

A sample of insulation is placed in one arm *CD* of the Schering bridge. Under balanced condition the other three arms are as follows:

AD = 109 *pF*, *BC* = 100 ohms and *AB* = 309 ohm in parallel with a loss free capacitance of 0.5 μF. Determine the capacitance equivalent series resistance and p.f. of the insulation in the arm *CD*. Derive balanced conditions and draw phasor diagram. (340 pF, 460 K Ω, 0.05)

6.25. A sheet of bakelite 4.57 mm thick is tested at 50 Hz between electrodes 12.10 cms in diameter. The Schering bridge employed has a standard compressed air capacitor of 106 pF a non-inductive resistor of 1000/π ohm in parallel with a variable capacitance *C*, and a non-inductive variable resistor *R*. Balance is obtained with *C* = 0.5 μ*F* and *R* = 260 ohm. Calculate the p.f. and the permittivity of the sheet.

(0.05, 5.88)

6.26. To determine the permittivity of a material following two measurements were made on the Schering bridge.

Without the specimen between the electrodes.

Standard capacitor 150 pF in arm *BC*

Arm *CD* 120 pF in parallel with 5000 Ω

Arm *DA* 120 pF in parallel with 5000 Ω

Arm *DA* 120 pF in parallel with 5000 Ω

Arm *AB* Test electrodes

With specimen between the electrodes

AB BC 900 pF

Arm *CD* 1000 pF in parallel with 5000 Ω

Arm *DA* 1000 pF in parallel with 5000 Ω

The angular frequency of supply is 500 rad/sec.

Determine the relative permittivity and p.f. of the specimen. (6.0, 0.02)

REFERENCES

Kuffel E., Zaengl W. *High Voltage Engineering-Fundamentals,* Pergamon Press 1984.

Boggs S.A., Electromagnetic techniques for fault and PD-location in gas-insulated cables and substations, *IEEE Tran PAS* - 101 (1982), pp 1935–41.

Mole G. *et al*, Measurement of the magnitude of internal discharged in power capacitor, Proc. *IEE* Vol. 116, No.5 (1969).

Papoulis A., *The Fourier Integrais and its' applications* Mc Graw Hill 1962.

Schwab A.J., *High Voltage Measurement Techniques,* MIT Press 1972.

7 Transients in Power Systems and Insulation Coordination

7.1 INTRODUCTION

Transient phenomenon is an aperiodic function of time and does not last longer. The duration for which they last is very insignificant as compared with the operating time of the system. Yet they are very important because depending upon the severity of these transients, the system may result into black out in a city, shut down of a plant, fires in some buildings, etc.

The power system can be considered as made up of linear impedance elements of resistance, inductance and capacitance. The circuit is normally energized and carries load until a fault suddenly occurs. The fault, then, corresponds to the closing of a switch (or switches, depending upon the type of fault) in the electrical circuit. The closing of this switch changes the circuit so that a new distribution of currents and voltages is brought about. This redistribution is accompanied in general by a transient period during which the resultant currents and voltages may momentarily be relatively high. It is very important to realize that this redistribution of currents and voltages cannot take place instantaneously for the following reasons:

1. The electromagnetic energy stored by an inductance L is $\frac{1}{2} LI^2$ where I is the instantaneous value of current. Assuming inductance to be constant the change in magnetic energy requires change in current which an inductor is opposed by an *emf* of magnitude $L \frac{dI}{dt}$. In order to change the current instantaneously $dt = 0$ and therefore $L \frac{dI}{0}$ is infinity, *i.e.*, to bring about instantaneous change in current the *emf* in the inductor should become infinity which is practically not possible and, therefore, it can be said that the change of energy in an inductor is gradual.

2. The electrostatic energy stored by a capacitor C is given by $\frac{1}{2} CV^2$ where V is the instantaneous value of voltage. Assuming capacitance to be constant, the change in energy requires change in voltage across the capacitor.

Since, for a capacitor, $\frac{dV}{dt} = \frac{I}{C}$, to bring instantaneous change in voltage, *i.e.*, for $dt = 0$ the change in current required is infinite which again can not be achieved in practice and, therefore, it can be said that change in energy in a capacitor is also gradual.

There are only two components L and C in an electrical circuit which store energy and we have seen that the change in energy through these components is gradual and, therefore, the redistribution of energy following a circuit change takes a finite time. The third component, the resistance R, consumes energy. At any time, the principle of conservation of energy in an electrical circuit applies, *i.e.* the rate of generation of energy is equal to the rate of storage of energy plus the rate of energy consumption.

It is clear that the three simple facts, namely,

1. The current cannot change instantaneously through an inductor,

2. The voltage across a capacitor cannot change instantaneously,

3. The law of conservation of energy must hold good, are fundamental to the phenomenon of transients in electric power systems.

From the above it can be said that in order to have transients in an electrical system the following requirements should be met:

1. Either inductor or capacitor or both should be present.

2. A sudden change in the form of a fault or any switching operation should take place.

There are two components of voltages in a power system during transient period: (*i*) Fundamental frequency voltages, and (*ii*) Natural frequency voltages usually of short duration which are superimposed upon the fundamental frequency voltages. There is third component also known as harmonic voltages resulting from unbalanced currents flowing in rotating machines in which the reactances in the direct and quadrature axes are unequal.

Natural frequency voltages appear immediately after the sudden occurrence of a fault. They simply add to the fundamental frequency voltages. Since resultant voltages are of greater importance from a practical viewpoint it will be preferable to speak of the fundamental frequency and natural frequency components simply as a transient voltage. The transient voltages are affected by the number of connections and the arrangements of the circuits.

Transients in which only one form of energy-storage, magnetic or electric is concerned, are called single energy transients, where both magnetic and electric energies are contained in or accepted by the circuit, double energy transients are involved.

7.2 TRANSIENTS IN SIMPLE CIRCUITS

For analysing circuits for transients we will make use of Laplace transform technique which is more powerful and easy to handle the transient problems than the differential equation technique. We will assume here lumped impedances only. The transients will depend upon the driving source also, *i.e.*, whether it is a d.c. source or an a.c. source. We will begin with simple problems and then go to some complicated problems.

1. D.C. Source

(*a*) *Resistance only* (*Fig. 7.1 (a)*)

As soon as the switch S is closed, the current in the circuit will be determined according to Ohm's law.

$$I = \frac{V}{R}$$

Now transients will be there in the circuit.

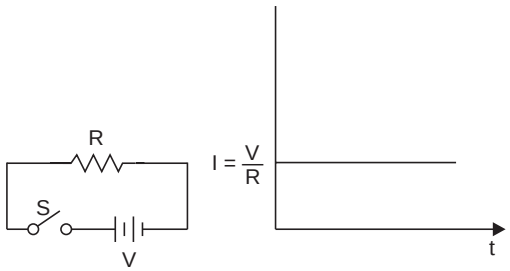

Fig. 7.1 (*a*) Resistive circuit.

(*b*) *Inductance only* (*Fig. 7.1 (b)*)

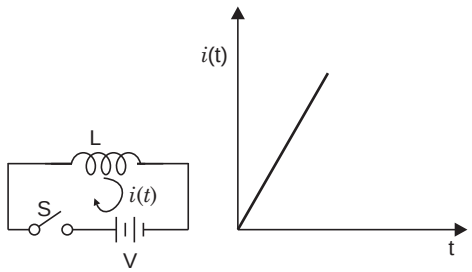

Fig. 7.1 (*b*) Inductive circuit.

When switch *S* is closed, the current in the circuit will be given by

$$I(s) = \frac{V(s)}{Z(s)} = \frac{V}{s} \cdot \frac{1}{Ls} = \frac{V}{L} \cdot \frac{1}{s^2}$$

$$i(t) = \frac{V}{L} t$$

This shows that when a pure inductance is switched on to a d.c. source, the current at $t = 0_+$ is zero and this increases linearly with time till for infinite time it becomes infinity. In practice, of course, a choke coil will have some finite resistance, however small; the current will settle down to the value *V*/*R*, where *R* is the resistance of the coil.

(*c*) *Capacitance only* (*Fig. 7.1 (c)*)

When switch *S* is closed, the current in the circuit is given by

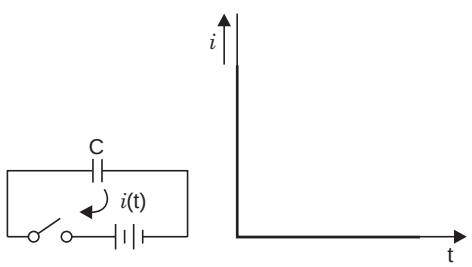

Fig. 7.1 (*c*) Capacitance circuit.

$$I(s) = \frac{V(s)}{Z(s)} = \frac{V}{s}\, Cs = VC$$

which is an impulse of strength (magnitude) *VC*.

(*d*) *R-L Circuit* (*Fig. 7.1 (d)*)

When switch *S* is closed, the current in the circuit is given by

$$I(s) = \frac{V(s)}{Z(s)} = \frac{V}{s}\,\frac{1}{R+Ls} = \frac{V}{s}\,\frac{1/L}{s+R/L}$$

$$= \frac{V}{L}\left[\frac{1}{s} - \frac{1}{s+R/L}\right]\frac{L}{R}$$

$$= \frac{V}{R}\left[\frac{1}{s} - \frac{1}{s+R/L}\right]$$

$$i(t) = \frac{V}{R}\left[1 - \exp\left(-\frac{R}{L}t\right)\right]$$

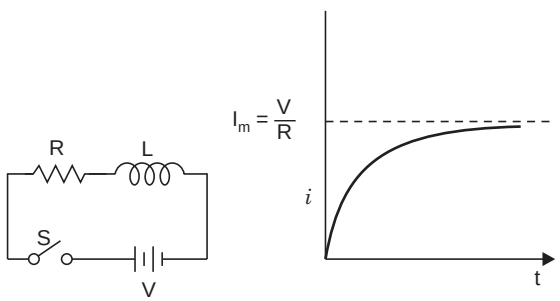

Fig. 7.1(*d*) R-L circuit.

The variation of current is shown in Fig. 12.1(*d*). It can be seen from the expression that the current will reach *V*/*R* value after infinite time. Also it can be seen that the inductor just after closing of the switch behaves as an open circuit and that is why the current at $t = 0_+$ is zero. When $t = L/R$,

$$i(t) = \frac{V}{R}\left(1 - \frac{1}{e}\right) = I_m\left(1 - \frac{1}{e}\right) = 0.632\ I_m$$

At time $t = L/R$ the current in the circuit is 63.2% of the maximum value reached in the circuit. This time in seconds is called the time-constant of the circuit. The larger the value of inductance in the circuit as compared with resistance the slower will be the build up of current in the circuit. The energy stored in the inductor under steady state condition will be $\frac{1}{2}LI_m^2$, where $I_m = V/R$.

(*e*) *R-C circuit* (*Fig. 7.1(e)*)

After the switch *S* is closed, current in the circuit is given by

$$I(s) = \frac{V(s)}{Z(s)} = \frac{V}{s}\,\frac{1}{R+1/Cs}$$

$$= \frac{V}{s}\,\frac{(1/RC)Cs}{s+1/RC} = \frac{V}{R}\,\frac{1}{s+1/RC}$$

$$i(t) = \frac{V}{R}\, e^{-t/CR}$$

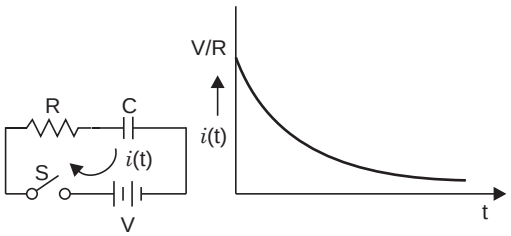

Fig. 7.1(*e*) R-C circuit

It is seen that at $t = 0$ the capacitor acts as a short-circuit to the d.c. source and the current is V/R limited only by the resistance of the circuit. At $t = \infty$ the current in the circuit is zero and the capacitor is charged to a voltage V. The energy stored by the capacitor is $\frac{1}{2}CV^2$.

(*f*) *R-L-C circuit (Fig. 7.1(f))*

After the switch S is closed, the current in the circuit is given by

$$I(s) = \frac{V}{s} \cdot \frac{1}{R + Ls + 1/Cs}$$

$$= \frac{V}{s} \cdot \frac{Cs}{RCs + LCs^2 + 1}$$

$$= \frac{V}{s} \cdot \frac{1/L}{s^2 + \frac{R}{L}s + \frac{1}{LC}}$$

$$= \frac{V}{L} \cdot \frac{1}{\left\{s + \left(\frac{R}{2L} - \sqrt{\frac{R^2}{4L^2} - \frac{1}{LC}}\right)\right\}\left\{s + \left(\frac{R}{2L} + \sqrt{\frac{R^2}{4L^2} - \frac{1}{LC}}\right)\right\}}$$

Let $\frac{R}{2L} = a$ and $\sqrt{\frac{R^2}{4L^2} - \frac{1}{LC}} = b$; then

$$I(s) = \frac{V}{L} \frac{1}{(s + a - b)(s + a + b)}$$

$$= \frac{V}{2bL}\left[\frac{1}{(s + a - b)} - \frac{1}{(s + a + b)}\right]$$

$$i(t) = \frac{V}{2bL}\, [e^{-(a-b)t} - e^{-(a+b)t}]$$

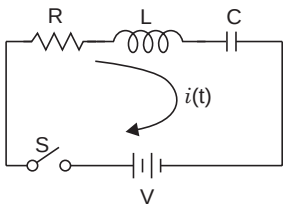

Fig. 7.1(*f*) R-L-C circuit

There are three conditions based on the value of b.

(*i*) If $\frac{R^2}{4L^2} > \frac{1}{LC}$, b is real

(*ii*) If $\frac{R^2}{4L^2} = \frac{1}{LC}$, b is zero

(*iii*) If $\frac{R^2}{4L^2} < \frac{1}{LC}$, b is imaginary.

Case I: When b is real

The expression for current will be

$$i(t) = \frac{V}{2\sqrt{\frac{R^2}{4L^2} - \frac{1}{LC}} \cdot L} \left[\exp\left\{ -\left(\frac{R}{2L} + \sqrt{\frac{R^2}{4L^2} - \frac{1}{LC}} \right) t \right\} - \exp\left\{ -\left(\frac{R}{2L} - \sqrt{\frac{R^2}{4L^2} - \frac{1}{LC}} \right) t \right\} \right]$$

and the variation of current is given in Fig. 7.1(*g*).

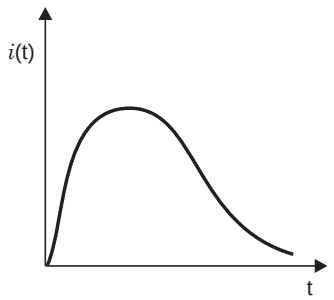

Fig. 7.1 (*g*) Waveform when b is real

Case II: When $b = 0$.

The expression for current becomes

$$i(t) = \frac{V}{2bL} [e^{-at} - e^{-at}]$$

which is indeterminate. Therefore, differentiating $i(t)$ with respect to b gives

$$i(t) = \frac{V}{2L} \cdot t[e^{-(a-b)t} + e^{-(a+b)t}]$$

Now at $b = 0$

$$i(t) = \frac{V}{L} te^{-at} = \frac{V}{L} te^{-(R/2L)t}$$

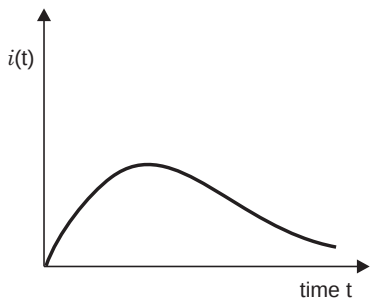

Fig. 7.1(*h*) Waveform when $b = 0$

The variation of current is given in Fig. 7.1(*h*).

Case III: When b is imaginary

$$i(t) = \frac{V}{2bL} (e^{-at} \cdot e^{jbt} - e^{-at} \cdot e^{-jbt}) = \frac{V}{2bL} e^{-at} 2 \sin bt$$

$$= \frac{V}{2L\sqrt{\frac{R^2}{4L^2} - \frac{1}{LC}}} e^{-at} 2 \sin\left(-\frac{R^2}{4L^2} + \frac{1}{LC} \right) t$$

The wave shape of the current is shown in Fig. 7.1(*i*).

When b is positive or zero, the variation of current is non-oscillatory whereas it is oscillatory when b is imaginary. Because of the presence of the capacitance, the current in all the three cases dies down to zero value with d.c. source in the circuit.

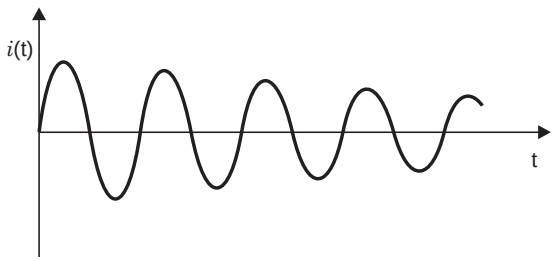

Fig. 7.1(*i*) Wave form when b is imaginary

2. A.C. Source

R-L circuit (*Fig. 7.2*)

When switch S is closed, the current in the circuit is given by

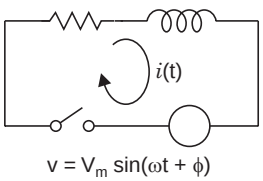

Fig. 7.2

$$I(s) = \frac{V(s)}{Z(s)} = V_m \left\{ \frac{\omega \cos\phi}{s^2+\omega^2} + \frac{s \sin\phi}{s^2+\omega^2} \right\} \frac{1}{R+Ls}$$

$$= \frac{V_m}{L} \left\{ \frac{\omega \cos\phi}{s^2+\omega^2} + \frac{s \sin\phi}{s^2+\omega^2} \right\} \frac{1}{s+R/L}$$

Let $\frac{R}{L} = a$; then

$$I(s) = \frac{V_m}{L} \left\{ \frac{\omega \cos\phi}{(s+a)(s^2+\omega^2)} + \frac{s \sin\phi}{(s+a)(s^2+\omega^2)} \right\}$$

Now $$\frac{1}{(s+a)(s^2+\omega^2)} = \frac{1}{(a^2+\omega^2)} \left\{ \frac{1}{(s+a)} + \frac{a}{(s^2+\omega^2)} - \frac{s}{(s^2+\omega^2)} \right\}$$

and $$\frac{s}{(s+a)(s^2+\omega^2)} = \frac{1}{(a^2+\omega^2)} \left\{ \frac{as}{s^2+\omega^2} + \frac{\omega^2}{s^2+\omega^2} - \frac{a}{s+a} \right\}$$

Therefore $$L^{-1}I(s) = \frac{V_m}{(a^2+\omega^2)L} \left[\omega \cos\phi \left\{ e^{-at} + \frac{a}{\omega} \sin\omega t - \cos\omega t \right\} \right.$$

$$\left. + \sin\phi \{ a \cos\omega t + \omega \sin\omega t - a e^{-at} \} \right]$$

The equation can be further simplified to

$$i(t) = \frac{V_m}{L\sqrt{a^2+\omega^2}} \{ \sin(\omega t + \phi - \theta) - \sin(\phi - \theta) e^{-at} \}$$

$$= \frac{V_m}{(R^2+\omega^2 L^2)^{1/2}} \{ \sin(\omega t + \phi - \theta) - \sin(\phi - \theta)\, e^{-at} \}$$

where $$\theta = \tan^{-1} \frac{\omega L}{R} .$$

The variation of current is shown in Fig. 7.3.

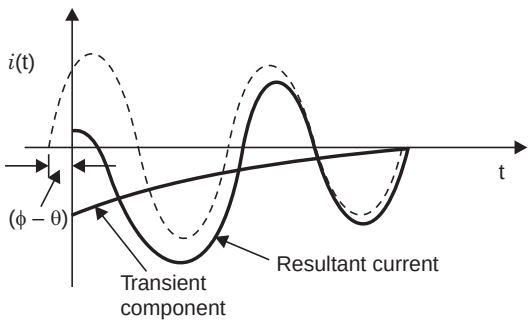

Fig. 7.3 Asymmetrical alternating current

The first term in the expression above is the steady state sinusoidal variation and the second term is the transient part of it which vanishes theoretically after infinite time. But practically, it vanishes very quickly after two or three cycles. The transient decay as is seen depends upon the time constant $\frac{1}{a} = \frac{L}{R}$ of the circuit. Also at $t = 0$ it can be seen that the transient component equals the steady state component and since the transient component is negative the net current is zero at $t = 0$. It can be seen that the transient component will be zero in case the switching on of the voltage wave is done when $\theta = \phi$, *i.e.*, when the wave is passing through an angle $\phi = \tan^{-1} \frac{\omega L}{R}$. This is the situation when we have no transient even though the circuit contains inductance and there is switching operation also. On the other hand if $\phi - \theta = \pm \pi/2$, the transient term will have its maximum value and the first peak of the resulting current will be twice the peak value of the sinusoidal steady state component.

7.3 TRAVELLING WAVES ON TRANSMISSION LINES

So far, we have analysed the transient behaviour of various circuits with lumped parameters. However, there are some parts of a power system where this approach is inadequate. The most obvious example is the transmission line. Here the parameters *L*, *C* and *R* are uniformly distributed over the length of the line. For steady state operation of the line the transmission lines could be represented by lumped parameters but for the transient behaviour of the lines they must be represented by their actual circuits *i.e.*, distributed parameters. We say that for a 50 Hz supply and short transmission line the sending end current equals the receiving end current and the change in voltage from sending end to receiving end is smooth. This is not so when transmission line is subjected to a transient.

To understand the travelling wave phenomenon over transmission line consider Fig. 7.4 (*a*). The line is assumed to be lossless. Let *L* and *C* be the inductance and capacitance respectively per unit length of the line. The line has been represented in Fig. 7.4. (*b*) by a large number of *L* and *C* sections. The closing of the switch is similar to opening the valve at the end of a channel, thereby admitting water to the channel from some reservoir behind. When the valve is opened the channel does not get filled up instantaneously. We observe the water advancing down the channel. At any instant the channel ahead of the wave front is dry while that behind is filled with water to the capacity. Similarly, when

the switch S is closed the voltage does not appear instantaneously at the other end. When switch S is closed, the inductance L_1 acts as an open circuit and C_1 as short circuit instantaneously. The same instant the next section cannot be charged because the voltage across the capacitor C_1 is zero. So unless the capacitor C_1 is charged to some value whatsoever, charging of the capacitor C_2 through L_2 is not possible which, of course, will take some finite time. The same argument applies to the third section, fourth section and so on. So we see that the voltage at the successive sections builds up gradually. This gradual build up of voltage over the transmission line conductors can be regarded as though a voltage wave is travelling from one end to the other end and the gradual charging of the capacitances is due to the associated current wave.

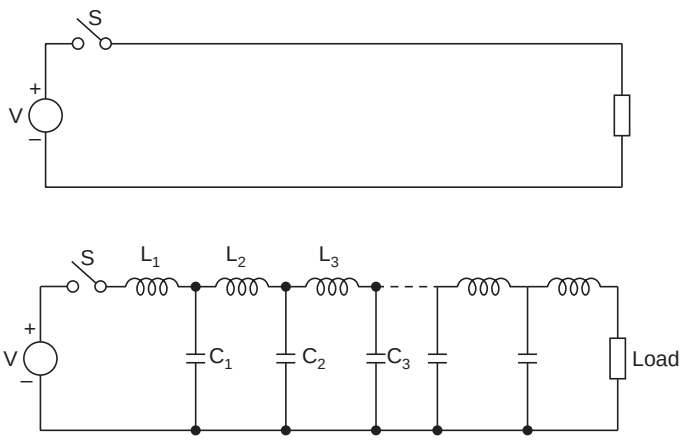

Fig. 7.4 (*a*) Long transmission line, (*b*) Equivalent section of a long transmission line

Now it is desired to find out expressions for the relation between the voltage and current waves travelling over the transmission lines and their velocity of propagation.

Suppose that the wave after time t has travelled through a distance x. Since we have assumed lossless lines whatever is the value of voltage and current waves at the start, they remain same throughout the travel. Consider a distance dx which is travelled by the waves in time dt. The electrostatic flux is associated with the voltage wave and the electromagnetic flux with the current wave. The electrostatic flux which is equal to the charge between the conductors of the line upto a distance x is given by

$$q = VCx \tag{7.1}$$

The current in the conductor is determined by the rate at which the charge flows into and out of the line.

$$I = \frac{dq}{dt} = VC\frac{dx}{dt} \tag{7.2}$$

Here dx/dt is the velocity of the travelling wave over the line conductor and let this be represented by v. Then

$$I = VCv \tag{7.3}$$

Similarly the electromagnetic flux linkages created around the conductors due to the current flowing in them upto a distance of x is given by

$$V = ILx \tag{7.4}$$

The voltage is the rate at which the flux linkages link around the conductor

$$V = IL\frac{dx}{dt} = ILv \tag{7.5}$$

Dividing equation (7.5) by (7.3), we get

$$\frac{V}{I} = \frac{ILv}{VCv} = \frac{IL}{VC}$$

or $$\frac{V^2}{I^2} = \frac{L}{C}$$

or $$\frac{V}{I} = \sqrt{\frac{L}{C}} = Z_n \tag{7.6}$$

The expression is a ratio of voltage to current which has the dimensions of impedance and is therefore, here designated as surge impedance of the line. It is also known as the natural impedance because this impedance has nothing to do with the load impedance. It is purely a characteristic of the transmission line. The value of this impedance is about 400 ohms for overhead transmission lines and 40 ohms for cables.

Next, multiplying equations (7.3) with (7.5), we get

$$VI = VCv\ ILv = VILCv^2$$

or $$v^2 = \frac{1}{LC}$$

or $$v = \frac{1}{\sqrt{LC}} \tag{7.7}$$

Now expressions for L and C for overhead lines are

$$L = 2 \times 10^{-7} \ln \frac{d}{r} \text{ H/metre}$$

$$C = \frac{2\pi\varepsilon}{\ln \frac{d}{r}} \text{ F/metre}$$

Substituting these values in equation (7.7), the velocity of propagation of the wave

$$v = \frac{1}{\left(2\times10^{-7} \ln \frac{d}{r}\frac{2\pi\varepsilon}{\ln d/r}\right)^{1/2}}$$

$$= \frac{1}{\sqrt{4\pi\varepsilon\, 10^{-7}}} = \frac{1}{\sqrt{4\pi \frac{1}{36\pi} \times 10^{-9} \times 10^{-7}}}$$

$$= 3 \times 10^8 \text{ metres/sec.}$$

This is the velocity of light. This means the velocity of propagation of the travelling waves over the overhead transmission lines equals the velocity of light. In actual practice because of the resistance and leakance of the lines the velocity of the travelling wave is slightly less than the velocity of light. Normally a velocity of approximately 250 m/μ sec is assumed. It can be seen from the expression that the velocity of these waves over the cables will be smaller than over the overhead lines because of the permittivity term in the denominator.

Since $\varepsilon = \varepsilon_0\varepsilon_r$ for overhead lines $\varepsilon_r = 1$ whereas for cables where the conductor is surrounded by some dielectric material for which $\varepsilon_r > 1$, the term ε is greater for cables than for overhead lines and therefore the velocity of the waves over the cables is smaller than over the overhead lines.

Let us study the behaviour of these lines to the travelling waves when they reach the other end of the lines or whenever they see a change in the impedance (impedance other than characteristic impedance of the line).

Open End Line

Consider a line with the receiving end open-circuited as shown in Fig. 7.5.

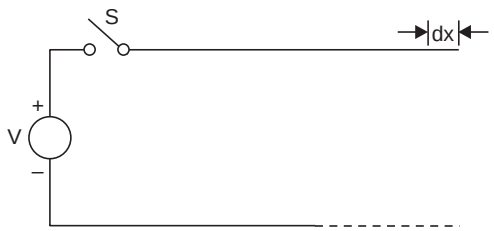

Fig. 7.5 Case of an open-ended line

When switch *S* is closed, a voltage and current wave of magnitudes *V* and *I* respectively travel towards the open end. These waves are related by the equation:

$$\frac{V}{I} = Z$$

Where *Z* is the characteristic impedance of the line. Consider the last element *dx* of the line, because, it is here where the wave is going to see a change in impedance, an impedance different from *Z* (infinite impedance as the line is open-ended).

The electromagnetic energy stored by the element *dx* is given by $\frac{1}{2}\ LdxI^2$ and electrostatic energy in the element *dx*, $\frac{1}{2}\ CdxV^2$. Since the current at the open end is zero, the electromagnetic energy vanishes and is transformed into electrostatic energy. As a result, let the change in voltage be *e*; then

$$\frac{1}{2}\ LdxI^2 = \frac{1}{2}\ Cdxe^2$$

or
$$\left(\frac{e}{I}\right)^2 = \frac{L}{C}$$

or
$$e = IZ = V$$

This means the potential of the open end is raised by *V* volts; therefore, the total potential of the open end when the wave reaches this end is

$$V + V = 2V$$

The wave that starts travelling over the line when the switch *S* is closed, could be considered as the incident wave and after the wave reaches the open end, the rise in potential *V* could be considered

due to a wave which is reflected at the open end and actual voltage at the open end could be considered as the refracted or transmitted wave and is thus

Refracted wave = Incident wave + Reflected wave

We have seen that for an open end line a travelling wave is reflected back with positive sign and coefficient of reflection as unity.

Let us see now about the current wave.

As soon as the incident current wave I reaches the open end, the current at the open end is zero, this could be explained by saying that a current wave of I magnitude travels back over the transmission line. This means for an open end line, a current wave is reflected with negative sign and coefficient of reflection unity. The variation of current and voltage waves over the line is explained in Fig. 7.6.

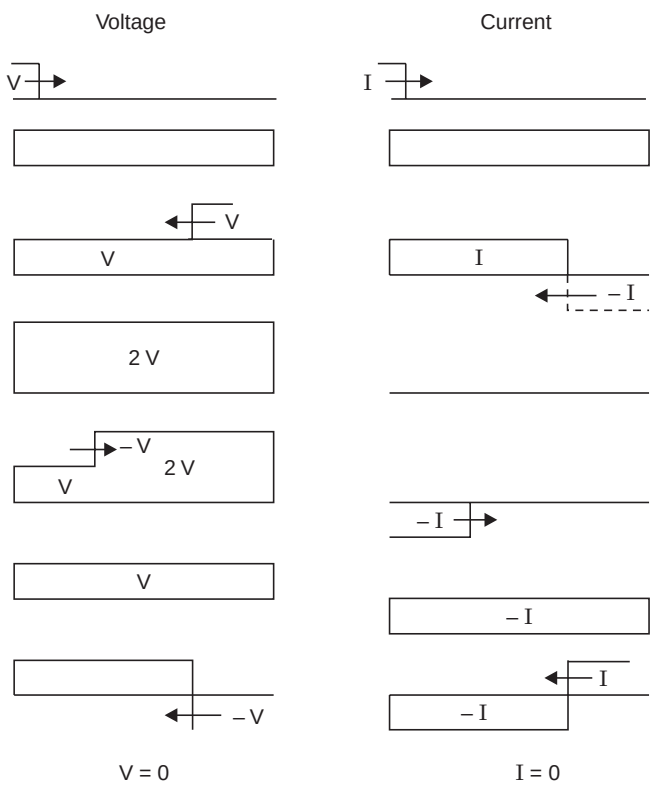

Fig. 7.6 Variation of voltage and current in an open-ended line

After the voltage and current waves are reflected back from the open end, they reach the source end, the voltage over the line becomes $2V$ and the current is zero. The voltage at source end cannot be more than the source voltage V, therefore, a voltage wave of $-V$ and current wave of $-I$ is reflected back into the line (Fig. 7.6). It can be seen that after the waves have travelled through a distance of $4l$ where l is the length of the line, they would have wiped out both the current and voltage waves, leaving the line momentarily in its original state. The above cycle repeats itself.

Short Circuited Line

Consider the line with receiving end short-circuited as shown in Fig. 7.7.

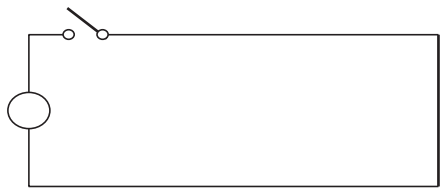

Fig. 7.7 Case of a short-circuited line

When switch S is closed, a voltage wave of magnitude V and current wave of magnitude I start travelling towards the shorted end. Consider again the last element dx where the electrostatic energy stored by the element is $\frac{1}{2} CdxV^2$ and electromagnetic energy $\frac{1}{2} LdxI^2$. Since the voltage at the shorted end is zero, the electrostatic energy vanishes and is transformed into electromagnetic energy. As a result, let the change in the current be i; then

$$\frac{1}{2} CdxV^2 = \frac{1}{2} Ldxi^2$$

or $$V = iZ$$

or $$i = \frac{V}{Z} = I$$

This means the increase in current is I amperes. As a result the total current at the shorted end, when the current wave reaches the end is $(I + I) = 2I$ amperes. This could be considered due to a reflected current wave of magnitude I amperes. Therefore, for a short-circuited end the current wave is reflected back with positive sign and coefficient of reflection as unity. Since the voltage at the shorted end is zero, a voltage wave of $-V$ could be considered to have been reflected back into the line, *i.e.*, the current wave in case of short-circuited end is reflected back with positive sign and with coefficient of reflection as unity, whereas the voltage wave is reflected back with negative sign and coefficient of reflection as in the variation of voltage and current over the line is explained in Fig. 7.8.

It is seen from above that the voltage wave periodically reduces to zero after it has travelled through a distance of twice the length of the line whereas after each reflection at either end the current is built up by an amount $V/Z_n = I$. Theoretically, the reflections will be infinite and therefore, the current will reach infinite value. But practically in an actual system the current will be limited by the resistance of the line and the final value of the current will be $I' = V/R$, where R is the resistance of transmission line.

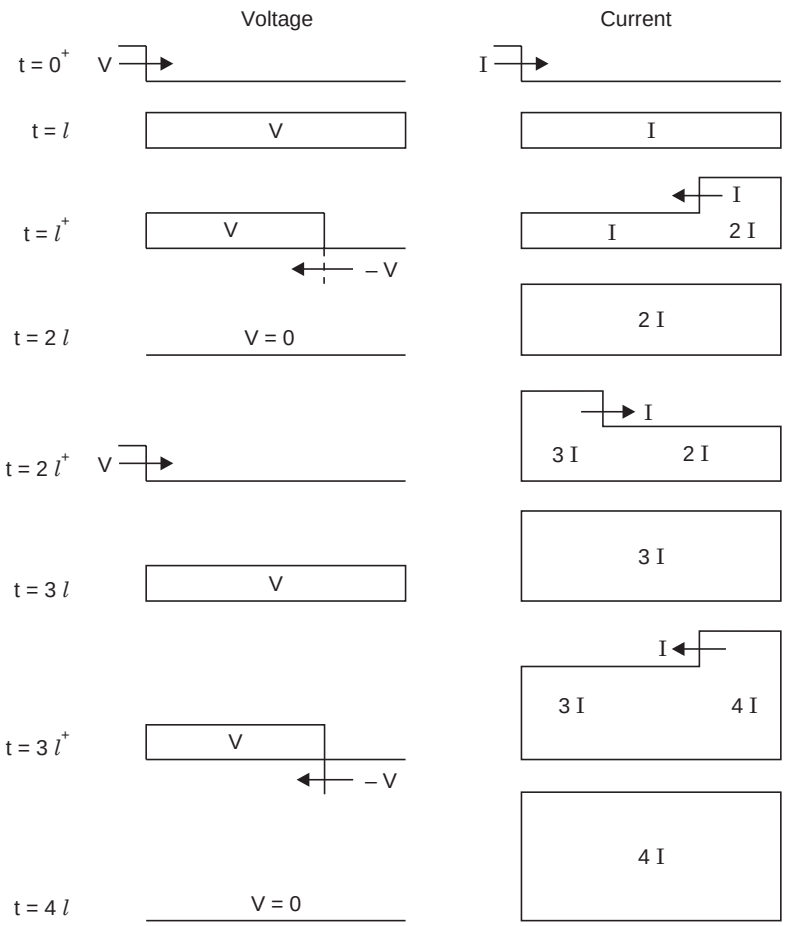

Fig. 7.8 Variation of voltage and current in a short ended line

Line Terminated Through a Resistance

Let Z be the surge impedance of the line terminated through a resistance R (Fig. 7.9). It has been seen in the previous sections that what ever be the value of the terminating impedance whether it is open or short circuited, one of the two voltage or current waves is reflected back with negative sign. Also, since the reflected wave travels along the overhead line or over the line along which the incident wave travelled, therefore, the following relation holds good for reflected voltage and current waves.

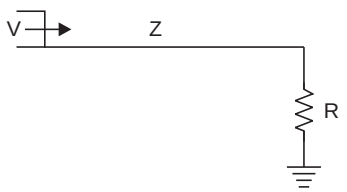

Fig. 7.9 Line terminated through a resistance

$$I' = -\frac{V'}{Z}$$

where V' and I' are the reflected voltage and current waves. Also,

Refracted or transmitted wave = Incident wave + Reflected wave

Let V'' and I'' be the refracted voltage and current waves into the resistor R when the incident waves V and I reach the resistance R. The following relations hold good:

$$I = \frac{V}{Z}$$

$$I' = -\frac{V'}{Z}$$

$$I'' = \frac{V''}{Z}$$

Since $I'' = I + I'$ and $V'' = V + V'$, using these relations, we have

$$\frac{V''}{R} = \frac{V}{Z} - \frac{V'}{Z} = \frac{V}{Z} - \frac{V'' - V}{Z} = \frac{2V}{Z} - \frac{V''}{Z} \tag{7.8}$$

or $$V'' = \frac{2VR}{Z + R} \tag{7.9}$$

and current $$I'' = \frac{2V}{R + Z} = \frac{V}{Z} \cdot \frac{2Z}{R + Z} = I \cdot \frac{2Z}{R + Z} \tag{7.10}$$

Similarly substituting for V'' in terms of $(V + V')$, equation (7.8) becomes

$$\frac{V + V'}{R} = \frac{V}{Z} - \frac{V'}{Z}$$

or $$V' = V \frac{R - Z}{R + Z} \tag{7.11}$$

and $$I' = -\frac{V'}{Z} = -\frac{V}{Z} \frac{(R - Z)}{R + Z} \tag{7.12}$$

From the relations above, the coefficient of refraction for current waves

$$= \frac{2Z}{R + Z}$$

and for voltage waves $$= \frac{2R}{R + Z}$$

Similarly, the coefficient of reflection for current waves

$$= -\frac{R - Z}{R + Z}$$

and for voltage waves $$= +\frac{R - Z}{R + Z}$$

Now the two extreme cases can be derived out of this general expression. For open circuit,

$$R \to \infty$$

and coefficient of refraction for current waves

$$\frac{2Z}{\infty + Z} = 0$$

and coefficient of refraction for voltage waves

$$= \frac{2R}{R+Z} = \frac{2}{1+Z/R} = \frac{2}{1+Z/\infty} = 2$$

Similarly, coefficient of reflection for current waves

$$= -\frac{R-Z}{R+Z} = -\frac{1-Z/R}{1+Z/R} = -1$$

and coefficient of reflection for voltage waves

$$= \frac{R-Z}{R+Z} = 1$$

Similarly, to find out the coefficients of reflection and refraction for current and voltage waves for the short circuit case, the value of $R = 0$ is to be substituted in the corresponding relations as derived in this section.

It is, therefore, seen here that whenever a travelling wave looks into a change in impedance, it suffers reflection and refraction. It is shown below that in case $Z = R$ *i.e.*, the line is terminated through a resistance whose value equals the surge impedance of the line (*i.e.*, no change in the impedance) there will be no reflection and the wave will enter fully into the resistance, *i.e.*, the coefficient of refraction will be unity whereas the coefficient of reflection will be zero.

When $R = Z$, substituting this, the coefficient of reflection for current wave

$$= -\frac{R-Z}{R+Z} = \frac{Z-Z}{Z+Z} = 0$$

and for voltage wave $$= \frac{R-Z}{R+Z} = 0$$

The coefficient of refraction for current wave

$$= \frac{2Z}{R+Z} = \frac{2Z}{2Z} = 1$$

and for voltage wave $$= \frac{2R}{R+Z} = 1$$

It is seen that when a transmission line is terminated through a resistance equal to its surge impedance the wave does not suffer reflection and, therefore, such lines could be said to be of infinite length. Such lines are also called as matched lines and the load corresponding to this is known as surge impedance loading or natural impedance loading.

Line Connected to a Cable

A wave travels over the line and enters the cable (Fig. 7.10). Since the wave looks into a different impedance, it suffers reflection and refraction at the junction and the refracted voltage wave is given by

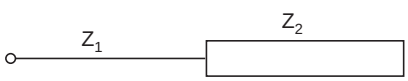

Fig. 7.10 Line connected to a cable

$$V'' = V \frac{2Z_2}{Z_1 + Z_2}$$

The other waves can be obtained by using the relations (7.10–7.12). The impedance of the overhead line and cable are approximately 400 ohms and 40 ohms respectively. With these values it can be seen that the voltage entering the cable will be

$$V'' = V \cdot \frac{2 \times 40}{40 + 400} = \frac{2}{11} V$$

i.e., it is about 20% of the incident voltage V. It is for this reason that an overhead line is terminated near a station by connecting the station equipment to the overhead line through a short length of underground cable. Besides the reduction in the magnitude of the voltage wave, the steepness is also reduced because of the capacitance of the cable. This is explained in the next section. The reduction in steepness is very important because this is one of the factors for reducing the voltage distribution along the windings of the equipment. While connecting the overhead line to a station equipment through a cable it is important to note that the length of the cable should not be very short (should not be shorter than the expected length of the wave) otherwise successive reflections at the junction may result in piling up of voltage and the voltage at the junction may reach the incident voltage.

Reflection and Refraction at a *T*-junction

A voltage wave V is travelling over the line with surge impedance Z_1 as shown in Fig. 7.11. When it reaches the junction, it looks a change in impedance and, therefore, suffers reflection and refraction. Let V_2'', I_2'' and V_3'', I_3'' be the voltages and currents in the lines having surge impedances Z_2 and Z_3 respectively. Since Z_2 and Z_3 form a parallel path as far as the surge wave is concerned, $V_2'' = V_3'' = V''$. Therefore, the following relations hold good.

$$V + V' = V''$$

$$I = \frac{V}{Z_1}, \; I' = -\frac{V'}{Z_1}$$

$$I_2'' = \frac{V''}{Z_2} \quad \text{and} \quad I_3'' = \frac{V''}{Z_3}$$

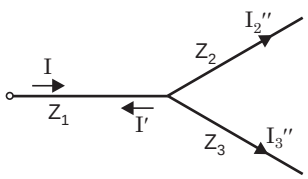

Fig. 7.11 A bifurcated line

and
$$I + I' = I_2'' + I_3'' \tag{7.13}$$

Substituting in equation (7.13) the values of currents

$$\frac{V}{Z_1} - \frac{V'}{Z_1} = \frac{V''}{Z_2} + \frac{V''}{Z_3}$$

Substituting for $V' = V'' - V$,

$$\frac{V}{Z_1} - \frac{V'' - V}{Z_1} = \frac{V''}{Z_2} + \frac{V''}{Z_3}$$

$$\frac{2V}{Z_1} = V'' \left(\frac{1}{Z_1} + \frac{1}{Z_2} + \frac{1}{Z_3} \right)$$

or
$$V'' = \frac{2V/Z_1}{\frac{1}{Z_1} + \frac{1}{Z_2} + \frac{1}{Z_3}} \tag{7.14}$$

Similarly other quantities can be derived.

Example 7.1. *A 3-phase transmission line has conductors 1.5 cms in diameter spaced 1 metre apart in equilateral formation. The resistance and leakance are negligible. Calculate (i) the natural impedance of the line, (ii) the line current if a voltage wave of 11 kV travels along the line, (iii) the rate of energy absorption, the rate of reflection and the state and the form of reflection if the line is terminated through a star connected load of 1000 ohm per phase, (iv) the value of the terminating resistance for no reflection and (v) the amount of reflected and transmitted power if the line is connected to a cable extension with inductance and capacitance per phase per cm of 0.5 × 10^{-8} H and 1 × 10^{-6} F respectively.*

Solution: The inductance per unit length

$$= 2 \times 10^{-7} \ln \frac{d}{r} \text{ H/metre}$$

$$= 2 \times 10^{-7} \ln \frac{100}{0.75}$$

$$= 2 \times 10^{-7} \ln 133.3$$

$$= 2 \times 10^{-7} \times 4.89$$

$$= 9.78 \times 10^{-7} \text{ H/m}$$

The capacitance per phase per unit length

$$= \frac{2\pi\varepsilon_0}{\ln d/r} \text{ F/metre}$$

$$= \frac{2 \times 10^{-9}}{36 \ln d/r} = \frac{1}{18} \times \frac{10^{-9}}{4.89} = 1.136 \times 10^{-11}$$

$\therefore$ The natural impedance $= \sqrt{\frac{L}{C}} = \sqrt{\frac{9.78 \times 10^{-7}}{1.136 \times 10^{-11}}} = 294$ ohms. **Ans.**

(*ii*) The line current $= \frac{11000}{\sqrt{3} \times 296} = 21.6$ amps. **Ans.**

(*iii*) Since the terminating resistance is of higher value as compared to the value of the surge impedance of the line, the reflection is with a positive sign.

$$E'' = \frac{2Z_2E}{Z_1 + Z_2}$$

where Z_1 = line surge impedance, Z_2 = terminating impedance and E = incident voltage.

$$E'' = 2 \times \frac{11000}{\sqrt{3}} \frac{1000}{1294} = 9.8 \text{ kV}$$

$\therefore$ The rate of power consumption $= \frac{3E''^2}{R}$ MW

$$= \frac{3 \times 9.8 \times 9.8}{1000} \times 1000 \text{ kW}$$

$$= 288 \text{ kW} \quad \textbf{Ans.}$$

The reflected voltage $$E' = \frac{Z_2 - Z_1}{Z_2 + Z_1} E = \frac{1000 - 294}{1294} \times \frac{11}{\sqrt{3}} \text{ kV}$$

$$= \frac{706}{1294} \times \frac{11}{\sqrt{3}} = 3.465 \text{ kV}$$

$\therefore$ The rate of reflected energy $= \frac{3 \times 3.465^2}{294} \times 1000$ kW

$= 121.8$ kW **Ans.**

(*iv*) In order that the incident wave when reaches the terminating resistance, does not suffer reflection, the terminating resistance should be equal to the surge impedance of the line, *i.e.*, 294 ohms.

(*v*) The surge impedance of the cable $= \sqrt{\frac{L}{C}} = \sqrt{\frac{0.5 \times 10^{-8}}{10^{-12}}}$

$= 70.7$ ohm

The refracted voltage $= \frac{2 \times 70.7}{294 + 70.7} \times \frac{11}{\sqrt{3}}$

$= \frac{2 \times 70.7 \times 11}{\sqrt{3} \times 364.7} = 2.46$ kV

The reflected voltage $= \frac{70.7 - 294}{364.7} \times \frac{11}{\sqrt{3}}$

$= \frac{-223.3 \times 11}{\sqrt{3} \times 364.7} = -3.9$ kV

$\therefore$ The refracted and reflected powers are respectively.

$\frac{3 \times 2.46^2}{70.7} \times 1000 = 256$ kW and $\frac{3 \times 3.9^2}{294} \times 1000 = 155$ kW. **Ans.**

Example 7.2. *A surge of 15 kV magnitude travels along a cable towards its junction with an overhead line. The inductance and capacitance of the cable and overhead line are respectively 0.3 mH, 0.4* μ*F and 1.5 mH, 0.012* μ*F per km. Find the voltage rise at the junction due to the surge.*

Solution: In this problem the surge travels from the cable towards the overhead line and hence there will be positive voltage reflection at the junction.

The natural impedance of the cable $= \sqrt{\frac{0.3 \times 10^{-3}}{0.4 \times 10^{-6}}} = \sqrt{\frac{3 \times 10^{-4}}{0.4 \times 10^{-6}}} = 27.38$

The natural impedance of the line $= \sqrt{\frac{1.5 \times 10^{-3}}{0.012 \times 10^{-6}}}$

$= \sqrt{\frac{1.5 \times 10^{-3}}{0.12 \times 10^{-7}}} = 353$ ohms.

The voltage rise at the junction is the voltage transmitted into the overhead line as the voltage is zero before the surge reaches the junction.

$$E'' = \frac{2 \times 353 \times 15}{353 + 27} = \frac{2 \times 353 \times 15}{380} = 27.87 \text{ kV} \quad \textbf{Ans.}$$

Example 7.3. *A surge of 100 kV travelling in a line of natural impedance 600 ohms arrives at a junction with two lines of impedances 800 ohms and 200 ohms respectively. Find the surge voltages and currents transmitted into each branch line.*

Solution: The problem deals with a reflection at a T-joint. The various natural impedances are: Z_1 = 600 ohms, Z_2 = 800 ohms, Z_3 = 200 ohms. The surge magnitude is 100 kV.

The surge as it reaches the joint suffers reflection and here the two lines are in parallel; therefore, the transmitted voltage will have the same magnitude and is given by

$$E'' = \frac{2E/Z_1}{\frac{1}{Z_1} + \frac{1}{Z_2} + \frac{1}{Z_3}} = \frac{2 \times 100/600}{\frac{1}{600} + \frac{1}{800} + \frac{1}{200}}$$

$$= \frac{0.333}{(1.67 + 1.25 + 5.0) \times 10^{-3}} = \frac{0.333 \times 10^3}{7.92}$$

$$= \frac{33.3}{7.92} \times 10 = 42.04 \text{ kV} \quad \textbf{Ans.}$$

The transmitted current in line $Z_2 = \dfrac{42.04 \times 1000}{800}$ amps = 52.55 amps **Ans.**

The transmitted current in line $Z_3 = \dfrac{42.04 \times 1000}{200}$ amps = 210.2 amps. **Ans.**

Line Terminated through a Capacitance

We consider here that a d.c. surge of infinite length travels over the line of surge impedance Z and is incident on the capacitor as shown in Fig. 7.12. We are interested in finding out the voltage across the capacitor *i.e.*, the refracted voltage. The refracted voltage, using equation (7.9),

$$V''(s) = \frac{2 \times 1/Cs}{Z + 1/Cs} \cdot \frac{V}{s} = \frac{2V}{s} \frac{1}{ZCs + 1}$$

$$= \frac{2V}{s} \cdot \frac{1/ZC}{s + 1/ZC} = 2V \left[\frac{1}{s} - \frac{1}{s + 1/ZC} \right]$$

$$v''(t) = 2V[1 - e^{-t/ZC}] \qquad (7.15)$$

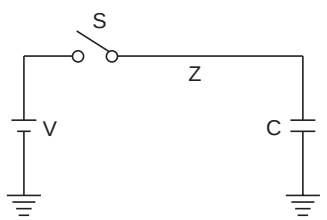

Fig. 7.12 Line terminated through a capacitance

The variation of voltage is shown in Fig. 7.13 (*b*).

It is to be noted that since terminating impedance is not a transmission line, therefore, $V''(s)$ is not a travelling wave but it is the voltage across the capacitor C.

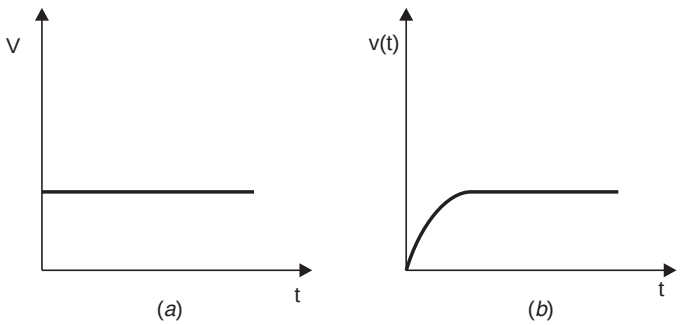

Fig. 7.13 (*a*) Incident voltage and (*b*) Voltage across capacitor

Capacitor Connection at a *T*

The voltage across capacitor is given by the equation

$$V''(s) = \frac{2V/Z_1 s}{\frac{1}{Z_1} + \frac{1}{Z_2} + Cs} = \frac{2VZ_2}{s} \cdot \frac{(1/Z_1 Z_2 C)}{\frac{Z_1 + Z_2}{Z_1 Z_2 C} + s} = \frac{2V}{sZ_1 C} \cdot \frac{1}{s + \frac{Z_1 Z_2}{Z_1 Z_2 C}}$$

Let $\frac{Z_1 + Z_2}{Z_1 Z_2 C} = \alpha$; then

$$V''(s) = \frac{2V}{s} \cdot \frac{1/Z_1 C}{s + \alpha}$$

or

$$V''(s) = \frac{2V}{s} \cdot \frac{Z_2}{Z_1 + Z_2} \cdot \frac{(Z_1 + Z_2)/Z_1 Z_2 C}{(s + \alpha)}$$

$$= \frac{2V}{s} \cdot \frac{Z_2}{Z_1 + Z_2} \cdot \frac{\alpha}{s + \alpha} = \frac{2VZ_2}{Z_1 + Z_2} \left[\frac{1}{s} - \frac{1}{s + \alpha}\right]$$

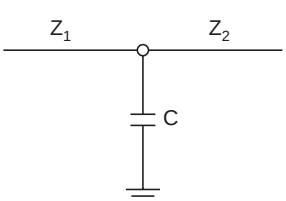

Fig. 7.14 Capacitor connected at *T*

or

$$v''(t) = \frac{2V \cdot Z_2}{Z_1 + Z_2} \left[1 - \exp\left(-\frac{Z_1 + Z_2}{Z_1 Z_2 C} t\right)\right] \quad (7.16)$$

The variation of the wave is shown in Fig. 7.15.

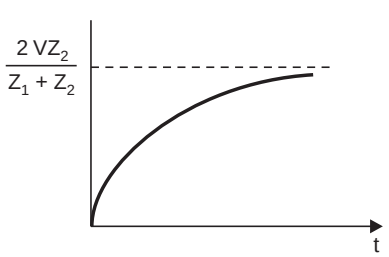

Fig. 7.15 Variation of voltage across the capacitor

We have assumed in the derivation of the expression for voltage across the capacitor in the previous section that the travelling surge is of infinite length. Let us now derive the expression when the surge is of finite duration say τ (Fig. 7.16). Also, let the magnitude of this wave be V units. The wave could be decomposed into two waves.

Here $f(t) = Vu(t) - Vu(t - \tau)$

$Vu(t - \tau) = V$ for $t \geq \tau$

$= 0$ for $t < \tau$

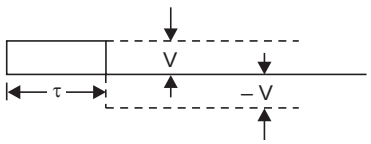

Fig. 7.16 Surge of finite length

With this, voltage across the capacitor is given by

$$V''(s) = L\{f(t)\} \cdot \frac{2/Z_1}{\frac{1}{Z_1} + \frac{1}{Z_2} + Cs} = \frac{2V/Z_1 s}{\frac{1}{Z_1} + \frac{1}{Z_2} + Cs} - \frac{(2V/Z_1 s) \cdot e^{-\tau s}}{\frac{1}{Z_1} + \frac{1}{Z_2} + Cs}$$

$$v''(t) = 2V \cdot \frac{Z_2}{Z_1 + Z_2}\left[1 - \exp\left(-\frac{Z_1 + Z_2}{Z_1 Z_2 C} t\right)\right]$$

$$- \frac{2VZ_2}{Z_1 + Z_2}\left[1 - \exp\left\{-\frac{Z_1 + Z_2}{Z_1 Z_2 C}(t - \tau)\right\}\right]$$

The variation of voltage is shown in Fig. 7.17.

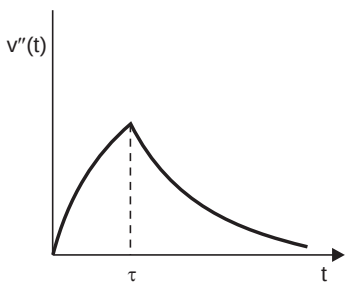

Fig. 7.17 Variation of voltage across the capacitor with finite duration incident surge

Thus for time $0 < t < \tau$ only the first term in the expression is active and for $t \geq \tau$ both the terms are active. The rise in voltage is maximum at $t = \tau$ when the value will be

$$V''(t) = \frac{2VZ_2}{Z_1 + Z_2}\left[1 - \exp\left(-\frac{Z_1 + Z_2}{Z_1 Z_2 C}\tau\right)\right] - \frac{2VZ_2}{Z_1 + Z_2}(1 - e^0)$$

$$= \frac{2VZ_2}{Z_1 + Z_2}\left[1 - \exp\left(-\frac{Z_1 + Z_2}{Z_1 Z_2 C}\tau\right)\right] \qquad (7.17)$$

It is, therefore, clear that the attenuation in the magnitude of voltage for a short wave is much more rapid than for long wave.

We have seen that the effect of a shunt capacitor is to reduce the steepness and magnitude of the wave reaching an equipment. Since an inductor is dual to a capacitor, an inductor in series of the lines should give the same effect.

Example 7.4: *A 500 kV 2 μ sec rectangular surge on a line having a surge impedance of 350 ohms approaches a station at which the concentrated earth capacitance is 3000 pF. Determine the maximum value of the transmitted wave.*

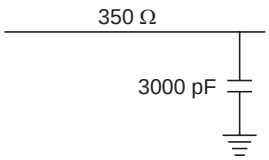

Fig. Ex.7.4

Solution: The diagram corresponding to the problem is as follows:

The maximum value of voltage will be

$$E'' = 2E\left[1 - \exp\left(-\frac{\tau}{ZC}\right)\right]$$

$$= 2 \times 500\left[1 - \exp\left(-\frac{2\times10^{-6}\times10^{12}}{350\times3000}\right)\right] = 2 \times 500\left[1 - \exp\left(-\frac{2\times10^{3}}{350\times3}\right)\right]$$

$$= 2 \times 500[1 - 0.15]$$

$$= 850 \text{ kV.}$$ **Ans.**

Example 7.5. *An inductance of 800 μH connects two sections of a transmission line each having a surge impedance of 350 ohms. A 500 kV 2μs rectangular surge travels along the line towards the inductance. Determine the maximum value of the transmitted wave.*

Solution: The maximum value of the transmitted surge is given by

$$E'' = E\left[1 - \exp\left(-\frac{2Z}{L}\tau\right)\right]$$

$$= 500\left[1 - \exp\left(-\frac{2\times350}{800}\times2\right)\right]$$

$$= 500\,[1 - e^{-0.875\times2}]$$

$$= 500\,[1 - e^{-1.750}]$$

$$= 500\,[1 - 0.173]$$

$$= 413.5 \text{ kV.}$$ **Ans.**

7.3.1 Attenuation of Travelling Waves

Let R, L, C and G be the resistance, inductance, capacitance and conductance respectively per unit length of a line (Fig. 7.18). Let the value of voltage and current waves at $x = 0$ be V_0 and I_0. Our objective is to find the values of voltage and current waves when they have travelled through a distance of x units over the overhead line. Let the time taken be t units when voltage and current waves are V and I respectively. To travel a distance of dx, let the time taken be dt. The equivalent circuit for the differential length dx of the line is shown in Fig. 7.19.

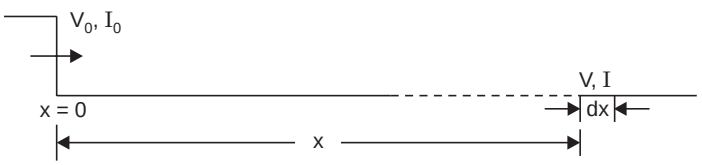

Fig. 7.18 Travelling wave on a lossy line

The power loss in the differential element is

$$dp = I^2R\,dx + V^2G\,dx \tag{7.18}$$

Also power at a distance x . $VI = p = I^2Z_n$

Differential power, $dp = -2IZ_n dI$ (7.19)

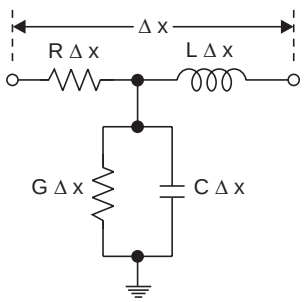

Fig. 7.19 Differential element of transmission line

where Z_n is the natural impedance of the line. Here negative sign has been assigned as there is reduction in power as the wave travels with time.

Equating the equation (7.18) and (7.19)

$$-2IZ_n dI = I^2Rdx + V^2Gdx$$
$$= I^2Rdx + I^2Z_n{}^2Gdx$$

or $$dI = -\frac{I(R + GZ_n^2)}{2Z_n}dx$$

or $$\frac{dI}{I} = -\frac{(R + GZ_n^2)}{2Z_n}dx$$

or $$\ln I = -\frac{(R + GZ_n^2)}{2Z_n}x + A$$

At $x = 0$, $I = I_0$, $\therefore \quad A = \ln I_0$

or $$\ln \frac{I}{I_0} = -\frac{R + GZ_n^2}{2Z_n}x = -ax \text{ (say)}$$

where $$a = \frac{R + GZ_n^2}{2Z_n}.$$

$\therefore$ $$I = I_0 e^{-ax}.$$ (7.20)

Similarly it can be proved that $V = V_0 e^{-ax}$. This shows that the current and voltage waves get attenuated exponentially as they travel over the line and the magnitude of attenuation depends upon the parameters of the line. Since the value of resistance depends not only on the size of the conductors but also on the shape and length of the waves. An empirical relation due to Foust and Menger takes into account the shape and length of the wave for calculating the voltage and current at any point on the line after it has travelled through a distance x units and is given as

$$V = \frac{V_0}{1 + KxV_0}$$ (7.21)

where x is in kms, V and V_0 are in kV and K is the attenuation constant, of value

$K = 0.00037$ for chopped waves
$= 0.00019$ of short-waves
$= 0.0001$ for long-waves.

Example 7.6. *A travelling wave of 50 kV enters an overhead line of surge impedance 400 ohms and conductor resistance 6 ohm per km. Determine (i) the value of the voltage wave when it has travelled through a distance of 50 km, and (ii) the power loss and the heat loss of the wave during the time required to traverse this distance. Neglect the losses in the insulation and assume a wave velocity of 3×10^5 km per second. Determine the corresponding values for a cable having surge impedance of 40 ohms and relative permittivity 4.*

Solution: (*i*) Since the line has some specific resistance, the wave as it travels gets attenuated in magnitude.

The magnitude of the wave is given by

$$e = e_0 \varepsilon^{-1/2^{(R/Z + GZ)\,x}}$$

where e = the value of voltage when travelled through a distance of x kilometres, R, G the resistance and leakance per kilometre length of the line and Z is the surge impedance, e_0 = initial magnitude of the surge voltage, ε the Naperian base.

Here in this problem $e_0 = 50$ kV, $x = 50$ km, $R = 6$ ohm and $Z = 400$ ohm and $G = 0.0$ mhos.

Substituting these values,

$$e = 50\varepsilon^{-1/2(6/400)50} = 50 \times^{-0.375} = 50 \times 0.69 = 34.5 \text{ kV.}$$

(*ii*) The power loss is the instantaneous quantity and is required to be calculated when the wave travels the distance of 50 km where the voltage magnitude is 34.5 kV.

$$\text{The power loss} = \frac{34.5 \times 34.5}{400} \times 1000 \text{ kW} = 2975 \text{ kW}$$

The heat loss is the integrated value of power over the distance (or time) the wave has travelled.

$$\text{Heat loss} = \int ei\, dt$$

Now $e = e_0 \varepsilon^{-1/2\, R/Z\, x}$ and similarly, $i = i_0 \varepsilon^{-1/2\, R/Z\, x}$.

Now, $x = vt$

$$\therefore \quad e = e_0\, \varepsilon^{-1/2}\, \frac{R}{Z}\, vt \quad \text{and} \quad i = i_0 \varepsilon^{-1/2}\, \frac{R}{Z}\, vt$$

Substituting these values, we get

$$\text{Heat loss} = \int_0^t e_0 i_0\, \varepsilon^{-(R/Z)vt\, dt}$$

where v = the velocity of the wave

$$t = \frac{x}{v} = \frac{50}{3 \times 10^5} = 16.67 \times 10^{-5} \text{ sec}$$

and

$$i_0 = \frac{e_0}{Z} = \frac{50 \times 1000}{4000} = 125 \text{ amps.}$$

$$\therefore \quad \text{Heat loss} = -\int_0^{16.67 \times 10^{-5}} 50 \times 125 \varepsilon^{-(R/Z)vt}\, dt$$

$$= -50 \times 125 \times \frac{400}{6 \times 3 \times 10^5} [e^{-0.75} - 1]$$

$$= 0.736 \text{ kJ or } 176 \text{ cal. } \textbf{Ans.}$$

7.4 CAPACITANCE SWITCHING

The switching of a capacitance such as disconnecting a line or a cable or a bank of capacitor poses serious problems in power systems in terms of abnormally high voltages across the circuit breaker contacts. Under this situation the current leads the voltage by about 90°. Assuming that the current interruption takes place when it is passing through zero value the capacitor will be charged to maximum voltage. Since the capacitorm is now isolated from the source, it retains its charge as shown in Fig. 7.20 (*c*) and because of trapping of this charge, half a cycle after the current zero the voltage across the circuit breaker contact is 2*V* which may prove to be dangerous and may result in the circuit breaker restrike. This is equivalent to closing the switch suddenly which will result into oscillations in the circuit at the natural frequency

$$f = \frac{1}{2\pi\sqrt{LC}}$$

The circuit condition corresponds to Fig. 7.20 (*e*). The only difference between the two circuits is that whereas in Fig. 7.20 the capacitor is charged to a voltage *V*, in Fig. 7.20 (*e*) it is assumed to be without charge. Therefore, the voltage across the capacitor reaches 3*V*. Since the source voltage is *V*, the voltage across the breaker contacts after another half cycle will be 4*V* which may cause another restrike. This phenomenon may theoretically continue indefinitely, increasing the voltage by successive increments of 2*V*. This may result into an external flashover or the failure of the capacitor. This is due to the inability of the circuit breaker to provide sufficient dielectric strength to the contacts to avoid restrikes after they are opened first.

This problem is practically solved by using air blast circuit breakers or multibreak breakers.

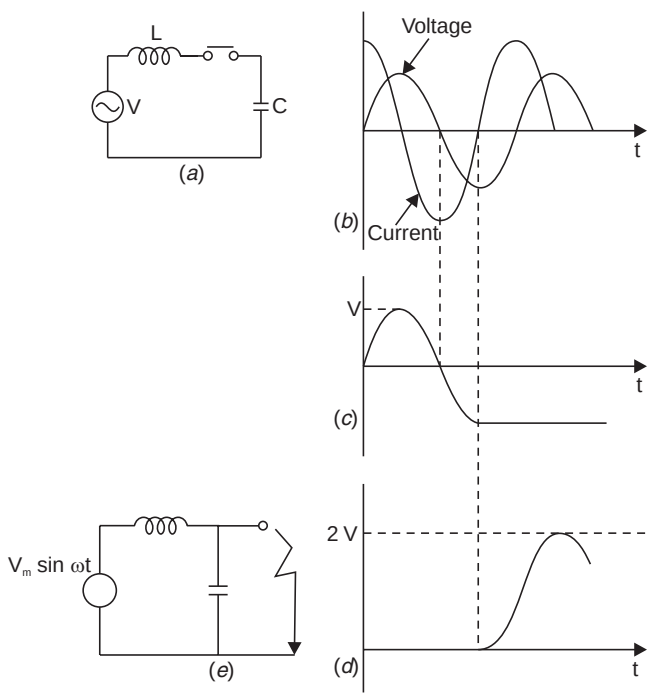

Fig. 7.20 (*a*) Equivalent circuit for capacitor switching; (*b*) System voltage and current; (*c*) Capacitor voltage; (*d*) Voltage across the switch; (*e*) Equivalent circuit for 3-ϕ fault.

7.5 OVER VOLTAGE DUE TO ARCING GROUND

Fig. 7.21 shows a 3-phase system with isolated neutral. The shunt capacitances are also shown. Under balanced conditions and complete transposed transmission lines, the potential of the neutral is near the ground potential and the currents in various phases through the shunt capacitors are leading their corresponding voltages by 90°. They are displaced from each other by 120° so that the net sum of the three currents is zero (Fig. 7.21). Say there is line-to-ground fault on one of the three phases (say phase '*c*'). The voltage across the shunt capacitor of that phase reduces to zero whereas those of the healthy phases become line-to-line voltages and now they are displaced by 60° rather than 120°. The net charging current now is three times the phase current under balanced conditions (Fig. 7.21 (*c*)). These currents flow through the fault and the windings of the alternator. The magnitude of this current is often sufficient to sustain an arc and, therefore, we have an arcing ground. This could be due to a flashover of a support insulator. Here this flashover acts as a switch. If the arc extinguishes when the current is passing through zero value, the capacitors in phases *a* and *b* are charged to line voltages. The voltage across the line and the grounded points of the post insulator will be the super-position of the capacitor voltage and the generator voltage and this voltage may be good enough to cause flashover which is equivalent to restrike in a circuit breaker. Because of the presence of the inductance of the generator winding, the capacitances will form an oscillatory circuit and these oscillations may build up to still higher voltages and the arc may reignite causing further transient disturbances which may finally lead to complete rupture of the post insulators.

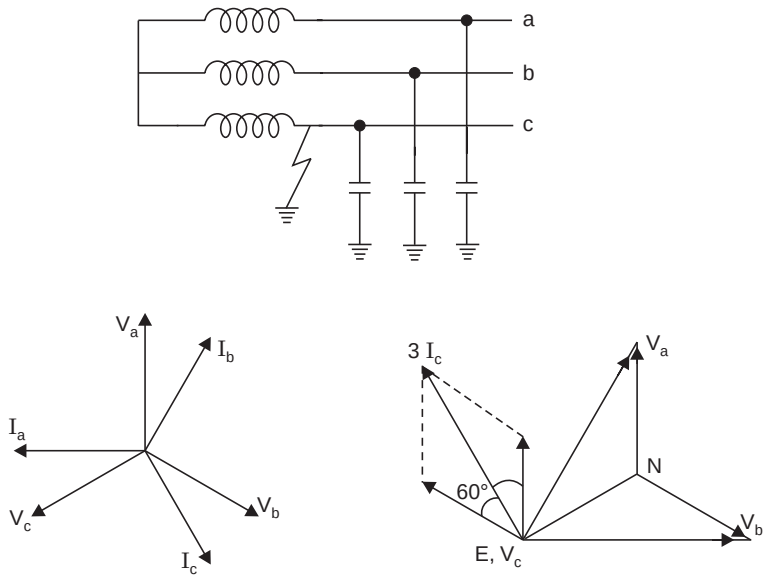

Fig. 7.21 (*a*) 3-phase system with isolated neutral; (*b*) Phasor diagram under healthy condition; (*c*) Phasor diagram under faulted condition.

7.6 LIGHTNING PHENOMENON

Lightning has been a source of wonder to mankind for thousands of years. Schonland points out that any real scientific search for the first time was made into the phenomenon of lightning by Franklin in 18th century.

Before going into the various theories explaining the charge formation in a thunder cloud and the mechanism of lightning, it is desirable to review some of the accepted facts concerning the thunder cloud and the associated phenomenon.

1. The height of the cloud base above the surrounding ground level may vary from 160 to 9,500 m. The charged centres which are responsible for lightning are in the range of 300 to 1500 m.

2. The maximum charge on a cloud is of the order of 10 coulombs which is built up exponentially over a period of perhaps many seconds or even minutes.

3. The maximum potential of a cloud lies approximately within the range of 10 MV to 100 MV.

4. The energy in a lightning stroke may be of the order of 250 kWhr.

5. Raindrops:

(*a*) Raindrops elongate and become unstable under an electric field, the limiting diameter being 0.3 cm in a field of 100 kV/cm.

(*b*) A free falling raindrop attains a constant velocity with respect to the air depending upon its size. This velocity is 800 cms/sec. for drops of the size 0.25 cm dia. and is zero for spray. This means that in case the air currents are moving upwards with a velocity greater than 800 cm/sec, no rain drop can fall.

(*c*) Falling raindrops greater than 0.5 cm in dia become unstable and break up into smaller drops.

(*d*) When a drop is broken up by air currents, the water particles become positively charged and the air negatively charged.

(*e*) When an ice crystal strikes with air currents, the ice crystal is negatively charged and the air positively charged.

Wilson's Theory of Charge Separation

Wilson's theory is based on the assumption that a large number of ions are present in the atmosphere. Many of these ions attach themselves to small dust particles and water particles. It also assumes that an electric field exists in the earth's atmosphere during fair weather which is directed downwards towards the earth (Fig. 7.22(*a*)). The intensity of the field is approximately 1 volt/cm at the surface of the earth and decreases gradually with height so that at 9,500 m it is only about 0.02 V/cm. A relatively large raindrop (0.1 cm radius) falling in this field becomes polarized, the upper side acquires a negative

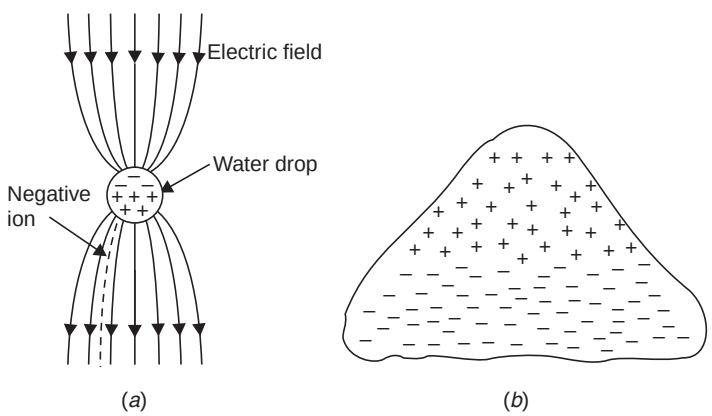

Fig. 7.22(*a*) Capture of negative ions by large falling drop; (*b*) Charge separation in a thunder cloud according to Wilson's theory.

charge and the lower side a positive charge. Subsequently, the lower part of the drop attracts –ve charges from the atmosphere which are available in abundance in the atmosphere leaving a preponderance of positive charges in the air. The upwards motion of air currents tends to carry up the top of the cloud, the +ve air and smaller drops that the wind can blow against gravity. Meanwhile the falling heavier raindrops which are negatively charged settle on the base of the cloud. It is to be noted that the selective action of capturing –ve charges from the atmosphere by the lower surface of the drop is possible. No such selective action occurs at the upper surface. Thus in the original system, both the positive and negative charges which were mixed up, producing essentially a neutral space charge, are now separated. Thus according to Wilson's theory since larger negatively charged drops settle on the base of the cloud and smaller positively charged drops settle on the uper positions of the cloud, the lower base of the cloud is negatively charged and the upper region is positively charged (Fig. 7.22(*b*)).

Simpson's and Scarse Theory

Simpson's theory is based on the temperature variations in the various regions of the cloud. When water droplets are broken due to air currents, water droplets acquire positive charges whereas the air is negatively charged. Also when ice crystals strike with air, the air is positively charged and the crystals negatively charged. The theory is explained with the help of Fig. 7.23.

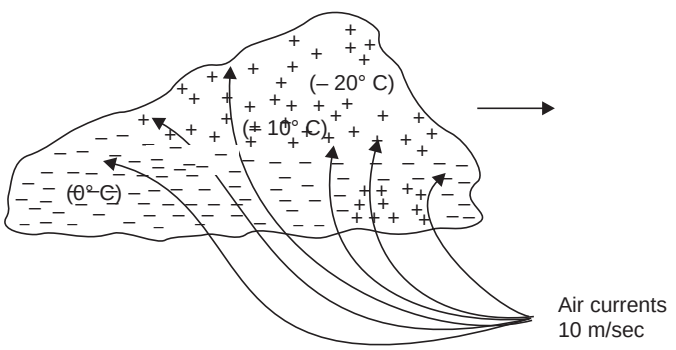

Fig. 7.23 Charge generation and separation in a thunder cloud according to Simpson's theory

Let the cloud move in the direction from left to right as shown by the arrow. The air currents are also shown in the diagram. If the velocity of the air currents is about 10 m/sec in the base of the cloud, these air currents when collide with the water particles in the base of the cloud, the water drops are broken and carried upwards unless they combine together and fall down in a pocket as shown by a pocket of positive charges (right bottom region in Fig. 7.23). With the collision of water particles we know the air is negatively charged and the water particles positively charged. These negative charges in the air are immediately absorbed by the cloud particles which are carried away upwards with the air currents. The air currents go still higher in the cloud where the moisture freezes into ice crystals. The air currents when collide with ice crystals the air is positively charged and it goes in the upper region of cloud whereas the negatively charged ice crystals drift gently down in the lower region of the cloud. This is how the charge is separated in a thundercloud. Once the charge separation is complete, the conditions are now set for a lightning stroke.

Mechanism of Lightning Stroke

Lightning phenomenon is the discharge of the cloud to the ground. The cloud and the ground form two plates of a gigantic capacitor and the dielectric medium is air. Since the lower part of the cloud is negatively charged, the earth is positively charged by induction. Lightning discharge will require the puncture of the air between the cloud and the earth. For breakdown of air at STP condition the electric field required is 30 kV/cm peak. But in a cloud where the moisture content in the air is large and also because of the high altitude (lower pressure) it is seen that for breakdown of air the electric field required is only 10 kV/cm. The mechanism of lightning discharge is best explained with the help of Fig. 7.24.

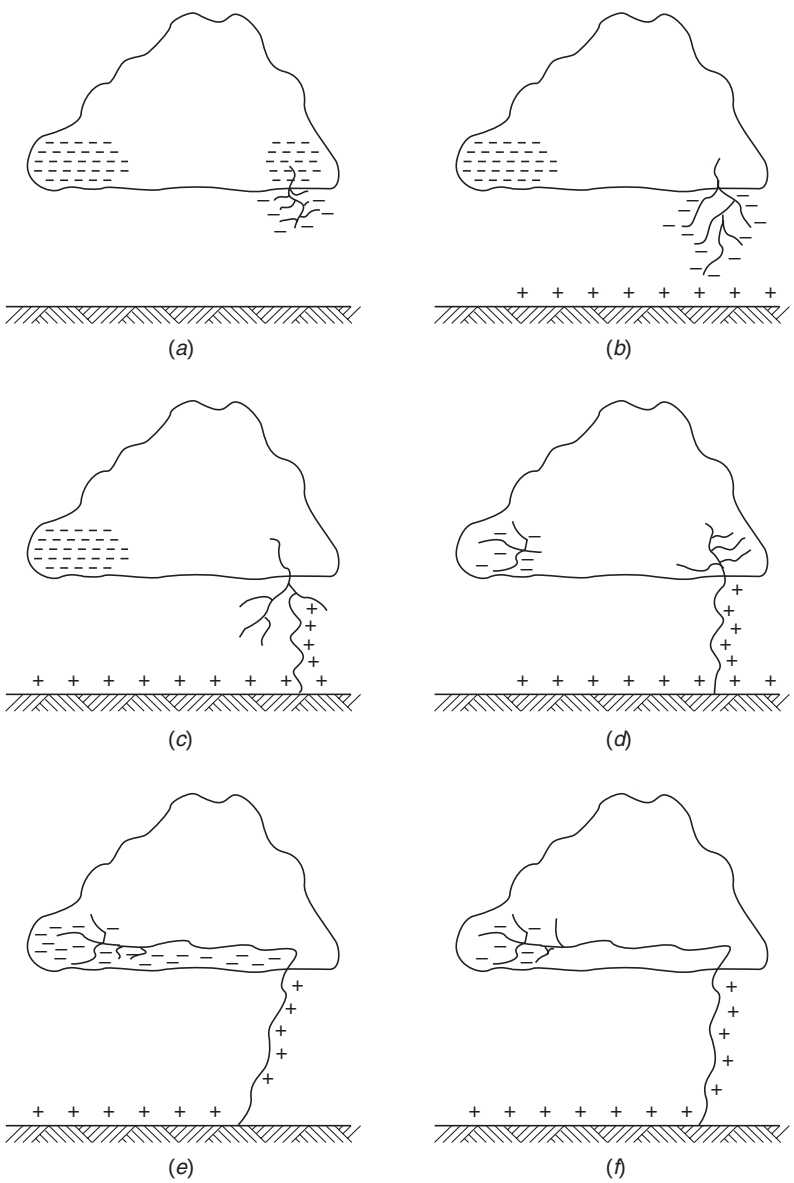

Fig. 7.24 Lightning mechanism

After a gradient of approximately 10 kV/cm is set up in the cloud, the air surrounding gets ionized. At this a streamer (Fig. 7.24(*a*)) starts from the cloud towards the earth which cannot be detected with the naked eye; only a spot travelling is detected. The current in the streamer is of the order of 100 amperes and the speed of the streamer is 0.16 m/μ sec. This streamer is known as pilot streamer because this leads to the lightning phenomenon. Depending upon the state of ionization of the air surrounding the streamer, it is branched to several paths and this is known as stepped leader (Fig. 7.24(*b*)). The leader steps are of the order of 50 m in length and are accomplished in about a microsecond. The charge is brought from the cloud through the already ionized path to these pauses. The air surrounding these pauses is again ionized and the leader in this way reaches the earth (Fig. 7.24(*c*)).

Once the stepped leader has made contact with the earth it is believed that a power return stroke (Fig. 7.24(*c*)) moves very fast up towards the cloud through the already ionized path by the leader. This streamer is very intense where the current varies between 1000 amps and 200,000 amps and the speed is about 10% that of light. It is here where the –ve charge of the cloud is being neutralized by the positive induced charge on the earth (Fig. 7.24(*d*)). It is this instant which gives rise to lightning flash which we observe with our naked eye. There may be another cell of charges in the cloud near the neutralized charged cell. This charged cell will try to neutralize through this ionised path. This streamer is known as dart leader (Fig. 7.24(*e*)). The velocity of the dart leader is about 3% of the velocity of light. The effect of the dart leader is much more severe than that of the return stroke.

The discharge current in the return streamer is relatively very large but as it lasts only for a few microseconds the energy contained in the streamer is small and hence this streamer is known as cold lightning stroke whereas the dart leader is known as hot lightning stroke because even though the current in this leader is relatively smaller but it lasts for some milliseconds and therefore the energy contained in this leader is relatively larger.

It is found that each thunder cloud may contain as many as 40 charged cells and a heavy lightning stroke may occur. This is known as multiple stroke.

7.7 LINE DESIGN BASED ON LIGHTNING

The severity of switching surges for voltage 400 kV and above is much more than that due to lightning voltages. All the same it is desired to protect the transmission lines against direct lightning strokes. The object of good line design is to reduce the number of outages caused by lightning. To achieve this the following actions are required.

(*i*) The incidence of stroke on to power conductor should be minimised.

(*ii*) The effect of those strokes which are incident on the system should be minimized.

To achieve (*i*) we know that lightning normally falls on tall objects; thus tall towers are more vulnerable to lightning than the smaller towers. In order to keep smaller tower height for a particular ground clearance, the span lengths will decrease which requires more number of towers and hence the associated accessories like insulators etc. The cost will go up very high. Therefore, a compromise has to be made so that adequate clearance is provided, at the same time keeping longer span and hence lesser number of towers.

With a particular number of towers the chances of incidence of lightning on power conductors can be minimized by placing a ground wire at the top of the tower structure. Refer to article 7.11 for ground wires.

Once the stroke is incident on the ground wire, the lightning current propagates in both the directions along the ground wire. The tower presents a discontinuity to the travelling waves; therefore they suffer reflections and refraction. The system is, then, equivalent to a line bifurcated at the tower point.

We know that the voltage and current transmitted into the tower will depend upon the surge impedance of the tower and the ground impedance (tower footing resistance) of the tower. If it is low, the wave reflected back up the tower will largely remove the potential existing due to the incident wave. In this way the chance of flashover is eliminated. If, on the other hand, the incident wave encounters a high ground impedance, positive reflection will take place and the potential on the top of the tower structure will be raised rather than lowered. It is, therefore, desired that for good line design high surge impedances in the ground wire circuits, the tower structures and the tower footing should be avoided. Various methods for lowering the tower footing resistances have been discussed in article 7.11

7.8 SWITCHING SURGE TEST VOLTAGE CHARACTERISTICS

Switching surges assume great importance for designing insulation of overhead lines operating at voltages more than 345 kV. It has been observed that the flashover voltage for various geometircal arrangements under unidirectional switching surge voltages decreases with increasing the front duration of the surge and the minimum switching surge corresponds to the range beetween 100 and 500 μ sec. However, time to half the value has no effect as flashover takes place either at the crest or before the crest of the switching surge. Fig. 7.25 gives the relationship between the critical flashover voltage per metre as a function of time to flashover for on a 3 m rod-rod gap and a conductor-plane gap.

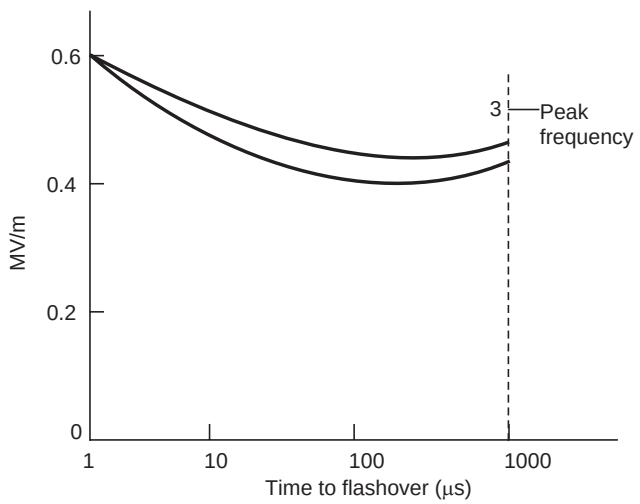

Fig. 7.25 Variation of F.O. V/m as a function of time to flashover

It can be seen that the standard impulse voltage (1/50 μ sec) gives highest flashover voltage and switching surge voltage with front time varyling between 100 to 500 μ sec has lower flashover voltage as compared to power frequency voltage. The flashover voltage not only depends upon the crest time but upon the gap spacing and humidity for the same crest time surges. It has been observed that the

switching surge voltage per meter gap length decreases drastically with increase in gap length and, therefore, for ultra high voltage system, costly design clearances are required. Therefore, it is important to know the behaviour of external insulation with different configuration under positive switching surges as it has been found that for nearly all gap configurations which are of paractical interest positive switching impulse is lower then the negative polarity switching impulse. It has also been observed that if the humidity varies between 3 to 16 gm/m^3, the breakdown voltage of positive and gaps increases approximately 1.7% for 1 gm/m^3 increase in absolute humidity.

For testing purposes the switching surge has been standardized with wave front time 250 μ sec ± 20% and wave tail time 2500 to ± 60% μ sec.

It is known that the shape of the electrode has a decided effect on the flashover voltage of the insulation. Lot of experimental work has been carried on the switching surge flash over voltage for long gaps using rod-plane gap and it has been attempeted to correlate these voltages with switching surge flash over voltage of other configuration electrodes. Several investigators have shown that if the gap length varies between 2 to 8 m, the 50% positive switching surge flash over for any configuration is given by the expression

$$V_{50} = 500\ kd^{0.6}\ \text{kV}$$

where d is the gap length in metres, k is the gap factor which is a function of electrode geometry. For rod-plane gaps $K = 1.0$. Thus K represents a propertionality contant and is equal to 50% flash over voltage of any gap geometry to that of a rod-plane gap for the same gap spacing *i.e.*,

$$k = \frac{V_{50}}{V_{50}\text{rod} - \text{plane gap}}$$

The expression for V_{50} applies to switching impulse of constant crest time. A more general expression which applies to longer times to crest has been proposed as follows :

$$V_{50} = \frac{3450\ K}{1 + \frac{8}{d}}\ \text{kV}$$

here K and d have the same meaning as in the equation above. The gap factor K depends mainly on the gap geomatry and hence on the field distribution in the gap. Table 7.1 gives values of K for different gap configurations.

Table 7.1

Gap factor k for different configurations

Configuration	*Figure*	*d = 2m*	*3m*	*4m*	*6m*
		K	K	K	K
Rod-plane	*a*	1	1	1	1
Conductor-plane	*b*	1.08	1.1	1.14	1.15
Rod-rod gap	*c*	1.27	1.26	1.21	1.14
Conductor cross arm	*d*	1.57	1.68	1.65	1.54
Rod-structure	*e*	1.08	—	1.07	1.06

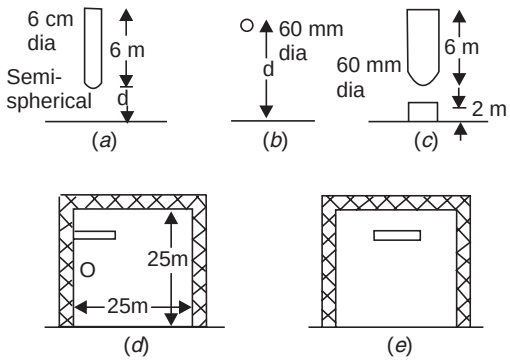

Fig. 7.26 Different gap geometries

Above two expressions for V_{50} and the Table 7.1 can be used to evaluate clearances in designing extra and ultra-high voltage lines and structures.

7.9 INSULATION COORDINATION AND OVERVOLTAGE PROTECTION

Insulation coordination means the correlation of the insulation of the various equipments in a power system to the insulation of the protective devices used for the protection of those equipments against overvoltages. In a power system various equipments like transformers, circuit breakers, bus supports etc. have different breakdown voltages and hence the volt-time characteristics. In order that all the equipments should be properly protected it is desired that the insulation of the various protective devices must be properly coordinated. The basic concept of insulation coordination is illustrated in Fig. 7.27. Curve *A* is the volt-time curve of the protective device and *B* the volt-time curve of the equipment to be protected. Fig. 7.27 shows the desired positions of the volt-time curves of the protecting device and the equipment to be protected. Thus, any insulation having a withstand voltage strength in excess of the insulation strength of curve *B* is protected by the protective device of curve *A*.

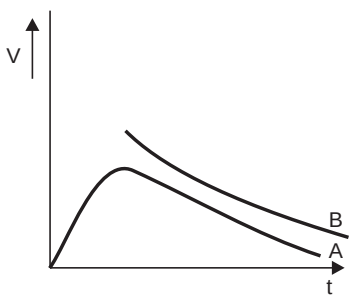

Fig. 7.27 Volt-time curve *A* (protecting device and) volt-time curve *B* (device to be protected)

The 'volt-time curve' expression will be used very frequently in this chapter. It is, therefore, necessary to understand the meaning of this expression.

7.9.1 Volt-Time Curve

The breakdown voltage for a particular insulation of flashover voltage for a gap is a function of both the magnitude of voltage and the time of application of the voltage. The volt-time curve is a graph showing the relation between the crest flashover voltages and the time to flashover for a series of impulse applications of a given wave shape. For the construction of volt-time curve the following procedure is adopted. Waves of the same shape but of different peak values are applied to the insulation whose volt-time curve is required. If flashover occurs on the front of the wave, the flashover point gives one point on the volt-time curve. The other possibility is that the flashover occurs just at the peak value

of the wave; this gives another point on the *V-T* curve. The third possibility is that the flashover occurs on the tail side of the wave. In this case to find the point on the *V-T* curve, draw a horizontal line from the peak value of this wave and also draw a vertical line passing through the point where the flashover takes place. The intersection of the horizontal and vertical lines gives the point on the *V-T* curve. This procedure is nicely shown in Fig. 7.28.

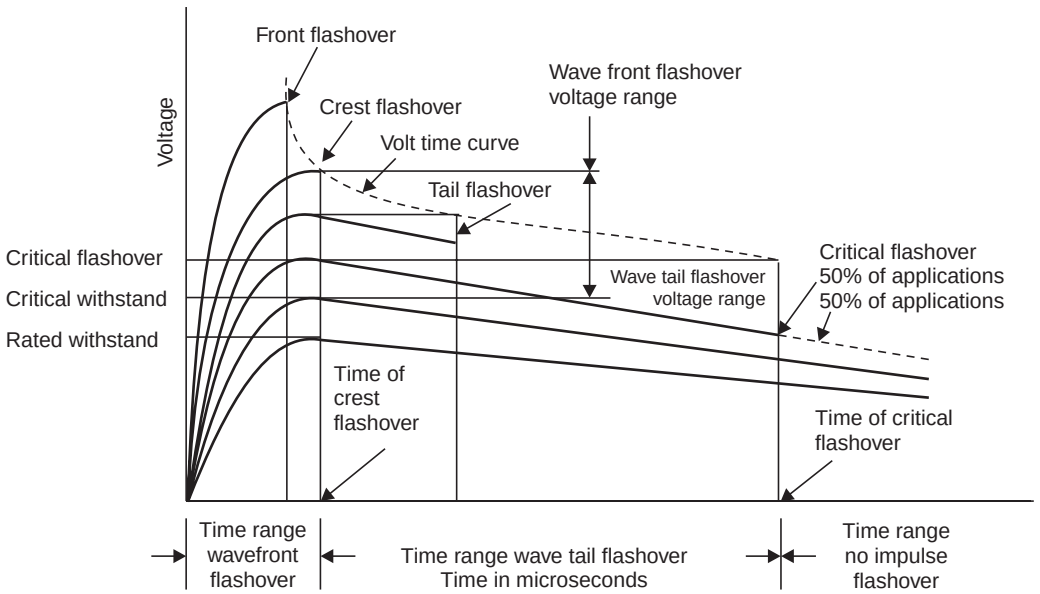

Fig. 7.28 Volt-time curve (construction)

The overvoltages against which coordination is required could be caused on the system due to system faults, switching operation or lightning surges. For lower voltages, normally upto about 345 kV, over voltages caused by system faults or switching operations do not cause damage to equipment insulation although they may be detrimental to protective devices. Overvoltages caused by lightning are of sufficient magnitude to affect the equipment insulation whereas for voltages above 345 kV it is these switching surges which are more dangerous for the equipments than the lightning surges.

The problem of coordinating the insulation of the protective equipment involves not only guarding the equipment insulation but also it is desired that the protecting equipment should not be damaged.

To assist in the process of insulation coordination, standard insulation levels have been recommended. These insulation levels are defined as follows.

Basic impulse insulation levels (BIL) are reference levels expressed in impulse crest voltage with a standard wave not longer than 1.2/50 μ sec wave. Apparatus insulation as demonstrated by suitable tests shall be equal to or greater than the basic insulation level.

The problem of insulation coordination can be studied under three steps:

1. Selection of a suitable insulation which is a function of reference class voltage (*i.e.,* 1.05 × operating voltage of the system). Table 7.2 gives the BIL for various reference class voltages.

Table 7.2 Basic impulse insulation levels

Reference class kV	*Standard Basic impulse level kV*	*Reduced insulation levels*
23	150	
34.5	200	
46	250	
69	350	
92	450	
115	550	450
138	650	550
161	750	650
196	900	
230	1050	900
287	1300	1050
345	1550	1300

2. The design of the various equipments such that the breakdown or flashover strength of all insulation in the station equals or exceeds the selected level as in (1).

3. Selection of protective devices that will give the apparatus as good protection as can be justified economically.

The above procedure requires that the apparatus to be protected shall have a withstand test value not less than the kV magnitude given in the second column of Table 7.2, irrespective of the polarity of the wave positive or negative and irrespective of how the system was grounded.

The third column of the table gives the reduced insulation levels which are used for selecting insulation levels of solidly grounded systems and for systems operating above 345 kV where switching surges are of more importance than the lightning surges. At 345 kV, the switching voltage is considered to be 2.7 p.u., *i.e.*, 345 × 2.7 = 931.5 kV which corresponds to the lightning level. At 500 kV, however, 2.7 p.u. will mean 2.7 × 500 = 1350 kV switching voltage which exceeds the lightning voltage level. Therefore, the ratio of switching voltage to operating voltage is reduced by using the switching resistances between the C.B. contacts. For 500 kV it is has been possible to obtain this ratio as 2.0 and for 765 kV it is 1.7. With further increase in operating voltages, it is hoped that the ratio could be brought to 1.5. So, for switching voltages the reduced levels in third column are used *i.e.*, for 345 kV, the standard BIL is 1550 kV but if the equipment can withstand even 1425 kV or 1300 kV it will serve the purpose.

Fig. 7.29 gives the relative position of the volt-time curves of the various equipments in a substation for proper coordination. To illustrate the selection of the BIL of a transformer to be operated on a 138 kV system assume that the transformer is of large capacity and its star point is solidly

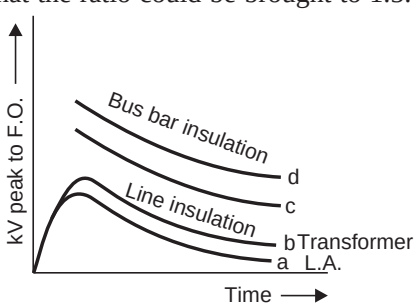

Fig. 7.29 Volt-time curves

grounded. The grounding is such that the line-to-ground voltage of the healthy phase during a ground fault on one of the phases is say 74% of the normal *L-L* voltage. Allowing for 5% overvoltage during operating conditions, the arrester rms operating voltage will be 1.05 × 0.74 × 138 = 107.2 kV. The nearest standard rating is 109 kV. The characteristic of such a L.A. is shown in Fig. 7.30. From the figure the breakdown value of the arrester is 400 kV. Assuming a 15% margin plus 35 kV between the insulation levels of L.A. and the transformer, the insulation level of transformer should be at least equal to 400 + 0.15 × 400 + 35 = 495 kV. From Fig. 7.30 (or from the table the reduced level of transformer for 138 kV is 550 kV) the insulation level of transformer is 550 kV; therefore a lightning arrester of 109 kV rating can be applied.

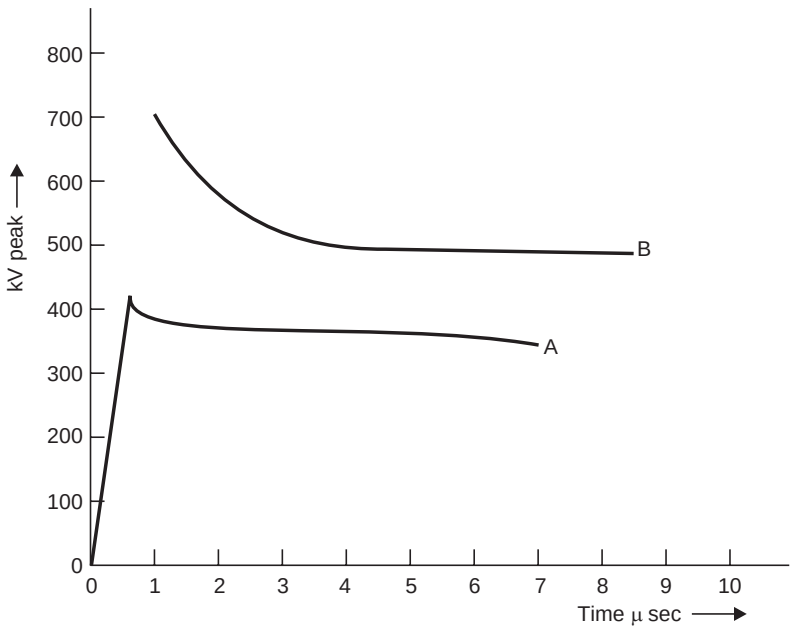

Fig. 7.30 Coordination of transformer insulation with lightning arrester:
A–Lightning arrester 109 kV, *B*–Transformer insulation withstand characteristic

It is to be noted that low voltage lines are not as highly insulated as higher voltage lines so that lightning surges coming into the station would normally be much less than in a higher voltage station because the high voltage surges will flashover the line insulation of low voltage line and not reach the station.

The traditional approach to insulation coordination requires the evaluation of the highest overvoltages to which an equipment may be subjected during operation and selection of standardized value of withstand impulse voltage with suitable safety margin. However, it is realized that overvoltages are a random phenomenon and it is uneconomical to design plant with such a high degree of safety that they sustain the infrequent ones. It is also known that insulation designed on this basis does not give 100% protection and insulation failure may occur even in well designed plants and, therefore, it is desired to limit the frequency of insulation failures to the most economical value taking into account equipment cost and service continuity. Insulation coordination, therefore, should be based on evaluation and limitation of the risk of failure than on the prior choice of a safety margin.

The modern practice, therefore, is to make use of probabilistic concepts and statistical procedures especially for very high voltage equipments which might later on be extended to all cases where a close adjustment of insulation to system conditions proves economical. The statistical methods even though laborious are quite useful.

7.9.2 Statistical Methods for Insulation Coordination

Both the over voltages due to lightning or switching and the breakdown strength of the insulating media are of statistical nature. Not all lightning or switching surges are dangerous to the insulation and particular specimen need not necessarily flashover or puncture at a particular voltage. Therefore, it is important to design the insulation of the various equipments to be protected and the devices used for protection not for worst possible condition but for worst probable condition as the cost of insulation for system of the voltage more than 380 kV are proportional to square of the voltage and, therefore any small saving in insulation will result in a large sums when considered for such large modern power system. This, however, would involve some level of risk failure. It is desired to accept some level of risk of failure than to design a risk-free but a very costly system.

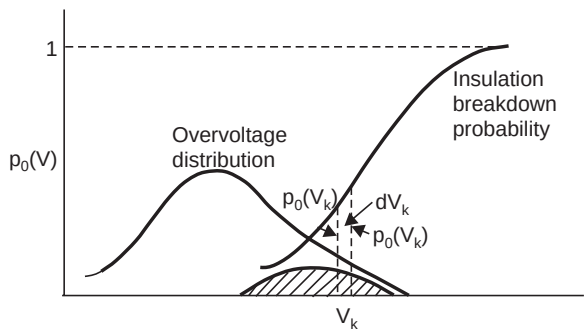

Fig. 7.31 Overvoltage distribution and Insulation breakdown probability

The statistical methods, however, call for a very rigorous experimentation and analysis work so as to find probability of occurence of overvoltages and probability of failure of insulation. It is found that the distribution of breakdown for a given gap follows with some exceptions approximately normal or Gaussian distribution. Similarly the distribution of over voltages on the system also follows the Gaussian distribution. In order to coordinate electrical stresses due to overvoltages with the electrical strengths of the dielectric media, it has been found convenient to represent overvoltage distribution in the form of probability density function and the insulation breakdown probability by the cumulative distribution function as shown in Fig. 7.31.

Suppose $P_0(V_k)$ is the probability density of an overvoltage V_k and $P_0(V_k)\, dV_k$ the probability of occurence of the over voltages having a peak value V_k. To obtain the probability to disruptive discharges due to these overvoltages having a value between V_k and $V_k + dV_k$, their probability of occurrence $P_0(V_k)\, dV_k$, shall be multiplied by $P_b(V_k)$ that an impulse of the given type and of value V_k will produce a discharge. The resultant probability or risk of failure for overvoltage between V_k and $V_k + dV_k$ is thus,

$$dR = P_b(V_k)\, P_0(V_k)\, dV_k$$

For the total voltage range we obtain the total probability of failure or risk of failure.

$$R = \int_0^\infty P_b(V_k)\, P_0(V_k) dV_k$$

The risk of failure will thus be given by the shaded area under the curve. In actual practice, however, it is uneconomical to use the complete distribution functions for the occurrence of overvoltage and for the withstand of insulation and, thereforem, a compromise solution is adopted as shown in Fig. 7.32 (*a*) and (*b*). Fig. 7.32 shows probability of occurrence of overvoltages which will result into breakdown, by the shaded area for voltage greater than V_s known as statistical overvoltage.

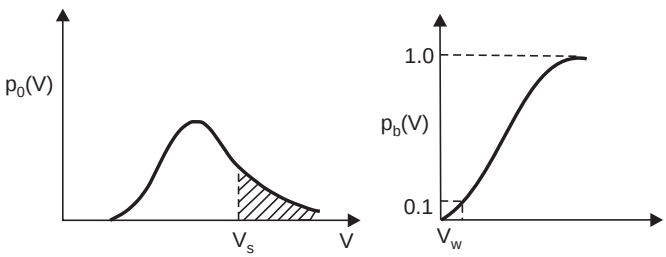

Fig. 7.32 Reference probabilities for overvoltage and for insulation withstand voltage

In Fig. 7.32(*b*) V_w is the withstand voltage which results in flashover only in 10% of applications and for remaining 90% of applied impulsed, no breakdown of insulation occurs. This voltage is known as statistical withstand voltage V_w.

Fig. 7.33 (*a*) to (*c*) show the functions $P_b(V)$ and $P_0(V)$ plotted for three different cases of insulation strength, keeping the overvoltage distribution the same. The density function $P_0(V_k)$ is the same in (*a*) to (*c*) whereas the cumulative function giving the undetermined withstand voltage is gradually shifted along the *V*-axis towards high values of *V*. The shifting of the cumulative distribution curve to right is equivalent to increasing the insulation strength by either using thicker insulation or material of high dielectric strength.

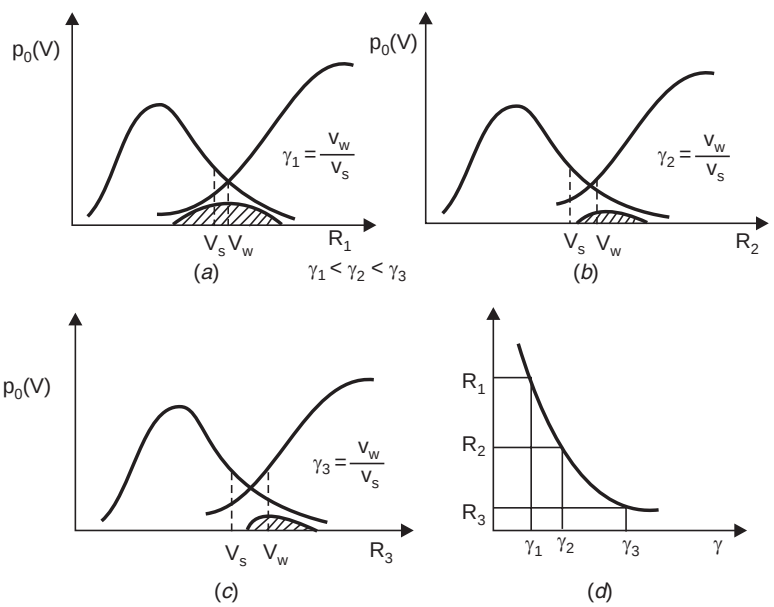

Fig. 7.33 Risk of failure as a function of statistical safety factor

Let the statistical factor of safety be defined as $\gamma = V_w/V_s$ and as the withstand characteristic is shifted towards right, the statistical factor of safety increases and hence the risk of failure decreases as shown in Fig. 7.33 (*d*). However, the cost of insulation goes up as the factor of safety is increased.

7.10 OVERVOLTAGE PROTECTION

The causes of overvoltages in the system have been studied extensively in previous sections. Basically, there are two sources: (*i*) external overvoltages due to mainly lightning, and (*ii*) internal overvoltages mainly due to switching operation. The system can be protected against external overvoltages using what are known as shielding methods which do not allow an arc path to form between the line conductors and ground, thereby giving inherent protection in the line design. For protection against internal voltages normally non-shielding methods are used which allow an arc path between the ground structure and the line conductor but means are provided to quench the arc. The use of ground wire is a shielding method whereas the use of spark gaps, and lightning arresters are the non-shielding methods. We will study first the non-shielding methods and then the shielding methods. However, the non-shielding methods can also be used for external over voltages.

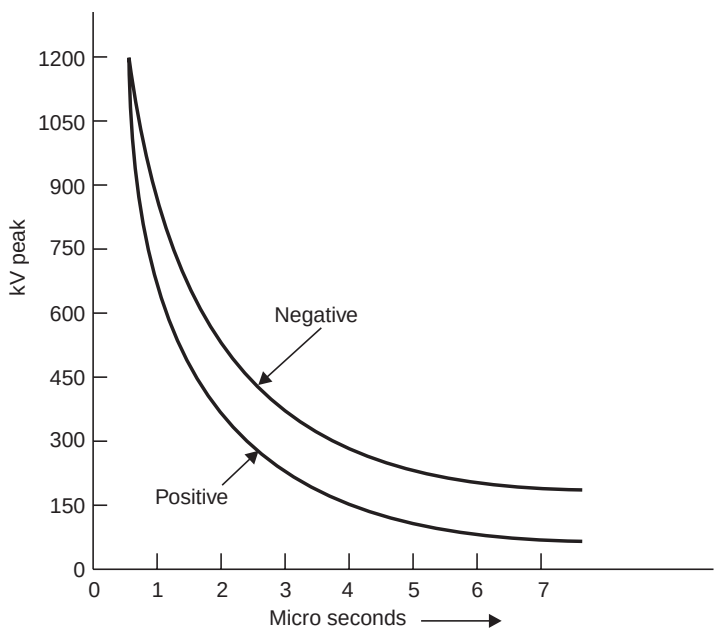

Fig. 7.34 Volt-time curves of gaps for positive and negative polarity

The non-shielding methods are based upon the principle of insulation breakdown as the overvoltage is incident on the protective device; thereby a part of the energy content in the overvoltage is discharged to the ground through the protective device. The insulation breakdown is not only a function of voltage but it depends upon the time for which it is applied and also it depends upon the shape and size of the electrodes used. The steeper the shape of the voltage wave, the larger will be the magnitude of voltage required for breakdown; this is because an expenditure of energy is required for the rupture of any dielectric, whether gaseous, liquid or solid, and energy involves time. The energy

criterion for various insulations can be compared in terms of a common term known as Impulse Ratio which is defined as the ratio of breakdown voltage due to an impulse of specified shape to the breakdown voltage at power frequency. The impulse ratio for sphere gap is unity because this gap has a fairly uniform field and the breakdown takes place on the field ionization phenomenon mainly whereas for a needle gap it varies between 1.5 to 2.3 depending upon the frequency and gap length. This ratio is higher than unity because of the non-uniform field between the electrodes. The impulse ratio of a gap of given geometry and dimension is greater with solid than with air dielectric. The insulators should have a high impulse ratio for an economic design whereas the lightning arresters should have a low impulse ratio so that a surge incident on the lightning arrester may be-by passed to the ground instead of passing it on to the apparatus.

The volt-time characteristics of gaps having one electrode grounded depend upon the polarity of the voltage wave. From Fig. 7.34 it is seen that the volt-time characteristic for positive polarity is lower than the negative polarity, *i.e.* the breakdown voltage for a negative impulse is greater than for a positive because of the nearness of earthed metal or of current carrying conductors. For post insulators the negative polarity wave has a high breakdown value whereas for suspension insulators the reverse is true.

Horn Gap

The horn gap consists of two horn-shaped rods separated by a small distance. One end of this is connected to be line and the other to the earth as shown in Fig. 7.35, with or without a series resistance. The choke connected between the equipment to be protected and the horn gap serves two purposes: (*i*) The steepness of the wave incident on the equipment to be protected is reduced. (*ii*) It reflects the voltage surge back on to the horn.

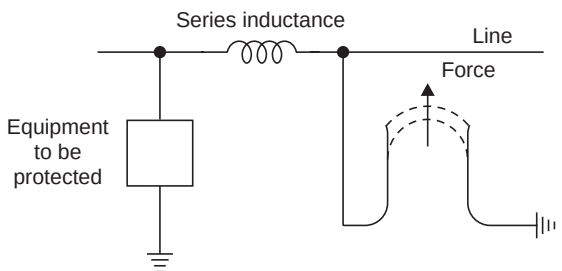

Fig. 7.35 Horn gap connected in the system for protection

Whenever a surge voltage exceeds the breakdown value of the gap a discharge takes place and the energy content in the rest part of the wave is by-passed to the ground. An arc is set up between the gap, which acts like a flexible conductor and rises upwards under the influence of the electro-magnetic forces, thus increasing the length of the arc which eventually blows out.

There are two major drawbacks of the horn gap; (*i*) The time of operation of the gap is quite large as compared to the modern protective gear. (*ii*) If used on isolated neutral the horn gap may constitute a vicious kind of arcing ground. For these reasons, the horn gap has almost vanished from important power lines.

Surge Diverters

The following are the basic requirements of a surge diverter:

(*i*) It should not pass any current at normal or abnormal (normally 5% more than the normal voltage) power frequency voltage.

(*ii*) It should breakdown as quickly as possible after the abnormal high frequency voltage arrives.

(*iii*) It should not only protect the equipment for which it is used but should discharge the surge current without damaging itself.

(*iv*) It should interrupt the power frequency follow current after the surge is discharged to ground.

There are mainly three types of surge diverters: (*i*) Rod gap, (*ii*) Protector tube or expulsion type of lightning arrester, (*iii*) Valve type of lightning arrester.

Rod gap

This type of surge diverter is perhaps the simplest, cheapest and most rugged one. Fig. 7.36 shows one such gap for a breaker bushing. This may take the form of arcing ring. Fig. 7.37 shows the breakdown characteristics (volt-time) of a rod gap. For a given gap and wave shape of the voltage, the time for breakdown varies approximately inversely with the applied voltage.

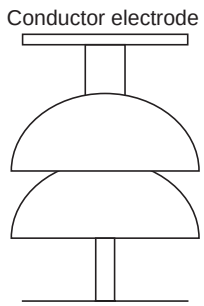

Fig. 7.36 A rod gap

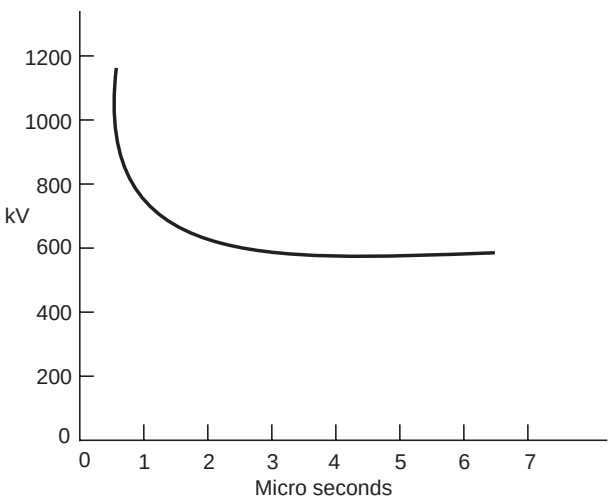

Fig. 7.37 Volt-time characteristic of rod gap

The time to flashover for positive polarity are lower than for negative polarities. Also it is found that the flashover voltage depends to some extent on the length of the lower (grounded) rod. For low values of this length there is a reasonable difference between positive (lower value) and negative flashover voltages. Usually a length of 1.5 to 2.0 times the gap spacing is good enough to reduce this difference to a reasonable amount. The gap setting normally chosen is such that its breakdown voltage is not less than 30% below the voltage withstand level of the equipment to be protected.

Even though rod gap is the cheapest form of protection, it suffers from the major disadvantage that it does not satisfy one of the basic requirements of a lightning arrester listed at no. (*iv*) *i.e.*, it does not interrupt the power frequency follow current. This means that every operation of the rod gap results

in a *L-G* fault and the breakers must operate to de-energize the circuit to clear the flashover. The rod gap, therefore, is generally used as back up protection.

Expulsion type of lightning arrester

An improvement of the rod gap is the expulsion tube which consists of (*i*) a series gap (1) external to the tube which is good enough to withstand normal system voltage, thereby there is no possibility of corona or leakage current across the tube; (*ii*) a tube which has a fibre lining on the inner side which is a highly gas evolving material; (*iii*) a spark gap (2) in the tube; and (*iv*) an open vent at the lower end for the gases to be expelled (Fig. 7.38). It is desired that the breakdown voltage of a tube must be lower than that of the insulation for which it is used. When a surge voltage is incident on the expulsion tube the series gap is spanned and an arc is formed between the electrodes within the tube.

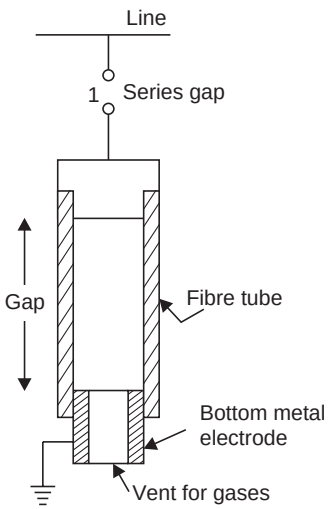

Fig. 7.38 Expulsion type lightning arrester

The heat of the arc vaporizes some of the organic material of the tube wall causing a high gas pressure to build up in the tube. The resulting neutral gas creates lot of turbulence within the tube and is expelled out from the open bottom vent of the tube and it extinguishes the arc at the first current zero. At this instant the rate of build up of insulation strength is greater than the RRRV. Very high currents have been interrupted using these tubes. The breakdown voltage of expulsion tubes is slightly lower than for plain rod gaps for the same spacing. With each operation of the tube the diameter of the tube (fibre lining) increases; thereby the insulation characteristics of the tube will lower down even though not materially. The volt-time characteristics (Fig. 7.39) of the expulsion tube are somewhat better than the rod gap and have the ability to interrupt power voltage after flashover.

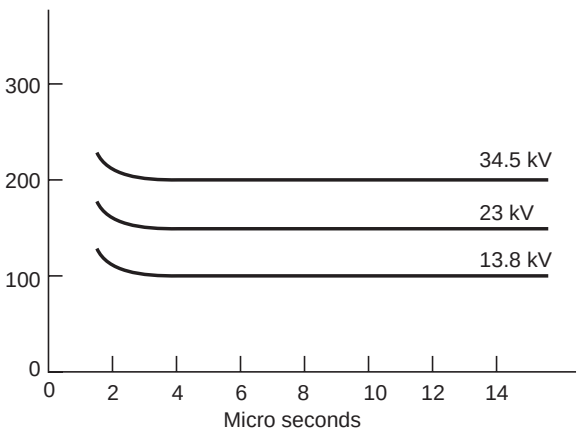

Fig. 7.39 Volt-time characteristic of expulsion gaps

Valve type lightning arresters

An improved but more expensive surge diverter is the valve type of lightning arrester or a non-linear surge diverter. A porcelain bushing (Fig. 7.40) contains a number of series gaps, coil units and the

valve elements of the non-linear resistance material usually made of silicon carbide disc, the latter possessing low resistance to high currents and high resistance to low currents. The characteristic is usually expressed as $I = KV^n$ where n lies between 2 and 6 and K is constant, a function of the geometry and dimension of the resistor. The non-linear characteristic is attributed to the properties of the electrical contacts between the grains of silicon carbide. The discs are 90 mm in dia and 25 mm thick. A grading ring or a high resistance is connected across the disc so that the system voltage is evenly distributed over the discs. The high resistance keeps the inner assembly dry due to some heat generated.

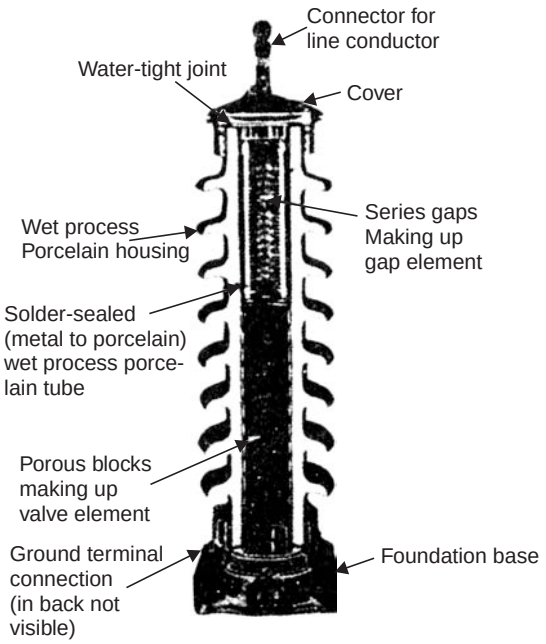

Fig. 7.40 Valve-type lightning arrester

Figure 7.41 shows the volt-ampere characteristics of a non-linear resistance of the required type. The closed curve represents the dynamic characteristic corresponding to the application of a voltage surge whereas the dotted line represents the static characteristic. The voltage corresponding to the horizontal tangent to the dynamic characteristic is known as the residual voltage (IR drop) and is the peak value of the voltage during the discharge of the surge current. This voltage varies from 3 kV to 6 kV depending upon the type of arrester *i.e.*, whether station or line type, the magnitude and wave shape of the discharge current. The spark gaps are so designed that they give an impulse ratio of unity to the surge diverter and as a result they are unable to interrupt high values of current and the follow up currents are limited to 20 to 30 *A*. The impulse breakdown strength of a diverter is smaller than the residual voltage, and therefore, from the point of view of insulation coordination residual voltage decides the protection level.

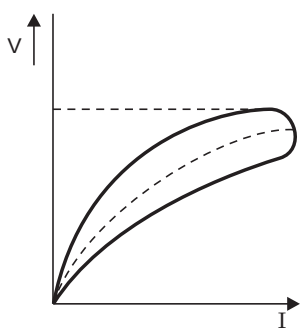

Fig. 7.41 Volt-ampere characteristic of valve-type LA

The operation of the arrester can be easily understood with the help of Fig. 7.42 (*a*) and (*b*). When a surge voltage is incident at the terminal of the arrester it causes the two gap units to flashover, thereby a path is provided to the surge to the ground through the coil element and the non-linear resistor element. Because of the high frequency of the surge, the coil develops sufficient voltage across its terminals to cause the by-pass gap to flashover. With this the coil is removed from the circuit and the voltage across the *LA* is the *IR* drop due to the non-linear element. This condition continues till power frequency currents follow the preionized path. For power frequency the impedance of the coil is very low and, therefore, the arc will become unstable and the current will be transferred to the coil (Fig. 7.42 (*b*)). The magnetic field developed by the follow current in the coil reacts with this current in the arcs of the gap assemblies, causing them to be driven into arc quenching chambers which are an integral part of the gap unit. The arc is extinguished at the first current zero by cooling and lengthening the arc and also because the current and voltage are almost in phase. Thus the diverter comes back to normal state after discharging the surge to the ground successfully.

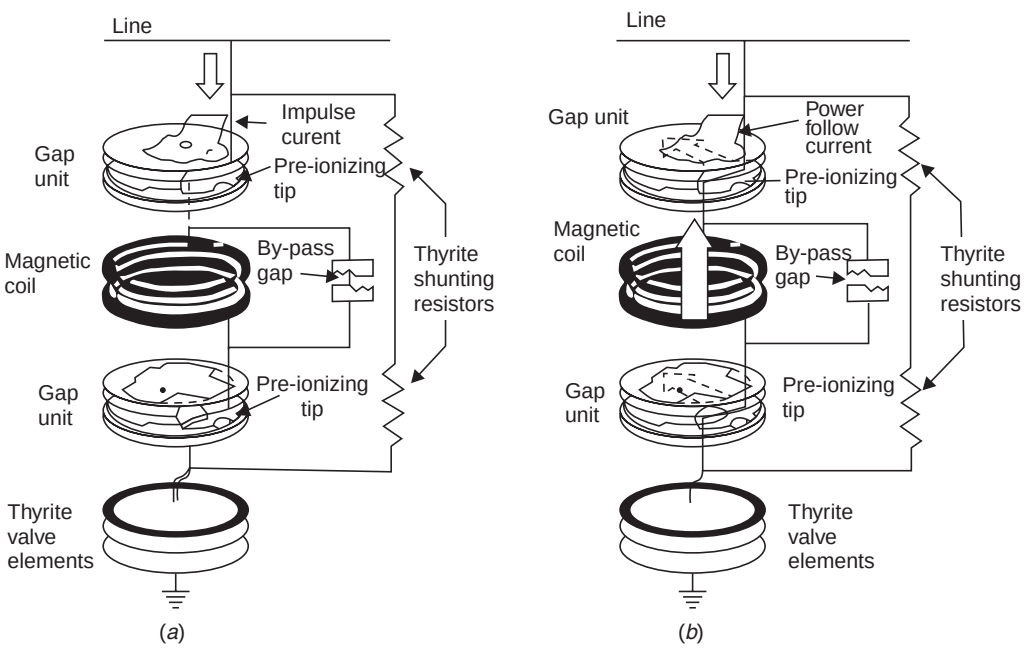

Fig. 7.42 Schematic diagram of valve-type arrester indicating path of (*a*) Surge current, (*b*) Follow current.

Location of lightning arresters

The normal practice is to locate the lightning arrester as close as possible to the equipment to be protected. The following are the reasons for the practice: (*i*) This reduces the chances of surges entering the circuit between the protective equipment and the equipment to be protected. (*ii*) If there is a distance between the two, a steep fronted wave after being incident on the lightning arrester, which sparks over corresponding to its spark over voltage, enters the transformer after travelling over the lead between the two. The wave suffers reflection at the terminal and, therefore, the total voltage at the terminal of the transformer is the sum of reflected and the incident voltage which approaches nearly twice the incident voltage *i.e.,* the transformer may experience a surge twice as high as that of the

lightning arrester. If the lightning arrester is right at the terminals this could not occur. (*iii*) If L is the inductance of the lead between the two, and IR the residual voltage of the lightning arrester, the voltage incident at the transformer terminal will be

$$V = IR + L\frac{di}{dt}$$

where di/dt is the rate of change of the surge current.

It is possible to provide some separation between the two, where a capacitor is connected at the terminals of the equipment to be protected. This reduces the steepness of the wave and hence the rate di/dt and this also reduces the stress distribution over the winding of the equipment.

There are three classes of lightning arresters available:

(*i*) *Station type:* The voltage ratings of such arresters vary from 3 kV to 312 kV and are designed to discharge currents not less than 100,000 amps. They are used for the protection of substation and power transformers.

(*ii*) *Line type:* The voltage ratings vary from 20 kV to 73 kV and can discharge currents between 65,000 amps and 100,000 amps. They are used for the protection of distribution transformers, small power transformers and sometimes small substations.

(*iii*) *Distribution type:* The voltage ratings vary from 8 kV to 15 kV and can discharge currents upto 65,000 amperes. They are used mainly for pole mounted substation for the protection of distribution transformers upto and including the 15 kV classification.

Rating of lightning arrester

A lightning arrester is expected to discharge surge currents of very large magnitude, thousands of amperes, but since the time is very short in terms of microseconds, the energy that is dissipated through the lightning arrester is small compared with what it would have been if a few amperes of power frequency current had been flown for a few cycles. Therefore, the main considerations in selecting the rating of a lightning arrester is the line-to-ground dynamic voltage to which the arrester may be subjected for any condition of system operation. An allowance of 5% is normally assumed, to take into account the light operating condition under no load at the far end of the line due to Ferranti effect and the sudden loss of load on water wheel generators. This means an arrester of 105% is used on a system where the line to ground voltage may reach line-to-line value during line-to-ground fault condition.

The overvoltages on a system as is discussed earlier depend upon the neutral grounding condition which is determined by the parameters of the system. We recall that a system is said to be solidly grounded only if

$$\frac{R_0}{X_1} \leq 1$$

and

$$\frac{X_0}{X_1} \leq 3$$

and under this condition the line to ground voltage during a *L-G* fault does not exceed 80% of the *L-L* voltage and, therefore, an arrester of (80% + 0.05 × 80%) = 1.05 × 80% = 84% is required. This is the extreme situation in case of solidly grounded system. In the same system the voltage may be less than 80%; say it may be 75%. In that case the rating of the lightning arrester will be 1.05 × 75% = 78.75%.

The overvoltages can actually be obtained with the help of precalculated curves. One set of curves corresponding to a particular system is given in Fig. 7.43.

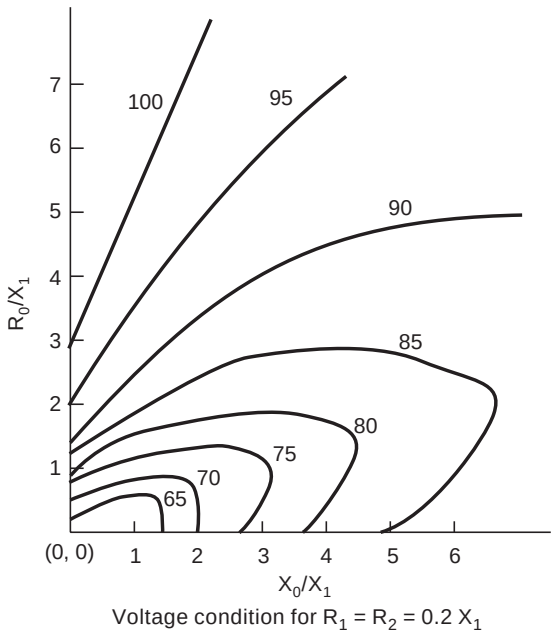

Fig. 7.43 Maximum line-to-ground voltage at fault location for grounded neutral system under any fault condition

For system grounded through Peterson coil, the overvoltages may be 100% if it is properly tuned and, therefore, it is customary to apply an arrester of 105% for such systems. Even though there is a risk of overvoltage becoming more than 100% if it is not properly tuned, but it is generally not feasible to select arresters of sufficiently high rating to eliminate all risks of arrester damage due to these reasons. The voltage rating of the arrester, therefore, ranges between 75% to 105% depending upon the neutral grounding condition.

So far we have discussed the non-shielding method. We now discuss the shielding method *i.e.*, the use of ground wires for the protection of transmission lines against direct lightning strokes.

7.11 GROUND WIRES

The ground wire is a conductor running parallel to the power conductors of the transmission line and is placed at the top of the tower structure supporting the power conductors (Fig. 7.44 (*a*)). For horizontal configuration of the power line conductors, there are two ground wires to provide effective shielding to power conductors from direct lightning stroke whereas in vertical configuration there is one ground wire. The ground wire is made of galvanized steel wire or in the modern high voltage transmission lines ACSR conductor of the same size as the power conductor is used. The material and size of the conductor are more from mechanical consideration rather than electrical. A reduction in the effective ground resistance can be achieved by other relatively simpler and cheaper means. The ground wire serves the following purposes: (*i*) It shields the power conductors from direct lightning strokes. (*ii*) Whenever a

lightning stroke falls on the tower, the ground wires on both sides of the tower provide parallel paths for the stroke, thereby the effective impedance (surge impedance) is reduced and the tower top potential is relatively less. (*iii*) There is electric and magnetic coupling between the ground wire and the power conductors, thereby the changes of insulation failure are reduced.

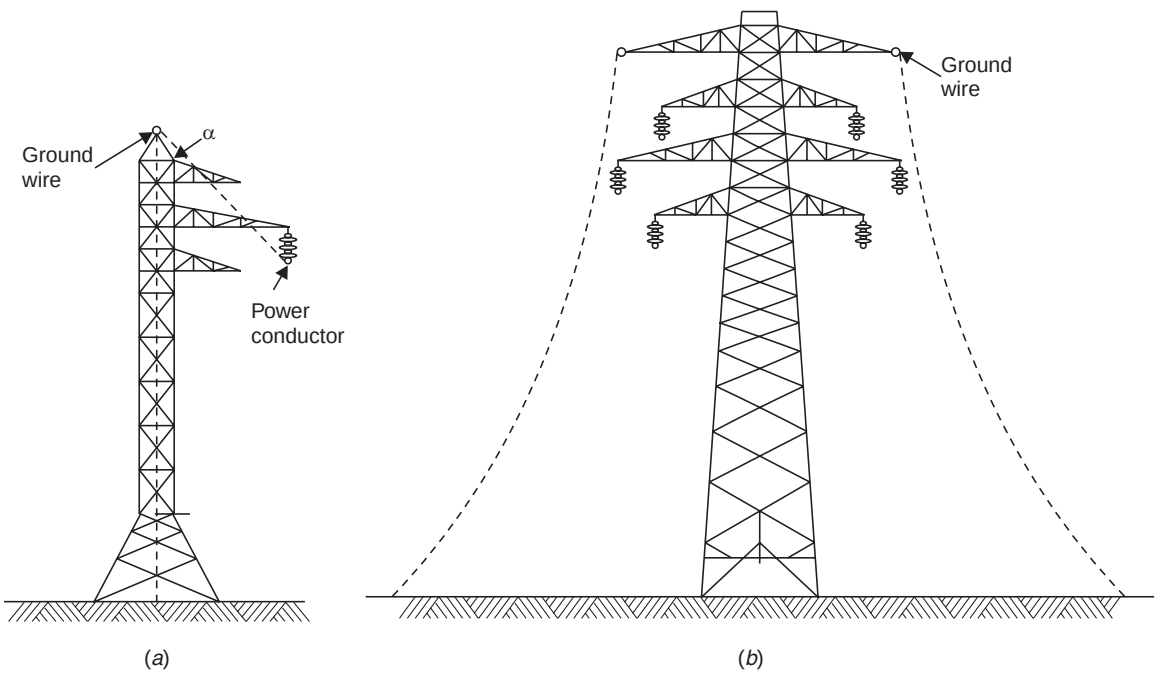

Fig. 7.44 (*a*) Protective angle; (*b*) Protection afforded by two ground wires

Protective angle of the ground wire is defined as the angle between the vertical line passing through the ground wire and the line passing through the outermost power conductor (Fig. 7.44 (*a*)) and the protective zone is the zone which is a cone with apex at the location of the ground wire and surface generated by line passing through the outermost conductor. According to Lacey, a ground wire provides adequate shielding to any power conductor that lies below a quarter circle drawn with its centre at the height of ground wire and with its radius equal to the height of the ground wire above the ground. If two or more ground wires are used, the protective zone between the two adjacent wires can be taken as a semi-circle having as its diameter a line connecting the two ground wires (Fig. 7.44 (*b*)). The field experience alongwith laboratory investigation has proved that the protective angle should be almost 30° on plain areas whereas the angle decreases on hilly areas by an amount equal to the slope of the hill.

The voltage to which a transmission tower is raised when a lightning strikes the tower, is independent of the operating voltage of the system and hence the design of transmission line against lightning for a desired performance is independent of the operating voltage. The basic requirement for the design of a line based on direct stroke are: (*i*) The ground wires used for shielding the line should be mechanically strong and should be so located that they provide sufficient shield. (*ii*) There should be

sufficient clearance between the power conductors themselves and between the power conductors and the ground or the tower structure for a particular operating voltage. (*iii*) The tower footing resistance should be as low as can be justified economically.

To meet the first point the ground wire as is said earlier is made of galvanized steel wire or ACSR wire and the protective angle decides the location of the ground wire for effective shielding. The second factor, *i.e.,* adequate clearance between conductor and tower structure is obtained by designing a suitable length of cross arm such that when a string is given a swing of 30° towards the tower structure the air gap between the power conductor and tower structure should be good enough to withstand the switching voltage expected on the system, normally four times the line-to-ground voltage (Fig. 7.45).

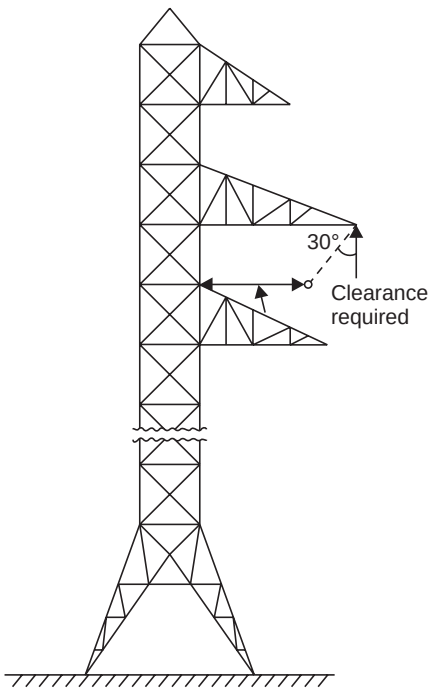

Fig. 7.45 Clearance determination or cross arm length determination

The clearances between the conductors also should be adjusted by adjusting the sag so that the mid span flashovers are avoided.

The third requirement is to have a low tower footing resistance economically feasible. The standard value of this resistance acceptable is approximately 10 ohms for 66 kV lines and increases with the operating voltage. For 400 kV it is approx. 80 ohms. The tower footing resistance is the value of the footing resistance when measured at 50 Hz. The line performance with regard to lightning depends upon the impulse value of the resistance which is a function of the soil resistivity, critical breakdown gradient of the soil, length and type of driven grounds or counterpoises and the magnitude of the surge current. If the construction of the tower does not give a suitable value of the footing resistance, following methods are adopted.

One possibility could be the chemical treatment of the soil. This method is not practically possible because of the long length of the lines and because this method needs regular check up about the soil conditions. It is not possible to check up the soil conditions at each and every tower of the line which runs in several miles. Therefore, this method is used more for improving the grounds of the substation.

The methods normally used for improving the grounds of transmission towers are the use of (*i*) ground rods, and (*ii*) counterpoises.

Ground Rods

Ground rods are used to reduce the tower footing resistance. These are put into the ground surrounding the tower structure. Fig. 7.46 shows the variation of ground resistance with the length and thickness of the ground rods used. It is seen that the size (thickness) of the rod does not play a major role in reducing the ground resistance as does the length of the rod. Therefore, it is better to use thin but long rods or many small rods.

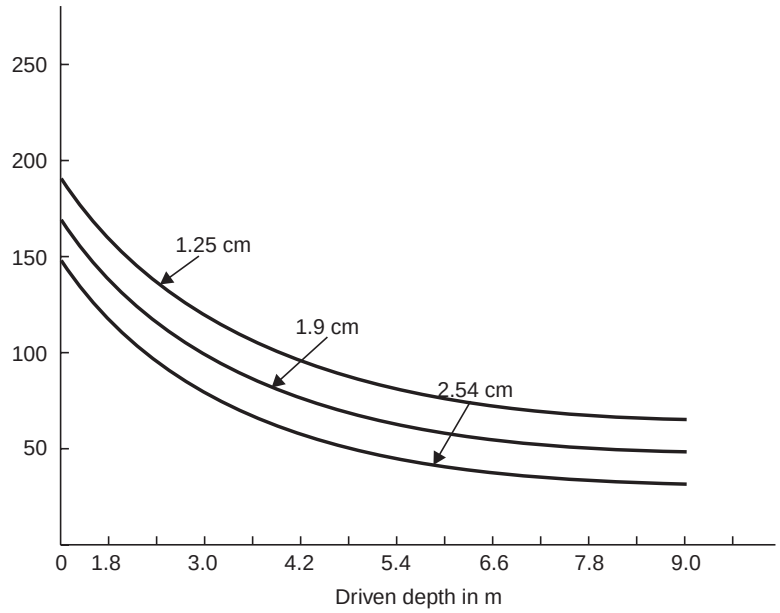

Fig. 7.46 Ground rod resistance as a function of rod length

Counterpoise

A counterpoise is galvanized steel wire run in parallel or radial or a combination of the two, with respect to the overhead line. The various configurations used are shown in Fig. 7.47.

The corners of the squares indicate the location of the tower legs. The lightning stroke as is incident on the tower, discharges to the ground through the tower and then through the counterpoises. It is the surge impedance of the counterpoises which is important initially and once the surge has travelled over the counterpoise it is the leakage resistance of the counterpoise that is effective. While selecting a suitable counterpoise it is necessary to see that the leakage resistance of the counterpoise should always be smaller than the surge impedance; otherwise, positive reflections of the surge will take place and hence instead of lowering the potential of the tower (by the use of counterpoise) is will be raised.

The leakage resistance of the counterpoise depends upon the surface area, *i.e.*, whether we have one long continuous counterpoise say 1000 m or four smaller counterpoises of 250 m each, as far as the leakage resistance is concerned it is same, whereas the surge impedance of say 1000 m if it is 200 ohms, then it will be 200/4, if there are four counterpoises of 250 m. each, as these four wires will now be connected in parallel. Also if the surge takes say 6 micro-seconds to travel a distance of 1000 m to reduce the surge impedance to leakage impedance, with four of 250 m it will take 1.5. μ sec, that is, the surge will be discharged to ground faster, the shorter the length of the ground wire. It is, therefore, desirable to have many short counterpoises instead of one long counterpoise. But we should not have too many short counterpoises, otherwise the surge impedance will become smaller than the leakage resistance (which is fixed for a counterpoise) and positive reflections will occur.

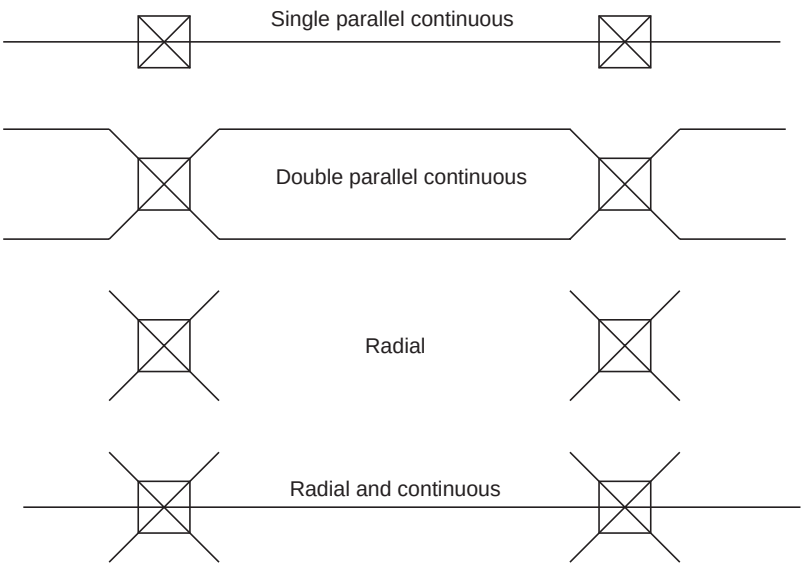

Fig. 7.47 Arrangement of counterpoise

The question arises as to why we should have a low value of tower footing resistance. It is clear that, whenever a lightning strikes a power line, a current is injected into the power system. The voltage to which the system will be raised depends upon what impedances the current encounters. Say if the lightning stroke strikes a tower, the potential of the tower will depend upon the impedance of the tower. If it is high, the potential of the tower will also be high which will result in flashover of the insulator discs and result in a line-to-ground fault. The flashover will take place from the tower structure to the power conductor and, therefore, it is known as back flashover,

Surge Absorbers

A surge absorber is a device which absorbs energy contained in a travelling wave. Corona is a means of absorbing energy in the form of corona loss. A short length of cable between the equipment and the overhead line absorbs energy in the travelling wave because of its high capacitance and low inductance. Another method of absorbing energy is the use of Ferranti surge absorber which consists of an air core inductor connected in series with the line and surrounded by an earthed metallic sheet called a dissipator. The dissipator is insulated from the inductor by the air as shown in Fig. 7.48.

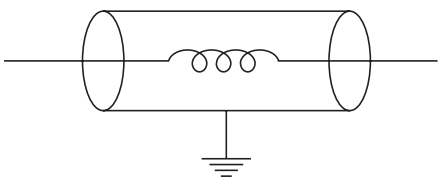

Fig. 7.48 Ferranti surge absorber

The surge absorber acts like an air cored transformer whose primary is the low inductance inductor and the dissipator acts as the single turn short circuit secondary. Whenever the travelling wave is incident on the surge absorber a part of the energy contained in the wave is dissipated as heat due to transformer action and by eddy currents. Because of the series inductance, the steepness of the wave also is reduced. It is claimed that the stress in the end turns is reduced by 15% with the help of surge absorber.

7.12 SURGE PROTECTION OF ROTATING MACHINE

A rotating machine is less exposed to lightning surge as compared to transformers. Because of the limited space available, the insulation on the windings of rotating machines is kept to a minimum. The main difference between the winding of rotating machine and transformer is that in case of rotating machines the turns are fewer but longer and are deeply buried in the stator slots. Surge impedance of rotating machines in approx. 1000 Ω and since the inductance and capacitance of the windings are large as compared to the overhead lines the velocity of propagation is lower than on the lines. For a typical machine it is 15 to 20 metres/ μ sec. This means that in case of surges with steep fronts, the voltage will be distributed or concentrated at the first few turns. Since the insulation is not immersed in oil, its impulse ratio is approx. unity whereas that of the transformer is more than 2.0.

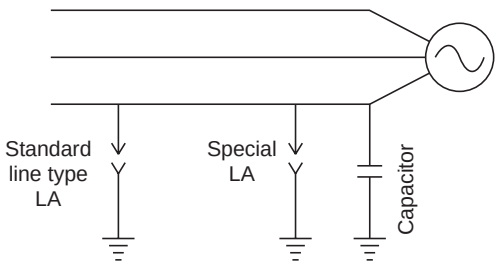

Fig. 7.49 Surge protection of rotating machine

The rotating machine should be protected against major and minor insulations. By major insulation is meant the insulation between winding and the frame and minor insulation means inter-turn insulation.

The major insulation is normally determined by the expected line-to-ground voltage across the terminal of the machine whereas the minor insulation is determined by the rate of rise of the voltage. Therefore, in order to protect the rotating machine against surges requires limiting the surge voltage magnitude at the machine terminals and sloping the wave front of the incoming surge. To protect the major insulation a special lightning arrester is connected at the terminal of the machine and to protect the minor insulation a condenser of suitable rating is connected at the terminals of the machine as shown in Fig. 7.49.

PROBLEMS

7.1. Given an *RL* circuit with a sudden 50 Hz sinusoidal voltage applied where R = 20 ohms, L = 0.36 H and voltage V = 220 V.

(*a*) The switch is closed at such a time as to permit maximum transient current. What is the instantaneous value of V upon closing the switch ?

(*b*) What is the maximum value of current in part (*a*) ?

(*c*) Let the switch be closed so as to yield minimum transient current. What instantaneous values of V and α correspond to this instant of closing the switch ?

7.2. Determine the relative attenuation occurring in two cycles in the over voltage surge set up on a 132 kV cable fed through an air blast breaker when the breaker opens on a system short circuit. The breaker uses critical resistance switching. The network parameters are R = 10 ohms, L = 8 mH and C = 0.08 μF.

7.3. Explain with neat diagrams two different theories of charge generation and separation in a thunder cloud.

7.4. Explain with neat sketches the mechanism of lightning discharge.

7.5. Differentiate between a hot lightning stroke and a cold lightning stroke.

7.6. Show that a travelling wave moves with a velocity of light on the overhead line and its speed is proportional to $1/\sqrt{\varepsilon_r}$ on a cable with dielectric material of permittivity ε_r.

7.7. Explain the variation of current and voltage on an overhead line when one end of the line is (*i*) short-circuited, and (*ii*) open-circuited and at the other end a source of constant e.m.f. *V* is switched in.

7.8. What is a travelling wave ? Explain the development of such a wave on an overhead line.

7.9. An overhead transmission line with surge impedance 400 ohms is 300 km long. One end of this line is short-circuited and at the other end a source of 11 kV is suddenly switched in. Calculate the current at the source end 0.005 sec after the voltage is applied.

7.10. Explain why a short length of cable is connected between the dead end tower and the terminal apparatus in a station. An over-head line with surge impedance 400 ohms is connected to a terminal apparatus through a short length of cable of surge impedance 40 ohms.

A travelling wave of constant magnitude 100 kV and infinite duration originates in the overhead line and travels towards the junction with the cable. Calculate the energy transmitted into the cable during a period of 5 μ sec after the arrival of the wave at the junction.

7.11. An overhead line with inductance and capacitance per km of 1.24 mH and 0.087 μF respectively is connected in series with an underground cable having inductance and capacitance of 0.185 mH/km and 0.285 μF/km. Calculate the values of transmitted and reflected waves of voltage and current at the junction due to a voltage surge of 110 kV travelling to the junction (*i*) along the line towards the cable, and (*ii*) along the cable towards the line.

7.12. An overhead line with surge impedance 400 ohms bifurcates into two lines of surge impedance 400 ohms and 40 ohms respectively. If a surge of 20 kV is incident on the overhead line, determine the magnitudes of voltage and current which enter the bifurcated lines.

7.13. A long overhead line has a surge impedance of 500 ohms and an effective resistance of 6 ohms per km. If a surge of 400 kV enters the line at a certain point, calculate the magnitude of this surge after it has traversed 100 km and calculate the power loss and heat loss of the wave over this distance. Assume velocity of wave as 3×10^8 m/sec.

7.14. A rectangular surge of 2 μ sec duration and magnitude 100 kV travels along a line of surge impedance 500 ohms. The latter is connected to another line of equal impedance through an inductor of 500 μH. Calculate the maximum value of surge transmitted to the second line.

7.15. The effective inductance and capacitance of a faulted system as viewed from the contacts of a breaker are 2.5 mH and 600 pF respectively. Determine the restriking voltage across the breaker contacts when a fault current of 150 amps is chopped.

7.16. What is arcing ground? Explain its effect on the performance of a power system.

7.17. What is "capacitance switching"? Explain its effect on the performance of the circuit breaker.

7.18. What are volt-time curves ? What is their significance in power system studies?

7.19. What are BILS? Explain their significance in power system studies?

7.20. Describe the construction, principle of operation and application of (*i*) Rod gaps; (*ii*) Expulsion gap; and (*iii*) Valve type lightning arrester.

7.21. Compare the relative performances of the following: (*i*) Rod gap; (*ii*) Expulsion gap; and (*iii*) Valve type l.A.

7.22. Explain clearly how the rating of a lightning arrester is selected. What is the best location of a lightning arrester and why?

7.23. What is tower-footing resistance? What are the methods to reduce this resistance? Why is it required to have this resistance as low as economically feasible?

7.24. What are ground rods and counterpoises? Explain clearly how these can be used to improve the grounding conditions. Give various arrangements of counterpoise.

7.25. "The leakage resistance of a counterpoise should be lower than its surge impedance." Why?

7.26. What is a ground wire? Discuss its location with respect to power conductors.

7.27. What are the requirements of a ground wire for protecting power conductors against direct lightning stroke? Explain how they are achieved in practice.

7.28. Explain the principle of operation of Ferranti surge absorber.

7.29. What are the basic requirements of a lightning arrester? Differentiate between (*i*) a lightning arrester and a lightning conductor, and (*ii*) a surge diverter and a surge absorber.

7.30. Explain clearly how a lightning arrester is selected for protecting a power transformer.

7.31. Give a scheme of protecting a rotating machine against overvoltages. Explain clearly how the scheme is different from protecting a power transformer.

REFERENCES

H. A. Peterson, *Power System Transients*, Dover, 1966.

Travelling Waves on Transmission Systems, Dover, 1961.

Allan Greenwood, *Electrical Transients in Power System*, John Wiley & Sons, 1971.

IEEE Committee Report on Switching Surges, *IEEE Trans*. on PAS, pp. 912, 1948.

V.A. Venikov, *Transients in Power System.*

H. Cotton, *The Transmission and Distribution of Electrical Energy.*

The Transmission and Distribution Reference Book, Westinghouse Elect. Corp., Pennsylvania, 1964.

B. M. Weedy, *Electric Power Systems*, John Wiley & Sons, 1974.

F. S. Young et al., Shielding of Transmission Lines, *IEEE Trans*. on PAS, 83, 132, 1963.

Kuffel, E., Zaengl, W.S., *High Voltage Engineering Fundamentals*, Pergamen Press, 1984.

Multiple Choice Questions

1. The process of ionisation is brought about by
   (*a*) Positive ions only (*b*) Photons only
   (*c*) metastables only (*d*) all of the above
2. The value of Townsends second ionization coefficient has
   (*a*) high value for low E/p ratio (*b*) Low value for low E/p ratio
   (*c*) no relation with E/p ratio (*d*) no application if the gas pressure is low
3. If α and v are the Townsends first and second ionisation coefficients, d the distance of separation between the plates, the Townsends Criterion for Threshold sparking is given as
   (*a*) $e^{\alpha d} = 1$ (*b*) $\gamma e^{\alpha d} = 1$ (*c*) $e^{\alpha d}/\gamma = 1$ (*d*) $\gamma e^{\alpha d} = 2$
4. When avalanche in the gap reaches a certain critical size, the electric spark discharge is due mainly to ionization of gas by
   (*a*) electron impact (*b*) positive ion bombardment
   (*c*) photoionization (*d*) all (*a*) (*b*) and (*c*)
5. If E_r is the radial field due to space charge and E_0 the externally applied field, the transformation of avalanche into a streamer takes place when
   (*a*) $E_r < E_0$ (*b*) $E_r > E_0$ (*c*) $E_r \approx E_0$
   (*d*) (*a*) and (*c*) (*e*) (*b*) and (*c*)
6. If p is the pressure of gas and d the distance of separation between the electrodes, the discharge voltage according to paschen's low is directly proportional to
   (*a*) p (*b*) d (*c*) pd (*d*) none of the above
7. Assuming p to be Constant and Townsend's second ionization coefficure to be small during the applicability of Paschen's law. Then if $(pd > (pd)_{min}$
   (*a*) electrons crossing in the gap make more frequent collisions with gas molecules than at $(pd)_{min}$
   (*b*) energy gained between successive collisions is smaller than at $(pd)_{min}$
   (*c*) energy gained between successive collisions is larger than at $(pd)_{min}$
   (*d*) (*a*) and (*b*)
   (*e*) (*a*) and (*c*)
8. The breakdown voltage of a specimen is 65 kV at STP. The breakdown voltage at 73 cm Hg pressure and 35° C is
   (*a*) 69 kV (*b*) 63.25 kV (*c*) 64.33 kV (*d*) 60.39

9. Penning effect explains
   (*a*) increase in dielectric strength of all mixture of gases
   (*b*) decrease in dielectric strength of many mixture of gases
   (*c*) increase in dielectric strength of many mixture of gases
   (*d*) none of the above
10. Trichel pulses are noticed in a point plane gap in air when
   (*a*) point is positive
   (*b*) point is negative
   (*c*) These pulses are seen in plane-sphere gap
   (*d*) These pulses are seen in point-sphere gap
11. The on-set voltage for Trichel pulses
   (*a*) increases with increases in gap length
   (*b*) increases with decrease in gap length
   (*c*) independent of gap length
12. The frequency of Trichel pulses
   (*a*) increases with voltage and gap pressure
   (*b*) increases with voltage but decreases with increase in pressure
   (*c*) decreases with increase in voltage and pressure
   (*d*) decreases with increase in voltage and increases with increase in pressure.
13. All parameters remaining same, the breakdown voltage is
   (*a*) higher with negative polarity at all pressures
   (*b*) lower with negative polarity at all pressures
   (*c*) higher with negative polarity at low pressures.
   (*d*) none of above
14. Liquids with solid impurities
   (*a*) have higher dielectric strength
   (*b*) of large size have higher dielectric strength
   (*c*) has lower dielectric strength as compared to pure liquids
   (*d*) none of the above
15. The electric field in a gas bubble which is immersed in a liquid of permittivity ε_z is
   (*a*) higher than that of the field in the liquid
   (*b*) lower than that of the field in the liquid
   (*c*) same as that in the liquid
   (*d*) none of the above is always true
16. Centrifugal methods of reconditioning transformer oil is effected for removal of
   (*a*) water (*b*) dissolved gases
   (*c*) solid impurities (*d*) all of the above

17. In order to prevent an excessive evaporation of the aromatics during reconditioning of transformer oil using filtrations under vacuum, the vapour pressure should be
(*a*) less than 10^{-4} torr (*b*) less than 10^{-2} torr
(*c*) less than 10^{-1} torr (*d*) none of the above

18 During reconditioning of transformer oil it is economical to use electrostatic filters if the water content of oil is
(*a*) greater than 4 ppm (*b*) greater than 2 ppm
(*c*) less than 2 ppm (*d*) electrostatic filters are never used

19. The accepted value of dielectric strength of transformer oil is
(*a*) 30 kV (*b*) 30 kV/cm
(*c*) 30 kV/cm for one min. (*d*) none of the above

20. While testing transformer oil for dielectric strength the spherical electrodes are placed in
(*a*) horizontal configuration (*b*) vertical configuration
(*c*) any configuration (*d*) spherical electrodes are not used

21. The breakdown of solid materials is roughly given by
(*a*) $V_b t_b$ = constant (*b*) V_b 1n t_b = constant
(*c*) t_b 1n V_b = constant (*d*) None of the above

22. While conducting intrinsic dielectric strength on a specimen, its shape should be so prepared that
(*a*) the electric stress is high at its centre
(*b*) the electric stress is high at its corner
(*c*) the electric stress is same all along the sample
(*d*) No definite consideration

23. To determine intrinsic dielectric strength, the time of application of voltage is of the order of
(*a*) 10^{-8} sec (*b*) 10^{-6} sec
(*c*) 10^{-4} sec (*d*) No such consideration

24. In case of impulse thermal breakdown of solid insulating materials, the critical electric filed is
(*a*) proportional to critical absolute temperature
(*b*) proportional to square of critical absolute temperature
(*c*) proportional to square of T_0
(*d*) None of the above is true

25. In case of impulse thermal breakdown of insulating materials, the critical time to breakdown is
(*a*) proportional to critical electric filed
(*b*) inversely proportional to critical electric field
(*c*) proportional to square of critical absolute temperature
(*d*) None of the above

26. The ripple voltage in the d.c. output is small if
(*a*) frequency of supply is small (*b*) the filtering capacitor is small
(*c*) the load current is large (*d*) none of the above is true

27. The voltage drop for a certain Cockroft and Walton circuit is small if
(*a*) the load current is small (*b*) the frequency of supply is small
(*c*) the capacitance of each stage is small (*d*) all of the above

28. All other parameters remaining identical, the ratio of voltage drop for an 8 stage to 4 stage Cockroft Walton circuit approximately is
(*a*) 2 (*b*) 8 (*c*) 4 (*d*) 2.828

29. In Cockrofts-Walton circuit, the optimum number of stages for maximum output voltage (for a fixed supply voltage magnitude) is directly proportional to
(*a*) frequency of supply (*b*) capacitance of each stage
(*c*) load current (*d*) none of the above

30. In a Cockroft-Walton circuit, input voltage 100 kV load current-100 mA, supply frequency 100 Hz, each capacitor 10 nF. The optimum no. of stages for maximum output voltage is
(*a*) 1 (*b*) 10 (*c*) 15 (*d*) 35

31. The maximum output voltage is question 30 is
(*a*) 133 kV (*b*) 300 kV (c) 500 kV (*d*) 1000 kV

32. In order to reduce ripples and/or voltage drop, it is more economical to use
(*a*) high frequency and high capacitance (*b*) high frequency and small capacitance
(*c*) low frequency and small capacitance (*d*) low frequency and high capacitance

33. In a Van de Graaf generator, the width of the belt is 1 m, and surface charge density permissible is 30×10^{-6} C/m^2. To supply a current of 300 μA, the velocity of belt should be
(*a*) 1 m/sec (*b*) 10 m/sec (*c*) 3.16 m/sec (*d*) None of the above

34. The surface charge density permissible in a Van de Graaf generator is 30×10^{-6} c/m^2. The radius of the electrode to charge to 10 MV is
(*a*) 0.295 m (*b*) 0.532 m (*c*) 1.234 m (*d*) 1.535 m

35. The radius of the ht electrode is 1 metre in Van de Graaf generator. If the permissible electric field is 21 kV/cm the maximum potential to which the electrode can be charged is
(*a*) 2.1 MV (*b*) 21 MV (*c*) 4.5 MV (*d*) None of the above

36. For a 3 stage Cascaded transformer if P1, P2, P3 are the loadings of I, II and III stages primaries, then
(*a*) P1 = P2 = P3 (*b*) P1 > P2 > P3 (*c*) P1 < P2 < P3 (*d*) P2 < P1 < P3

37. The short-circuit impedance of a three stage cascaded transformer as compared to a single unit transformer is
(*a*) 3 to 4 times (*b*) 8 to 9 times (*c*) 15 to16 times (*d*) 352 to 452 times

38. If the quality factor of the h.t. reactor in a.c. series resonant circuit is 49, and Q is the reactive power requirement of the test specimen, then the kW rating of the Feed Transformer is
(*a*) 49 Q (*b*) 7 Q (*c*) Q/7 (*d*) Q/49

39. If a single stage system using resonance test voltage is required, it is better to use
(*a*) series resonant circuit (*b*) parallel resonant circuit
(*c*) series-parallel resonant circuit (*d*) any one of the above

40. The impulse ratio for any particular object
(*a*) is a constant
(*b*) depends upon shape of wave
(*c*) depends upon the polarity of the impulse wave
(*d*) (*b*) and (*c*)

41. Impulse generator with circuit '*a*' configuration as compared with circuit '*b*' configuration
(*a*) has high voltage efficiency
(*b*) can be used for most of the equipments to be tested
(*c*) (*a*) and (*b*) (*d*) none of the above

42. The wave front and tail resistance and *IG* are 150 and 2000 Ω respectively. The impulse capacitance and load capacitances are 25 and 2 *nF* respectively. The approximate wave front time is
(*a*) 1 μ Sec. (*b*) 0.833 μ Sec. (*c*) 1.525 μ Sec. (*d*) 1.22 μ Sec.

43. The wave tail time for the above problem is
(*a*) 50.79 μ Sec. (*b*) 40.6 μ Sec. (*c*) 150 μ Sec. (*d*) 325.33 μ Sec.

44. For an impulse generator if $C_1/C_2 > 10$, for a given wave shape with different values of C_1/C_2
(*a*) wave front resistance is practically constant
(*b*) wave tail resistance is practically constant
(*c*) (*a*) and (*b*) (*d*) None of the above is true

45. The approximate voltage efficiency of *IG* for problem 42 is
(*a*) 99.45 % (*b*) 98.32 % (*c*) 92.60 % (*d*) 90.35 %

46. The minimum value of impulse capacitance to prevent oscillations on the tail of the impulse wave (1.5/40 μ Sec.) while testing inductive load with inductance of 10 H is
(*a*) 400 pF (*b*) 4 pF (*c*) 1628 pF (*d*) 1280 pF

47. The minimum value of impulse capacitance to impulse test a 3 ϕ, 200 kV, 5% impedance, power transformer is
(*a*) 4.5 nF (*b*) 0.22 nF (*c*) 0.826 nF (*d*) 0.02 μF

48. While impulse testing a power transformer, the impulse voltage is applied to
(*a*) one phase and the other two phases are short circuited, the secondary terminals are short circuited.
(*b*) one phase, the other two phases grounded, the secondary short circuited
(*c*) one phase, two phases left open, secondary left open
(*d*) one phase, two phases left open, secondary short circuited

49. If R_c is the charging resistance, R_2 wave tail resistance and R_1 the wave front control resistance then
(*a*) $R_c > R_2 < R_1$ (*b*) $R_c < R_2 < R_1$
(*c*) $R_1 > R_2 > R_c$ (d) None of the above

50. In order that Impulse circuit operates consistently, it is essential that
    (*a*) the first gap is slightly less than the second and so on
    (*b*) the axes of the gaps should be in the same vertical plane
    (*c*) (*a*) and (*b*)
    (*d*) None of the above is necessary
51. It is desirable to have wavefront control resistance
    (*a*) entirely within the impulse circuit
    (*b*) entirely outside the impulse circuit
    (*c*) partly inside and partly outside the impulse circuit
    (*d*) any where
52. The magnitude of pulse currents depends upon
    (*a*) voltage applied (*b*) no. of voids (*c*) (*a*) and (*b*)
53. The frequency spectrum of PD pulse current contains complete information concerning
    (*a*) the measurable charge in low frequency range
    (*b*) apparent charge in the low frequency range
    (*c*) apparent charge in the high frequency range
    (*d*) None of the above
54. In order to have proper integration of the pulse current it is desired that
    (*a*) time constant of pulse τ should be greater than time constant of the measuring circuit (T)
    (*b*) $\tau < T$ (*c*) $\tau = T$
    (*d*) time constant has nothing to do with integration of a pulse current
55. In narrow band PD detection circuit
    (*a*) Parallel combination of RLC forms measuring impedance
    (*b*) Parallel combination of RL forms measuring impedance
    (*c*) integration is carried out on the pulse current
    (*d*) (*a*) and (*c*)
56. Recurrent surge generator is used to generate
    (*a*) current of large magnitude
    (*b*) repetitive current surges
    (*c*) impulse voltage of smaller magnitude
    (*d*) (*b*) and (*c*)
57. For reducing tower footing resistance it is better to use
    (*a*) chemical and ground rods only (*b*) chemical and counterpoise only
    (*c*) ground rod and counterpoise only (*d*) chemical, ground rods and counter poise
58. The impulse ratio of a rod gap is:
    (*a*) unity (*b*) between 1.2 and 1.5
    (*c*) between 2.0 and 2.2 (*d*) between 1.6 and 1.8

59. The insulation of the modern EHV lines is designed based on:
(*a*) The lightning voltage (*b*) The switching voltage
(*c*) Corona (*d*) RI

60. High voltage d.c. testing for HV machines is resorted because
(*a*) Certain conclusions regarding the continuous ageing of an insulation can be drawn
(*b*) The stress distribution is a representation of the service condition
(*c*) Standardisation on the magnitude of voltage to be applied is available
(*d*) The stresses do not damage the coil and insulation

61. Standard impulse testing of a power transformer requires :
(*a*) Two applications of chopped wave followed by one application of a full wave
(*b*) One application of chopped wave followed by one applications of a full wave
(*c*) One application of chopped wave followed by two applications of a full wave
(*d*) None of the above

62. The velocity of a travelling wave through a cable of relative permittivity 9 is :
(*a*) 9×10^8 m/sec (*b*) 3×10^8 m/sec
(*c*) 10^8 m/sec (*d*) 2×10^8 m/sec

63. An overhead line with surge impedance 400 ohms is terminated through a resistance *R*. A surge travelling over the line does not suffer any reflection at the junction if the value of *R* is
(*a*) 20 ohms (*b*) 200 ohms
(*c*) 800 ohms (*d*) None of the above

64. When Oscilloscope is used as a null detector
(*a*) an inclined straight line shows magnitude unbalance
(*b*) an inclined straight line shows phase unbalance
(*c*) the area of the ellipse shows amptitude unbalance
(*d*) (*b*) and (*c*)

65. Current ratio arm bridge is used for
(*a*) low voltage high frequency application
(*b*) low voltage low frequency application
(*c*) high voltage low frequency application
(*d*) high voltage high frequency appliacation

66. Partial discharge can be detected by
(*a*) listening to hissing sound (*b*) a high tan δ
(*c*) optical methods (*d*) all of the above

67. During partial discharges if pulse currents through *CK* and *Ct* are observed simultaneously on the oscilloscope, it is found that
(*a*) these occupy same location (*b*) these have same polarity
(*c*) these have same magnitude (*d*) (*a*) and (*b*)
(*e*) (*a*) and (*c*)

68. The pulse currents through *CK* and *Ct* are supplied by
(*a*) source mainly (*b*) partial discharge mainly
(*c*) partly by source and partly be partial discharge
(*d*) impedance Z

69. If the source is not able to supply charging current required by the test cable, it is desirable to use
(*a*) shunt capacitor (*b*) series capacitor
(*c*) series inductor (*d*) (*a*) and (*c*)

70. Partial discharge measurement on a cable gives
(*a*) p.f. of the cable (*b*) loss angle of the cable
(*c*) location of fault (*d*) (*a*) and (*b*)

71. If tan δ_1, tan δ_2, and tan δ_3 are the loss angles of the test capacitors after 16, 24, and 48 hrs. respectively measured on *HV* schering bridge, it is desirable that
(*a*) $\tan \delta_1 \leq \tan \delta_2 \leq \tan \delta_3$ (*b*) $\tan \delta_1 \geq \tan \delta_2 \geq \tan \delta_3$
(*c*) $\tan \delta_1 \leq \tan \delta_2 + \tan \delta_3$ (*d*) None of the above

72. Non-destructive testing mehods require measurement of
(*a*) dielectric strength (*b*) Insulation resistance
(*c*) tan δ (*d*) (*a*) and (*b*)
(*e*) (*b*) and (*c*)

73. The mechanism responsible for dielectric loss in a dielectric are
(*a*) Conduction (*b*) Polarisation
(*c*) Ionisation (*d*) (*a*) and (*b*)
(*e*) (*b*) and (*c*)

74. The specific conductivity of a test specimen with $\varepsilon_r = 3.8$ and $\tan \delta = 0.008$ at 50 Hz is
(*a*) 0.27×10^{-12} s/m (*b*) 84.51×10^{-12}
(*c*) 10.56×10^{-9} (*d*) 22.24×10^{-12}

75. The specific conductivity of a test specimen with $\varepsilon_r = 4.0$ at 50 Hz is 10^{-12} S/m. It's loss angle is
(*a*) 9×10^{-5} (*b*) 5.65×10^{-4}
(*c*) 9×10^{-4} (*d*) 5.65×10^{-3}

76. A test specimen with specific conductivity 10^{-12} S/m is placed in an electric field of 100 kV/cm. The specific loss in the specimen is
(*a*) 10^{-5} W/m^3 (*b*) 100 W/m^3
(*c*) 10^9 W/m^3 (*d*) None of the above

77. High voltage Schering bridge is used to measure
(*a*) Large capacitance without additional element
(*b*) small capacitance without additional element
(*c*) medium value capacitances
(*d*) all values capacitances

78. Sphere gap is used for measurement of
(*a*) a.c. voltage only (*b*) d.c. voltage only
(*c*) Impulse voltage of any wave shape (*d*) (*a*) and (*b*)
(*e*) (*a*), (*b*), and (*c*)

79. Sphere gap when used for measurement of high voltage, the spheres are placed
(*a*) in horizontal configuration if spheres are small
(*b*) in vertical configuration if spheres are small
(*c*) in horizontal configuration if spheres are large
(*d*) (*b*) and (*c*)

80. Protective resistance to be connected between the sphere gap and the test equipment is required while measuring
(*a*) power frequency and higher frequency a.c. voltage
(*b*) power frequency and impulse voltage
(*c*) Higher frequency a.c. voltages and impulse voltage
(*d*) all kinds of voltages

81. If D is the diameter of the sphere, for better measurements, the gaps 'S' should be such that,
(*a*) $0.05\ D \le S \le 0.6\ D$ (*b*) $0.04\ D \le S \le 0.5\ D$
(*c*) $0.05\ D \le S \le 0.5\ D$ (*d*) $0.03\ D \le S \le 0.6\ D$

82. Tick out of the correct :
(*a*) The breakdown voltage in sphere gaps increases with increase in partial pressure of water vapour
(*b*) The increase in breakdown voltage as in (*a*) increases with increase in gap length
(*c*) (*a*) and (*b*)
(*d*) The breakdown voltage in sphere gaps decreases with increase in partial pressure of water vapour

83. Using uniform field spark gap, the breakdown voltage for 10 mm gap length is
(*a*) 34.25 kV (*b*) 30.30 kV (*c*) 36.25 kV (*d*) 32.73 kV

84. The voltage measurements using uniform spark gap are
(*a*) affected by nearby earthed objects (*b*) affected by polarity of supply
(*c*) affected by dust particles (*d*) all of (*a*) (*b*) and (*c*)

85. A generating voltmeter
(*a*) generates voltage (*b*) generates current
(*c*) is a variable capacitor device (*d*) (*b*) and (*c*)

86. A generating voltmeter uses
(*a*) a constant speed motor
(*b*) a variable speed motor
(*c*) a variable speed motor with a capacitor
(*d*) none of the above

87. A generating voltmeter is used to measure a.c. voltages if the angular frequency of voltage is
(*a*) half the angular frequency of motor used
(*b*) twice the angular frequency of motor used
(*c*) thrice the angular frequency of the motor used
(*d*) None of the above

88. A generating voltmeter has
(*a*) linear scale
(*b*) non-linear scale
(*c*) no contact with high voltage electrode
(*d*) (*a*) and (*c*)

89. A potential divider is normally connected
(*a*) Outside the generator circuit towards the load circuit
(*b*) within the generator circuit
(*c*) at a distance $V/100$ metres from the generator where V is the voltage to be measured in kV
(*d*) None of the above

90. For capacitor dividers, if damping resister is inserted in series with individual element of capacitor divider, the damped capacitive divider acts as
(*a*) capacitance divider only (*b*) resistance divider only
(*c*) resistance divider for high frequency (*d*) capacitance divider for high frequency

91. Klydonograph is used to record impulse voltages
(*a*) greater than 50 kV
(*b*) greater than 50 kV but less than 100 kV
(*c*) greater than 100 kV but less than 1000 kV
(*d*) None of the above

92. Klydonograph when used for measurement of voltages provides information on
(*a*) magnitude and polarity (*b*) polarity and frequency
(*c*) magnitude and frequency (*d*) all the three quantities

93. High power-frequency currents are normally measured using
(*a*) low shunt resistance (*b*) Hall element
(*c*) Current transformer (*d*) all of the above methods

94. High frequency and impulse currents are measured using
(*a*) resistive shunts (*b*) inductive elements
(*c*) Hall and Faraday effect devices (*d*) all of the above

95. Which element has flat frequency response upto 1000 MHz
(*a*) Bifilar shunt (*b*) Co-axial shunt
(*c*) Squirrel cage shunt (*d*) Rogowski coil

96. The breakdown voltage for air gap of 3 mm in a uniform field under standard atmospheric condition is
(*a*) 10.59 kV (*b*) 6.3 kV
(*c*) 9.2 kV (*d*) 7.25 kV.

Answers to Multiple Choice Questions

1 (*d*)	21 (*b*)	41 (*d*)	61 (*a*)	81 (*c*)
2 (*b*)	22 (*a*)	42 (*b*)	62 (*c*)	82 (*c*)
3 (*b*)	23 (*a*)	43 (*b*)	63 (*d*)	83 (*b*)
4 (*d*)	24 (*c*)	44 (*b*)	64 (*a*)	84 (*c*)
5 (*c*)	25 (*b*)	45 (*c*)	65 (*c*)	85 (*e*)
6 (*d*)	26 (*d*)	46 (*d*)	66 (*d*)	86 (*a*)
7 (*d*)	27 (*a*)	47 (*c*)	67 (*e*)	87 (*b*)
8 (*d*)	28 (*b*)	48 (*b*)	68 (*b*)	88 (*d*)
9 (*b*)	29 (*d*)	49 (*d*)	69 (*c*)	89 (*a*)
10 (*b*)	30 (*a*)	50 (*c*)	70 (*c*)	90 (*c*)
11 (*c*)	31 (*a*)	51 (*c*)	71 (*b*)	91 (*d*)
12 (*a*)	32 (*b*)	52 (*a*)	72 (*e*)	92 (*a*)
13 (*d*)	33 (*a*)	53 (*b*)	73 (*e*)	93 (*c*)
14 (*c*)	34 (*a*)	54 (*a*)	74 (*b*)	94 (*d*)
15 (*b*)	35 (*a*)	55 (*b*)	75 (*a*)	95 (*b*)
16 (*c*)	36 (*b*)	56 (*c*)	76 (*b*)	96 (*a*)
17 (*d*)	37 (*b*)	57 (*c*)	77 (*b*)	
18 (*c*)	38 (*d*)	58 (*b*)	78 (*d*)	
19 (*d*)	39 (*b*)	59 (*c*)	79 (*a*)	
20 (*a*)	40 (*d*)	60 (*a*)	80 (*a*)	

Index